

POWER SYSTEM CONFIGURATION STUDY
AND RELIABILITY ANALYSIS

FINAL REPORT

by
W.G. Binckley

07171-6001-R000

18 September 1967

This work was performed for the Jet Propulsion Laboratory,
California Institute of Technology, sponsored by the
National Aeronautics and Space Administration under
Contract No. 951574



One Space Park
Redondo Beach, California

Prepared for
JET PROPULSION LABORATORY
CALIFORNIA INSTITUTE OF TECHNOLOGY
Contract No. 951574

Prepared *W. G. Binckley*
W. G. Binckley
Project Manager

Approved *Arthur D. Schoenfeld*
A. D. Schoenfeld
Manager, Power Systems
and Conditioning Department

TRW Systems
One Space Park
Redondo Beach, California

DISCLAIMER CLAUSE

NOTICE

This report was prepared as an account of Government - sponsored work. Neither the United States, nor the National Aeronautics and Space Administration (NASA), nor any person acting on behalf of NASA:

- a. Makes warranty or representation, expressed or implied, with respect to the accuracy, completeness, or usefulness of the information contained in this report, or that the use of any information, apparatus, method, or process disclosed in this report may not infringe privately owned rights; or
- b. Assumes any liabilities with respect to the use of, or for damages resulting from, the use of any information, apparatus, method, or process disclosed in this report.

As used above, "person acting on behalf of NASA" includes any employee or contractor of NASA, or employee of such contractor, to the extent that such employees or contractor of NASA, or employee of such contractor prepares, disseminates, or provides access to, any information pursuant to his employment with such contractor.

Requests for copies of this report should be referred to:

National Aeronautics and Space Administration
Office of Scientific and Technical Information
Washington 25, D. C.

FOREWORD

This report covers work performed by TRW Systems for the Jet Propulsion Laboratory under Contract No. 951574 during the period 7 July 1966 to 8 September 1967. The author wishes to acknowledge the valuable contributions of the following personnel to this project: E.C. Jazwa, JPL technical representative, for his technical direction and guidance; W.S. Dixon, W.A. Klein and K.H. Meissner who formed the nucleus of the study team; P. Bauer, J.J. Biess, R.L. Brown, A.A. Conn, S. Green, W.R. Johnson, H.F. Meissinger, F.S. Osugi, B.M. Otzinger, A.D. Schoenfeld and J.W. Schrecengost for their significant technical contributions; and T. Byrne, G.A. Hetland and D.B. Ryder for their editorial assistance.

ABSTRACT

Analyses of photovoltaic electric power system configurations for interplanetary missions to Mercury, Venus, Mars and Jupiter are covered in this report. Seven model missions and spacecraft configurations and representative power levels and required load power characteristics for each model are presented. Analyses of alternative methods of configuring electric power systems and of implementing the various system functions are discussed. Candidate power system configurations are defined and methods of improving power system reliability and the effects of these improvements on the weight and efficiency of each unit are described. A computer program developed in this program for assessing the reliability and weight of candidate systems and selecting optimum system configurations on the basis of maximum reliability and minimum weight is described. Preliminary definitions of optimum power system configurations for each model mission/spacecraft resulting from the use of this computer program are presented. Salient design considerations in implementing these systems are discussed and include electromagnetic compatibility, thermal interfaces, and command and telemetry provisions.

CONTENTS

	Page
1. INTRODUCTION	1-1
1.1 Definition of Terms	1-4
2. MISSION AND SPACECRAFT ANALYSES	2-1
2.1 Model Spacecraft	2-1
2.2 Model Power Requirements	2-9
3. BASELINE POWER SYSTEM CONFIGURATIONS	3-1
3.1 Power System Synthesis	3-1
3.2 Solar Array Analysis	3-9
3.2.1 Determination of Current-Voltage Characteristics	3-9
3.2.2 Comparison of Solar Array Capability With Load Profile	3-10
3.3 Solar Array - Battery Integration	3-19
3.3.1 Selection of Battery Type and Control Approach	3-19
3.3.2 Battery Control Implementation	3-24
3.3.3 Solar Array Control Implementation	3-42
3.4 Power Conditioning Analysis	3-49
3.4.1 Line Regulators	3-49
3.4.2 Load Power Conditioning Equipment	3-49
3.5 Selection of Baseline System Configurations	3-63
3.6 Solar Array Power Utilization	3-68
4. RELIABILITY ANALYSIS	4-1
4.1 Reliability Weight Optimization Method	4-1
4.1.1 Computer Program Description	4-2
4.2 Reliability Improvement Methods	4-20
4.2.1 Implementation of Redundancy	4-21
4.2.2 Selected Redundant Configurations and Parts Counts	4-26
4.2.3 Failure Mode Effects	4-41
4.3 Effects of Reliability Improvements on Unit Weight and Efficiency	4-74
4.3.1 Electronic Equipment	4-74
4.3.2 Batteries	4-75

CONTENTS (Continued)

	Page
4.4 Results of Reliability - Weight of Optimization	4-88
4.4.1 Venus Orbiter No. 1	4-88
4.4.2 Venus Orbiter No. 2	4-90
4.4.3 Mercury Flyby	4-90
4.4.4 Mars Orbiter	4-91
4.4.5 Jupiter Flyby	4-92
4.4.6 Jupiter Orbiters	4-93
5. QUALITATIVE SYSTEM COMPARISONS	5-1
5.1 Electromagnetic Compatibility	5-1
5.2 Thermal Control	5-5
5.3 Power System Flexibility	5-7
5.4 System Design Considerations	5-11
5.4.1 Command Provisions	5-11
5.4.2 Telemetry Provisions	5-15
5.4.3 Load Fault Protection	5-19
5.4.4 Electromagnetic Interference Control	5-22
6. CONCLUSIONS AND RECOMMENDATIONS	6-1
6.1 Conclusions	6-1
6.1.1 Reliability-Weight Optimization Computer Program	6-1
6.1.2 Preferred Power System Configurations	6-3
6.1.3 Preferred Power Systems	6-5
6.2 Recommended Future Study Areas	6-7
6.2.1 Optimization Program Refinements	6-7
6.2.2 Mathematical Analysis of Reliability-Weight Characteristics	6-9

ILLUSTRATIONS

		Page
1.	Mission Profile: Mercury Flyby	2-5
2.	Mission Profile: Venus Orbiter	2-5
3.	Mission Profile: Mars Orbiter (Launch May 1971)	2-6
4.	Mission Profile: Jupiter Orbiter (Launch March 1972)..	2-6
5.	Eclipse Durations for Assumed Mars Orbit	2-8
6.	Eclipse Durations for Assumed Venus Orbit	2-8
7.	Flow Diagram - Baseline System Configuration Analysis	3-2
8.	Generalized Power System Concepts	3-3
9.	Basic Functional Power System Configurations	3-4
10.	Simplified System Operating Points for Basic Functional Power System Configurations	3-5
11.	Comparison of Special Solar Cell with Standard Solar Cell at Light Intensity of 20 Suns	3-9
12.	Mercury Flyby Solar Array Characteristics	3-11
13.	Venus Orbiter Solar Array Characteristics	3-11
14.	Mars Orbiter Solar Array Characteristics	3-12
15.	Jupiter Orbiter Solar Array Characteristics	3-12
16.	Solar Array Maximum Power Capability and Conditioned Load Power Requirements versus Time - Mercury Flyby Mission	3-15
17.	Solar Array Maximum Power Capability and Conditioned Load Power Requirements versus Time - Venus Orbiter No. 1 Mission	3-15
18.	Solar Array Maximum Power Capability and Conditioned Load Power Requirements versus Time - Venus Orbiter No. 2 Mission	3-16
19.	Solar Array Maximum Power Capability and Conditioned Load Power Requirements versus Time - Mars Orbiter Mission	3-16

ILLUSTRATIONS (Continued)

		Page
20.	Solar Array Maximum Power Capability and Conditioned Load Power Requirements versus Time – Jupiter Flyby Mission	3-17
21.	Solar Array Maximum Power Capability and Conditioned Load Power Requirements versus Time – Jupiter Orbiter No. 1 Mission	3-17
22.	Solar Array Maximum Power Capability and Conditioned Load Power Requirements versus Time – Jupiter Orbiter No. 2 Mission	3-18
23.	Comparison of Required Solar Array Capabilities With and Without Momentary Line Booster for Unregulated Lens Systems	3-23
24.	Dissipative Series Charger	3-26
25.	PWM Buck Series Charger	3-26
26.	PWM Buck-Boost Charger, Array Regulator or Line Regulator	3-27
27.	Dissipative Battery Charge Regulator	3-27
28.	PWM Buck Battery Charge Regulator	3-28
29.	Momentary Line Booster, Used With Boost Charger . . .	3-28
30.	PWM Boost Discharge Regulator, Boost Line Regulator or Momentary Line Booster Used With Buck Charger	3-29
31.	Battery Controls Block Diagram Bucking Charger and Discharge Switch	3-30
32.	System Operating Points for Bucking Charger	3-31
33.	Battery Controls Block Diagram Bucking Charger, Discharge Switch, and Line Booster	3-33
34.	System Operating Points for Bucking Charger With Line Booster	3-35
35.	Battery Controls Block Diagram Boost Charger and Discharge Switch	3-36
36.	System Operating Points for Boost Charger	3-38

ILLUSTRATIONS (Continued)

	Page
37. Battery Controls Block Diagram Boost Charger, Discharge Switch, and Line Booster	3-39
38. System Operating Points for Boost Charger with Live Booster	3-40
39. Battery Controls Block Diagram Bucking Charge Regulator, Boost Discharge Regulator	3-42
40. Zener Diode Solar Array Voltage Limiter	3-46
41. Active Shunt Solar Array Voltage Limiter	3-47
42. PWM Bucking Solar Array Voltage Limiter or Line Regulator	3-47
43. Maximum Power Tracker	3-48
44. Dissipative Line Regulator	3-50
45. Block Diagram of Load Power Conditioning Equipment Configuration - DC Distribution	3-53
46. Block Diagram Unregulated DC-DC Converter	3-53
47. Block Diagram of Load Power Conditioning Equipment Configuration - AC Distribution	3-54
48. Selected Alternative Methods of Implementing Basic Functional Configurations Having Unregulated Main Bus	3-64
49. Selected Methods of Implementing Basic Functional Configurations Having Regulated Main Bus	3-64
50. Solar Array Sizing Factors for Mercury Flyby Mission	3-73
51. Solar Array Utilization Factors for Venus Orbiter No. 1 Mission	3-76
52. Solar Array Sizing Factors for Venus Orbiter No. 2 Mission	3-78
53. Solar Array Sizing Factors for Mars Orbiter Mission . .	3-79
54. Solar Array Sizing Factors for Jupiter Missions	3-80
55. Reliability - Weight Optimization Matrix	4-6

ILLUSTRATIONS (Continued)

	Page
56. Basic System Reliability Model	4-23
57. Parallel Redundant System Reliability Model	4-23
58. Standby Redundant System Reliability Model	4-25
59. Quad Redundant System Reliability Model	4-25
60. Majority Voting System Reliability Model	4-26
61a. Nonredundant Voltage Sensing and Error Amplifier Block Diagram	4-28
61b. Majority Voting Redundant Configuration of Voltage Sensing and Error Amplifier	4-28
62. Methods of Implementing Part Redundancy	4-33
63. Array Controls, Baseline, Weight versus Power Output .	4-77
64. Array Controls, Redundant, Weight versus Power Output	4-77
65. Array Controls, Baseline, Efficiency versus Power Output	4-78
66. Array Controls, Redundant, Efficiency versus Power Output	4-78
67. Battery Controls, Baseline, Weight versus Power Output	4-79
68. Battery Controls, Redundant, Weight versus Power Output	4-79
69. Battery Controls, Baseline, Efficiency versus Power Output	4-80
70. Battery Controls, Redundant, Efficiency versus Power Output	4-80
71. Low Voltage Battery Controls, Efficiency versus Power Output	4-81
72. Low Voltage Battery Controls, Weight versus Power Output	4-81

ILLUSTRATIONS (Continued)

	Page
73. Line Regulator, Baseline, Weight versus Power Output .	4-82
74. Line Regulator, Redundant, Weight versus Power Output	4-82
75. Line Regulator, Baseline, Efficiency versus Power Output	4-83
76. Line Regulator, Redundant, Efficiency versus Power Output	4-83
77. Load Power Conditioning Equipment, Baseline, Weight versus Power Output	4-84
78. Load Power Conditioning Equipment, Redundant, Weight versus Power Output	4-84
79. Load Power Conditioning Equipment, Baseline, Efficiency versus Power Output	4-85
80. Load Power Conditioning Equipment, Redundant, Efficiency versus Power Output	4-86
81. Bucking Line Regulator Power Loss Weight Product versus Switching Frequency	4-86
82. Twenty-cell Silver-cadmium and Fifteen-cell Silver-zinc Battery Weights, Baseline	4-87
83. Three-cell Battery Weights, Redundant	4-87
84. Locus of Optimum System Configurations, Venus Orbiter No. 1	4-94
85. Comparison of Optimum System Configurations, Venus Orbiter No. 1	4-95
86. Locus of Optimum System Configurations, Venus Orbiter No. 2	4-96
87. Comparison of Optimum System Configurations, Venus Orbiter No. 2	4-97
88. Locus of Optimum System Configurations, Mercury Flyby	4-98
89. Comparison of Optimum System Configurations, Mercury Flyby	4-99

ILLUSTRATIONS (Continued)

	Page
90. Locus of Optimum System Configurations, Mars Orbiter	4-100
91. Comparison of Optimum System Configurations, Mars Orbiter	4-101
92. Locus of Optimum System Configurations, Jupiter Flyby	4-102
93. Comparison of Optimum System Configurations, Jupiter Flyby	4-103
94. Locus of Optimum System Configurations, Jupiter Orbiter No. 1	4-104
95. Comparison of Optimum System Configurations, Jupiter Orbiter No. 1	4-105
96. Locus of Optimum System Configurations, Jupiter Orbiter No. 2	4-106
97. Comparison of Optimum System Configurations, Jupiter Orbiter No. 2	4-107

TABLES

	Page
1. Model Spacecraft Configurations	2-2
2. Conditioned Power Requirements (in watts) as Function of Mission Phase - Mercury Flyby Model	2-10
3. Conditioned Power Requirements (in watts) as Function of Mission Phase - Venus Orbiter Model No. 1	2-11
4. Conditioned Power Requirements (in watts) as Function of Mission Phase - Venus Orbiter Model No. 2	2-12
5. Conditioned Power Requirements (in watts) as Function of Mission Phase - Mars Orbiter Model	2-13
6. Conditioned Power Requirements (in watts) as Function of Mission Phase - Jupiter Flyby Model	2-14
7. Conditioned Power Requirements (in watts) as Function of Mission Phase - Jupiter Orbiter Model No. 1	2-15
8. Conditioned Power Requirements (in watts) as Function of Mission Phase - Jupiter Orbiter Model No. 2	2-16
9. Load Equipment Typical Input Power Characteristics	2-18
10. Mercury Flyby Mission, Load Power Conditioning Equipment	3-56
11. Venus Orbiter No. 1 Mission, Load Power Conditioning Equipment	3-57
12. Venus Orbiter No. 2 Mission, Load Power Conditioning Equipment	3-58
13. Mars Orbiter Mission, Load Power Conditioning Equipment	3-59
14. Jupiter Flyby Mission, Load Power Conditioning Equipment	3-60
15. Jupiter Orbiter No. 1 Mission, Load Power Conditioning Equipment	3-61
16. Jupiter Orbiter No. 2 Mission, Load Power Conditioning Equipment	3-62

TABLES (Continued)

		Page
17.	Summary of Selected Baseline Power System Configurations	3-71
18.	Justifications for Deletions of Power System Configurations	3-72
19.	Recommended Failure Rates for Power System Configuration Study	4-4
20.	Part Type Demonstrated Orbital Operating Hours (Vela and OGO)	4-5
21.	Part Group Total Number of Orbital Parts (Vela and OGO)	4-5
22.	Weight Calculations for DC Distribution Systems	4-9
23.	Weight Calculations for AC Distribution Systems	4-10
24.	Glossary of Terms	4-11
25.	Example of Computer Printout for Optimization of One System	4-14
26.	Power System Configuration Code	4-15
27.	Example of Ranking by Type for Given Reliability Constraint, Venus Orbiter No. 1 Mission	4-18
28.	Array Controls, Baseline Parts Count	4-30
29.	Array Controls, Redundant Parts Count	4-31
30.	Battery Controls, Baseline Parts Count	4-36
31.	Battery Controls, Redundant Parts Count	4-37
32.	Line Regulators, Baseline Parts Count	4-39
33.	Line Regulators, Redundant Parts Count	4-40
34.	Load Power Conditioning Equipment, Baseline Parts Count, Mercury Flyby, AC Distribution System	4-46
35.	Load Power Conditioning Equipment, Redundant Parts Count, Mercury Flyby, AC Distribution System	4-47

TABLES (Continued)

	Page
36. Load Power Conditioning Equipment, Baseline Parts Count, Mercury Flyby, DC Distribution System	4-48
37. Load Power Conditioning Equipment, Redundant Parts Count, Mercury Flyby, DC Distribution System	4-49
38. Load Power Conditioning Equipment, Baseline Parts Count, Venus Orbiter No. 1, AC Distribution System. . . .	4-50
39. Load Power Conditioning Equipment, Redundant Parts Count, Venus Orbiter No. 1, AC Distribution System. . . .	4-51
40. Load Power Conditioning Equipment, Baseline Parts Count, Venus Orbiter No. 1, DC Distribution System. . . .	4-52
41. Load Power Conditioning Equipment, Redundant Parts Count, Venus Orbiter No. 1, DC Distribution System. . . .	4-53
42. Load Power Conditioning Equipment, Baseline Parts Count, Venus Orbiter No. 2, AC Distribution System. . . .	4-54
43. Load Power Conditioning Equipment, Redundant Parts Count, Venus Orbiter No. 2, AC Distribution System. . . .	4-55
44. Load Power Conditioning Equipment, Baseline Parts Count, Venus Orbiter No. 2, DC Distribution System. . . .	4-56
45. Load Power Conditioning Equipment, Redundant Parts Count, Venus Orbiter No. 2, DC Distribution System. . . .	4-57
46. Load Power Conditioning Equipment, Baseline Parts Count, Mars Orbiter, AC Distribution System.	4-58
47. Load Power Conditioning Equipment, Redundant Parts Count, Mars Orbiter, AC Distribution System.	4-59
48. Load Power Conditioning Equipment, Baseline Parts Count, Mars Orbiter, DC Distribution System.	4-60
49. Load Power Conditioning Equipment, Redundant Parts Count, Mars Orbiter, DC Distribution System.	4-61
50. Load Power Conditioning Equipment, Baseline Parts Count, Jupiter Flyby, AC Distribution System.	4-62

TABLES (Continued)

	Page
51. Load Power Conditioning Equipment, Redundant Parts Count, Jupiter Flyby, AC Distribution System.	4-63
52. Load Power Conditioning Equipment, Baseline Parts Count, Jupiter Flyby, DC Distribution System.	4-64
53. Load Power Conditioning Equipment, Redundant Parts Count, Jupiter Flyby, DC Distribution System.	4-65
54. Load Power Conditioning Equipment, Baseline Parts Count, Jupiter Orbiter No. 1, AC Distribution System . . .	4-66
55. Load Power Conditioning Equipment, Redundant Parts Count, Jupiter Orbiter No. 1, AC Distribution System . . .	4-67
56. Load Power Conditioning Equipment, Baseline Parts Count, Jupiter Orbiter No. 2, DC Distribution System . . .	4-68
57. Load Power Conditioning Equipment, Redundant Parts Count, Jupiter Orbiter No. 2, DC Distribution System . . .	4-69
58. Load Power Conditioning Equipment, Baseline Parts Count, Jupiter Orbiter No. 2, AC Distribution System . . .	4-70
59. Load Power Conditioning Equipment, Redundant Parts Count, Jupiter Orbiter No. 2, AC Distribution System . . .	4-71
60. Load Power Conditioning Equipment, Baseline Parts Count, Jupiter Orbiter No. 2, DC Distribution System . . .	4-72
61. Load Power Conditioning Equipment, Redundant Parts Count, Jupiter Orbiter No. 2, DC Distribution System . . .	4-73
62. Configuration Code	4-89
63. Analog Telemetry Measurements and Priorities	5-17

1. INTRODUCTION

This is the final report covering work performed by TRW Systems for the Jet Propulsion Laboratory under Contract 951574, "Power System Configuration Study and Reliability Analysis. "

The design of an electric power system for any spacecraft application necessarily begins with the comparative analysis of alternative power system configurations. These configurations are normally defined by a block diagram representing each of the functional elements within the system. The functions essential to any photovoltaic power system which includes batteries are the power source, power source control, energy storage (battery and battery controls), line voltage regulation and load power conditioning.

Since a large variety of power system configurations are conceptually feasible, it is normally necessary to limit the scope of these comparisons by selecting relatively few preferred approaches for comparison. The preferences leading to these selections are usually subjective in nature and tend to reflect to a large extent the experience of the organization or individual charged with the responsibility of performing this important phase of the system design task. The specific design requirements for the power system and the optimization criteria used to evaluate candidate configurations vary from one application to another. The two most common criteria exclusive of cost, however, are the conflicting requirements of maximizing reliability and minimizing weight. The validity of these preliminary system tradeoffs will clearly be reflected in the degree of optimization achieved in all subsequent phases of the power system design effort.

This study project, therefore, was directed primarily toward the development and application of a method of conducting preliminary tradeoffs of photovoltaic power system configurations to select optimized system with

respect to reliability and weight. The method was applied to seven specific spacecraft configuration models spanning the following five basic interplanetary missions:

Mission 1 — 0.3 AU Probe (Mercury Flyby)

Mission 2 — Venus Orbiter (Two Spacecraft Models)

Mission 3 — Mars Orbiter

Mission 4 — 5.2 AU Probe (Jupiter Flyby)

Mission 5 — Jupiter Orbiter (Two Spacecraft Models)

The study included analyses of each mission to determine realistic spacecraft configurations based on booster capabilities, scientific objectives, vehicle stabilization methods, data transmission requirements and first approximations of spacecraft power requirements. Mission profiles were determined for each to include definition of mission phases, important events, Sun-spacecraft and Earth-spacecraft distance variations with time and orbit characteristics where appropriate. From these spacecraft models, representative power requirements were ascertained to serve as a basis for the power system analyses. The results of these analyses are presented in Section 2 of this report.

A systematic approach to determining feasible candidate power system configurations for each model set of requirements was then undertaken. This approach includes analyses of the solar array output characteristics for each mission and the ability of the various power system configurations to effectively utilize the solar array power capability. The analyses leading to the definition of candidate power systems and the selection of specific designs for the various power system functions are covered in Section 3 of this report.

Investigations of methods of improving the reliability of each candidate power system were performed and preferred methods of implementing unit redundancy were selected. Parametric data covering the weight and

efficiency of each unit of the power system as a function of output power were generated and the effects on these parameters of implementing redundancy were determined. The analyses of alternative methods of improving unit reliability through the use of redundancy and the effects of these reliability improvements on unit parts count, weight and efficiency are reported in Section 4 of this report.

Section 4 also reports the power system optimization process which makes use of a computer program to evaluate the reliability and weight of the 156 candidate system configurations for each model spacecraft. Minimum weight configurations of each possible system were selected by means of these computations from the large number (256 to 1024) of configurations for each system generated by various combinations of redundant and non-redundant units. The optimized configurations of each of the 156 systems were then compared and ranked, and minimum weight power systems were selected for each of twenty different reliability values.

Following these spacecraft analyses and the definition of preferred power system configurations, the design implementation phase of the power system development can then be initiated. The salient design considerations which influence the implementation of a selected power system configuration are related primarily to the electrical, thermal and mechanical interfaces between the power system and the spacecraft. Specific considerations include electromagnetic compatibility, power system command and telemetry provisions, load fault protection, heat dissipation, temperature limits and dimensional constraints. Although command and telemetry provisions and load fault detection are essentially common to all power system configurations, electromagnetic interference considerations, together with thermal and mechanical interface considerations, will influence the selection of a power system to a varying degree depending upon the particular application. As a result, investigations of these design considerations were included in the study and are reported in Section 5.

The final selection of an optimum power system configuration must be made in conjunction with overall spacecraft reliability-weight tradeoffs. The results of the power system optimization analyses reported herein serve as inputs to these spacecraft level tradeoffs which determine the proper apportionment of the booster-imposed weight limit to each of the spacecraft systems to achieve a maximum spacecraft reliability.

1.1 DEFINITION OF TERMS

For purposes of this study, the term "system" was applied to the combined electric power equipment including the solar array, battery, regulators, controls and load power conditioning equipment. The load power conditioning equipment consists of unregulated converters or unregulated inverters and transformer rectifiers which convert power from a regulated dc power bus to the various dc and ac power outputs of the system. The term "unit" was used to identify the major functional elements of the power system such as a battery, line regulator, converter, etc. The term "part" was applied to the discrete components contained within a unit such as a transistor, diode, relay, etc.

2. MISSION AND SPACECRAFT ANALYSES

2.1 MODEL SPACECRAFT

The five interplanetary missions specified by JPL as the subject for this study were analyzed to synthesize realistic spacecraft configurations and mission profiles for each. Two spacecraft models were defined for each mission based on consideration of propulsion capabilities, scientific objectives, estimated power levels, and spacecraft geometry. Spacecraft configurations were determined from adaptations of existing vehicles and design concepts which included Mariner, Voyager, Advanced Planetary Probe, and Pioneer VI. The spacecraft investigations included consideration of the use of electric propulsion systems on two of the missions to produce a relatively large power requirement in keeping with the original goal of investigating power systems in the 200- to 4000-w range.

Seven of the ten spacecraft configurations resulting from these analyses were selected by JPL for further use in the power system studies. Elimination of three of the models was based on establishing a suitable balance between the number of systems analyzed and the depth of each analysis within the scope of the project. Preference was given to those model configurations in which the system configurations and power system design constraints were based on well established technology. As a result, one of the 0.3 AU probe models using a despun heat shield for thermal control and two models employing electric propulsion were eliminated. A summary of the seven selected model spacecraft configurations is given in Table I. In each case, salient features of the spacecraft subsystems having significant effects on the power subsystem are listed.

Model 1, the 0.3 AU probe, was interpreted as a Mercury Flyby mission as can be seen in Table I. Similarly, Model 5, the 5.2 AU probe, was interpreted as a Jupiter flyby mission. In the case of both the Venus and Jupiter orbiters, two classes of spacecraft were configured as reflected by two weight categories and two power levels. In each case the power levels listed represent a rough estimate of the payload and spacecraft

requirements. Detailed analysis of representative power requirements for the equipment and experiments carried on each of the missions were performed subsequently.

Each of the spacecraft models is three-axis stabilized with exception of the 5.2 AU probe. In this case spin stabilization was selected with the spin axis of the vehicle directed towards the earth. The attitude control system for this model uses gas jets which precess the spin axis of the vehicle as required and which are controlled from the ground by scanning the RF beam from the vehicle.

The data rates for each of the spacecraft models were assigned as a function of the missions and objectives specified. Those models having larger payload capabilities and therefore greater quantities of experiment data to transmit require the higher bit rates. In all cases, high gain antennas are used to maintain the transmitter power requirements within reasonable levels and reduce system weight. A primary example of the system tradeoff between antenna gain and transmitter power is evident in comparing the Jupiter Orbiter No. 1 and Jupiter Flyby models. For the Jupiter Orbiter, a relatively large 32-ft diameter paraboloid antenna is employed with a 10-w rf TWT transmitter to achieve a data rate of 2800 bits-per-second at an earth-spacecraft distance of 6.0 AU. By way of comparison, Model 5, the Jupiter probe, utilizes a smaller 7-ft dish with a 20-w transmitter and achieves a bit rate of only 270 bits-per-second at the same distance. This order of magnitude reduction in the achievable data rate results from the fact that the data rate is proportional to the square of the antenna diameter and directly proportional to the radiated power. It appeared clearly advantageous to make use of large deployable antennas for the more distant mission, and thereby reduce the power requirements of the communications systems to reflect a lighter power system weight.

The close proximity of Mercury to the Sun dictates special provisions to maintain solar array temperatures within an acceptable range for Model No. 1. The selected method employs temperature-controlled

Mission Definition Spacecraft Type	1 0.3 AU Probe (or Mercury Flyby) Mariner Class With Variable-Angle Array	2 Venus Orbiter No. 1 Mariner Class With Orbit Insertion Engine	V V E
Primary mission objectives	1. Interplanetary particles and fields 2. Mercury scan	1. Interplanetary and planetary particles and fields 2. Venus scan	1. Ven 2. Ven 3. Int
Mission C_3 (km^2/sec^2)	91 (50 to 60 for Mercury flyby)	14	
Launch vehicle	Atlas/Centaur/HEKS or Titan IIIC/Centaur	Atlas/Centaur	Saturn large Saturn
Spacecraft injected weight (lb)	900	1500	
Mission duration (yr)			
Transit	{ 0.25 to perihelion	0.4	
Orbit	{ 0.25 - 0.32 to Mercury	0.5	
Approx Power capability (w)			
At Earth	350	250	
At target (planet)	350	300	
Weight breakdown (lb)			
Injected weight	900	1490	
Propellant exp en route	(4 lb midcourse, if Mercury flyby)	60	
Propellant exp orbit insertion	-	750	
Lander or entry capsule	-	-	
Total weight expended	-	810	
Total weight remaining	900	680	
Science payload	60	50	
Orbit characteristics			
Period (Earth days)	-	0.74, 1.52	0.74,
Size (planetary radii from center of planet)	-	1.5 x 9.	1.5 x 9
Inclination	-	0 deg	0 deg
Worst-case eclipse (h)	-	2.2	2.2
Configuration	Octagonal body, roll axis toward sun. Gimbale antenna and most experiment sensors away from sun.	Mariner II (Venus), with orbit insertion engine incorporated so as to point toward sun along roll axis. Thrust \approx 400 lb.	Similar (Phas LEM to 25 inject
Stabilization and control	3-axis stabilized, using sun and Canopus optical sensors for errors, and gas jets. (Mariner).	3-axis stabilized, using sun and Canopus optical sensors and gas jets. Gimbale engines and gyros during firing.	3-axis optical Gimb durin
Communications (downlink to 210-ft dish)	3-ft (Mariner) dish (23.3 db), double gimbale, and 20-w TWT transmitter gives 650 b/sec at 1.6 AU. (Earth-Spacecraft distance)	3-ft (Mariner) dish (23.3 db), double gimbale, and 10-w solid-state transmitter: 3000 b/sec at 0.5 AU (Earth-s/c distance at encounter) 250 b/sec at 1.7 AU (1 year after launch)	6-ft di gimb trans 25,00 (enco 2,000 after
Thermal control	Reflecting shield on sun side of equipment compartment.	Standard Mariner	Louven
Estimated solar array size and configuration	Four panels totaling 75 ft^2 extend as elements of a cross from spacecraft perpendicular to roll axis. Each panel is oriented about its axis for temperature control.	Two panels totaling 40 ft^2 .	Four p

3 Canopus Orbiter No. 2 Voyager Class With Entry Probe	4 Mars Orbiter Voyager Class Second-Generation With Lander	5 5.2 AU Probe (or Jupiter Flyby) APP Class Spin Stabilized	6 Jupiter Orbiter No. 1 APP Class Second-Generation	7 Jupiter Orbiter No. 2 Voyager Class With Multiple Entry Probes
Interplanetary environment Interplanetary atmosphere (scan and probe) Interplanetary environment	1. Interplanetary/planetary science 2. Mars environment, atmos- phere, and surface data (including biological data, if any)	1. Interplanetary particles and fields 2. Jupiter scan	1. Interplanetary exploration 2. Jupiter environment and orbital scan	1. Planetary/interplanetary data 2. Jupiter orbiter/entry probes
14	<25	85 or 95 (Jupiter flyby)	90 to 100	90 to 100
IB/Centaur (or two vehicles on one in V)	Saturn V (two spacecraft per launch)	Atlas/Centaur/TE-364 (C ₃ ≤ 86) or Atlas/Centaur/ HEKS (crowded)	Saturn IB/Centaur/HEKS	Saturn V
9000	20,500	650	2800	16,000
0.4 0.5	0.5 0.5	2.0 -	2.0 0.5	2.0 0.5
1000 1000	1010 600	>5000 200	>7000 300	>14,000 600
9150 50	20,500 1,400	650 -	2800 80	16,000 170
4600	9,650 plus 320 lb for orbit trim	-	1100	6,400
1000	3,000	-	-	1,000
5650	14,370	-	1180	7,570
3500	6,130	650	1620	8,430
250	400	50	250	500
1.52	0.60	-	8.45	8.45
	1.6 x 7	-	1.5 x 32	1.5 x 32
	45 deg	-	0 deg	0 deg
	2.3	-	1.6	1.6
to TRW Mars Voyager the IA Task B, using (stage), but scaled down 10 lb thrust, 9000 lb total weight.	Sun/Canopus oriented. 3-axis stabilized with fixed solar array and gimbaled h.g. antenna dish. Deployed planetary scan platform. Basic spaceframe is octagonal, with liquid propellant retro stage.	Similar to APP spin-stabilized 500 lb spacecraft. Solar panels surrounding 7-ft D dish.	First sun/Canopus oriented; later Earth/Canopus oriented; large fixed antenna. Deployed solar panels.	Same as 6
using sun and Canopus sensors and gas jets. Solid engines and gyros g firing.	3-axis stabilized; requires sun and Canopus sensors, gyro package, possibly Mars sen- sors. TVC by retro engine gimbals. MC maneuvers by throttled retro.	Spin-stabilized. Axis near sun until 1.3 AU, then directed toward Earth. Conical scan RF tracking and jet preces- sion.	3-axis stabilized; gas jets; sun and Canopus sensors plus gyro package. Bias correc- tion for Earth pointing based on signal strength. TVC by jet vanes.	Same as 6
h (29.3 db), double- ended, and 20-w TWT mitter: 0 b/sec at 0.5 AU (enter) b/sec at 1.7 AU (1 year launch)	12-ft paraboloid dish, gimbal mounted. 50-w TWT transmitter 15,000 b/sec at 2.6 AU (end of mission)	7-ft dish (30.9 db), body- mounted, 20-w, Klystron transmitter. 270 b/sec at 6.0 AU.	32-ft dia paraboloid antenna 10-w TWT transmitter 2800 b/sec at 6 AU	Same as 6, except 40-w TWT 11,000 b/sec
s on equipment bays	Louvered equipment mounting panels, aluminized Mylar in- sulation. Thermostatically controlled heaters; thermal control of lander to be included.	Insulation from sun; thermal switches.	Insulation from sun; thermal switches or louvers	Same as 6
panels totaling 140 ft ² .	20-ft dia circular array around retro engine nozzle. Eight fixed modular array plates; 280 ft ²	1 panels (475 ft ² , deployed from perimeter of 7 ft dia rigid antenna and unfolded.	Deployed 8-panel array (each 10 x 10 ft) around sunflower antenna dish. Sequential deployment of solar array and antenna; (must with- stand orbit insertion loads.	Same (but each panel 12.5 x 16 ft)

Table 1. Model Spacecraft
Configurations

orientation of the solar panels away from normal to the sun vector to maintain a maximum 150°C limit. The increased solar intensity near Mercury, of course, compensates for the resultant reduction in effective panel area.

Mission profiles, as shown in Figures 1 through 4, were prepared to show variations in earth-spacecraft and sun-spacecraft distances with mission time. Significant mission events, such as midcourse maneuvers, planetary encounter and orbit insertion, were identified. In addition, the angle between the sun and the earth as viewed from the spacecraft was plotted as a function of mission time. This latter characteristic is particularly significant for the Jupiter missions where both the antenna and solar panels are earth-oriented after reaching a sun-spacecraft distance of approximately 1.3 AU. This permits a significant simplification of the spacecraft in that separate orientation of the solar array and antenna is not required. It can be seen in Figure 4 that the solar array orientation error resulting from this approach is only slightly greater than 10 degrees at Jupiter. In the worst case this produces a solar array power loss of less than 2 percent. The trajectory data presented in Figures 3 and 4 are based on assumed launch dates for the Mars and Jupiter missions. Variations in these data with launch date will chiefly affect the early portion of the sun-spacecraft-earth angle time history, and the late portion of the earth-spacecraft distance time history.

The major interests in the power system analysis for orbital missions are the eclipse time and sunlight time for any given orbit and the variations in these parameters during the assumed 6-month orbital phase of the missions. Detailed analyses of possible orbit parameters for the Venus and Jupiter missions were necessarily beyond the scope of this study. Therefore, orbits were assumed to be in the ecliptic plane for these planets. The Mars orbit selection and resultant eclipse profile were based on analyses performed in the course of TRW's Voyager studies. The orbit parameters and variations in eclipse duration for the Mars and

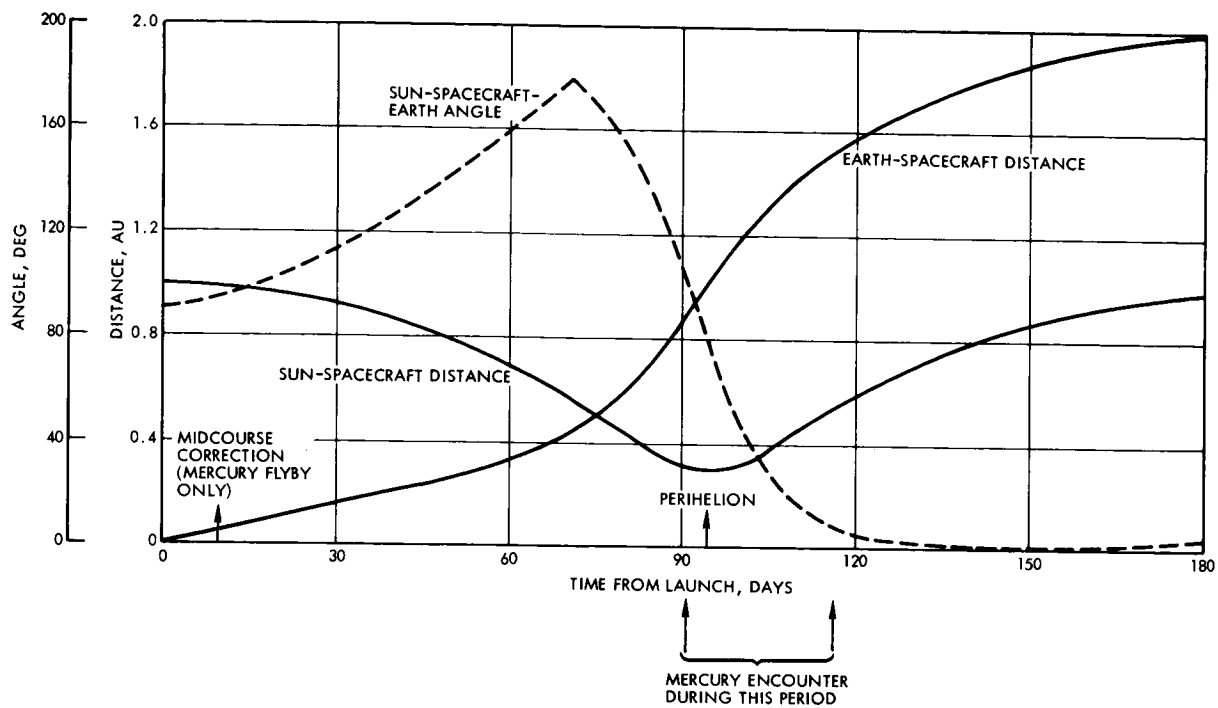


Figure 1. Mission Profile: Mercury Flyby

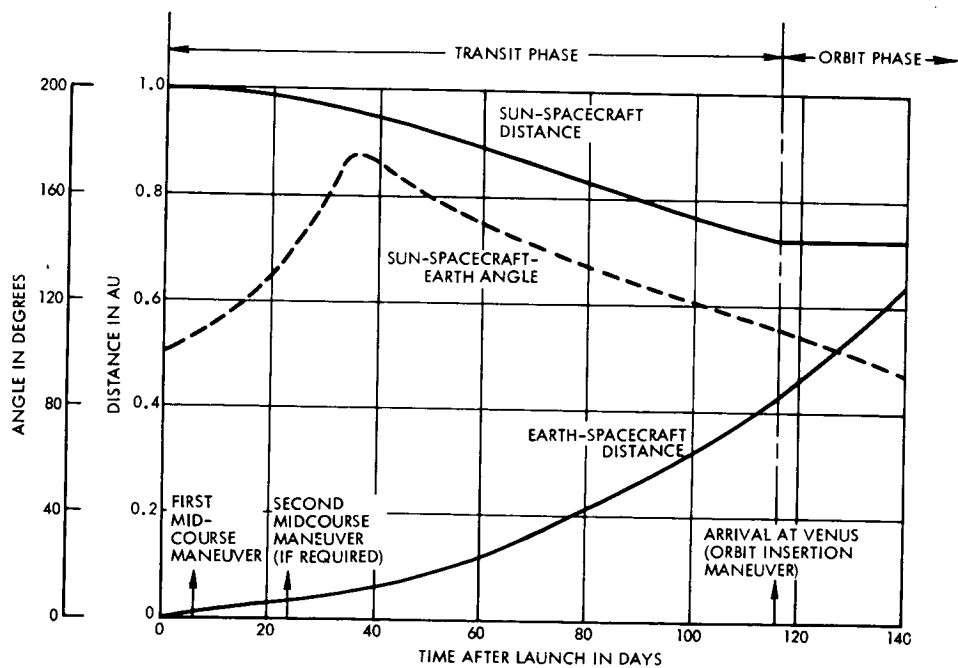


Figure 2. Mission Profile: Venus Orbiter

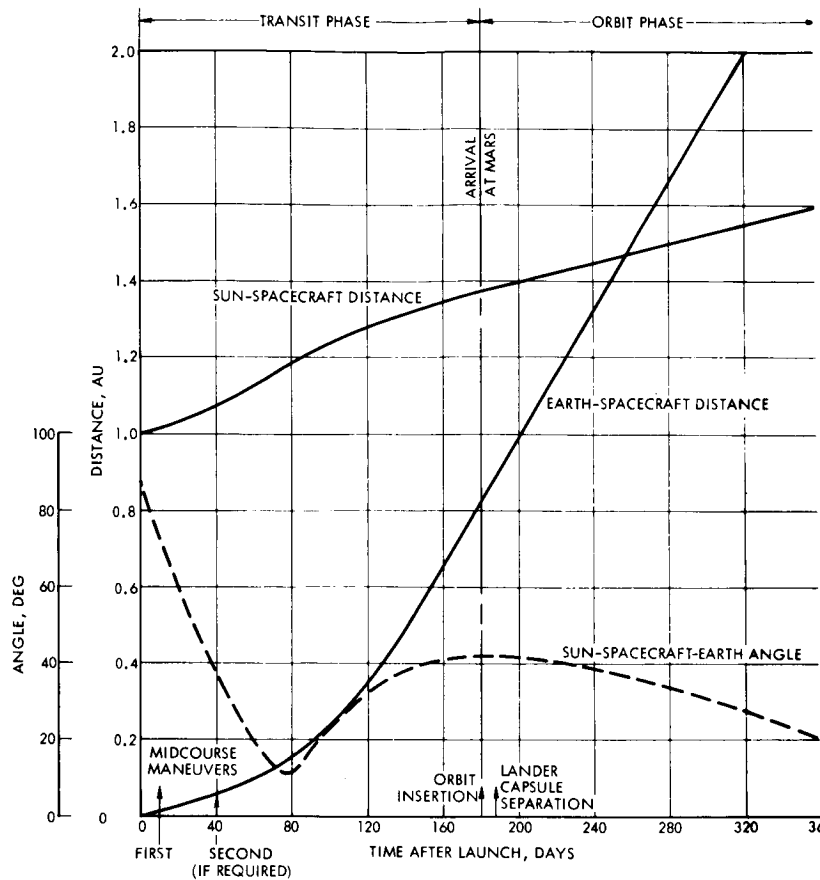


Figure 3. Mission Profile: Mars Orbiter (Launch May 1971)

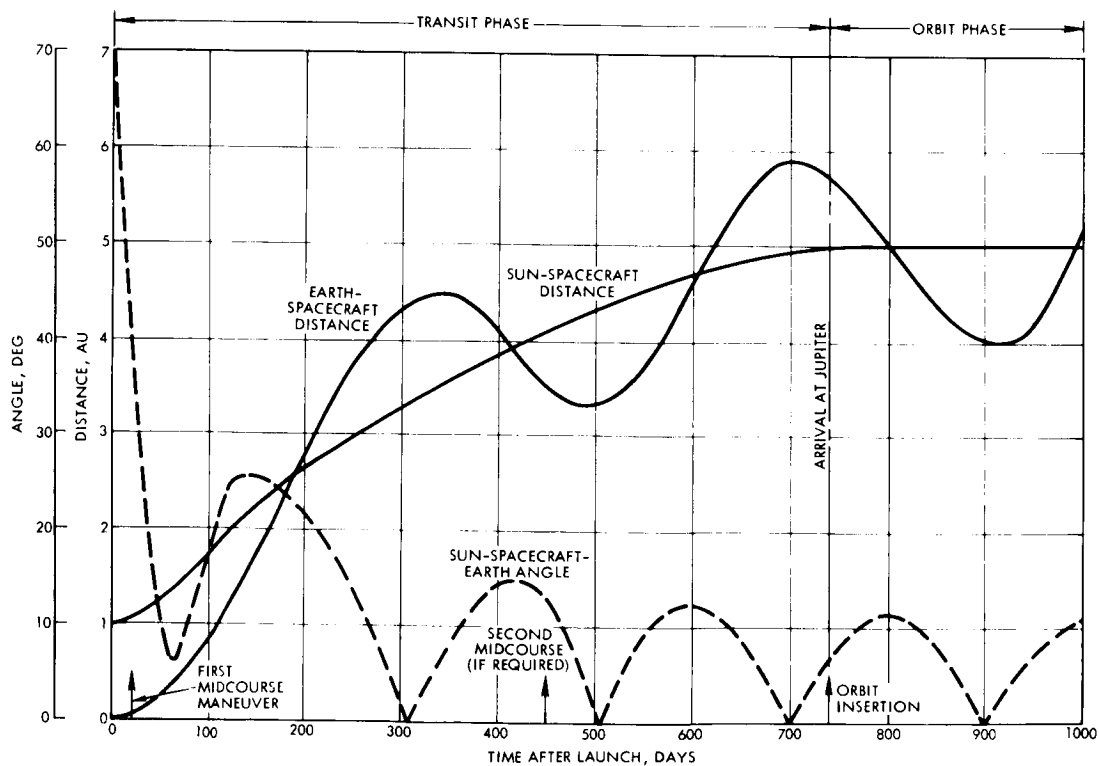


Figure 4. Mission Profile: Jupiter Orbiter (Launch March 1972)

Venus missions are shown in Figures 5 and 6. The parameters for the assumed Jupiter orbit are as follows:

Orbit Period	203 hr
Eclipse Duration	1.6 hr maximum 1.1 hr minimum
Periapsis Altitude	105,000 km
Apoapsis Altitude	2,170,000 km

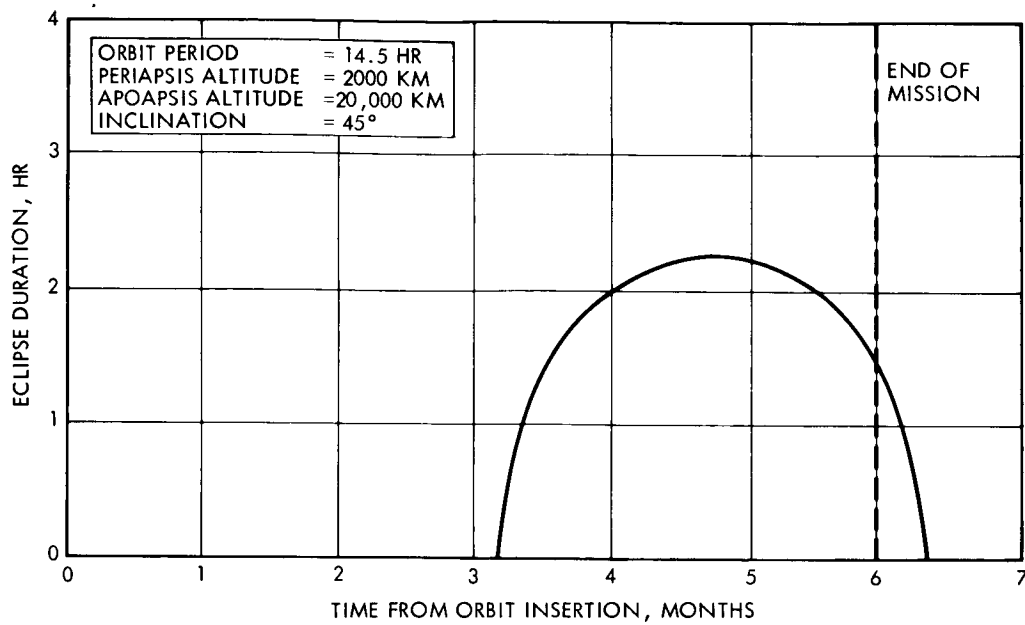


Figure 5. Eclipse Durations for Assumed Mars Orbit

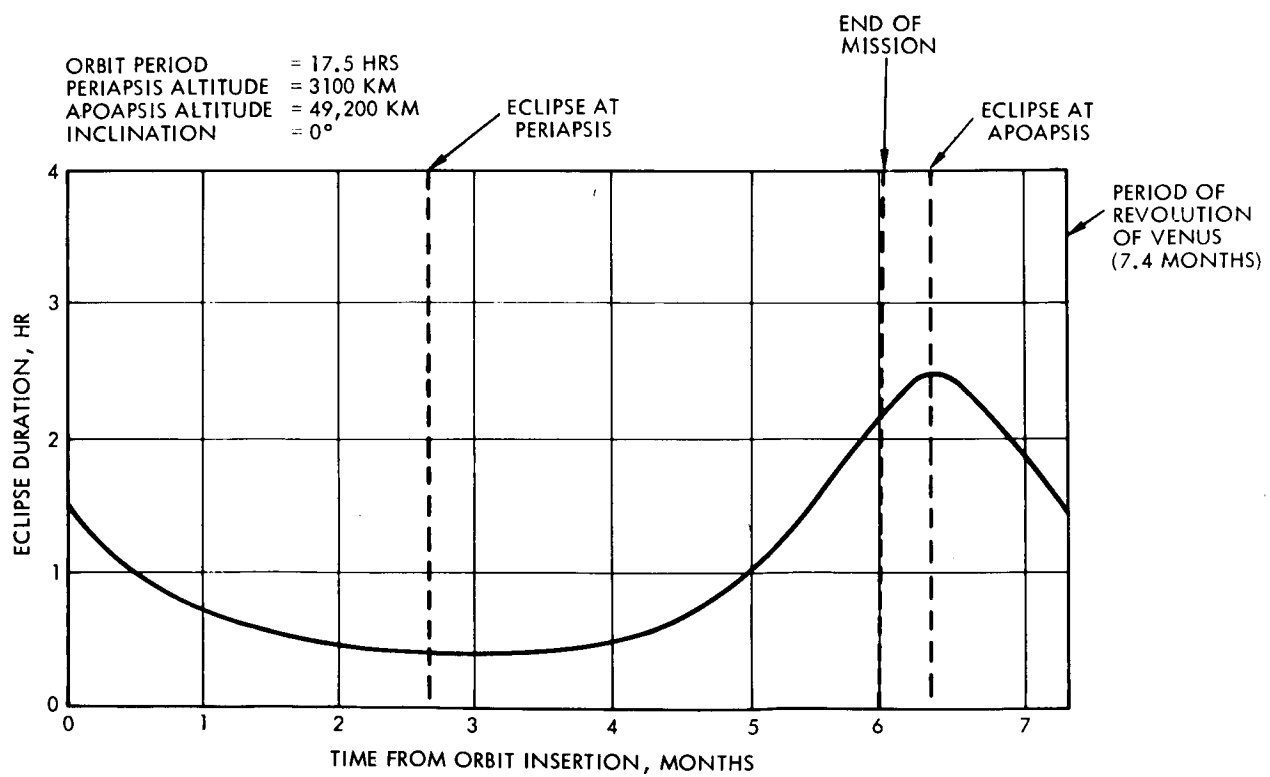


Figure 6. Eclipse Durations for Assumed Venus Orbit

2.2 MODEL POWER REQUIREMENTS

Each of the model spacecraft configurations was analyzed to define typical equipment categories required in each of the subsystems (i. e., stabilization and control, communications and data handling, propulsion, thermal control, and science/payload). These equipment categories were investigated for each model and their power consumption was estimated as a function of mission phase for each case. Selected load power requirements are shown in Tables 2 through 8 for each spacecraft model. These estimates were based primarily on load data from existing spacecraft designs such as Mariner, Pioneer, and Voyager. A significant result of these analyses was the determination that power levels in the largest spacecraft configurations fell in the lower end of the 200- to 4000-w range originally specified for analysis. The investigations of probable scientific experiments to be performed on these missions disclosed that, in most cases, individual equipment power levels of less than 10 w would adequately fulfill the scientific objectives. Television systems requiring approximately 25 w of power constituted the highest single equipment requirement in the science category. Relatively high power requirements for thermal control of lander/probe payloads were assumed for the orbiting spacecraft missions based on the 200-w requirement used in the Voyager studies. In most cases, this requirement represents the largest single load in the spacecraft. A second major power-consuming load is the transmitter required to achieve suitable data rates at the extreme distances being considered in these studies. Use of a 32-ft diameter-paraboloid antenna at the large earth-spacecraft distances encountered in the Jupiter Orbiter No. 2 mission permitted selection of a relatively low power transmitter having a 40-w output rating, and requiring an input power level of 135 w. The largest transmitter considered in these evaluations was a 100-w TWT which was judged to represent a reasonable upper limit on state-of-the-art advancements for flight usage during the 1970 to 1980 time period assumed in the study. The largest transmitter selected, however, is the 50-w TWT used on the Mars Orbiter model. In addition to the TWT, transmitters of the klystron and solid-state types

Table 2. Conditioned Power Requirements (in watts) as Function of Mission Phase - Mercury Flyby Model

LOAD GROUP	EQUIPMENT	PRE-LAUNCH	LAUNCH	ACQUIRE	CRUISE	MANUEVER	ENCOUNT.	PLAYBACK
Stab and Control	Gyros and Electronics	25	25	25	0	25	0	0
	Sensors	4	4	4	4	4	4	4
	Control Elect.	12	12	12	5	25	5	5
	Valves	0	0	0/0/30*	0/0/30	0/1/30	0/0/30	0/0/30
Propulsion	Valves	(Not used for this model)						
Integration	Actuators	(Not used for this model)						
	Comp. Sequencer	5	5	5	5	5	5	5
Thermal Control	Deploy. Actuators	(Not used for this model)						
	Heaters	(Not used for this model)						
	Transmitter **	1	1	1/70/70	70	70	70	70
	Tape Recorder	0	0	0	0	0	6	4
Communications	Data Handling	20	60	20	20	20	20	20
	Cmd. Receiver	5	5	5	5	5	5	5
	Cmd. Decoder	3	3	3	3	3	3	3
	Relay Receiver	(Not used for this model)						
Science/Payload	Lander/Probe	(Not used for this model)						
	TV System	0	0	0	0	0	17	0
	Exp. Pkg. Orient.	0	0	0	0	0	7	0
	Dual Freq. Receiver	0	0	0	2	2	2	2
	Trap. Radiation Det.	0	0	0	1	1	1	1
	Plasma Probe	0	0	0	2	2	2	2
	Spectrophotometer	0	0	0	0	0	25	0
	Magnetometer	0	0	0	7	7	7	7
	IR Radiometer	0	0	0	0	0	3	0
	Cosmic Dust Det.	0	0	0	1	1	1	1
	Cosmic Ray Telescope	0	0	0	1	1	1	1
Total Conditioned Power Ave		75	75	144	126	172	183	130

*Indicates Min/Ave/Max power levels.

** 20 w TWT and driver.

Table 3. Conditioned Power Requirements (in watts) as Function of Mission Phase - Venus Orbiter Model No. 1

LOAD GROUP	EQUIPMENT	PRE-LAUNCH	LAUNCH	ACQUIRE	CRUISE	MANUEVER	INSERTION	ORBIT (SUN)	ORBIT (ECLIPSE)
Stab and Control	Gyros and Electronics	25	25	25	0	25	25	0	25
	Sensors	4	4	4	4	4	4	4	4
Propulsion	Control Elect.	12	12	12	5	25	25	22	22
	Valves	0	0	0/0/30*	0/0/30	0/1/30	0/1/30	0/0/30	0/0/30
Integration	Valves	0	0	0	0	0/2/10	0/2/10	0	0
	Actuators	0	0	0	0	0/10/40	0/35/140	0	0
Thermal Control	Comp. Sequencer	5	5	5	5	5	5	5	5
	Deploy. Actuators		Squibs						
Communications	Heaters **	(Not used for this model)							
	Transmitter **	50	50	50	50	50	50	50	50
Science/Payload	Tape Recorder	0	0	0	0/4/10	0	0	0/4/10	0/4/10
	Data Handling	9	9	34	34	34	34	34	34
	Cmd. Receiver	8	8	8	8	8	8	8	8
	Cmd. Decoder	3	3	3	3	3	3	3	3
	Relay Receiver	(Not used for this model)							
	Antenna Orient.	0	0	0/2/8	0/2/8	0/2/25	0/2/25	0/2/25	0/2/25
	Lander/Probe	(Not used for this model)							
	TV System	(Not used for this model)							
	Exp. Pkg. Orient.	0	0	0	0	0	0	0/1/10	0/1/10
	Dual Freq. Receiver	0	0	0	2	2	2	2	2
	Trap Radiation Det.	0	0	0	1	1	1	1	1
	Plasma Probe	0	0	0	3	3	3	3	3
	UV Photometer	0	0	0	5	5	5	5	5
	Magnetometer	0	0	0	7	7	7	7	7
	IR Radiometer	0	0	0	0	0	0	3	3
	Cosmic Dust Det.	0	0	0	2	2	2	2	2
Total Conditioned Power		116	116	143	135	189	214	156	181

* Indicates Min/Ave/Max power levels.

** 10 w solid state.

Table 4. Conditioned Power Requirements (in watts) as Function of Mission Phase - Venus Orbiter Model No. 2

LOAD GROUP	EQUIPMENT	PRE-LAUNCH	LAUNCH	ACQUIRE	CRUISE	MANUEVER	INSERTION	ORBIT (SUN)	ORBIT (ECLIPSE)	CAPSULE SEPARATE	ORBIT (SUN)	ORBIT (ECLIPSE)
Stab and Control	Gyros and Electronics	25	25	25	0	25	25	0	25	0	0	25
	Sensors	4	4	4	4	4	4	4	4	4	4	4
Propulsion	Control Elect.	9/9/45*	9/9/45	9/9/45	9/9/45	9/9/45	9/9/45	9/9/45	9/9/45	9/9/45	9/9/45	9/9/45
	Valves	0	0	0/0/50	0/0/50	0/1/50	0/1/50	0/0/50	0/0/50	0/0/50	0/0/50	0/0/50
	Valves	0	0	0	0	0/2/15	0/2/15	0	0	0	0	0
	Actuators	0	0	0	0	0/20/80	0/70/280	0	0	0	0	0
Integration	Comp. Sequencer	18	18	18	18	18	18	18	18	18	18	18
	Deploy. Actuators	Squibs	Squibs							Squibs		
Thermal Control	Heaters **	1	1	1/70/70	70	70	70	70	70	70	70	70
	Transmitter **	0	0	0	0/7/12	0/4/12	0/4/12	0/17/60	0/17/60	0/17/60	0/17/60	0/17/60
Communications	Tape Recorder	10	10	40	40	40	40	40	40	40	40	40
	Data Handling	8	8	8	8	8	8	8	8	8	8	8
	Cmd. Receiver	3	3	3	3	3	3	3	3	3	3	3
	Cmd. Decoder	0	0	0	0	0	0	0	0	0	0	0
Science/Payload	Relay Receiver	0	0	0	0	0	0	0	0	0	0	0
	Antenna Orient.	0	0	0/2/15	0/2/15	0/3/40	0/3/40	0/3/40	0/3/40	0/3/40	0/3/40	0/3/40
	Lander/Probe	0	0	0/200/200	200	200	200	200	200	0/200/200	0/200/200	0/200/200
	TV System	0	0	0	0	0	0	15	15	15	15	15
	Exp. Pkg. Orient	0	0	0	0	0	0	1/2/20	1/2/20	1/2/20	1/2/20	1/2/20
	Spectrometers (2)	0	0	0	0	0	0	30	30	30	30	30
	Bistatic Radar	0	0	0	0	0	0	3	3	3	3	3
	IR Radiometer	0	0	0	0	0	0	14	14	14	14	14
	Magnetometer (2)	0	0	0	6	6	9	9	9	3	3	3
	Ion Chamber	0	0	0	4	4	4	4	4	4	4	4
	Cosmic Ray Telescope	0	0	0	5	5	5	5	5	5	5	5
	Trap. Radiation Det	0	0	0	5	5	5	5	5	5	5	5
	Gamma Ray	0	0	0	5	5	5	5	5	5	5	5
	Plasma Probe	0	0	0	5	5	5	5	5	5	5	5
	Cosmic Dust Det.	0	0	0	2	2	2	2	2	2	2	2
		78	78	379	393	439	492	471	496	440	267	292
Total Conditioned Power												

* Indicates Min/Ave/Max power levels.

** 20 w TWT and driver.

Table 5. Conditioned Power Requirements (in watts) as Function of Mission Phase - Mars Orbiter Model

LOAD GROUP	EQUIPMENT	PRE-LAUNCH	LAUNCH	ACQUIRE	CRUISE	MANUEVER	INSERTION	ORBIT (SUN)	SEPARATE LANDER	ORBIT (SUN)	ORBIT (ECLIPSE)
Stab and Control	Gyros and Electronics	25	25	25	0	25	25	0	0	0	25
	Sensors	4	4	4	4	4	4	4	4	4	4
Propulsion	Control Elect.	9/9/45*	9/9/45	9/9/45	9/9/45	9/9/45	9/9/45	9/9/45	9/9/45	9/9/45	9/9/45
	Valves	0	0	0/0/50	0/0/50	0/0/50	0/0/50	0/0/50	0/0/50	0/0/50	0/0/50
	Valves	0	0	0	0	0/2/15	0/2/15	0	0	0	0
	Actuators	0	0	0	0	0/20/80	0/70/280	0	0	0	0
Integration	Comp. Sequencer	18	18	18	18	18	18	18	18	18	18
	Deploy. Actuators		Squibs						Squibs		
Thermal Control	Heaters	0	5	15	44	54	54	34	34	34	54
	Transmitter**	5	5	5/150/150	150	150	150	150	150	150	150
	Tape Recorder	0	0	0	0/4/12	0/4/12	0/17/60	0/17/60	0/17/60	0/17/60	0/17/60
	Data Handling	10	10	40	40	40	40	40	40	40	40
Science/Payload	Cmd. Receiver	8	8	8	8	8	8	8	8	8	8
	Cmd. Decoder	3	3	3	3	3	3	3	3	3	3
	Relay Receiver	0	0	0	0	0	0	0	0	0	0
	Lander/Probe	0	0	0/20/40	200	200	200	200	0/200/200	—	—
	TV System	0	0	0	0	0	0	26	26	26	26
	Exp. Pkg. Orient.	0	0	0	0	0	0	1/2/20	1/2/20	1/2/20	1/2/20
	Spectrometer (2)	0	0	0	0	0	0	30	30	30	30
	Radiometer	0	0	0	0	0	0	14	14	14	14
	Magnetometer	0	0	0	6	6	9	9	3	3	3
	Micrometeoroid	0	0	0	2	2	2	2	2	2	2
	Plasma Probe	0	0	0	5	5	5	5	5	5	5
	Trap. Radiation Det.	0	0	0	5	5	5	5	5	5	5
	Cosmic Ray (2)	0	0	0	10	10	10	10	10	10	10
	Bistatic Radar	0	0	0	0	0	0	3	3	3	3
	RF Noise Det.	0	0	0	3	3	3	3	3	3	3
	Ion Chamber	0	0	0	5	5	5	5	5	5	5
	Total Conditioned Power Ave	82	87	472	516	570	627	597	593	393	438

*Indicates Min/Ave/Max power levels.

** 50 w TWT and driver.

Table 6. Conditioned Power Requirements (in watts) as Function of Mission Phase - Jupiter Flyby Model

LOAD GROUP	EQUIPMENT	PRE-LAUNCH	LAUNCH	ACQUIRE	CRUISE	MANEUVER	ENCOUNT	PLAYBACK
Stab and control	Gyros and Electronics	(Not used for this model)						
	Sensors (sun)	(Negligible power consumption)						
	Control Elect.	5	5	5	5	5	5	5
	Valves	0	0	0/0/6*	0/0/6	0/0/6	0/0/6	0/0/6
Propulsion	Valves	0	0	0	0	Squibs	0	0
Integration	Actuators	(Not used for this model)						
	Comp Sequencers	5	5	5	5	5	5	5
	Deploy. Actuators		Squibs					
Thermal Control	Heaters	0	0	0	0/10/50	0	50	50
	Transmitter **	1	1	1/80/80	80	80	80	80
	Tape Recorder	0	0	0	0	0	6	4
	Data Handling	10	10	10	10	10	10	10
Communications	Cmd Receiver	2	2	2	2	2	2	2
	Cmd Decoder	2	2	2	2	2	2	2
	Relay Receiver							
	Antenna Orient.	(Not used for this model)						
Science/Payload	Lander/Probe							
	TV System	0	0	0	0	0	17	0
	Exp. Pkg. Orient.	0	0	0	0	0	7	0
	Magnetometer	0	0	0	4	4	4	4
	Trap. Radiation Det	0	0	0	2	2	2	2
	Plasma Probe	0	0	0	2	2	2	2
	Cosmic Dust	0	0	0	1	1	1	1
	Dual Freq Rec	0	0	0	2	2	2	2
	Radiometer, IR	0	0	0	7	7	7	7
	Cosmic Ray (2)	0	0	0	4	4	4	4
Total Conditioned Power		25	25	104	136	136	206	180

* Indicates Min/Ave/Max power levels.

** 20 w klystron and driver

Table 7. Conditioned Power Requirements (in watts) as Function of Mission Phase - Jupiter Orbiter Model No. 1

LOAD GROUP	EQUIPMENT	PRE-LAUNCH	LAUNCH	ACQUIRE	CRUISE	MANUEVER	INSERTION	ORBIT (SUN)	ORBIT (ECLIPSE)
Stab and Control	Gyros and Electronics	25	25	25	0	25	25	0	25
	Sensors	4	4	4	4	4	4	4	4
Propulsion	Control Elect.	12	12	12	5	25	25	22	22
	Valves	0	0	0/0/30*	0/0/30	0/1/30	0/1/30	0/1/30	0/0/30
Integration	Valves	0	0	0	0	0/2/20	0/4/20	0	0
	Actuators	0	0	0	0	0/6/12	0/6/12	0	0
Thermal Control	Comp. Sequencer	5	5	5	5	5	5	5	5
	Deploy. Actuators		Squibs						
Communications	Heaters	0	5	20	100	100	100	100	150
	Transmitter**	1	1	1/35/35	35	35	35	35	35
Science/Payload	Tape Recorder	0	0	0	0/4/10	0	0	0/4/10	0/4/10
	Data Handling	9	9	34	34	34	34	34	34
	Cmd. Receiver	8	8	8	8	8	8	8	8
	Cmd. Decoder	3	3	3	3	3	3	3	3
	Relay Receiver	(Not used for this model)							
	Lander/Probe	(Not used for this model)							
	RV System	0	0	0	0	0	0	15	15
	Exp. Pkg. Orient.	0	0	0	0	0	0	1/2/20	1/2/20
	Cosmic Ray (2)	0	0	0	4	4	4	4	4
	Plasma Probe	0	0	0	2	2	2	2	2
	Magnetometer	0	0	0	6	6	6	6	6
	Micrometeoroid	0	0	0	1	1	1	1	1
	Radio Propagation	0	0	0	3	3	3	3	3
	Trap. Radiation Det.	0	0	0	2	2	2	2	2
	IR Radiometer	0	0	0	0	0	0	3	3
	Auroral Detector	0	0	0	0	0	0	2	2
Total Conditioned Power Ave		67	72	146	216	266	268	255	330

* Indicates Min/Ave/Max power levels.

** 10 w TWT and driver.

Table 8. Conditioned Power Requirements (in watts) as Function of Mission Phase - Jupiter Orbiter Model No. 2

LOAD GROUP	EQUIPMENT	PRE-LAUNCH	LAUNCH	ACQUIRE	CRUISE	MIDCOURSE MANEUVER	ORBIT INSERTION	ORBIT (SUN)	ORBIT (ECLIPSE)	SEPARATE PROBE	TRACK PROBES	ORBIT (SUN)	ORBIT (ECLIPSE)
Subband Control	Gyros and Electronics	25	25	2	0	25	25	0	25	0	0	0	25
	Sensors	4	4	4	4	4	4	4	4	4	4	4	4
	Control Elect.	10	10	10/10/50*	10/10/50	10/10/50	10/10/50	10/10/50	10/10/50	10/10/50	10/10/50	10/10/50	10/10/50
	Valves	0	0	0/0/50	0/0/50	0/1/50	0/1/50	0/0/50	0/0/50	0/0/50	0/0/50	0/0/50	0/0/50
Propulsion	Valves	0	0	0	0	0/4/25	0/8/25	0	0	0	0	0	0
	Actuators	0	0	0	0	0/8/15	0/8/15	0	0	0	0	0	0
Integration	Comp Sequencer	20	20	20	20	20	20	20	20	20	20	20	20
	Deploy. Actuators		Squibs							Squibs			
Thermal Control	Heaters	0	0	0	200	200	200	200	250	200	200	200	250
	Transmitter**	5	5	5/135/135	135	135	135	135	135	135	135	135	135
	Tape Recorder	0	0	0	0/4/12	0/4/12	0/4/12	0/17/60	0/17/60	0/17/60	0/17/60	0/17/60	0/17/60
	Data Handling	10	10	40	40	40	40	40	40	40	40	40	40
Communications	Cmd Receiver	8	8	8	8	8	8	8	8	8	8	8	8
	Cmd Decoder	5	5	5	5	5	5	5	5	5	5	5	5
	Relay Receiver	0	0	0	0	0	0	0	0	2	2	2	2
	Antenna Orient		(Not used for this model)										
Science/Payload	Lander/Probe	0	0	0/150/150	150	150	150	150	150	150	0***	0***	0***
	TV System	0	0	0	0	0	0	26	26	26	26	26	26
	Exp Pkg Orient	0	0	0	0	0	0	2/4/40	2/4/40	2/4/40	2/4/40	2/4/40	2/4/40
	Cosmic Ray (2)	0	0	0	10	10	10	10	10	10	10	10	10
	Plasma Probe	0	0	0	5	5	5	5	5	5	5	5	5
	Magnetometers (2)	0	0	0	6	6	9	3	3	3	3	3	3
	Micrometeoroid	0	0	0	2	2	2	2	2	2	2	2	2
	Radio Propagation	0	0	0	3	3	3	3	3	3	3	3	3
	Trap Radiation	0	0	0	5	5	5	5	5	5	5	5	5
	Radiometers (2)	0	0	0	6	0	0	20	20	20	20	20	20
	Auroral Detector	0	0	0	0	0	0	2	2	2	2	2	2
	Spectrometer	0	0	0	0	0	0	15	15	15	15	15	15
	Topside Sounder	0	0	0	0	0	0	3	3	3	3	3	3
	Total Conditioned Power (Ave)		87	397	611	645	657	685	762	689	539/689	532	614

* Indicates Min/Ave/Max power levels

** 40 w TWT and driver

*** Average power decreases to zero with separation of last probe

were assumed for the Jupiter Flyby and Venus Orbiter No. 1 models respectively to reflect a broader spectrum of input power characteristics for the subsequent power system analyses.

The various load equipment groupings were analyzed further to ascertain their typical input voltage levels and voltage regulation requirements after power conditioning. In these investigations of representative voltage levels, the data for a large number of existing equipment designs were evaluated. These data were derived principally from the Mariner, Pioneer, OGO, Vela and Intelsat programs. In selecting voltages and regulation levels, considerable attention was given to the results of previous studies* which indicated the desirability of standardizing secondary voltage requirements of spacecraft systems. As a result, equipments were categorized and standardized voltages were selected for each. The advantages of such standardization are apparent in terms of the possibilities it affords for centralizing power conditioning equipment and thereby improving power system reliability, efficiency and weight. Obviously not all spacecraft load equipment can make use of such standardized voltages. A common exception is that of TWT transmitters. Certain experiments similarly require high voltages that are automatically excluded from any standardized secondary scheme. Low voltage requirements of less than 6 v should also be excluded from any centralized power distribution or power conversion configuration due to the significant losses that would be imposed on the system by trying to distribute these low voltages. Table 9 lists the selected voltages, regulation levels and apportionment of total power requirements among the several voltages for each item of load equipment or each group of equipment.

Consideration was given to the increased use of integrated circuits in newer equipment designs, particularly in the areas of control systems and data handling equipment. This was reflected in an increase in the percentage of total input power utilized at the lower voltage levels in comparison to that of earlier equipment designs. For each equipment category, the input power was apportioned among the required input voltages. These data, together with the load requirements data, define the required outputs of the power subsystem for each model spacecraft.

* Study and Analysis of Satellite Power Systems Configurations for Maximum Utilization of Power, Contract NAS5-9178.

Table 9. Load Equipment Typical Input Power Characteristics

<u>Equipment</u>	<u>Typical Voltages (volts)</u>	<u>Typical Regulation \pm(%)</u>	<u>Percent of Total Power</u>	<u>Remarks</u>
<u>Stabilization and Control</u>				
Gyros and electronics	26 ac	2	90	400 cps $\pm 0.01\%$, 3 ϕ
	+20	1	5	
	-20	1	5	
Star or sun sensor	20	1	100	
Control electronics	+20	2	5	
	-20	2	5	
	+15	1	20	
	-15	1	20	
	+6	1	25	
	-6	1	25	
Solenoid valves	bus	15	100	Peak only
Motor	bus	15	100	400 cps or dc
Heater	bus	15	100	
<u>Propulsion</u>				
Valve	bus	10 v min	100	Peak only
Solenoid	bus	15	100	Peak only
Heater	bus	15	100	
<u>Computer and Sequencer</u>				
	16	0.5	5	
	-16	0.5	5	
	+6	2	45	
	-3	2	45	
<u>Transmitters</u>				
10 w, solid state transmitter				
Driver	+6	1	5	
	-6	1	5	
Power amplifier	50	2	60	
	+15	1	5	
	-15	1	5	

Table 9. Load Equipment Typical Input Power Characteristics (Continued)

<u>Equipment</u>	<u>Typical Voltages (volts)</u>	<u>Typical Regulation ±(%)</u>	<u>Percent of Total Power</u>	<u>Remarks</u>
Thermoelectric cooler	+6	5	20	
20 w, Klystron transmitter				
Driver	+6 -6	1 1	5 5	
Klystron beam	1500	1	70	
Klystron heater	6	2	20	ac or dc
50 w, TWT transmitter				
Driver	+6 -6	1 1	5 5	
TWT helix	1500	0.2	70	
TWT collector	300	1	10	
TWT heater	6	1	10	dc
100 w, TWT transmitter				
Driver	16 6 -6	1 1 1	10	
TWT helix	3000	0.2	10	
TWT collector	800	1	60	
TWT heater	6	1	20	ac or dc
<u>Communications and Data Systems</u>				
Tape recorder	bus 16	2 1	50 50	
Data handling	bus -6 16 -16 +6 -6 16 -16	5 2 2 2 1 1 1 1	4 4 4 4 29 26 25 4	

Table 9. Load Equipment Typical Input Power Characteristics (Continued)

<u>Equipment</u>	<u>Typical Voltages (volts)</u>	<u>Typical Regulation \pm(%)</u>	<u>Percent of Total Power</u>	<u>Remarks</u>
Antenna deployment (squibs)	bus	15	0	Peaks only
Antenna orientation	bus 16	15 1	95 5	ac or dc
Receiver	bus +16 +6 -6	15 1 1 1	10 40 10 40	
Decoder	16 6 -6	2 2 2	20 40 40	
Switching and distribution	bus	5	0	Peaks only
<u>Science</u>				
Radio propagation	16 6 -6	1 0.1 0.1	40 30 30	
Whistlers	16	0.1	100	
Magnetometer	16 -16 6 -6 3	0.1 1 0.1 1 1	30 15 30 15 10	
Plasma probe	\pm 150 +6 165	1 1 1	30 65 5	
Coronagraph	3000 +16 -16 +6 -6	1 0.1 0.1 0.1 0.1	80 5 5 5 5	
Proton spectrometer	1000 +6 -6 +3 -3 -16	0.1 1 0.1 1 1 1	15 40 15 10 10 10	

Table 9. Load Equipment Typical Input Power Characteristics (Continued)

<u>Equipment</u>	<u>Typical Voltages (volts)</u>	<u>Typical Regulation \pm (%)</u>	<u>Percent of Total Power</u>	<u>Remarks</u>
Mass spectrometer	bus	5	25	
	3000	1	50	
	200	1	25	
	16	1		
	-16	1		
	+6	1		
	-6	1		
Cosmic ray	1000	0.1	50	
	16	1	30	
	6	1	20	
Ion chamber	6	1	100	
Scintollometer	1000	0.1	20	
	16	1	50	
	6	1	30	
Gamma ray	1000	0.1	10	
	16	0.1	90	
X-ray	1000	0.1	10	
	16	0.1	90	
Primary electrons	1500	0.1	20	
	16	0.5	50	
	3	2	30	
Micrometeorite	+12	1	60	
	-6	1	20	
	+3	1	20	
Television (ES vidicon)	500	0.2	5	Peaks only
	200	1	20	
	bus	5	0	
	+16	1	10	
	-16	1	5	
	+6	5	50	
	-6	0.2	10	
Probe/Lander	bus	15	100	Thermal control

Table 9. Load Equipment Typical Input Power Characteristics (Continued)

<u>Equipment</u>	<u>Typical Voltages (volts)</u>	<u>Typical Regulation \pm (%)</u>	<u>Percent of Total Power</u>	<u>Remarks</u>
Trapped radiation	1000	0.1	20	
	16	1	20	
	+6	1	30	
	-6	1	30	
IR radiometer (4 ch)	bus	2	20	Scanner
	6	1	40	
	-6	1	40	
UV spectrometer	bus	2	25	Scanner
	16	1	25	
	6	1	25	
	-6	1	25	
RF noise detector	+6	1	50	
	-6	1	50	
UV photometer	3000	1	70	
	35	1	10	
	± 20	1	10	
	± 10	1	10	
Bistatic radar	1500	1	70	
	+6	1	20	
	-6	1	10	

3. BASELINE POWER SYSTEM CONFIGURATIONS

3.1 POWER SYSTEM SYNTHESIS

The investigations and selection of candidate power system configurations for analysis were based on progression from generalized system concepts to specific baseline implementations as shown in the flow diagram, Figure 7. Initially, all photovoltaic power systems were divided into two generalized concepts as shown in Figure 8. From these two concepts, the basic functional power system configurations in Figure 9 were developed. These five functional system approaches were used to determine baseline system configurations by selecting specific designs for each functional element of each basic configuration.

In Figure 8, the first generalized concept combines the battery and solar array outputs at an unregulated bus with suitable controls. The unregulated bus supplies line regulation and power conditioning equipment which, in turn, supplies the regulated outputs of the system. The unregulated bus also can directly supply certain spacecraft loads such as heaters and solenoids. The second approach employs regulators for both the solar array and battery to permit their electrical connection to a regulated dc bus which supplies the load power conditioning equipment and direct connected loads.

The five basic functional configurations of Figure 9 were selected on the basis of their compatibility with the variations in load and solar array characteristics encountered during the interplanetary missions under consideration. In each system configuration, specific functions are identified which satisfy the regulation requirements of the applicable generalized concept. For generalized Configuration 1, the three alternative approaches to accomplish the line regulation function are shown. In general, voltage boosting (Configuration 1A) tends to minimize regulation losses at maximum sun-spacecraft distance (AU).

Figure 10A shows a simplified comparison of the current voltage characteristics of the solar array at minimum and maximum AU, with an assumed constant power load and the resultant operating points of the system. With the minimum AU solar array, the system will operate at

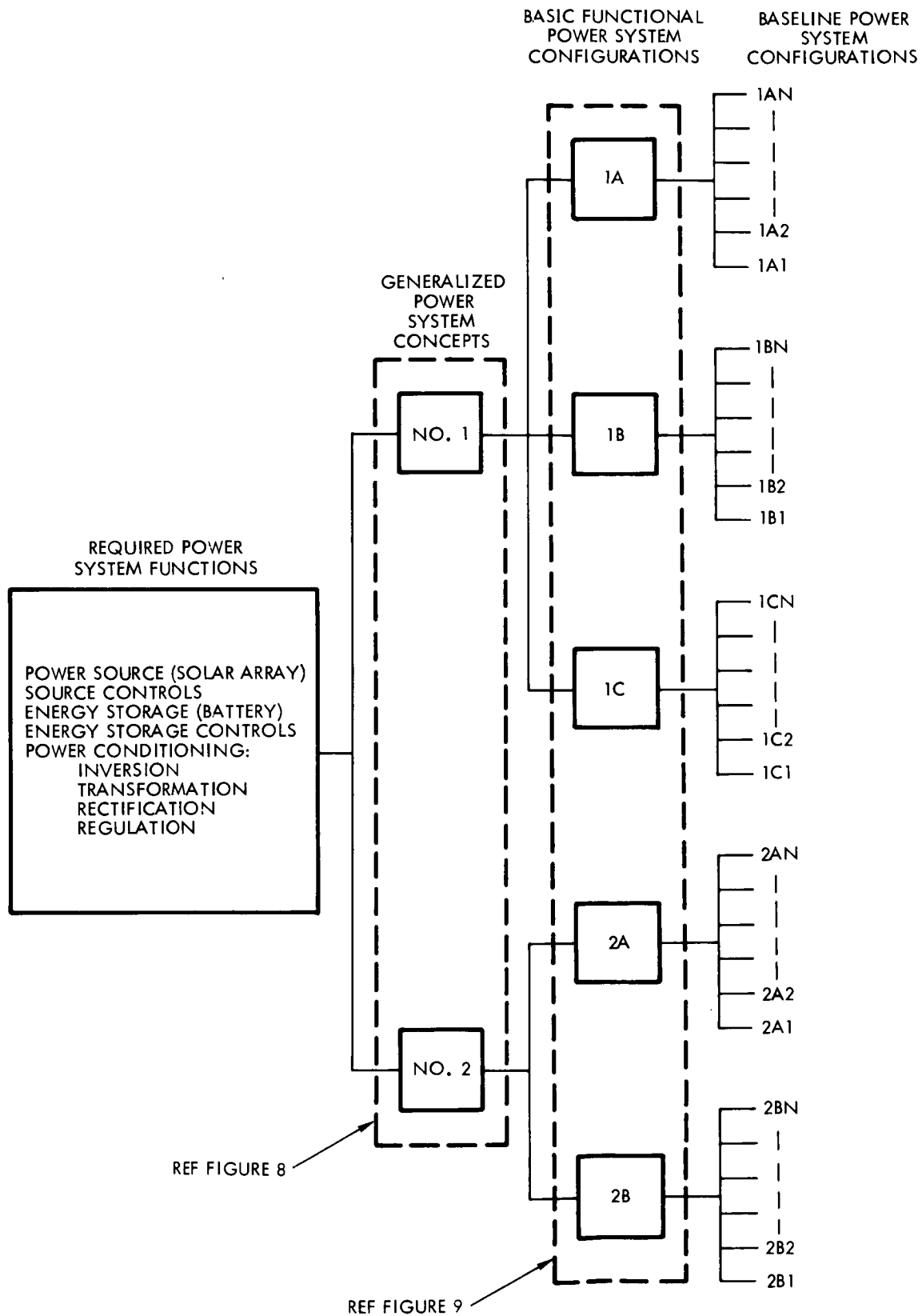


Figure 7. Flow Diagram - Baseline System Configuration Analysis

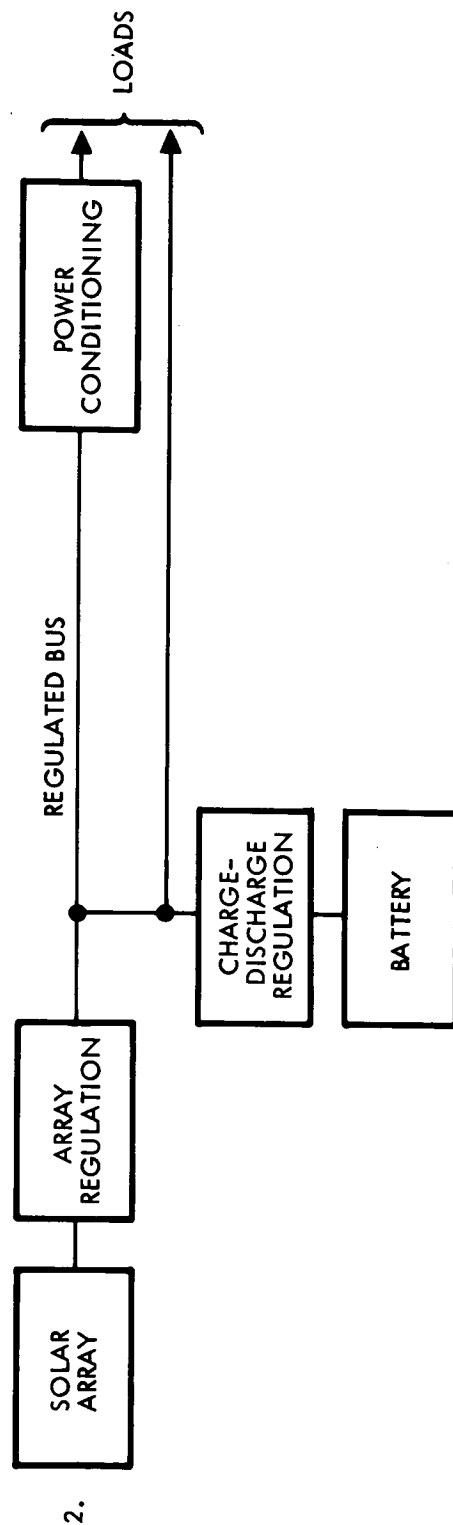
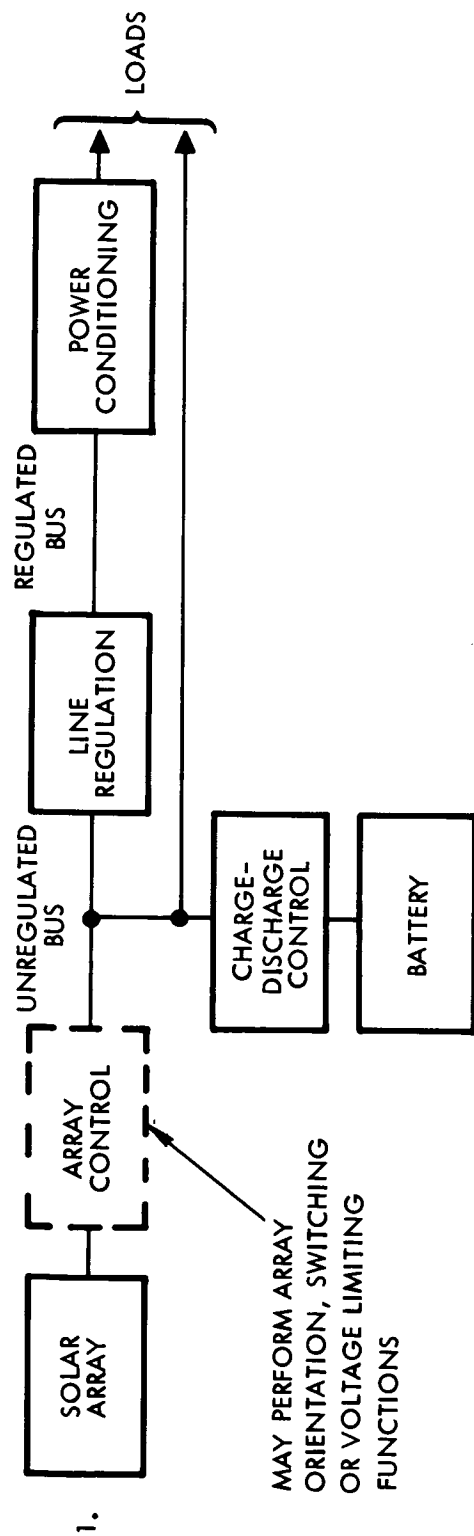


Figure 8. Generalized Power System Concepts

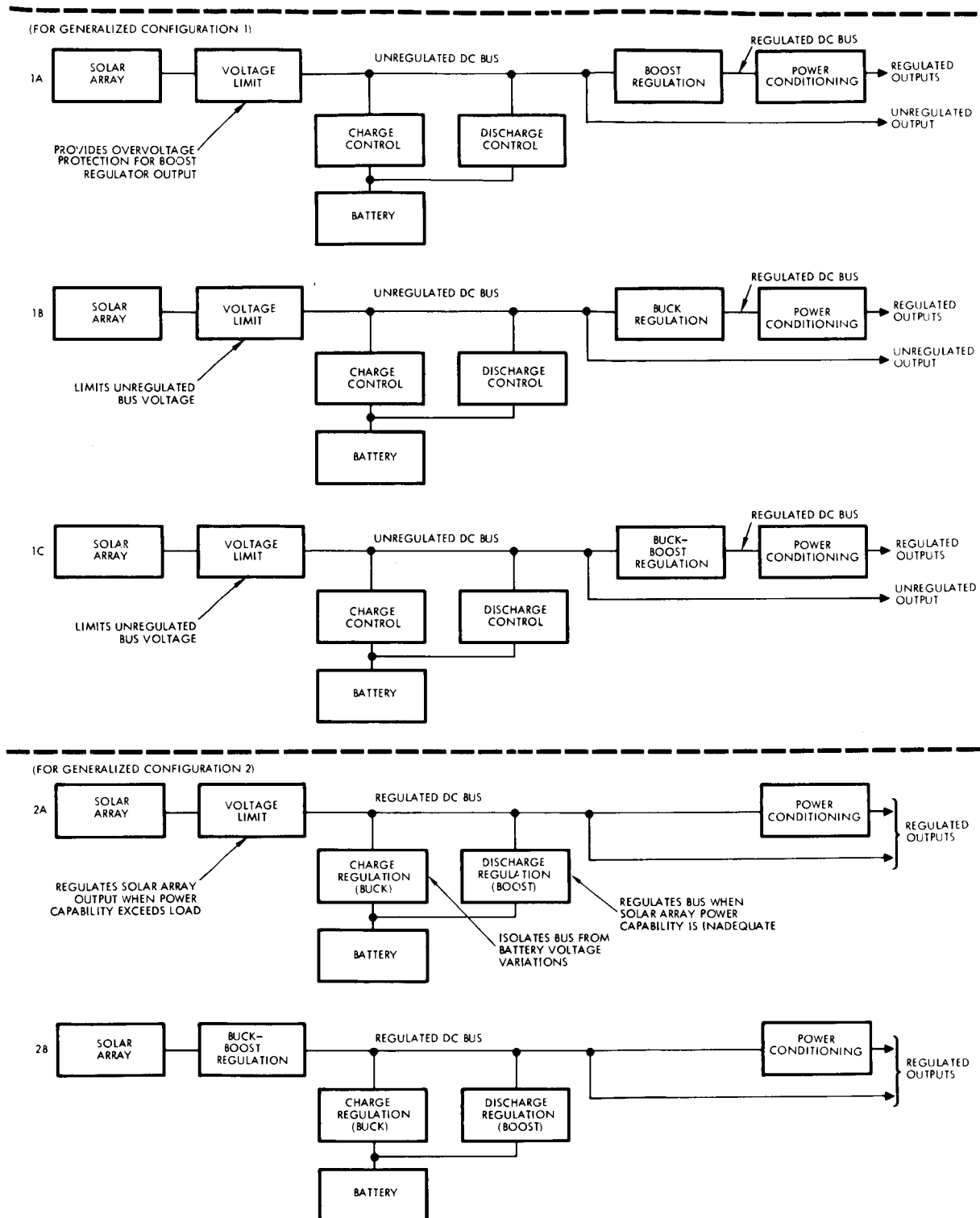
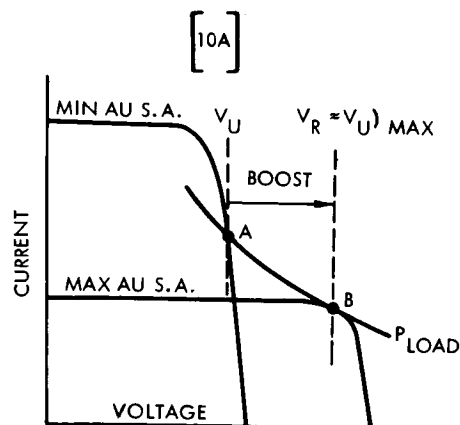
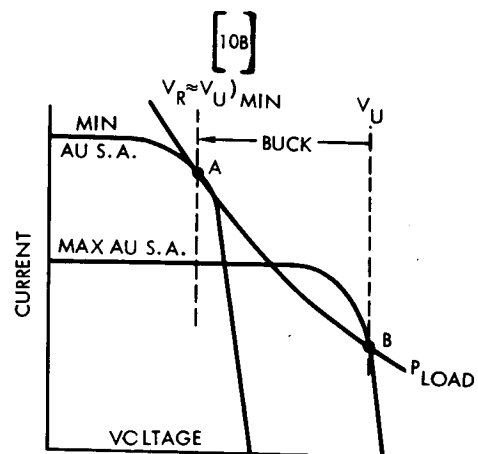


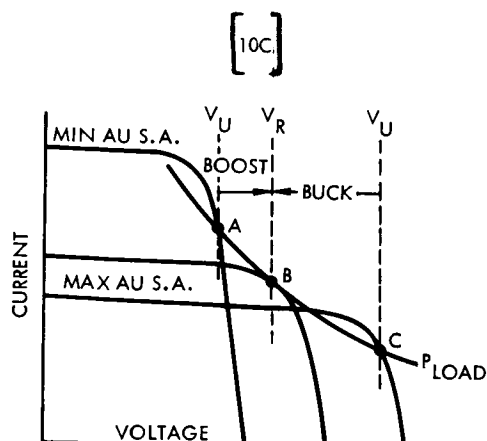
Figure 9. Basic Functional Power System Configurations



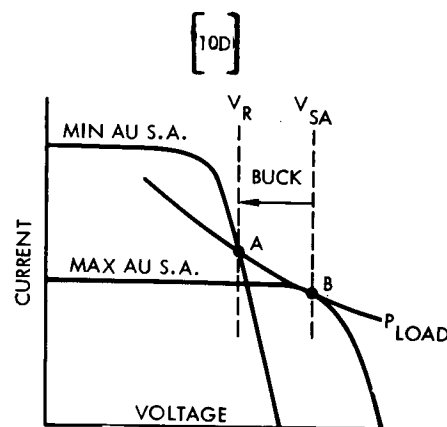
CONFIGURATION 1A
OPTIMIZED FOR MAX AU
(REQUIRES VOLT LIMIT ON SOLAR
ARRAY TO PREVENT $V_U > V_R$)



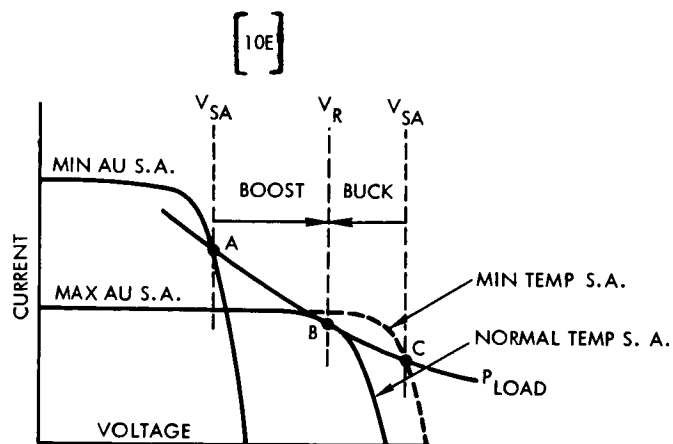
CONFIGURATION 1B
OPTIMIZED FOR MIN AU
(V_U MUST ALWAYS BE
GREATER THAN V_R)



CONFIGURATION 1C
OPTIMIZED FOR INTERMEDIATE
VALUE OF AU



CONFIGURATION 2A
OPTIMIZED FOR MAX AU



CONFIGURATION 2B
OPTIMIZED FOR MAX AU

V_U = UNREGULATED BUS VOLTAGE
 V_R = REGULATED BUS VOLTAGE
 V_{SA} = SOLAR ARRAY VOLTAGE

Figure 10. Simplified System Operating Points for Basic
Functional Power System Configurations

point A yielding an unregulated bus voltage V_U . The line booster then will increase this voltage to the regulated voltage V_R , with the boost regulator compensating for the reduced solar-array voltage capability at minimum AU due to the higher operating temperature. It is possible to set the regulated voltage V_R at or near the maximum power point of the solar array at maximum AU. This then would tend to permit the design of the array to support the required load at its maximum power point at the maximum AU conditions. As a result, the amount of voltage boosting required in the line regulator will be minimized at this condition, and result in a maximum line regulator efficiency. With this approach, a load reduction under maximum AU conditions would result in an overvoltage of the regulated bus. Therefore, a voltage limiter is required on the solar array to prevent this.

The use of the bucking line regulator (Configuration 1B of Figure 9) tends to minimize series losses in the line regulator at minimum AU conditions. Applying this approach, Figure 10B indicates that the regulator voltage can usually be selected at the maximum power point of the solar array at minimum AU conditions. The increased solar array voltage capability at increased AU value will produce a higher unregulated bus voltage corresponding to the operating Point B, shown in Figure 10B. The series line regulator will buck this voltage down to the proper regulated value. Maximum efficiency in the line regulator again will occur when the voltage drop across the line regulator is minimized, as represented by operating Point A. In contrast to the boost regulator approach described above, the bucking line regulator approach does not require a voltage limiter on the solar array. The voltage limiting of the array, however, may be required to prevent overvoltage on the unregulated bus when loads are energized directly from that bus.

The buck-boost line regulator (Configuration 1C of Figure 9) can be optimized with respect to line regulator efficiency at any selected value of AU. Figure 10C represents a hypothetical case where the solar array power capability at both minimum and maximum AU exceeds that at an intermediate value. Again a fixed constant power load is assumed, and by selecting the regulated bus voltage to correspond to operating Point B, maximum regulator efficiency will be achieved. As in the case of the

buckling line regulator, the buck-boost approach does not require the voltage limiting of the solar array in order to maintain the regulated bus voltage. Such voltage limiting may be required, however, to limit the maximum unregulated bus voltage in accordance with the requirements of the loads energized directly from the unregulated bus. The buck-boost approach would also permit optimizing the system with respect to line regulator efficiency at minimum AU or maximum AU as in the preceding two cases.

Figure 9 also shows two alternative approaches to provide the solar array regulation function for generalized Configuration 2. The voltage-limiting approach of Configuration 2A requires that the regulated bus voltage be selected at or below the minimum steady-state voltage of the array. This approach is similar to Configuration 1B in Figure 9, as it minimizes system losses at minimum AU. The operating conditions shown in Figure 10B would therefore apply, with the exception that the unregulated bus voltage would become the solar array voltage.

Figure 10D illustrates the use of this system configuration when the maximum AU solar array power capability is less than that at minimum AU. This reflects a situation where it is desirable to maximize the regulated bus voltage, to minimize the losses in the array regulator and similarly to operate the maximum AU solar array as close as possible to its maximum power point. Theoretically, with this system and a given constant power load, the operating points indicated as A and B can be achieved at minimum and maximum AU, respectively.

The use of a buck-boost array regulation approach (Configuration 2B of Figure 9) is similar to that of Configuration 1C in that it permits optimization at any AU value. The operating conditions for this system are shown in Figure 10C with the exception of the unregulated bus voltage V_U which is now the solar array voltage V_{SA} . Figure 10E, on the other hand, illustrates the application of the system when it is desirable to optimize for maximum AU conditions; the boosting capability of the solar array regulator permits setting the regulated bus voltage at the maximum power point of the maximum AU solar array. Thus, the possibility of a temperature excursion of the array has also been shown at maximum AU

conditions as typical in an orbiting application. The increased voltage capability of the solar array at reduced temperature is indicated by the dashed I-V curve. The solar array voltage increases to Point C with a constant power load, and the bucking function of the solar array control would be utilized to maintain the regulated output voltage.

The solar array characteristics, illustrated in Figure 10, are arbitrary representations of the effects of AU variations. Considerations of battery-operating voltages have been excluded from these initial considerations to simplify the discussion. Furthermore, the various regulation functions could be implemented in several different ways. An example is the array voltage limiter function which could use either a series-or shunt-type circuit, and each of these in turn could be implemented with either dissipative or switching (pulsewidth modulation) techniques. The method of implementing the regulation and control functions usually will have a significant impact on the operating conditions of the solar array and the ability to optimize the system for the various AU conditions. The load variations that occur during the various mission phases must also be taken into account. The succeeding sections of this report deal with the analyses of alternate methods of implementing each of the functions in the five basic configurations and the selection of appropriate methods for each.

3.2 SOLAR ARRAY ANALYSIS

3.2.1 Determination of Current-Voltage Characteristics

Representative solar array output current-voltage characteristics were computed for each mission as functions of sun-spacecraft distance. The solar cells used in the analysis of inbound missions to Venus and Mercury were those of a specially designed 1 x 2 cm size having a base resistivity of 10 ohm-cm, 10 percent AMO efficiency, and cover slides with a 420 μ cutoff filter. These cells were fabricated for high light intensity operation with a very low value of series resistance (approximately 0.2 ohm) through use of 12 grids rather than the usual 5. A comparison of the current-voltage characteristic of these cells, with standard solar cells at high solar intensity, is shown in Figure 11. The solar cell characteristics used in the analysis of the outbound missions to Mars and Jupiter were those of a 2 x 2 cm, 10.5 percent efficiency, 10 ohm-cm type covered by a 420 μ cutoff filter.

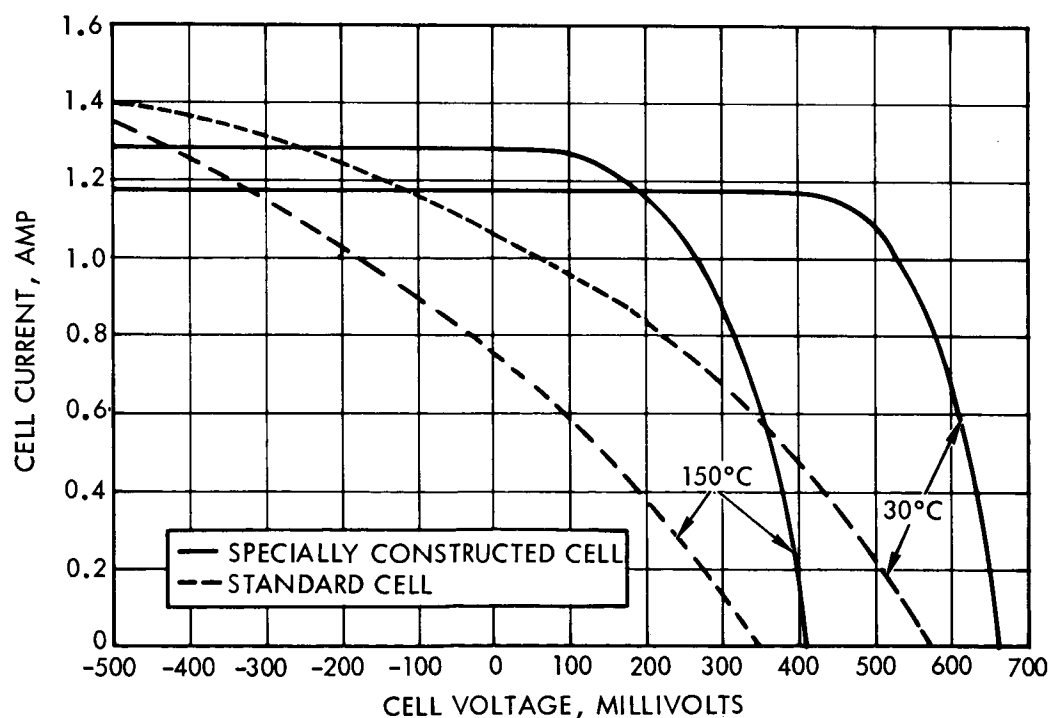


Figure 11. Comparison of Special Solar Cell with Standard Solar Cell at Light Intensity of 20 Suns

Solar array output calculations for each mission were based on a 10-series by 10-parallel solar cell array and utilized TRW Computer Programs AM 118 and AM 142. Program AM 118 is designed for the missions with decreasing solar intensity and Program AM 142 accounts for the effects of high solar intensity on cell performance as encountered on the Mercury and Venus models. In these analyses, a solar flare radiation environment equivalent to 10^{14} 1 mev electrons per cm^2 per year near the Earth (1 AU) was assumed. It was further assumed that the radiation levels at other than 1 AU varied inversely with the square of the sun-spacecraft distance.

Results of these solar array output calculations are shown in Figures 12, 13, 14 and 15 for the Mercury, Venus, Mars, and Jupiter missions, respectively. In addition to the array current-voltage characteristics at selected points in the mission, the variation in solar array current and voltage corresponding to the maximum power point throughout the mission is also indicated. For the Mercury mission, the maximum array power is shown to increase to a maximum and then to decrease at lower values of sun-spacecraft distance. This results from tilting the solar panels from their sun-oriented position to prevent excessive cell temperatures at the lower values of sun-spacecraft distance.

3. 2. 2 Comparison of Solar Array Capability with Load Profile

Figures 16 through 22 show the time profiles of the solar array capability in percent and the conditioned load requirements in watts for each of the model spacecraft. By comparing the relative solar array capability with the variations in load power requirements throughout the mission, it is possible to establish preliminary indications of the critical design points for each of the models. The critical design point is that condition during the mission at which the solar array power capability is a minimum relative to the power required from the solar array. Consequently at all other times during a given mission, the solar array power capability is greater than that required by the loads. The critical design point then determines the required solar array capability in order to adequately support the loads over the complete mission.

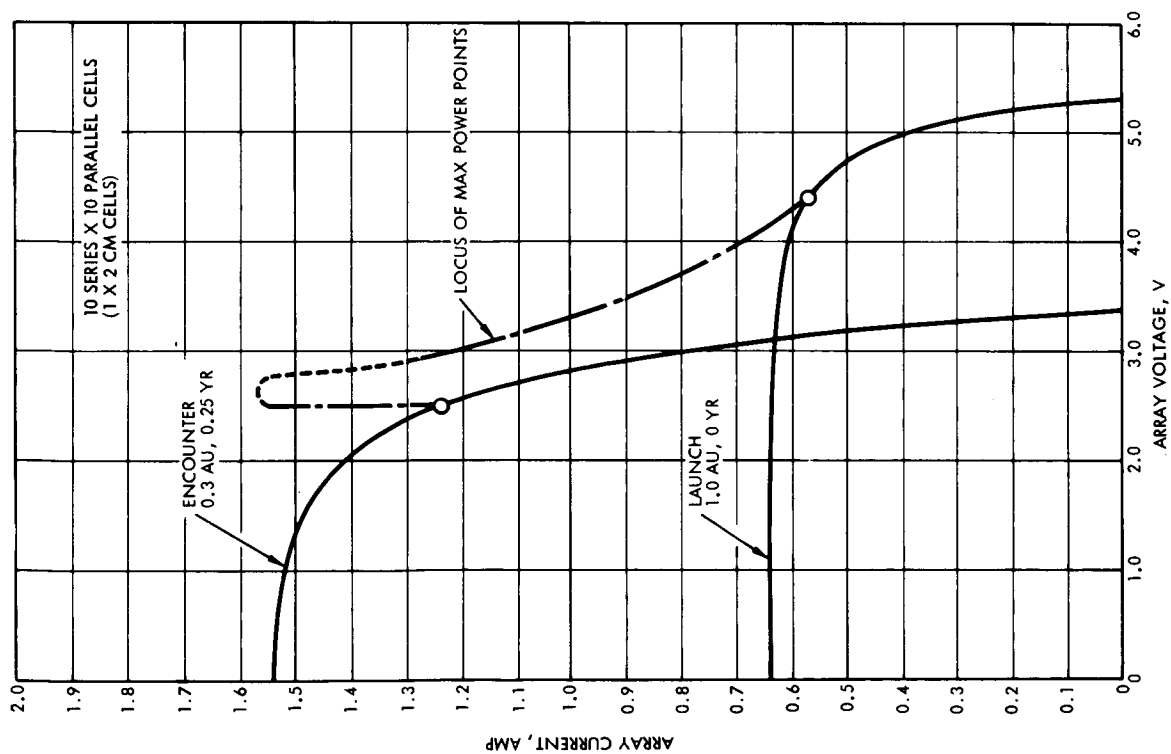


Figure 12. Mercury Flyby Solar Array Characteristics

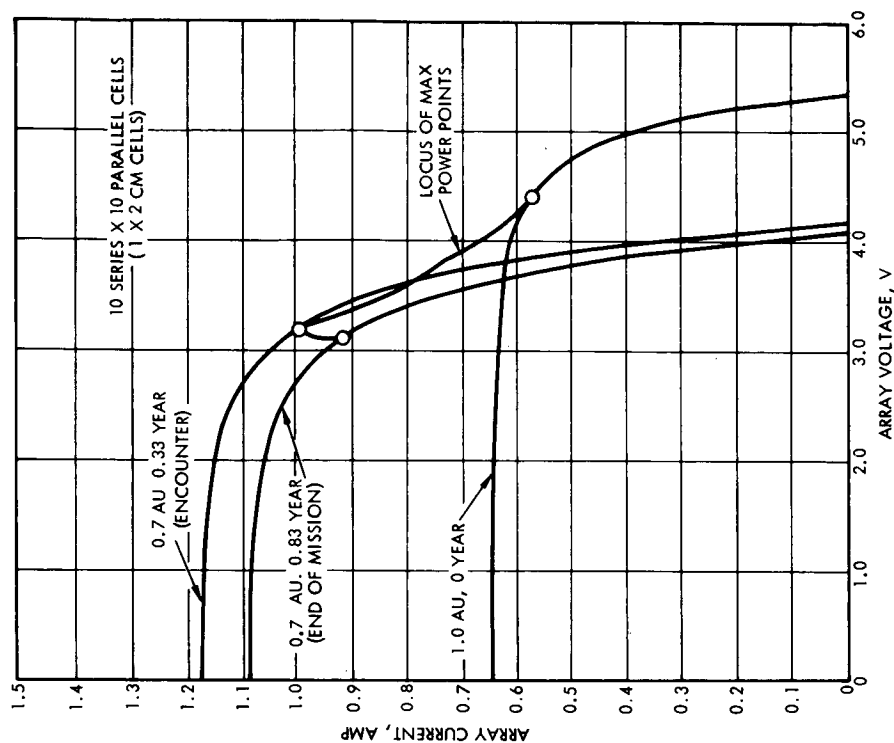


Figure 13. Venus Orbiter Solar Array Characteristics

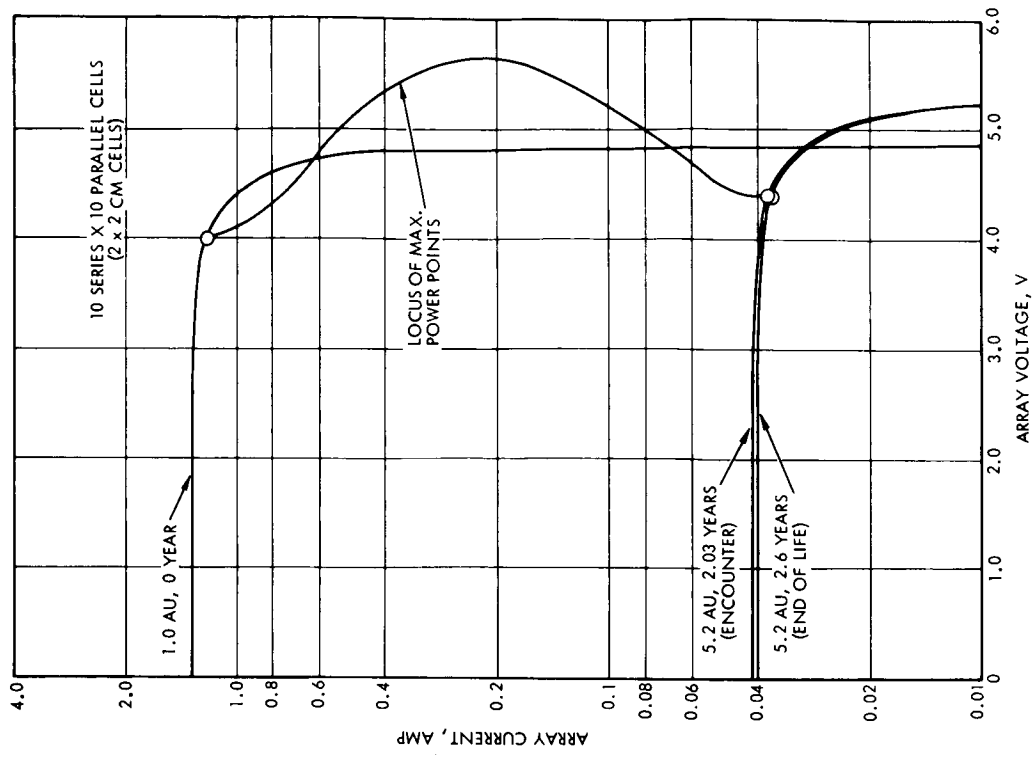


Figure 14. Mars Orbiter Solar Array Characteristics

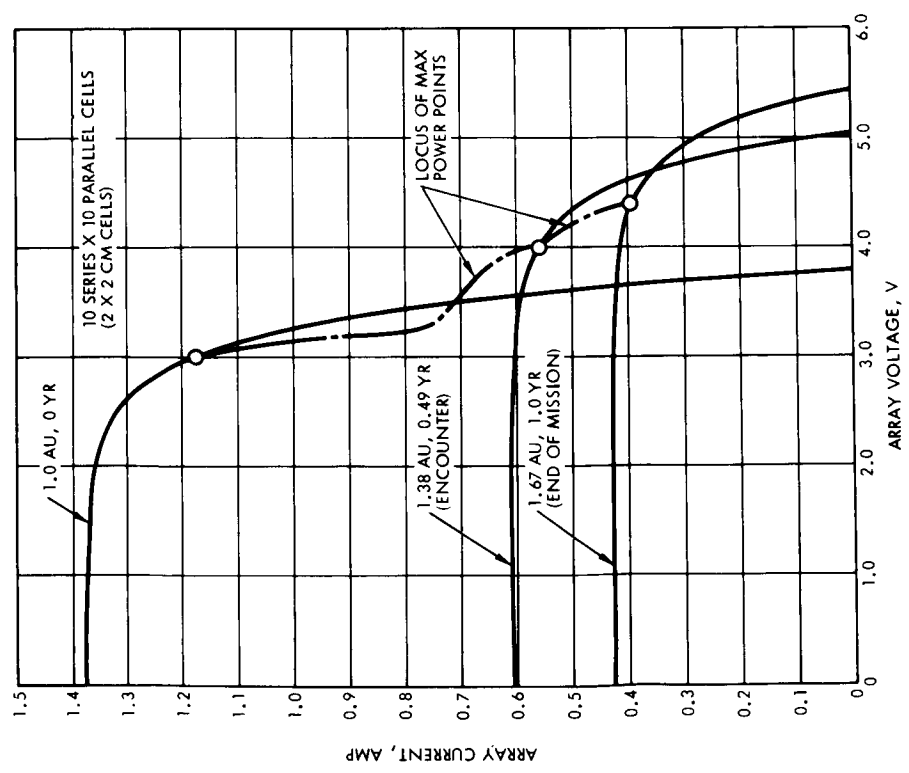


Figure 15. Jupiter Orbiter Solar Array Characteristics

Figure 16 for the Mercury Flyby mission shows the solar array power capability gradually increasing as the sun-spacecraft distance decreases, until such time as tilting of the panels is required to prevent excessive solar array temperatures. The maximum power capability of the array then degrades until the minimum AU condition is reached. Subsequently, the sun-spacecraft distance again increases throughout the duration of the mission. By comparing the solar array capability with the load requirements, it can be seen that if the solar array can support the 126-w cruise load at the beginning of the mission, its 123 percent capability at encounter would provide a load capability of 155 w. It was assumed that the battery would be utilized to share the load with the solar array during the encounter phase, based on an encounter period of 5 hours. The 28-w difference between the solar array capability and the load demand can be adequately handled by the battery designed to support the launch and midcourse maneuver in earlier phases of the mission. As a result, the critical design point for the Mercury mission appeared to be at one AU with the cruise load.

For the Venus Orbiter No. 1 model, Figure 17 shows that the solar array capability increases to 127 percent at encounter, and then degrades to 113 percent at end-of-life. The step decrease from 127 to 124 percent at encounter reflects an increased array temperature produced by the albedo of Venus. Comparison of the end-of-life load condition with the initial cruise load of 135 w indicates that the critical design point for the Venus Orbiter No. 1 is at end-of-life. It is assumed that the launch, orientation, midcourse maneuver and orbital insertion phase loads are all supplied by the battery.

For Venus Orbiter No. 2 (reference Figure 18) the solar array characteristics are identical to that of Venus Orbiter No. 1. The load profile differs, however, and the large load subsequent to orbit insertion, due to the presence of the probe on the spacecraft, determines the critical design point for the mission. It has been assumed that the probe will remain attached to the spacecraft for several orbits. The load is then reduced approximately 50 percent upon probe separation.

The solar array and load power profiles for the Mars Orbiter mission are shown in Figure 19. The maximum power capability of the solar array continuously decreases, due to the continual increase in sun-spacecraft distance over the course of the mission. This applies also during the orbit phase when the distance of Mars from the Sun increases from 1.38 AU to 1.67 AU for the particular launch date assumed for this mission. Comparing the solar array capability with the load requirements indicates that the 46 percent array power output at the end of mission is the critical design point. Although the load requirements are higher during the initial orbits prior to capsule separation, it has been assumed that no eclipses occur during this period; thus, the need for battery charging does not exist, and the 63 percent capability of the solar array during this phase of the mission is more than adequate to support the indicated load.

In the Jupiter probe (Figure 20) and Jupiter Orbiter No. 1 (Figure 21) missions, the maximum load is seen to occur at end-of-life and the minimum solar array capability at this same point clearly defines end-of-life as the critical design point for these missions. Figure 22, for the Jupiter No. 2 mission, reflects the presence of planetary probes on the spacecraft. Since these probes are ejected during the orbit phase, a maximum load condition occurs subsequent to insertion into orbit. As a result, the apparent design point for the Jupiter Orbiter No. 2 is at encounter. For all of the Jupiter Missions, an arbitrary 10 percent degradation of array performance has been assumed to reflect micro-meteoroid damage during passage through the asteroid region from approximately 2.0 to 4.0 AU.

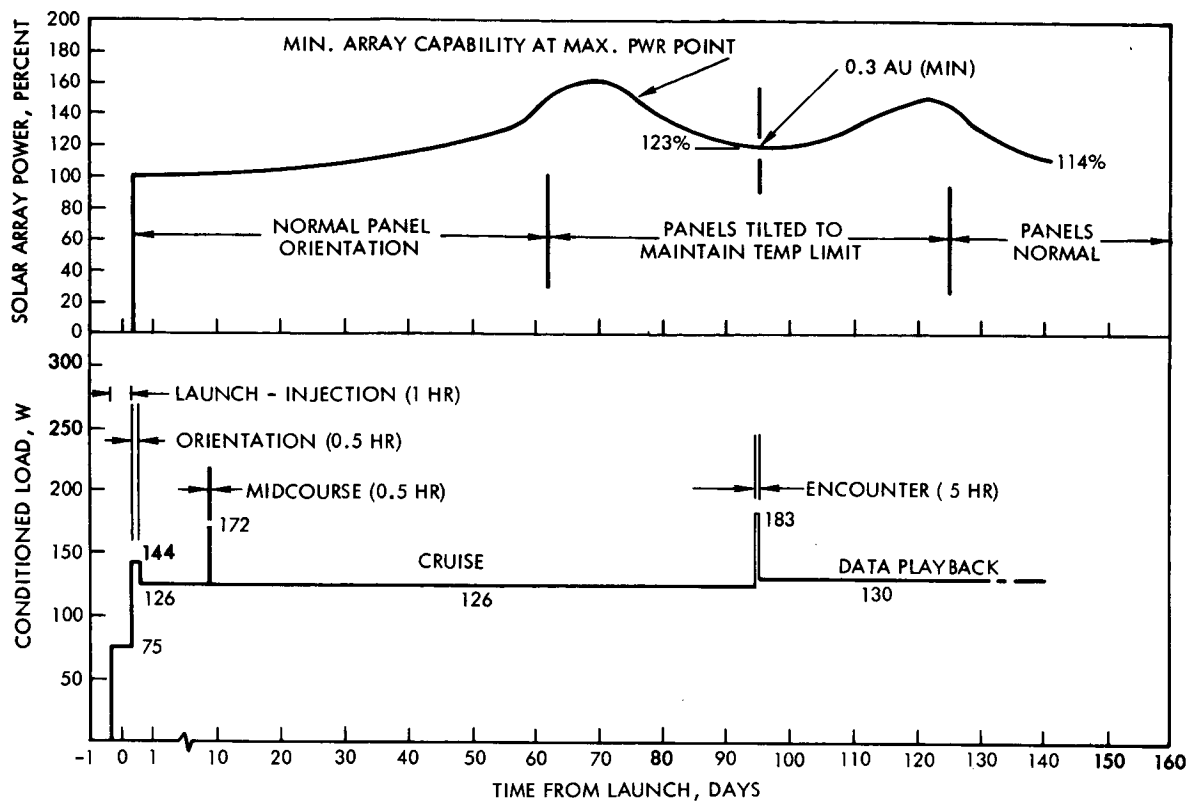


Figure 16. Solar Array Maximum Power Capability and Conditioned Load Power Requirements versus Time – Mercury Flyby Mission

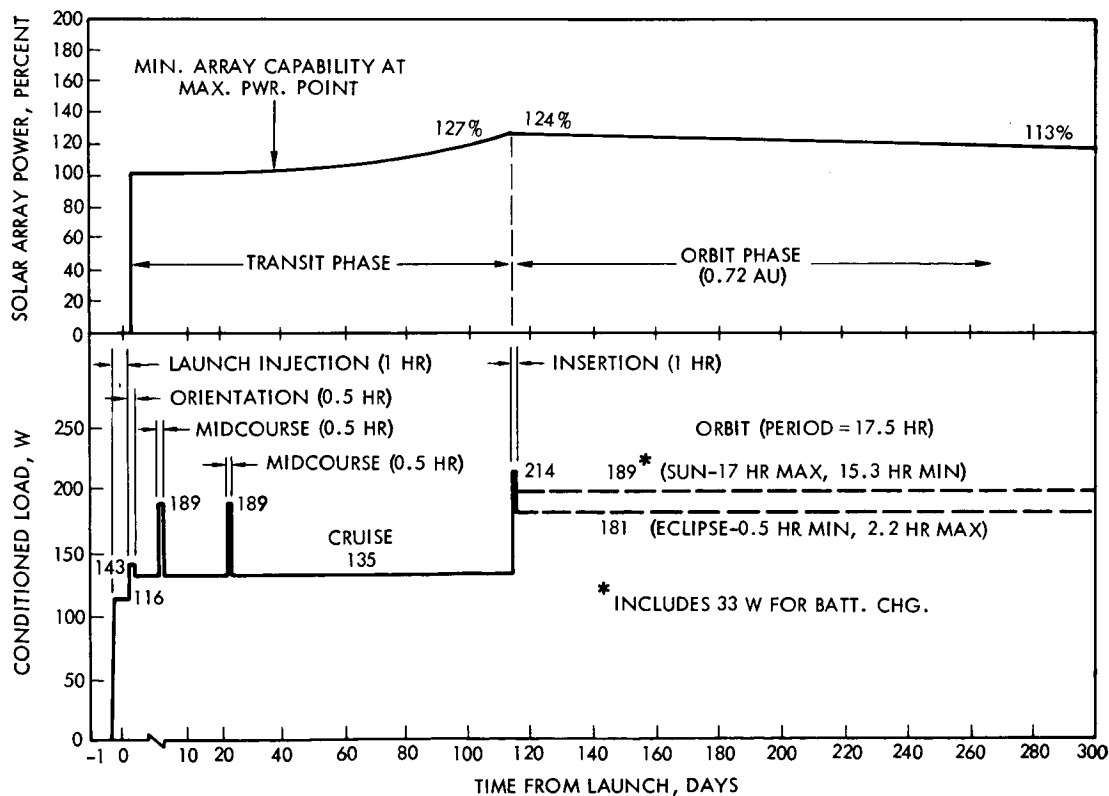


Figure 17. Solar Array Maximum Power Capability and Conditioned Load Power Requirements versus Time – Venus Orbiter No. 1 Mission

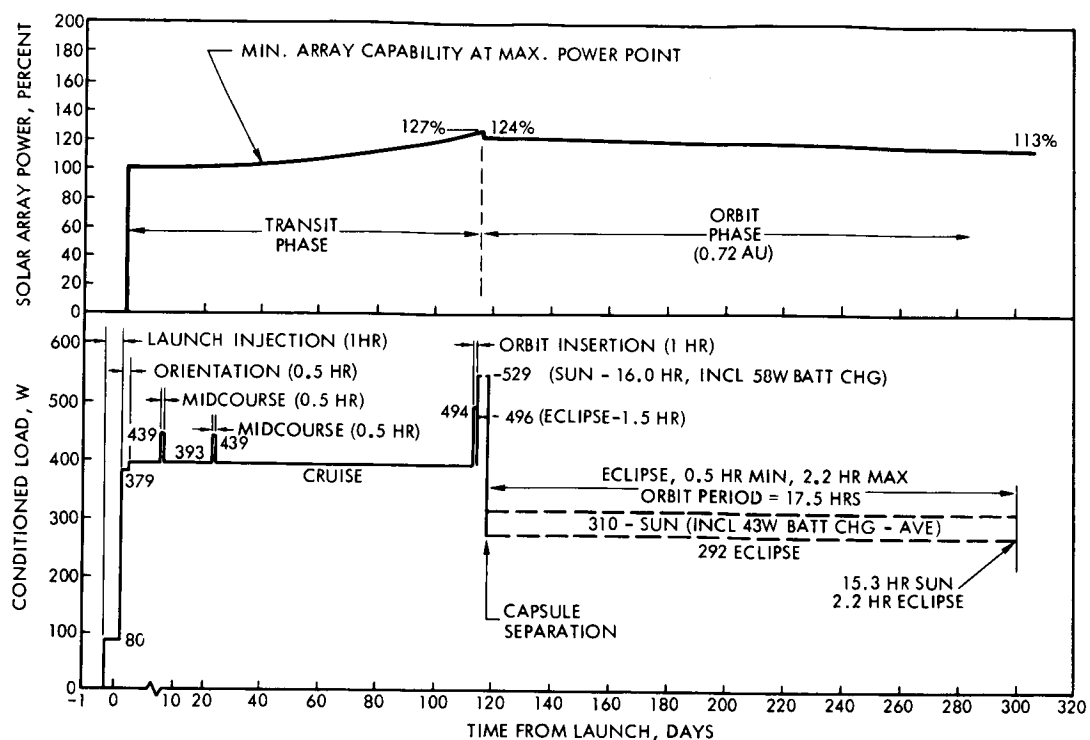


Figure 18. Solar Array Maximum Power Capability and Conditioned Load Power Requirements versus Time – Venus Orbiter No. 2 Mission

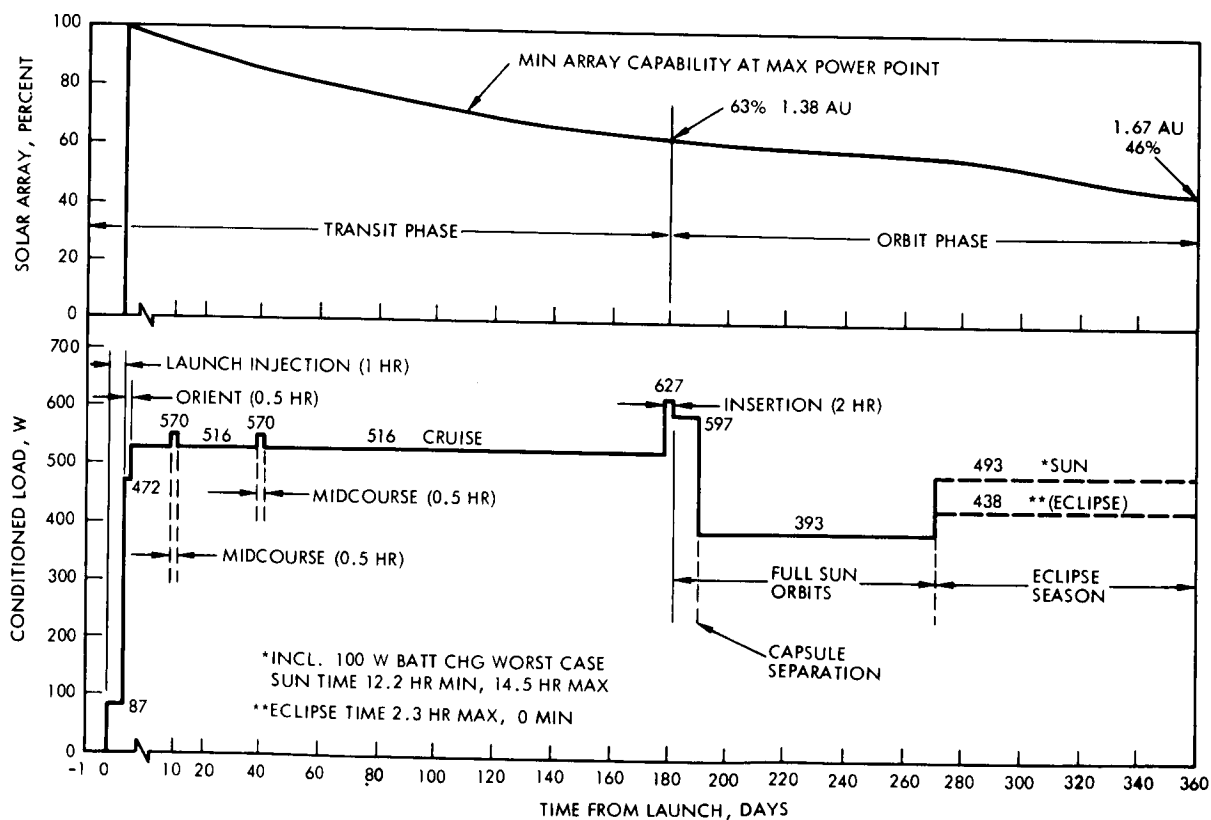


Figure 19. Solar Array Maximum Power Capability and Conditioned Load Power Requirements versus Time – Mars Orbiter Mission

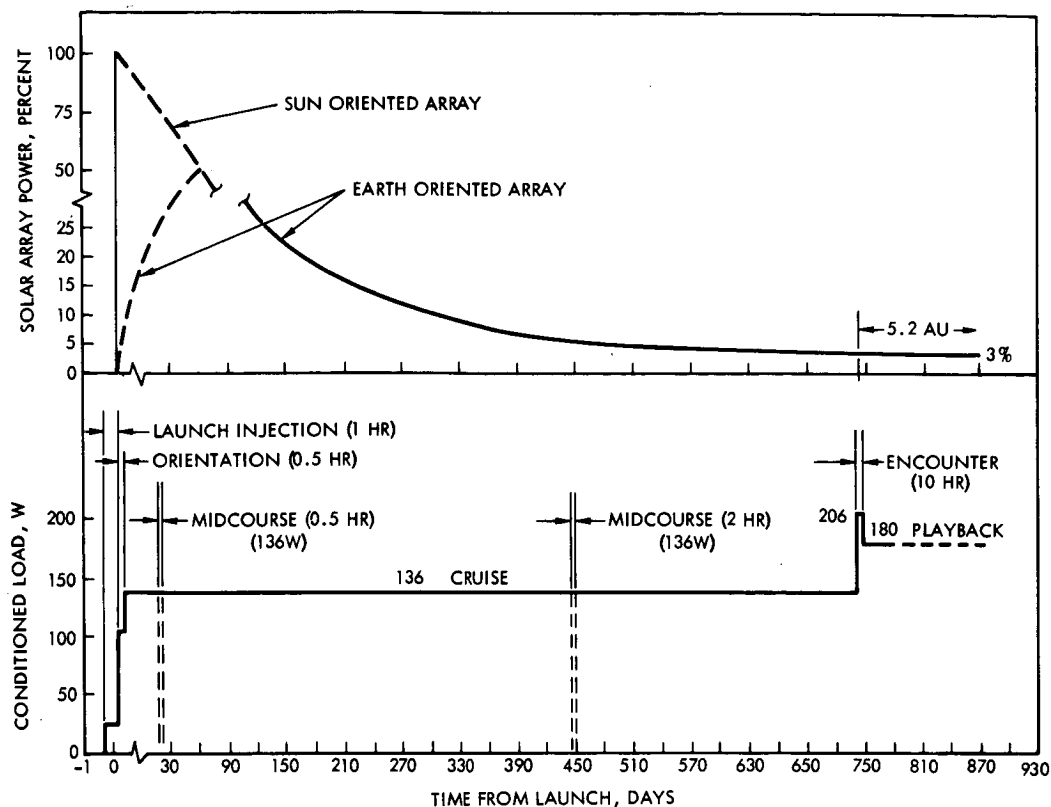


Figure 20. Solar Array Maximum Power Capability and Conditioned Load Power Requirements versus Time - Jupiter Flyby Mission

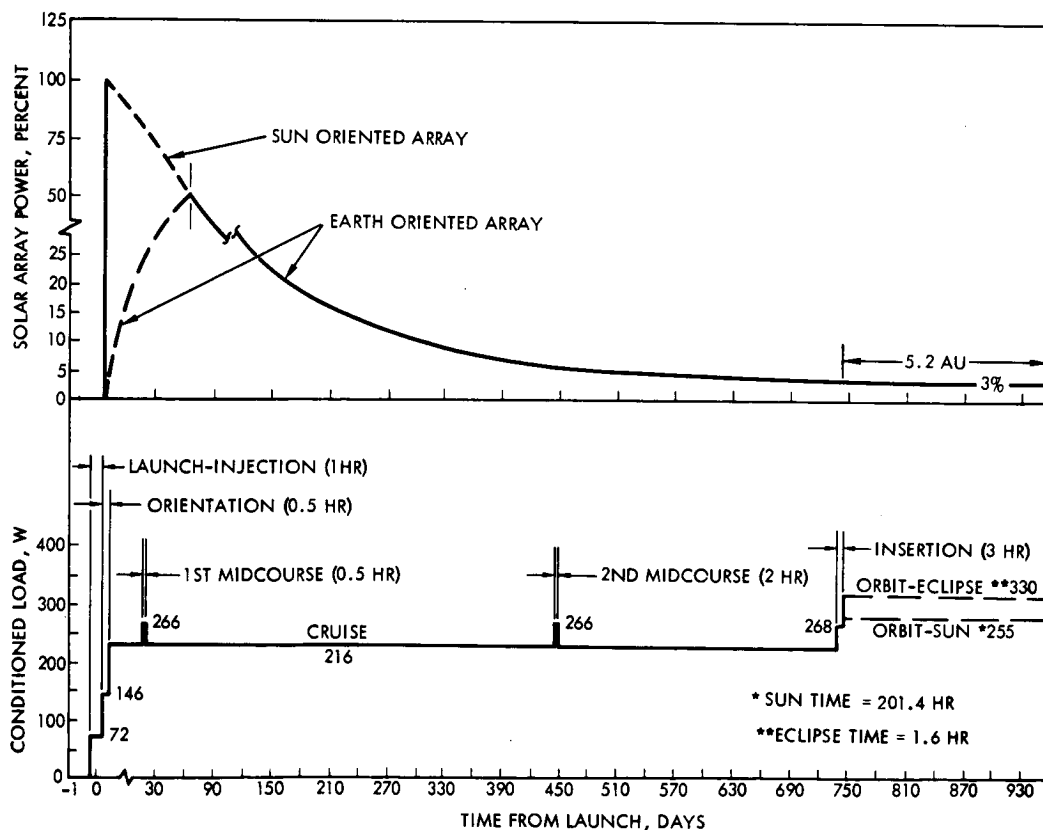


Figure 21. Solar Array Maximum Power Capability and Conditioned Load Power Requirements versus Time - Jupiter Orbiter No. 1 Mission

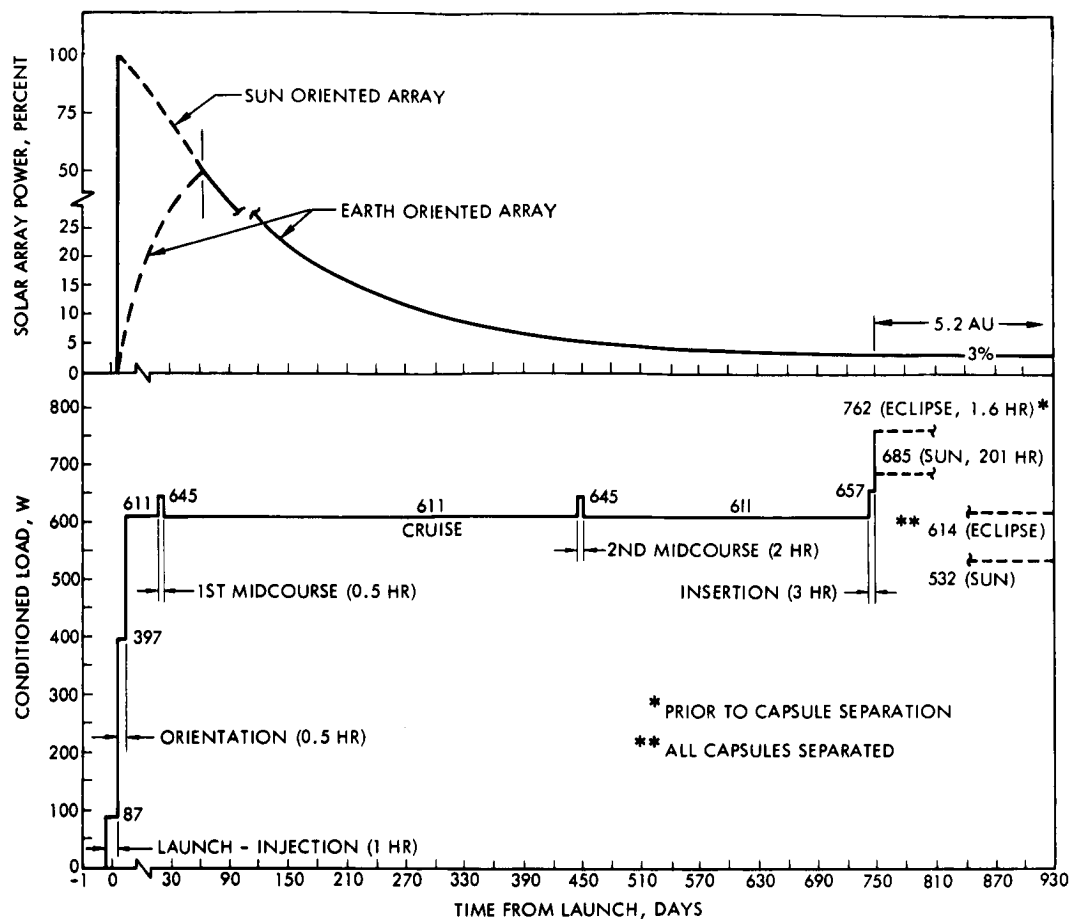


Figure 22. Solar Array Maximum Power Capability and Conditioned Load Power Requirements versus Time — Jupiter Orbiter No. 2 Mission

3.3 SOLAR ARRAY — BATTERY INTEGRATION

3.3.1 Selection of Battery Type and Control Approach

3.3.1.1 Battery Selection

The selection of batteries for each of the model missions was based primarily on straightforward tradeoffs of weight-and-cycle-life capability for the orbiting missions. The maximum number of cycles approach 300 for the Venus and Mars orbiters. This number of cycles is considerably lower than the capabilities of state-of-the-art silver-cadmium batteries operating at 50 percent depth-of-discharge. The competitive battery system for these missions is of course the nickel-cadmium type. The higher weight and higher fixed magnetic field associated with nickel-cadmium type in comparison to silver-cadmium, however, led to the selection of silver-cadmium batteries for the orbiting missions. For the flyby missions, the silver-zinc battery was selected because of the low-cycle life requirements and the improved energy density of the silver-zinc cell. Here again, a 50 percent maximum, depth-of-discharge was used in sizing the battery.

In some orbital applications, particularly low-altitude orbiting satellites, the need to recharge batteries rapidly during a relatively short sunlight period would make the selection of nickel-cadmium batteries possibly mandatory. Silver-cadmium batteries, however, operate more efficiently at lower charge rates and are susceptible to damage if charged at high rates. For the Venus and Mars orbiters, the ratio of sunlight time to eclipse time per orbit is relatively large at 7.7:1 and 5.3:1, respectively. As a result, the capability of silver-cadmium batteries to recharge at low rates during the relatively long sunlight period is desirable for these missions in order to minimize solar array power requirements.

For the selected Jupiter orbit, the ratio of sunlight to dark time is extremely large at 127:1. Because of the long (203 hr) orbit period, the total number of charge-discharge cycles which would occur over the 6-month-orbiting phase is significantly less for this mission. As a result, state-of-the-art silver-zinc batteries would appear to be contenders with the silver-cadmium type for this application. Studies have

indicated, however, that in order to utilize the silver-zinc type, it would be necessary to further reduce the depth-of-discharge from the 50 percent value assumed for the silver-cadmium batteries. As a result, the installed silver-zinc battery weight becomes more nearly equal to that of the silver-cadmium type. Recent developments in silver-zinc secondary batteries would tend to indicate that by the time a Jupiter orbital mission might become a reality, the silver-zinc approach could offer greater advantages in weight in comparison to the silver-cadmium type.

3.3.1.2 Charge Control

The characteristics of both the silver-zinc and silver-cadmium batteries require a charge control method which limits battery-charging current as a function of battery state-of-charge and prevents overcharge of the battery. The simplest scheme for implementing this method is to charge the battery from a constant potential bus through a series current limiting resistor. The voltage drop across the resistor will determine the amount of charging current to the battery. As the battery state-of-charge and its terminal voltage increase, the applied voltage across the series resistor will decrease and the charging current will similarly decrease until the battery approaches the applied constant potential and the charging current approaches zero.

When charging the battery from a power limited solar array, these control requirements become somewhat modified from the constant potential approach. At low states-of-charge, the battery can accept the maximum current available from the solar array over and above that required by the loads. The current limiting function can be implemented by the use of a resistor or by any type of current limiting regulator. The power losses associated with the use of a simple current limiting resistor would appear to be excessive for space applications, but with a 50-percent depth-of-discharge limitation, the silver-type batteries will be charged principally at their higher plateau voltage. As a result, assuming a bus voltage level equal to the maximum battery voltage allowable, the resistor losses will be small.

Since the silver-zinc and silver-cadmium batteries are subject to damage from over-charge, charge termination by means of disconnecting the battery from its charging power source is employed. Charge termination can be controlled in a variety of ways, such as, detecting a maximum voltage limit, a third electrode control signal, or determining that charging current has fallen below a low level which is indicative of full charge at a given voltage limit. This last method was adopted for purposes of this study.

For any dissipative charge control, charging current is measured by the use of a simple series resistor. In the case of the current limiting resistor approach, the resistor itself can serve as the current measuring device and the control signal, to indicate charge termination, may be derived by a voltage measurement across the charging resistor. In those cases where the maximum bus voltage is not equal to the maximum allowable battery voltage, a bucking or boosting regulator can be used for charge control. These regulators and their associated controls must limit battery voltage, limit battery current as a function of battery voltage, detect a decrease in charging current below the desired charge termination value and terminate charge by deenergizing the regulator. This basic charge control approach was used for all of the missions.

For those power supply configurations employing a regulated main dc bus, the charger includes bus-voltage feedback to further limit battery-charging current in those cases of marginal solar array capability where normal battery current could produce a main bus under-voltage condition.

3.3.1.3 Discharge Controls

For those power supplies in which the main bus voltage varies with the battery charge-discharge status, a switching function has been incorporated to provide a direct loss-less-discharge path from battery to bus. The alternative approach of relying on a diode to provide an unidirectional discharge path is considered undesirable because of the voltage drop and power loss associated with this approach. The added control complexity to implement this approach is considered a lesser penalty than the added battery weight to accommodate series diode losses, particularly in view

of the probable need for series redundant power diodes to ensure adequate reliability. However, a diode bypass of this discharge switch normally is provided to permit supplying transient or peak loads from the main bus without waiting for the relay to respond. The alternative approach is to supply transients or peak loads directly from the battery rather than from the main bus. For any of the charge control methods, the discharge switch must be open when the battery is charging. In those cases where a boost-type battery charger is used, the diode discharge path cannot be used as it would short-circuit the charger. For those systems employing a regulated main bus, a boost regulator must be used for battery discharge in order to maintain the required bus regulation.

3.3.1.4 Undesirable Solar Array Battery Load Sharing

A potentially large penalty in solar array sizing results from those system configurations which combine the battery and solar array electrically at an unregulated bus. In this type of a system the bus voltage is normally determined by the battery discharge status. As a result, the solar array when oriented must be capable of supporting the load over a relatively wide range of voltages. In a typical case, the load connected to the unregulated bus approaches a constant power characteristic as a function of bus voltage; therefore, at lower voltages, current demand is considerably higher than at the higher end of the bus voltage range. Unless the solar array is designed to supply the total load current at minimum unregulated bus voltage, or unless appropriate controls are included in the system, it is possible that a stable operating condition could exist in which the battery is required to share the load with the solar array, even though the solar array power capability at higher voltage would be adequate to support the entire load. Figure 23 illustrates the difference in required solar array capability between a system designed with appropriate controls to overcome this undesirable load-sharing condition and a system without such controls.

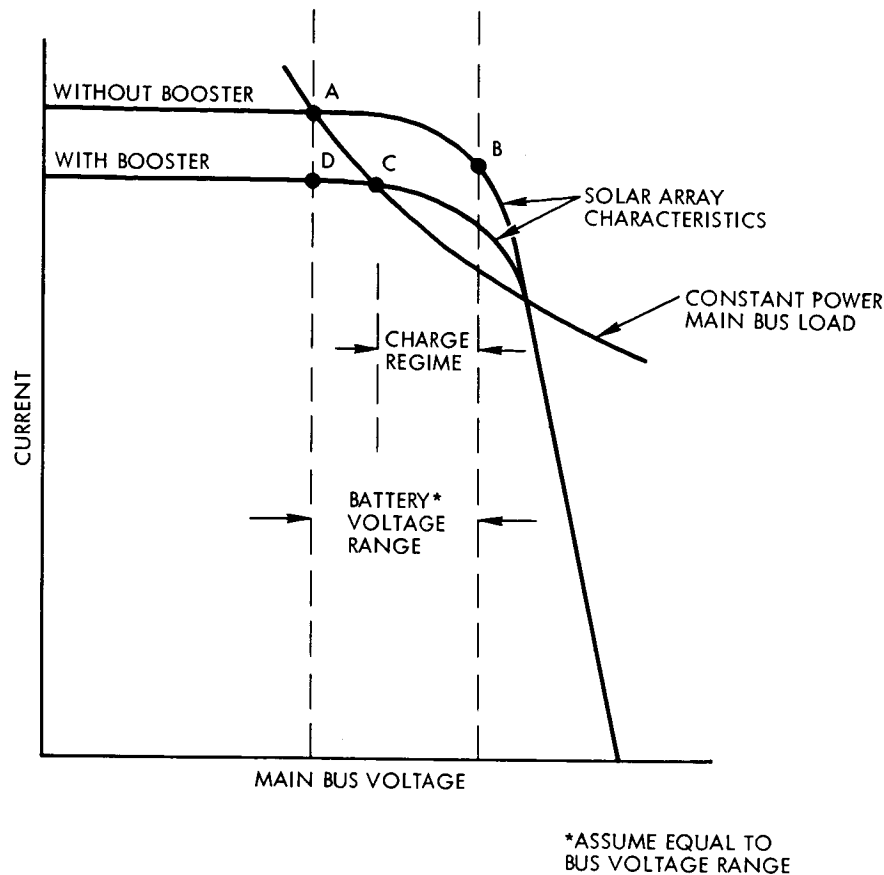


Figure 23. Comparison of Required Solar Array Capabilities With and Without Momentary Line Booster for Unregulated Lens Systems

In a simple case, such as emergence from a solar eclipse, the battery is normally discharging to support the total load and the bus voltage is at the lower end of its range. As the solar array is illuminated, it will deliver current to the load and must be sized to supply the total load current at the lower operating voltage (Figure 23, Point A). When the array current capability builds to the point at which battery discharge is no longer required, the bus voltage will rise, the load current will reduce, and the battery will begin accepting charge from the solar array. Since battery-charging current requirements are low, the array will tend to have a significant excess power capability at the higher voltages during battery charging (Point B). The inability to make use of the maximum solar array power capability at normal voltages clearly penalizes the power system from the standpoint of

solar array weight. The magnitude of this penalty is dependent on the relationship between the battery voltage range and the solar array maximum power point voltage.

To improve the utilization of array power, a momentary battery discharge booster may be employed to force the bus voltage to a higher level when an unnecessary load-sharing condition exists. With this approach, the solar array may be designed to provide required load current only at voltages corresponding to battery-charging conditions (Figure 23, Point C). The booster power capability need be adequate only to supply the difference in power between the load requirement at battery discharge voltage (Point A) and the solar array capability at that same voltage (Point D).

Power sources which generate a regulated dc bus directly by regulating both battery and solar array outputs independently require a continuous boosting regulator for battery discharge. This approach, of course, eliminates the problem of undesirable load sharing.

3.3.2 Battery Control Implementation

Basic system control and logic requirements were investigated and the battery charge and discharge control functions were established as necessary for proper operation of the integrated power systems. Specifically, the functions terminating battery charge, controlling the battery discharge switch used in many of the systems, detecting unnecessary battery load sharing, and controlling the momentary line booster to terminate this undesirable operating mode where applicable were analyzed.

The basic designs selected are:

- Bucking charger and discharge switch (Section 3.3.2.1)
- Bucking charger, discharge switch and momentary line booster (Section 3.3.2.2)
- Boost charger and discharge switch (Section 3.3.2.3)
- Boost charger, discharge switch and momentary line booster (Section 3.3.2.4)
- Bucking charge regulator and (continuous) boosting discharge regulator (Section 3.3.2.5).

Three methods of implementing the bucking charger approach were selected for analysis. For the unregulated bus systems, these consisted of first, a series current limiting resistor and disconnect relay to terminate battery charging; second, a series dissipative regulator controlled to limit maximum battery voltage and battery-charging current as a function of battery voltage, with charge termination by deenergizing the charger; third, a pulsewidth modulated series regulator, controlled to limit battery voltage and charging current, and terminate charging.

For the bucking charge regulator used with the regulated bus system, an active control is necessary to maintain the regulation of the main bus during battery charging. The appropriate methods of implementing this function are the dissipative and pulsewidth-modulated series regulators. In addition, the charge regulator is provided with a voltage feedback from the main bus which overrides the normal charge control functions to limit battery-charging current in accordance with the capability of the solar array to supply current and still maintain the main bus within voltage regulation limits. This approach prevents initial higher battery-charging currents from overloading the solar array at the regulated bus voltage.

The boost charger used with the unregulated bus systems and the boosting discharge regulator used with the regulated bus systems are dissimilar in that the former must have the capability of functioning in a bucking mode in those cases where the bus voltage exceeds the desired battery voltage limit. The momentary line booster used with the bucking charger is dissimilar from that used with a boosting charger in that the former is of the type wherein only an amount of power proportional to the difference in voltage between the battery and the bus is converted. This booster is similar to the continuous boosting discharge regulator and is designed with a series diode which passes the major portion of the power. With a boost charger, the momentary line booster must be designed without such a diode path since this would short circuit the charger. Simplified block diagrams for all of these chargers and regulators are illustrated in Figures 24 through 30.

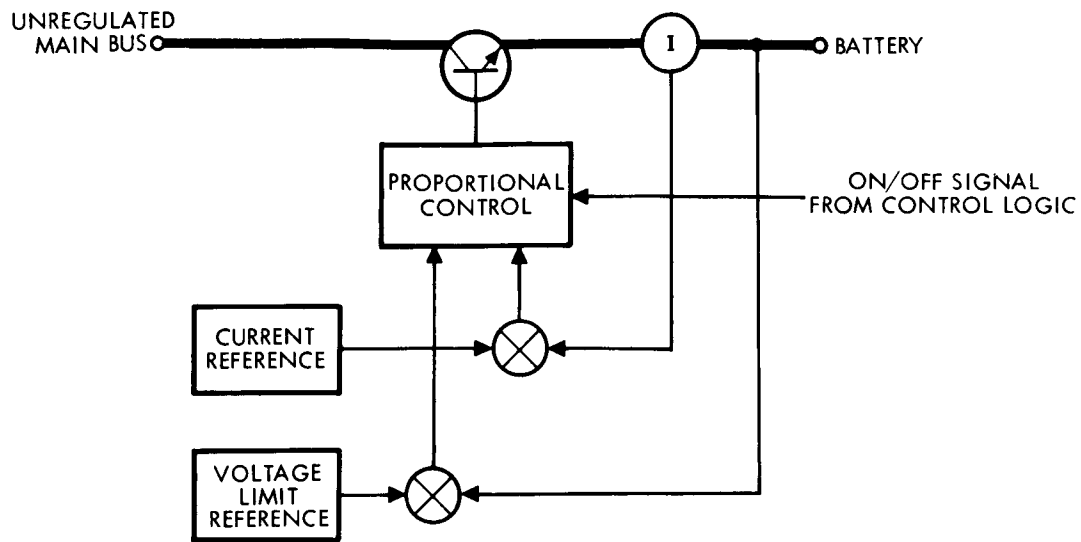


Figure 24. Dissipative Series Charger

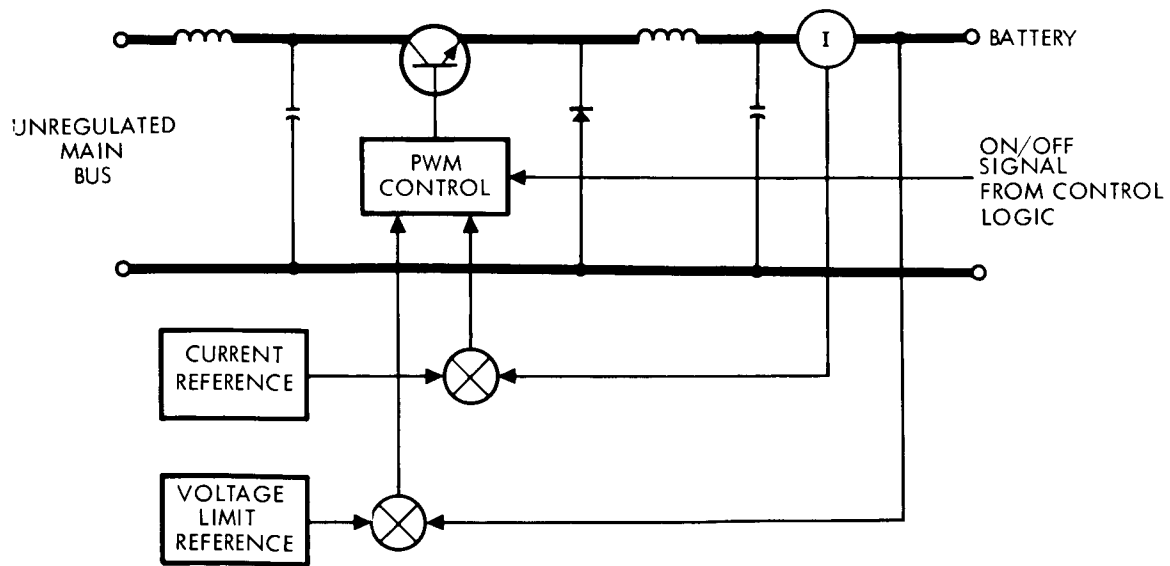


Figure 25. PWM Buck Series Charger

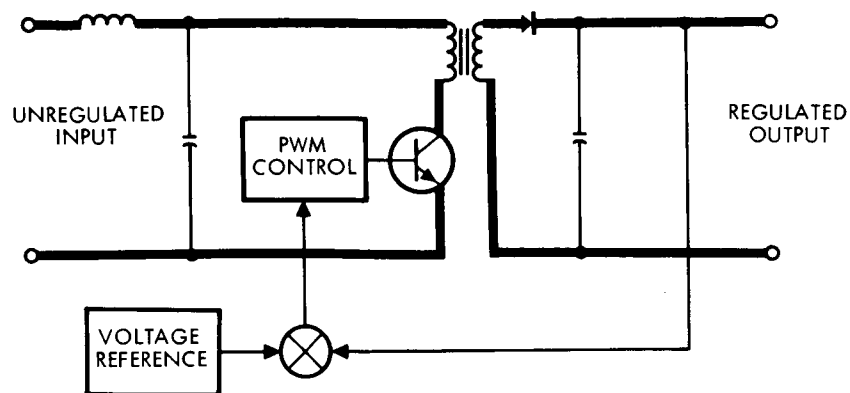


Figure 26. PWM Buck-Boost Charger, Array Regulator or Line Regulator

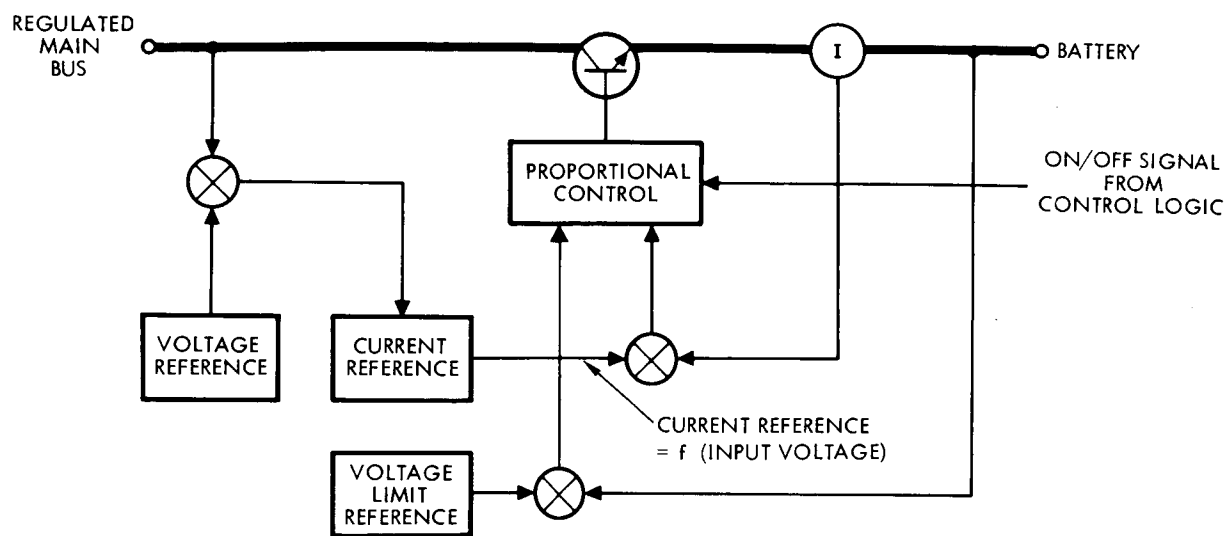


Figure 27. Dissipative Battery Charge Regulator

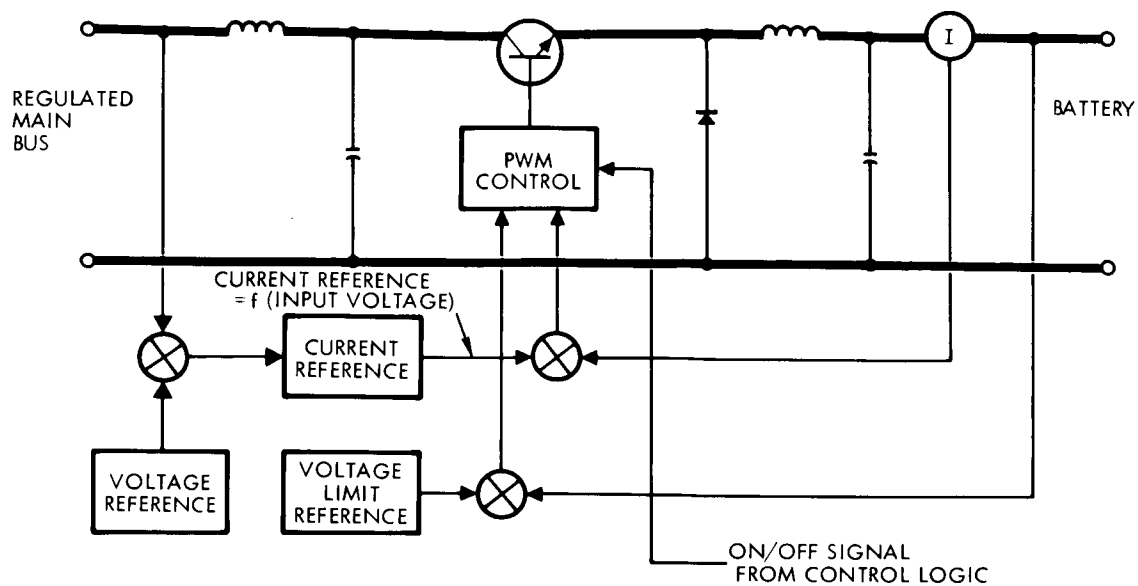


Figure 28. PWM Buck Battery Charge Regulator

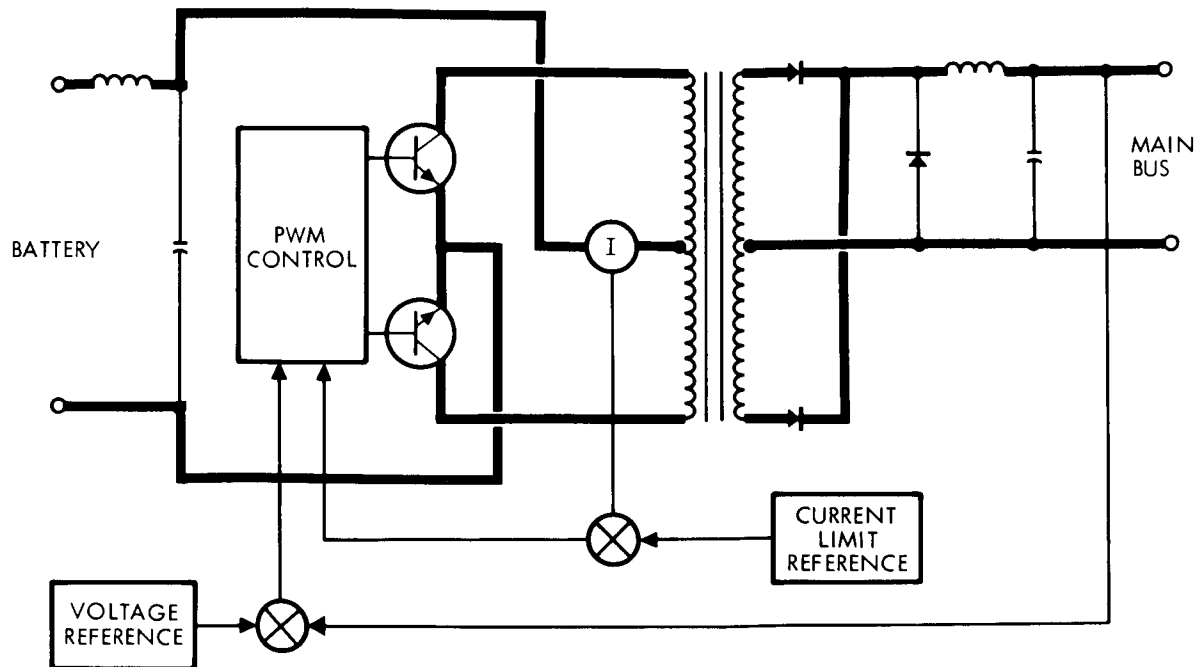


Figure 29. Momentary Line Booster, Used With Boost Charger

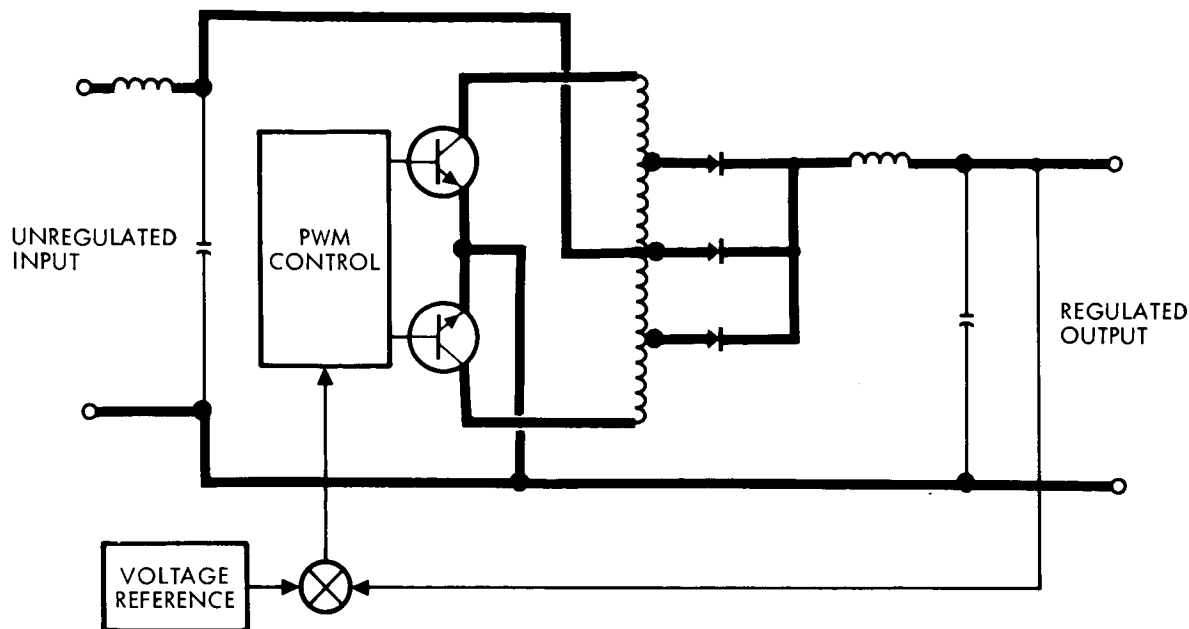


Figure 30. PWM Boost Discharge Regulator, Boost Line Regulator or Momentary Line Booster Used With Buck Charger

3.3.2.1 Bucking Charger

The bucking charger battery control is shown in Figure 31. At launch with the battery supplying the total load, the bus voltage is less than V_C and, as a result, the discharge switch is closed, the charger off, and the flipflop set. Upon entry into sunlight, the solar array takes over the load, the main bus voltage rises and the battery begins to charge through the discharge switch. As soon as the battery voltage increases to its minimum charging level, the charger is turned on and the discharge switch is opened. The time delay permits battery-charging current to be established and thereby prevents immediate reset of the flipflop. The battery charges to a voltage limit with decreasing charge current until such time as the charging current falls below I_1 , a value of approximately $C/100$, which is representative of a fully charged state. At this time, or in the event of an overtemperature of the battery, a signal is provided to

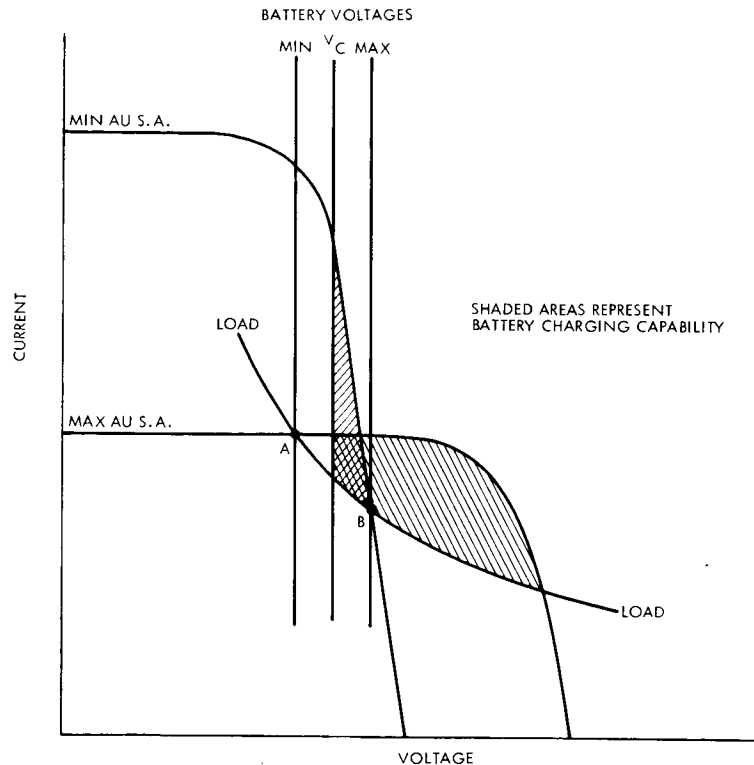


Figure 32. System Operating Points
for Bucking Charger

scheme must be capable of supporting the spacecraft load at the minimum voltage of the battery. When the battery is discharging, as during a maneuver or eclipse, the main bus voltage is determined by the battery load and state-of-charge. When the solar array is illuminated, the operating point on the array is at the voltage determined by the battery. The solar array must have adequate current capability to take over the load from the battery at this operating voltage (Point A). The assumption that this operating voltage is coincident with minimum battery voltage is conservative, in that the voltage regulation of the battery will result in some bus voltage increase as the solar array takes over any portion of the load. In the absence of adequate battery data on the behavior of the battery voltage as a function of the load current, taking into account the various states of charge and temperature conditions, it has been assumed that the battery voltage will remain at its minimum value until the discharge current is reduced to zero. When this occurs the battery voltage rises to its minimum charging level. With the assumed constant power characteristic of the unregulated bus load, this increase in bus voltage

results in a reduction in load current and enables the solar array to provide charging current.

Figure 32 is based on an assumed constant load for all AU conditions. The magnitude of the load, relative to the solar array characteristics shown, has been maximized. The maximum battery voltage with the bucking charger cannot exceed the voltage capability of the solar array at this load condition; therefore, the maximum battery voltage is constrained by the minimum AU solar array capability at Point B. The minimum battery voltage is assumed to be a fixed percentage of the maximum value and must be consistent with the load requirement and maximum AU solar array capability, as indicated by Point A. The load line shown then represents the maximum load, consistent with the assumed solar array characteristics. The shaded areas represent the maximum theoretical battery-charging capability. In order to utilize the relatively large charging capability of the maximum AU solar array, however, it is necessary that this system be designed in such a manner that the solar array voltage is not limited to the maximum battery voltage. This could be accomplished by the appropriate series regulator for the solar array control, or by charging the battery through a bucking charger that can sustain a significant voltage drop between the main bus and battery.

3.3.2.2 Bucking Charger with Line Booster

Figure 33 illustrates the system control logic for a bucking-type battery charger and a momentary line booster which eliminates the need for the solar array to take over the total bus load at minimum battery voltage, and permits making use of available increased solar array capability at higher voltages to support the load. For this system, during the launch phase, the solar array is not illuminated, the discharge switch is closed and the battery discharges directly to the main bus at a voltage less than V_C . Both the battery charger and the line booster are off.

Upon orientation of the solar array, the line booster flipflop is set, the line booster energized, and the discharge switch opened. As a result, the bus voltage is increased by the action of the line booster for a period of time determined by time delay TD2. After the completion of this time delay, the booster flipflop is reset and the booster deenergized. While

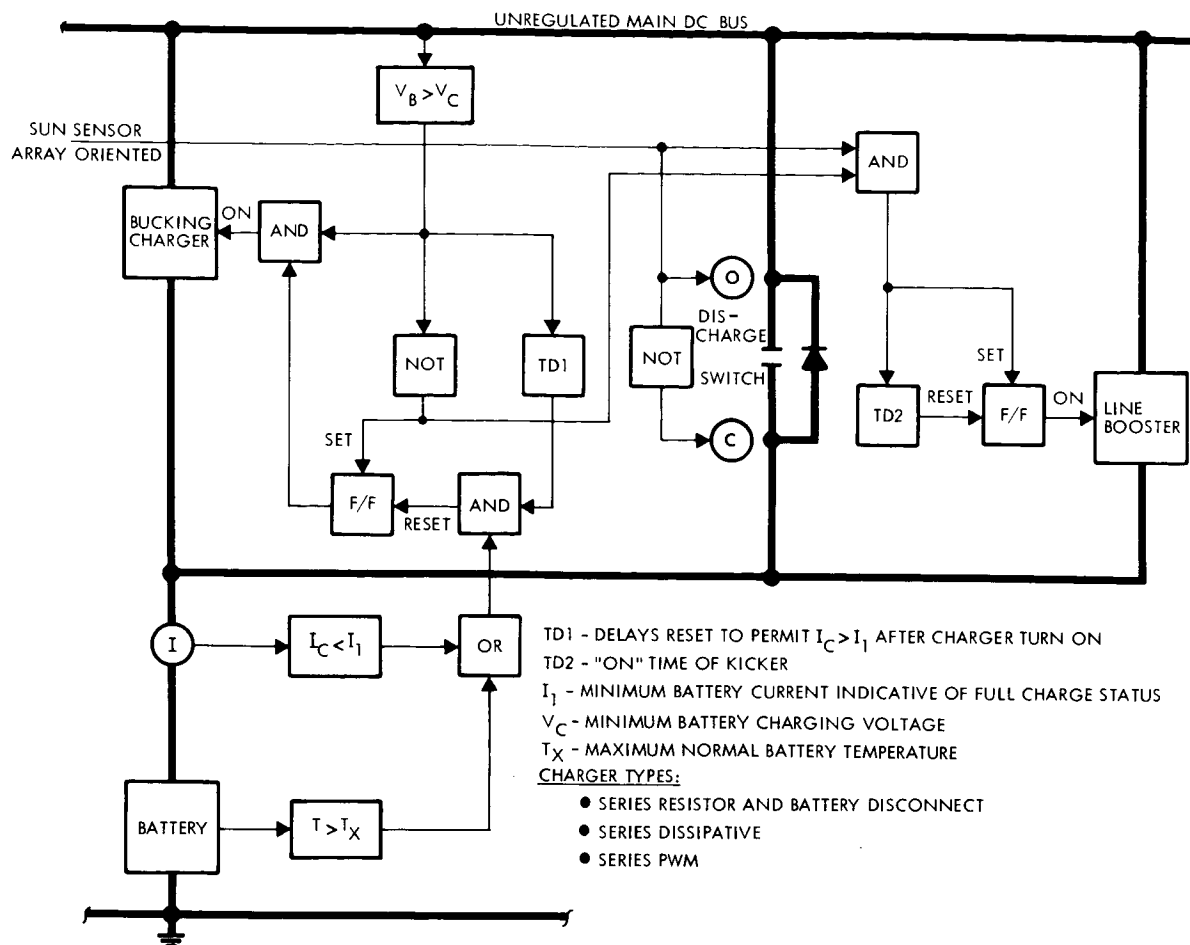


Figure 33. Battery Controls Block Diagram Bucking Charger, Discharge Switch, and Line Booster

the booster is on, the bus voltage is raised to a level at which the solar array can support the entire unregulated bus load. This higher voltage is sensed by the bus voltage sensor which then energizes the battery charger. The battery then charges until its current decays to less than I_1 at which time the charger flipflop is reset and the charger deenergized.

In the event of loss of solar array orientation or entry into an eclipse, the sun sensor signal is lost and the discharge switch closes. The line booster and battery charger remain off. Upon reacquisition of the sun or emergence into sunlight, the line-boosting functions and subsequent battery-charging functions are repeated. If an overload or marginal solar array capability exists, the battery shares the load with the solar array through the discharge diode. The bus voltage decreases to less

than V_C , the charger is deenergized and, assuming correct solar array orientation, the line booster is energized. After the line booster time delay, the line booster is reset, immediately energized again, and continues to cycle on and off until corrected by ground command. In all cases, the load is satisfied by the combined solar array and battery capability with the battery discharging primarily through the discharge diode and also through the line booster during its "on" periods. The design of the line booster controls could be implemented in such a manner that this cycling condition would be terminated automatically. This added complexity, however, has not been included in the design for this study.

Figure 34 illustrates the operating conditions for this system with two methods of implementing the battery charger function. The first of these employs a charge regulator of either the dissipative or pulsewidth modulated type. The load line shown (with charge regulator) is based on an assumed allowance for battery charging, between the maximum power Point D on the maximum AU solar array curve, and the load line. The intersection of this load line with the minimum AU solar array characteristic at Point C defines the maximum permissible battery voltage. The shaded area between the minimum charging voltage, V_C and Point C, indicates the available battery-charging capability of the minimum AU solar array.

By using a charge regulator for the battery in this scheme, the increased power capability of the maximum AU solar array at higher voltages can be effectively utilized, since the regulator will isolate the solar array voltage from that of the battery during charging. After an eclipse, the solar array capability at maximum AU will rise to the point where it supplies its available current at minimum battery voltage, designated at Point B. The corresponding load requirement at this voltage is Point A. The line booster will then be energized to force the solar array voltage to a sufficiently high level to permit it to supply the total load and recharge the battery at Point D.

For the same assumed solar array characteristics, the maximum load capability and battery-operating voltages for a simple resistor, battery charge current limiter are also shown. The solar array voltage is constrained by the battery voltage. The load line (with charge resistor)

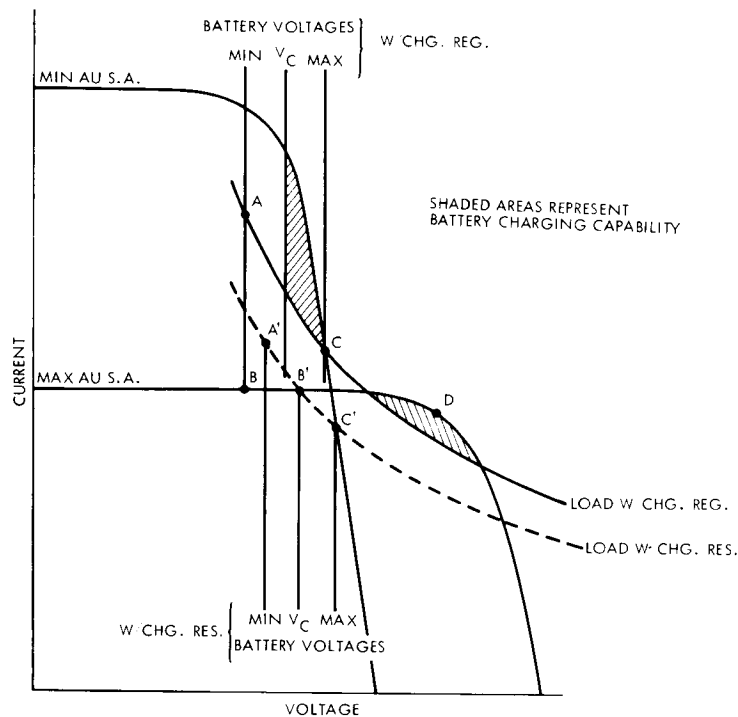


Figure 34. System Operating Points for Bucking Charger With Line Booster

is seen to intercept the minimum AU solar array capability at maximum battery voltage and the maximum solar array capability at the minimum charge voltage of the battery. The action of the line booster is to force the bus voltage from the initial operating condition at Point A', Figure 34, to a voltage equal to or greater than the minimum charge level Point B'. This will permit the battery to charge to its maximum at Point C'.

3.3.2.3 Boost Charger

Figure 35 illustrates the battery controls for a boost charger. An important difference between this system and the bucking charger systems is that a discharge diode would short circuit the charger and cannot be used. All requirements for battery support of the main bus load must be handled by the discharge switch. Clearly, the response of this switch, in the event of an overload condition, would produce transient under-voltage of the main bus until the switch closed to permit the battery to support the overload. This, however, is an abnormal condition and any

In the event of a reduction in solar array capability to the point where the solar array may no longer support the load, the bus voltage falls and the discharge switch closes as the bus voltage reaches the battery discharge plateau level ($<V_C$). Closure of the discharge switch sets the flipflop to enable subsequent turn-on of the boost charger upon recovery of solar array capability.

The boost charger permits optimizing the battery voltage range for higher solar array voltage capabilities at maximum sun-spacecraft distance. Since the maximum solar array operating voltage may exceed the battery maximum charge voltage, the boost charger normally must also have a bucking capability to limit battery-charging current and voltage. The advantages offered by this system are that at maximum AU conditions the solar array can take over the load from the battery at a higher minimum battery voltage, and the voltage difference between the unregulated main bus and the battery may be reduced in comparison to the straight bucking system, with an attendant improvement in charger efficiency. This is particularly true in comparing the boosting system with the simple dissipative bucking chargers.

Figure 36 illustrates the operating conditions for this type of battery control. The load line represents the maximum load relative to the solar array capability that can be supported. The presence of a boost charger permits setting the maximum voltage at a level higher than that which can be provided by the minimum AU solar array. However, the solar array capability does constrain the minimum charging voltage of the battery to the point at which the solar array can just support the load, Point B. Similarly, the limited current capability of the maximum AU solar array constrains the range of operating voltages to Point A, where the solar array can just support the load at minimum voltage. Adequate hysteresis must be provided in the bus voltage sensor as indicated by V_D , which must be at a level less than V_C so that the minimum AU solar array may operate at voltages less than V_C in order to recharge the battery through the boost charger. The shaded areas again represent the available battery-charging capability for the two solar array characteristics.

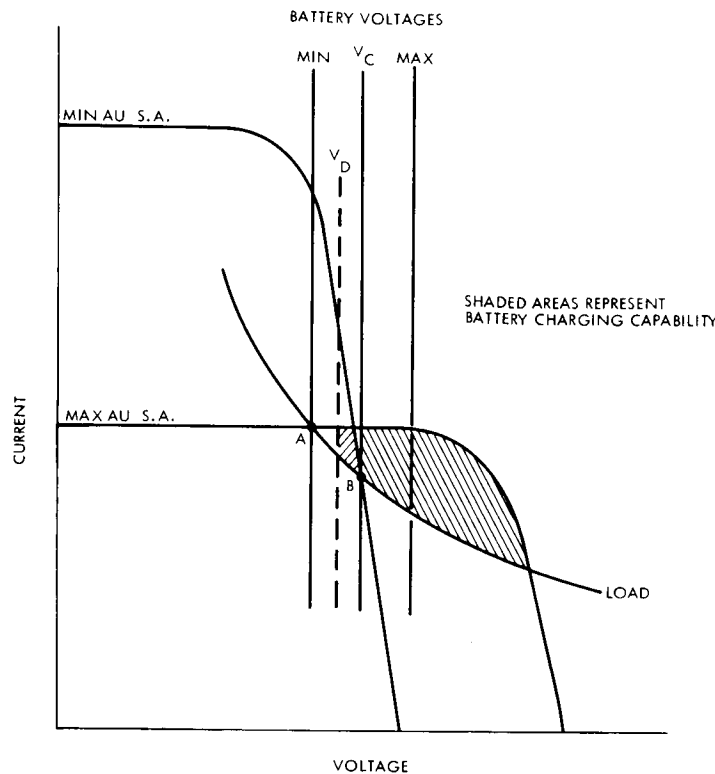


Figure 36. System Operating Points for Boost Charger

3.3.2.4 Boost Charger with Line Booster

Figure 37 represents the boost charge system with a momentary line booster added to permit the solar array to take over the load from the battery at a higher bus voltage. The difference between this configuration and the similar bucking charger configuration shown in Figure 33 is that the control of the discharge switch cannot be based strictly on the sun sensor signal which indicates that the solar array is oriented. If this were done, in the absence of a discharge diode, sharing between the solar array and battery would not be possible in sunlight conditions. As a result, the primary control method for the discharge switch is the sensing of main bus voltage. When the voltage is greater than the minimum charge voltage (V_C), the discharge switch is always open. If at any time the bus voltage is not greater than V_C and the line booster is not energized, the discharge switch is closed.

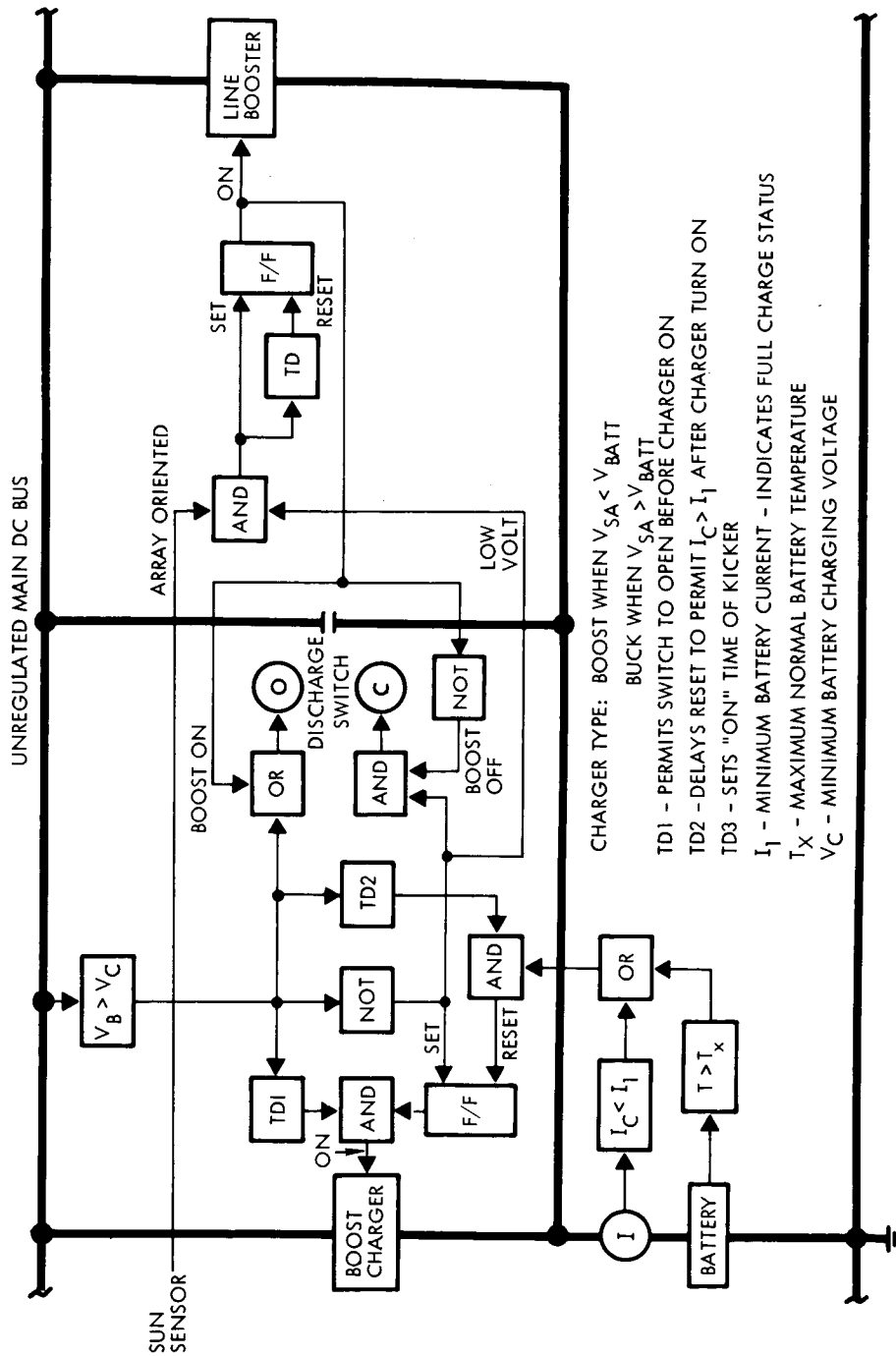


Figure 37. Battery Controls Block Diagram Boost Charger, Discharge Switch, and Line Booster

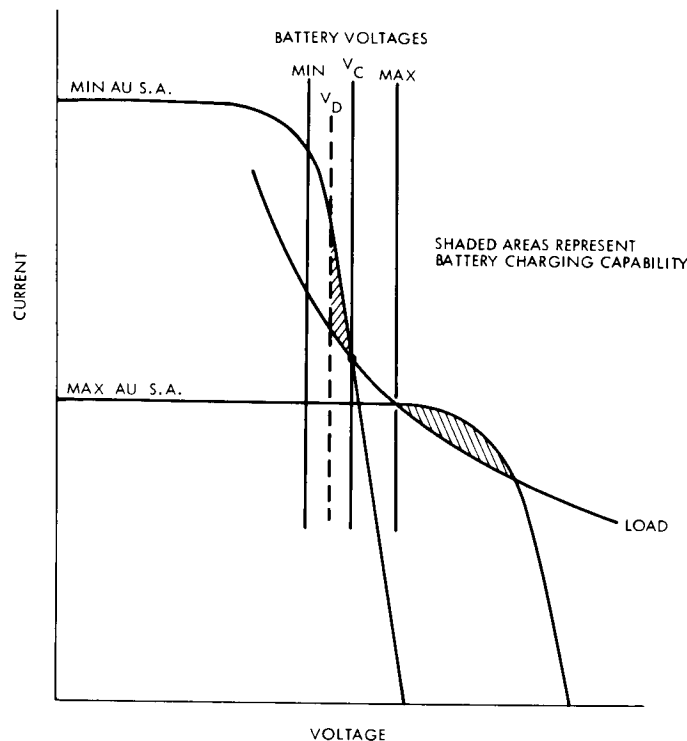


Figure 38. System Operating Points for Boost Charger with Live Booster

As a result, upon entry into sunlight after a maneuver, after receiving the array-orientation signal from the sun sensor, the line booster is energized and the discharge switch is open. The action of the line booster increases the solar array voltage to the point where the solar array can take over the load from the battery. This is indicated by the bus voltage rising to a value of greater than V_C , which in turn energizes the boost charger. TDI delays turn-on of the boost charger until after the line booster has been deenergized. In all other respects, such as control of the boost charger and charge termination by battery current sensing or overtemperature, the system is identical to those previously described.

The operating points for this system are illustrated in Figure 38. The addition of the line booster permits maximum use of the power capability of the maximum AU solar array, as shown in the figure. The load line is based on the maximum power point of this solar array characteristic with some arbitrary allowance for battery charging. The addition of the line booster in a boost charger system produces a reduction in

the levels of battery voltage relative to that of the solar array. As a result, some decrease in battery charging efficiency would be expected at minimum AU conditions. However, the improved utilization of the solar array capability, for both maximum and minimum AU conditions, far offsets any decrease in battery charging efficiency. The minimum AU solar array characteristic constrains the battery voltage at its minimum charging voltage to that voltage at which the solar array is just capable of supporting the load. Here again, voltage sensor hysteresis is represented by V_D , which is set below the minimum charging voltage so that the battery charger can make use of the increased solar array power capability at voltages less than V_C to charge the battery.

3.3.2.5 Bucking Charge Regulator with Boosting Discharge Regulator

Figure 39 illustrates the battery control logic for those systems utilizing a regulated main dc bus. The battery always discharges through a boost regulator to the main bus and the control logic is simply that required to terminate battery charging. This consists of a battery charge current sensor and overtemperature sensor and a charger control flip-flop circuit. The flipflop is necessary in order to prevent reenergizing the charger, after it has once been deenergized upon completing battery charging. The signal used to set the charger control flipflop is derived from the battery discharge regulator. Whenever the regulator is operative the set signal for the flipflop is present. As a result, at any time the battery power is required to support the load the charger flipflop will be set so that subsequently battery charging can occur. The operating points for this type of system are not illustrated, because the only constraint imposed by these battery controls is that the regulated main bus voltage be greater than the maximum battery voltage. As a result, with appropriate solar array controls, this regulated voltage can be established at the desired value to optimize the system with respect to solar array capability.

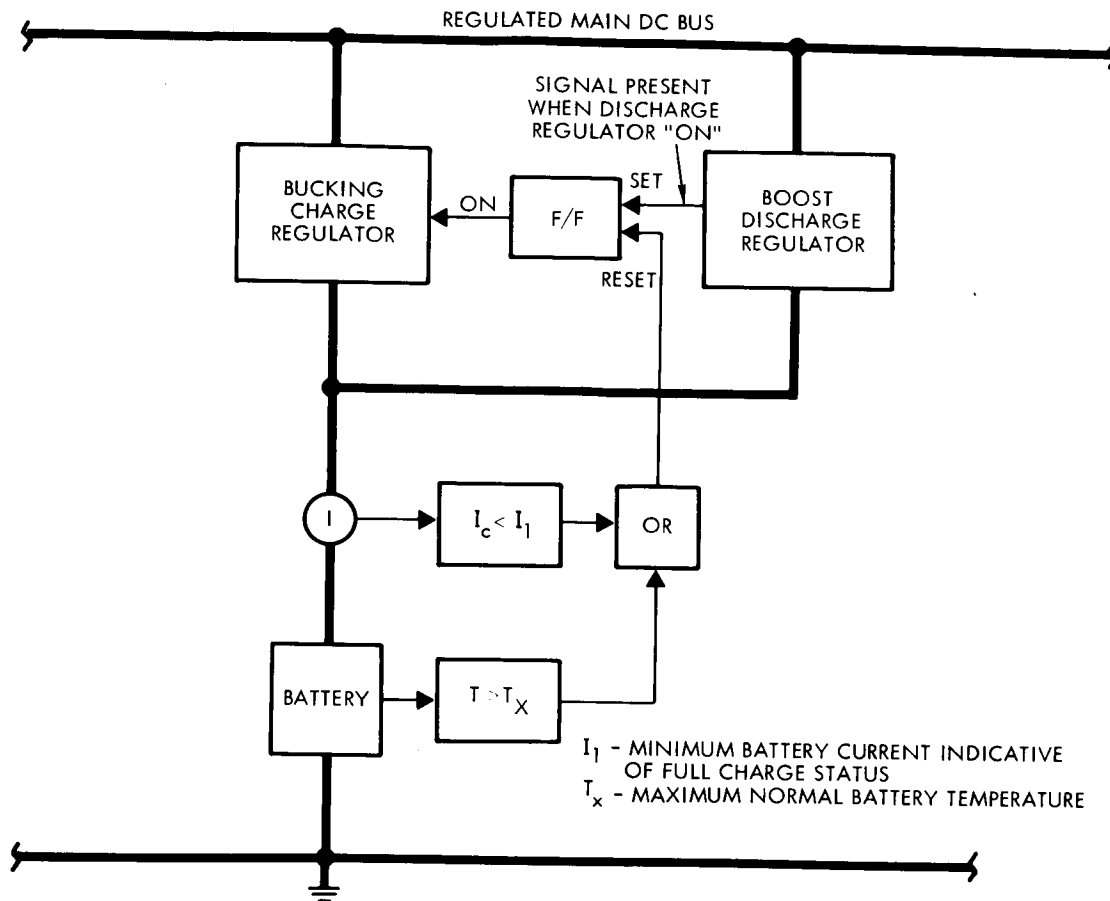


Figure 39. Battery Controls Block Diagram Bucking Charge Regulator, Boost Discharge Regulator

3.3.3 Solar Array Control Implementation

The solar array control functions consist of two principal types for the five basic functional system configurations (Figure 9). For all of the unregulated bus systems, the need for solar array control consists primarily of a need for voltage limiting of the solar array. The purpose of voltage limiting varies from system to system within the unregulated bus category but is principally required either to prevent an overvoltage condition of the regulated output bus or to limit the maximum voltage that will be applied to the battery or unregulated bus load equipment. In the regulated bus systems, the solar array control function may be a voltage limiter or a buck-boost voltage regulator.

3.3.3.1 Voltage Limiters

Voltage limiters used for solar array control may be either shunt or series types. Each of these may be either of the switching (pulse-width modulated) type or of the dissipative type. In general, the dissipative voltage limiter is less complex and has better response than its pulsewidth modulated counterpart. On the other hand, the dissipative regulator may penalize the system design in that its potentially large heat dissipation may introduce serious thermal control problems in the spacecraft. In addition, the dissipative type, if used in the series configuration, introduces a serious inefficiency in the power system. Series dissipative voltage limiters used as solar array controls were not considered for the study because of the relatively large range of solar array voltages that would be encountered and the resultant poor efficiency of the dissipative regulator.

Dissipative shunt regulators have found extensive application in a variety of spacecraft. The simplest application of this approach is the use of zener diodes to limit the solar array output voltage directly. A more accurate voltage limit can be achieved by sensing output voltage and controlling an active shunt element. This element in turn may be of either a dissipative or switching type. If connected in shunt with the entire solar array, the dissipative type must handle the maximum difference in power between the solar array capability at its voltage limit and the load demand. For the larger power systems under consideration in this study, this approach would be inappropriate because of the thermal control problems that would result.

Although a variety of designs have been considered for switching shunt regulators to eliminate thermal control problems, none has been developed thus far. In applying the dissipative shunt limiters to spacecraft systems, several methods have been developed to minimize their heat dissipation, and to minimize the effects of the dissipation on the spacecraft thermal control system. These methods consist chiefly of shunting only a portion of the series-connected solar cells in an array and controlling only a portion of the parallel-connected solar cells where possible to minimize the maximum dissipation of the shunt element. A further

variation of this approach is the use of the sequential shunt regulator scheme which employs several parallel-shunt regulated sections, with the sections controlled in a sequential manner such that one section will be limiting the array at a time. The remaining parallel sections will be either in a saturated or open-circuit condition.

Further techniques to minimize the impact of the shunt regulator on the spacecraft thermal control system have included mounting the heat dissipating elements externally to the spacecraft equipment compartment to permit direct radiation of their heat to space. In other cases, the shunt elements have been installed within the spacecraft and their localized heat dissipation minimized by distributing the shunt elements through the equipment compartment.

The implementation of a shunt voltage limiter scheme, for the missions under consideration, should include consideration of switching sections of the solar array during the course of the mission. An outstanding example where such solar array switching provisions would appear to be advantageous is the Jupiter missions. In this mission the 97 percent reduction in solar array capability from its initial capability at Earth to end-of-life would clearly present an unreasonable problem if shunt regulation techniques were used to control the entire array. Alternately, for these types of missions, if a spacecraft configuration employed an oriented-solar array, the solar array could be tilted away from the sun until needed, as done for Mercury mission configurations selected for this study to prevent excessive solar array temperatures. In considering the problems associated with orienting a very large solar array, however, a third alternative may be considered: delaying the deployment of sections of the array until needed in the mission.

Pulsewidth-modulated series regulators may be further divided into two categories for voltage-limiting applications. In the first category, the voltage limiter senses output voltage and adjusts the duty cycle of the series-switching element to maintain the desired output limit. With this approach, if the output voltage is less than the voltage limit, as in the case of the unregulated bus system configurations, the series switching element is driven into saturation and the limiter has the characteristic

of a small constant voltage drop between the solar array and the main bus. The second category of this basic approach is that of a series-voltage limiter controlled to provide maximum solar array power tracking capability. Properly designed, this approach permits nearly full utilization of the solar array maximum power capability despite its variations in magnitude and voltage as a function of solar intensity and array temperature. In those operating conditions where the maximum power capability of the array is not needed to support loads or charge batteries, a series regulator of this type reverts to a simple voltage-limiter.

A major advantage of the pulsewidth-modulated series regulators is the fact that this mode of operation causes excess solar array power capability to be rejected at the solar array rather than converting this power into heat within the regulator. As a result, the thermal interface between this type of regulator and the spacecraft is not a serious problem.

3.3.3.2 Buck Boost Voltage Regulator

The use of a buck-boost voltage regulator on the solar array eliminates constraints imposed on selection of the regulated main bus voltage by the solar array itself. At minimum AU conditions, when the solar array voltage is relatively low, the buck-boost voltage regulator would function in a boosting mode. At maximum AU condition, when the lower operating temperature of the array produces a higher voltage capability, the array control will operate in a bucking mode. This system permits establishing the regulated bus voltage level at a voltage consistent with the maximum power capability of the solar array at the critical design point. Properly implemented, it could also be utilized as a maximum power point tracker. The difference between this type of regulator and the maximum power tracking voltage limiter is the boosting capability of this sixth type of array control which would permit establishing the regulated bus level at a relatively high voltage condition.

3.3.3.3 Selected Methods

The selected alternative methods for implementing the array control functions are as follows:

- No array control
- Zener diode shunt
- Dissipative shunt voltage limiter
- Series pulsewidth-modulated voltage limiter
- Maximum power point tracker (series bucking)
- Series pulsewidth-modulated buck-boost regulator.

Simplified block diagrams of the five array controls are shown in Figures 40, 41, 42, 43 and 26, respectively.

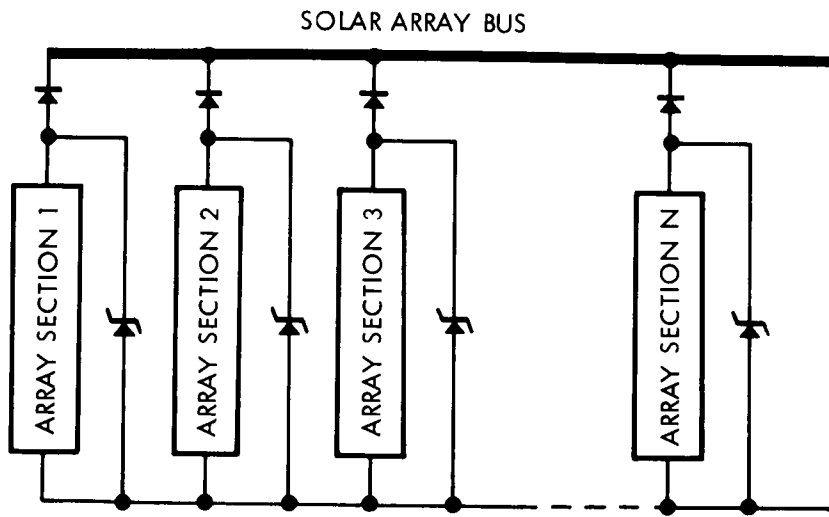


Figure 40. Zener Diode Solar Array Voltage Limiter

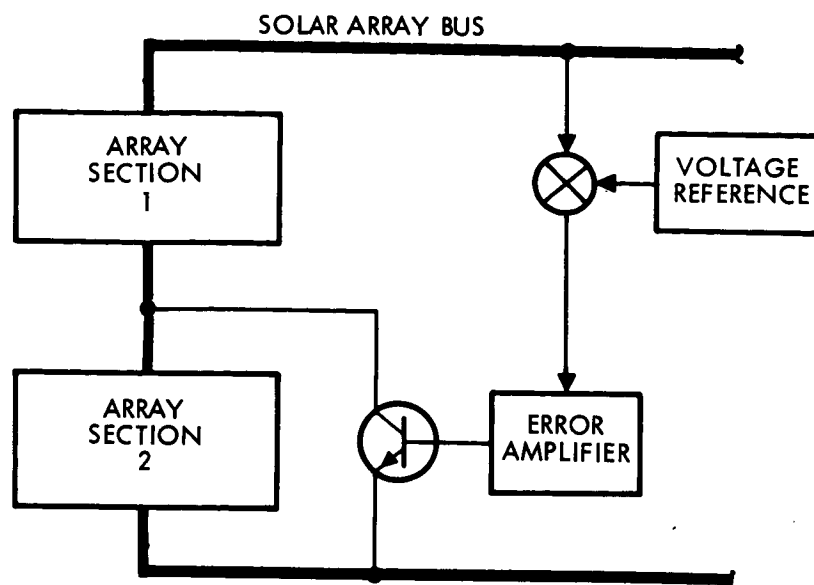


Figure 41. Active Shunt Solar Array Voltage Limiter

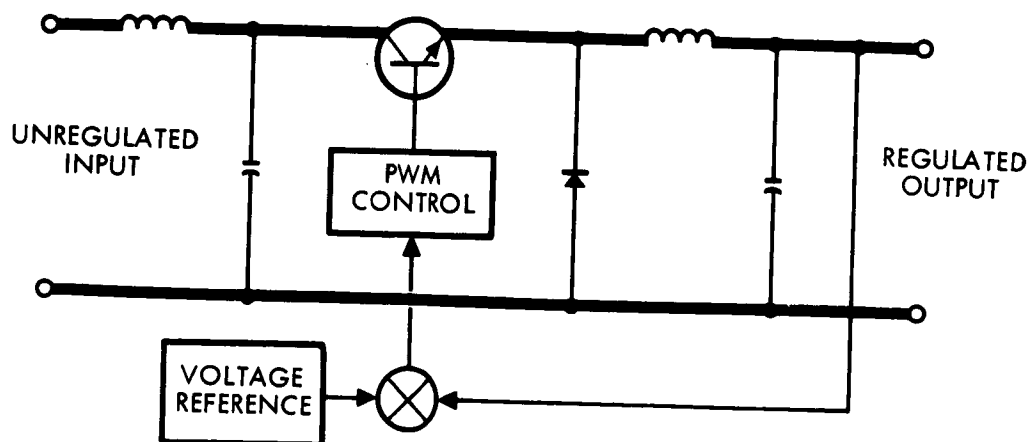


Figure 42. PWM Bucking Solar Array Voltage Limiter or Line Regulator

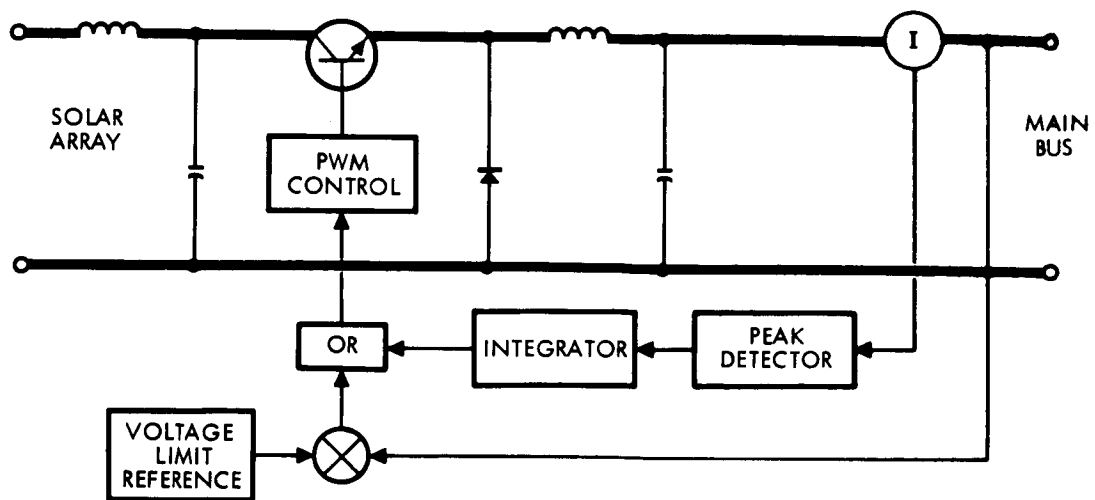


Figure 43. Maximum Power Tracker

3. 4 POWER CONDITIONING ANALYSIS

3. 4. 1 Line Regulators

For those basic functional configurations employing an unregulated bus, the line regulator function is either of the buck, boost, or buck-boost type. These line regulation functions can be incorporated within the load power conditioning equipment, such as converters or inverters. However by centralizing these regulation functions in one higher power unit, the efficiency of regulation can be improved and the reliability, in terms of the total parts required for regulation, can also be improved.

Whereas the boost and buck-boost regulators require pulsewidth modulation techniques to provide a regulated output voltage higher than the input voltage, the bucking regulator could be either a pulsewidth modulated or a dissipative type. However, the dissipative type regulator, discussed previously under array controls, imposes a serious efficiency penalty in the system if the ratio of input to output voltage is large. For this reason, examinations were made of various system configurations and only in those cases where the input voltage could be held to a small variation was the dissipative technique used. It was determined that the configuration under which these conditions applied is that in which the solar array voltage is limited to less than maximum battery voltage and the minimum unregulated bus voltage is the minimum battery voltage. Such a configuration would require a boost charger.

With the dissipative line regulator, the unregulated bus load becomes a constant current characteristic as a function of voltage as opposed to the constant power characteristic produced with the use of pulsewidth modulated line regulation techniques. Simplified block diagrams of the selected line regulators are illustrated in Figures 26, 30, 42, and 44.

3. 4. 2 Load Power Conditioning Equipment

Although a detailed analysis of load power-conditioning equipment was not within the scope of this study, it was considered essential to include a simplified investigation of these functions in order to more realistically assess overall system reliability and the impact of the efficiency of the load-conditioning equipment on the sizing of the power system elements. It was further desired that, in the comparison of

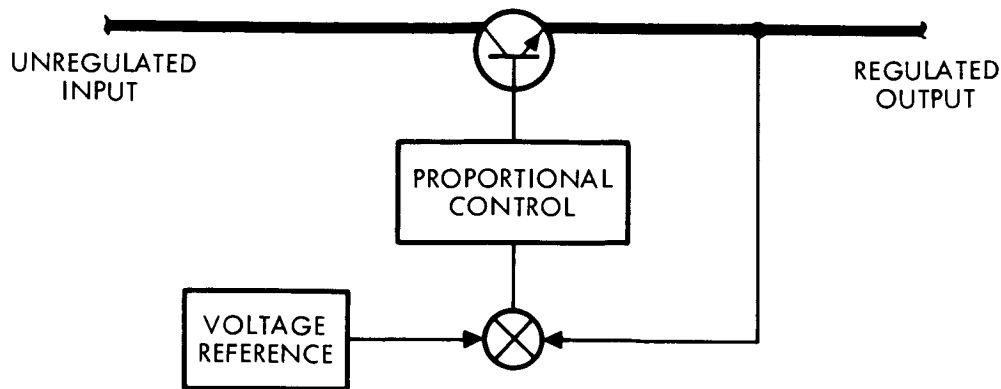


Figure 44. Dissipative Line Regulator

various system approaches, the relative advantages of ac distribution and dc distribution be evaluated. Several simplifying assumptions were made and a dc distribution configuration was selected as well as an ac distribution configuration for purposes of system analysis.

Although the load power conditioning equipment has not been considered part of all power systems in the past, it is essential that power system analyses include tradeoffs of conditioning equipment efficiency, weight and reliability with respect to their impact on the system weight and reliability to select an optimum system configuration. As in the case of the line regulation function described previously, centralizing the power conditioning equipment will normally lead to improved efficiency, lighter system weight and a reduction in the number of parts which increases system reliability.

In order to implement centralized load power conditioning, however, it is necessary that standardization of voltage requirements be established for the load equipment. In addition to improving system reliability by reducing the number of output stages required in the load power conditioning equipment, this approach also permits increasing the power handling capability of each of the stages. The result of increasing the power handled by individual items of conditioning equipment is an efficiency improvement attributable normally to the smaller ratio of standby losses to output power. Such standardization was considered in assigning voltages and regulation tolerances to the various load equipments for each of the model spacecraft. The selected standardized voltages of ± 20 volts, ± 16 volts,

and ± 6 volts reflect reasonable levels required in the design of the electronic load equipment considered. In recent applications of this standardized secondary voltage approach to an actual spacecraft applications, the selected voltages were slightly different from those used in this study. The fundamental concept, however, is the same and the six standardized voltages selected here are considered representative of practical application of this approach.

In general, four groups of equipment were excluded from this standardized centralized power conditioning approach. These were the transmitter converter which usually requires inputs of 1000 v or greater, the gyros which were assumed to require 400 Hz 3-phase power, and certain of the experiments which require voltages higher than 20 v or less than 6 v. The major simplifying assumption made in the analysis of load power conditioning equipment was that voltage regulation requirements of the loads to closer than ± 5 percent would not be included in this equipment. Since all of the power system configurations generate a regulated dc bus, the power conditioning equipment was simplified to consist of converters, inverters and transformer rectifier units which are unregulated.

In a real design application, the specific regulation requirements of each of the loads must be evaluated in defining the power conditioning equipment. Frequently, both line and load regulation functions can be combined in a given item of load power conditioning equipment, such as a dc-dc converter with an attendant improvement in efficiency, weight, and reliability, over the use of a separate line regulator as assumed for this study. In support of the assumption made for this study, however, it has been determined that when several loads are energized from a common secondary dc bus, isolation requirements and the sensitivity of the loads to noise generated on that bus by other loads (whether real or imagined) often lead to an input filter design for the particular load which is of an active type. The existence of such an active filter permits its use as a regulator and as a result, regulation to closer than ± 5 percent can be realistically assumed to be part of the load equipment. However, this is not necessarily the preferred approach for all applications.

Similarly, the assumed use of a separate line regulator is based primarily on maximizing the power handled by this function to improve its efficiency. A significant tradeoff exists between this approach and the improved efficiency resulting from combining this function with other regulation functions within the load power conditioning equipment. Therefore a rigorous analysis of voltage requirements and regulation requirements of each of the loads, and the implementation of conversion, inversion, rectification, transformation and/or regulation functions in an optimum manner is essential for optimizing any power system, regardless of where the actual circuitry that performs these load power conditioning functions is located.

Identification of the specific load power conditioning equipment for both ac and dc distribution approaches for each of the model spacecraft is shown in Tables 10 to 16. For dc distribution, these are divided normally into a main converter which supplies the standardized secondary voltage requirements of the majority of the load equipment, a transmitter converter, a gyro inverter, and auxiliary high voltage or low voltage converters to supply those loads not compatible with the standardized secondary voltages. Nonstandard power requirements of less than 1 w were excluded from these analyses and it was assumed that the necessary power conditioning in these few cases was a part of the load and included in the load power requirement.

As stated previously, all of these converters were assumed to be unregulated for purposes of this study. As a result, with a regulated dc input line at ± 1 percent, it is estimated that with typical temperature and load variations, a ± 3 to 5 percent regulation at the converter outputs is available. A block diagram of the selected load power conditioning equipment configuration is illustrated in Figure 45. This configuration is common to all baseline system configurations employing the dc distribution approach. A block diagram of the selected converter design is illustrated in Figure 46.

For the ac power distribution case, Figure 47, a central unregulated squarewave inverter was assumed to supply the major portion of the loads through transformer rectifier units. The transformer-rectifier units (TR's) were configured to combine as much power as possible in a main TR which

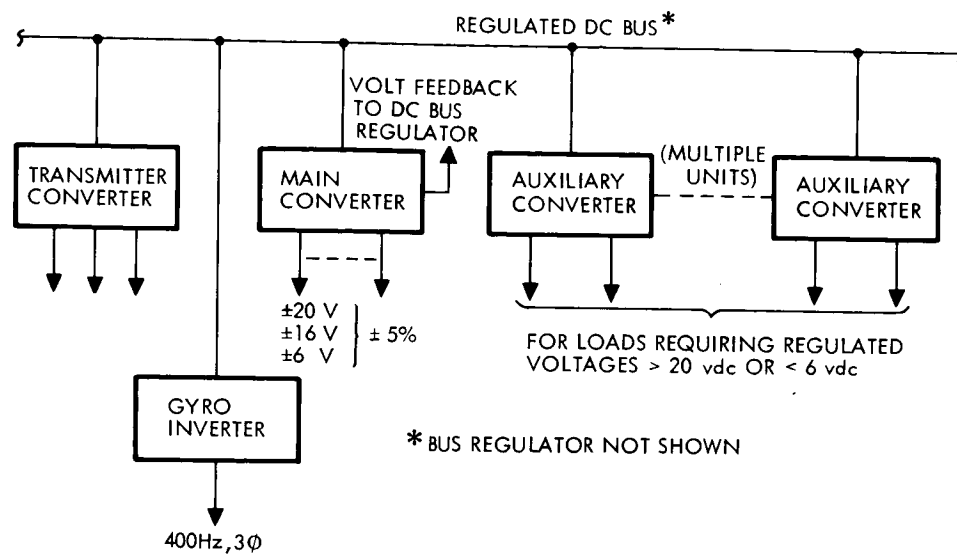


Figure 45. Block Diagram of Load Power Conditioning Equipment Configuration—DC Distribution

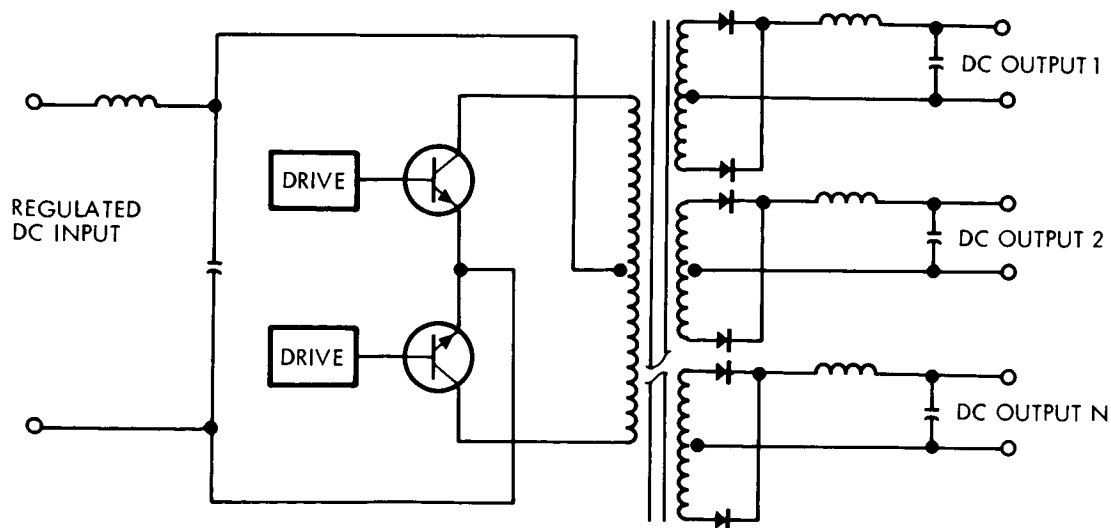
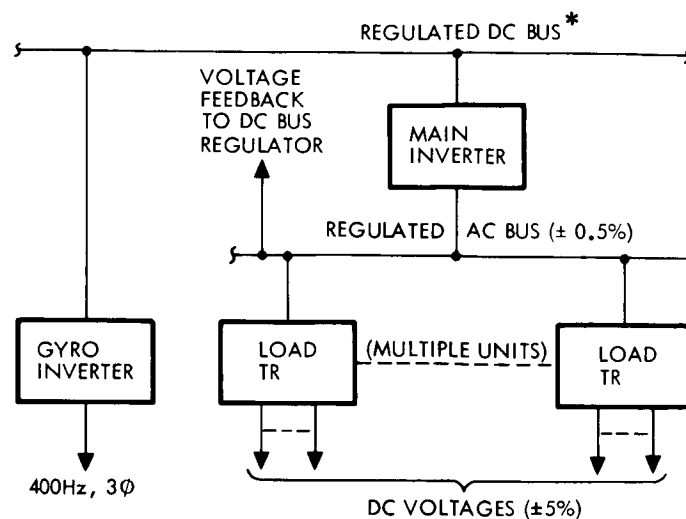


Figure 46. Block Diagram Unregulated DC-DC Converter



* BUS REGULATOR NOT SHOWN

Figure 47. Block Diagram of Load Power Conditioning Equipment Configuration—AC Distribution

furnished the standard secondary dc voltages common to both ac and dc approaches. Auxiliary TR's were selected to supply nonstandard voltages to the transmitter and experiments as required.

A separate unregulated gyro inverter is included to furnish the required 3φ 400Hz output. It was assumed that both the three-phase and single-phase inverters would supply squarewave outputs. While the large harmonic content associated with this approach tends to increase gyro-motor losses and EMC filtering requirements, the simple squarewave approach yields important advantages in inverter reliability and efficiency in comparison to either a trapazoidal waveform or sinusoidal waveform. This efficiency advantage and its impact on the weight of the solar array and battery in the system were considered more important than the attendant shielding and filtering disadvantages.

One approach to further improve the efficiency of an inverter above that of the simple squarewave approach is to employ a constant duty cycle control of the switching (push-pull) transistors. Such a control would delay turn-on on each half cycle for an interval greater than the storage

time of the transistors and thereby reduce commutation losses. This produces a quasi squarewave output of the inverter stage which also reduces the harmonic content of the generated waveform. Increased filter weight is required after rectification, however, because of the increased ripple of the rectified waveform. In addition, the control of the switching transistors in the inverter requires added circuitry and a resultant decrease in reliability.

It was estimated that the various output voltages of the TR's would be regulated to approximately ± 5 percent for typical temperature and load variations by sensing the ac bus voltage to control the dc line regulator. With this technique, degradation in voltage regulation produced by the main inverter as a function of load and temperature changes is eliminated. This technique improves the output regulation without penalizing the system with respect to either efficiency, weight or reliability. Similarly, referring to the dc system configuration, Figure 45, the output voltage regulation of the main converter is limited by sensing its average transformer flux by means of a separate secondary winding to control the dc line regulator.

Table 10. Mercury Flyby Mission, Load Power Conditioning Equipment

<u>DC Distribution</u>			
<u>No.</u>	<u>Unit</u>	<u>Output</u>	<u>Power Rating</u>
1	Gyro Inverter	26 vac 3 \emptyset , 400 Hz	22 va
2	Main Converter	± 20 , ± 16 , ± 6 vdc	73 watts
3	Transmitter (TWT) Converter	+1500, +300, ± 6 vdc	70 watts
4	TV Converter	+500, +200, ± 16 , ± 6 vdc	17 watts
5	Comp. -Sequencer Converter	± 16 , +6, -3 vdc	5 watts
6	Spectrophotometer Converter	+1000, -16, ± 6 , ± 3 vdc	25 watts

<u>AC Distribution</u>			
1	Gyro Inverter	26 vac, 3 \emptyset , 400 Hz	22 va
2	Main Inverter	1 \emptyset , 6 KHz	*
3	Transmitter TR	+1500, +300, ± 6 vdc	70 watts
4	TV TR	+500, +200, ± 16 , ± 6 vdc	17 watts
5	Equipment TR	± 20 , ± 16 , ± 6 vdc	78 watts
6	Spectrophotometer TR	+1000, -16, ± 6 , ± 3 vdc	25 watts

*Power rating = total input power to TR units.

Table 11. Venus Orbiter No. 1 Mission, Load Power Conditioning Equipment

<u>DC Distribution</u>			
<u>No.</u>	<u>Unit</u>	<u>Output</u>	<u>Power Rating</u>
1	Gyro Inverter	26 vac, 3 ϕ , 400 Hz	22 va
2	Transmitter (Solid State) Converter	+50, \pm 15, \pm 6 vdc	50 watts
3	Main Converter	\pm 20, \pm 16, \pm 6 vdc	94 watts
4	Comp. -Sequencer Converter	\pm 16, +6, -3 vdc	5 watts
5	UV Photometer Exp. Converter	+3000, +35, \pm 20, \pm 10 vdc	5 watts
6	Cosmic Dust Exp. Converter	+12, -6, +3 vdc	2 watts
<u>AC Distribution</u>			
1	Gyro Inverter	26 vac, 3 ϕ , 400 Hz	22 va
2	Main Inverter	1 ϕ , 6 KHz	*
3	Transmitter TR	+50, \pm 15, \pm 6 vdc	50 watts
4	Equipment TR	\pm 20, \pm 16, \pm 6, -3 vdc	99 watts
5	UV Photometer Exp. TR	+3000, +35, \pm 20, \pm 10 vdc	5 watts
6	Cosmic Dust Exp. TR	+12, -6, +3 vdc	2 watts

*Power rating = total input power to TR units.

Table 12. Venus Orbiter No. 2 Mission, Load Power
Conditioning Equipment

<u>DC Distribution</u>			
<u>No.</u>	<u>Unit</u>	<u>Output</u>	<u>Power Rating</u>
1	Gyro Inverter	26 vac, 3 \emptyset , 400 Hz	22 va
2	Transmitter (TWT) Converter	+1500, +300, ± 6 vdc	70 watts
3	Main Converter	± 20 , ± 16 , ± 6 vdc	137 watts
4	Comp. -Sequencer Converter	± 16 , +6, -3 vdc	18 watts
5	TV Converter	+500, +200, ± 16 , 26 vdc	15 watts
6	Bistatic Radar Converter	+1500, ± 6 vdc	3 watts
7	Plasma Probe Exp. Converter	+165, ± 150 , +6 vdc	5 watts

<u>AC Distribution</u>			
1	Gyro Inverter	26 vac, 3 \emptyset , 400 Hz	22 va
2	Main Inverter	1 \emptyset , 6 KHz	*
3	Transmitter TR	+1500, +300, ± 6 vdc	70 watts
4	Equipment TR	± 20 , ± 16 , ± 6 , -3 vdc	155 watts
5	TV TR	+500, +200, ± 16 , ± 6 vdc	15 watts
6	Bistatic Radar TR	+1500 ± 6 vdc	3 watts
7	Plasma Probe Exp. TR	± 165 , ± 150 , +6 vdc	5 watts

*Power rating = total input power to TR units.

Table 13. Mars Orbiter Mission, Load Power Conditioning Equipment

<u>DC Distribution</u>			
<u>No.</u>	<u>Unit</u>	<u>Output</u>	<u>Power Rating</u>
1	Gyro Inverter	26 vac, 3 ϕ , 400 Hz	22 va
2	Transmitter (TWT) Converter	+1500, +300, ± 6 vdc	150 watts
3	Main Converter	± 20 , ± 16 , ± 6 vdc	181 watts
4	TV Converter	+500, +200, ± 16 , ± 6 vdc	26 watts
5	Comp. -Sequencer Converter	± 16 , +6, -3 vdc	18 watts
6	Bistatic Radar Converter	+1500, ± 6 vdc	3 watts
7	Cosmic Ray Exp. Converter	+1000, +16, +6 vdc	10 watts
8	Plasma Probe Exp. Converter	+165, ± 150 , ± 16 , ± 6 vdc	5 watts
<u>AC Distribution</u>			
1	Gyro Inverter	26 vac, 3 ϕ , 400 Hz	22 va
2	Main Inverter	1 ϕ , 6 KHz	*
3	Transmitter TR	+1500, +300, ± 6 vdc	150 watts
4	Equipment TR	± 20 , ± 16 , ± 6 , -3 vdc	199 watts
5	TV TR	+500, +200, ± 16 , ± 6 vdc	26 watts
6	Bistatic Radar TR	+1500, ± 6 vdc	3 watts
7	Cosmic Ray Exp. TR	+1000, +16, +6 vdc	10 watts
8	Plasma Probe Exp. TR	+165, ± 150 , 216, ± 6 vdc	5 watts

* Power rating = total input power to TR units.

Table 14. Jupiter Flyby Mission, Load Power
Conditioning Equipment

DC Distribution

<u>No.</u>	<u>Unit</u>	<u>Output</u>	<u>Power Rating</u>
1	Transmitter (klystron) Converter	+1500, ± 6 vdc	80 watts
2	Main Converter	± 20 , ± 16 , ± 6 vdc	39 watts
3	TV Converter	+500, +200, ± 16 , ± 6 vdc	17 watts
4	Comp. -Sequencer Converter	± 16 , +6, -3 vdc	5 watts
5	Plasma Probe Exp. Converter	+165, ± 150 , ± 16 , ± 6 vdc	2 watts
6	Trap. Radiation Det. Exp. Conv.	+1000, ± 16 , ± 6 vdc	2 watts

AC Distribution

1	Main Inverter	1 \emptyset , 6 KHz	*
2	Transmitter TR	+1500, ± 6 vdc	80 watts
3	Equipment TR	± 20 , 216, 26, -3 vdc	44 watts
4	TV TR	+500, +200, ± 16 , ± 6 vdc	17 watts
5	Plasma Probe Exp. TR	+165, ± 150 , ± 16 , ± 6 vdc	2 watts
6	Trap. Radiation Det. Exp. TR	+1000, ± 16 , ± 6 vdc	2 watts

*Power rating = total input power to TR units.

Table 15. Jupiter Orbiter No. 1 Mission, Load Power Conditioning Equipment

<u>DC Distribution</u>			
<u>No.</u>	<u>Unit</u>	<u>Output</u>	<u>Power Rating</u>
1	Gyro Inverter	26 vac, 3 \emptyset , 400 Hz	22 va
2	Main Converter	± 20 , ± 16 , ± 6 vdc	92 watts
3	Transmitter (TWT) Converter	+1500, +300, ± 6 vdc	35 watts
4	TV Converter	+500, +200, ± 16 , ± 6 vdc	15 watts
5	Comp. -Sequencer Converter	± 16 , +6, -3 vdc	5 watts
6	Auroral Detector Exp. Converter	+3000, ± 16 , ± 6 vdc	2 watts
7	Plasma Probe Exp. Converter	+165, ± 150 , ± 16 , ± 6 vdc	2 watts
<u>AC Distribution</u>			
1	Gyro Inverter	26 vac, 3 \emptyset , 400 Hz	22 va
2	Main Inverter	1 \emptyset , 6 KHz	*
3	Transmitter TR	+1500, +300, ± 6 vdc	35 watts
4	TV TR	+500, +200, ± 16 , ± 6 vdc	15 watts
5	Equipment TR	± 20 , ± 16 , ± 6 vdc	97 watts
6	Auroral Detector Exp. TR	+3000, ± 16 , ± 6 vdc	2 watts
7	Plasma Probe Exp. TR	+165, ± 150 , ± 16 , ± 6 vdc	2 watts

*Power rating = total input power to TR units.

Table 16. Jupiter Orbiter No. 2 Mission, Load Power Conditioning Equipment

<u>DC Distribution</u>			
<u>No.</u>	<u>Unit</u>	<u>Output</u>	<u>Power Rating</u>
1	Gyro Inverter	26 vac, 3 \emptyset , 400 Hz	22 va
2	Transmitter (TWT) Converter	+1500, +300, ± 6 vdc	135 watts
3	Main Converter	± 20 , ± 16 , ± 6 vdc	111 watts
4	Comp. -Sequencer Converter	± 16 , +6, -3 vdc	20 watts
5	Cosmic Ray Exp. Converter	+1000, +16, +6 vdc	10 watts
6	Spectrometer Exp. Converter	+3000, +200, ± 16 , ± 6 vdc	15 watts

<u>AC Distribution</u>			
1	Gyro Inverter	26 vac, 3 \emptyset , 400 Hz	22 va
2	Main Inverter	1 \emptyset , 6 KHz	*
3	Transmitter TR	+1500, +300, ± 6 vdc	135 watts
4	Equipment TR	± 20 , ± 16 , ± 6 , -3 vdc	131 watts
5	Cosmic Ray Exp. TR	+1000, +16, +6 vdc	10 watts
6	Spectrometer Exp. TR	+3000, +200, ± 16 , ± 6 vdc	15 watts

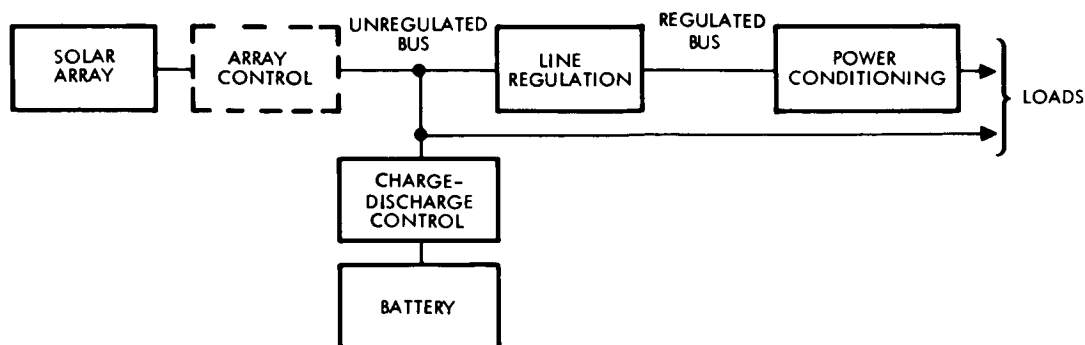
*Power rating = total input power to TR units.

3.5 SELECTION OF BASELINE SYSTEM CONFIGURATIONS

Based on the preceding analyses of alternative methods of implementing the power system regulation, control and conditioning provisions, each of the five basic functional configurations (Figure 9) was analyzed to select appropriate methods of implementing its various functions. The results of these analyses are shown in Figures 48 and 49. The variations from system to system are primarily in the array control and battery control approaches. Additional investigations were then made to determine logical combinations of these alternative control methods in each of the basic functional configurations to define baseline system configurations.

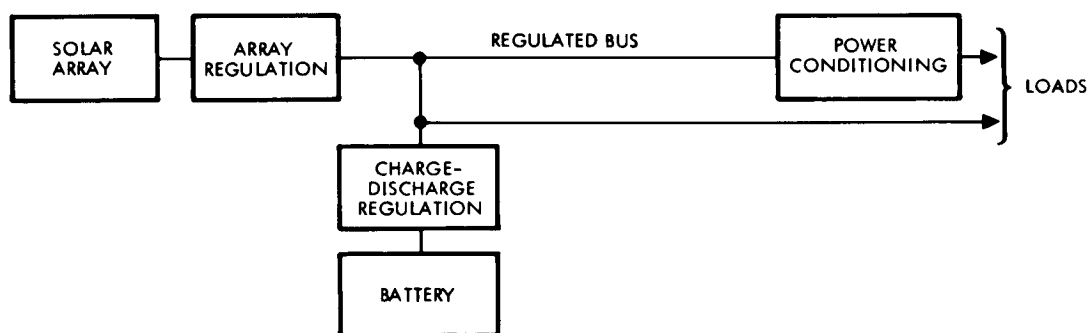
The selected baseline power system configurations are summarized in matrix form in Table 17. Since the study approach was based on utilizing a computer program to subsequently evaluate the reliability and weight of the alternative power system configurations for each model spacecraft, only those cases where specific combinations of regulation and control methods appeared illogical were excluded. As a result, the selected baseline system configurations represent a relatively large number of candidates (approximately 150). The need for the computer in evaluating this number of systems for each of the seven missions becomes readily apparent. Many of the candidate system configurations appear to be non-optimum because of their complexity or inefficiency in comparison to other systems. Qualitative judgements such as these, however, were excluded wherever possible in the study to permit more valid quantitative reliability and weight comparisons of the various systems.

In Table 17, the uncircled numbers listed in each matrix cell reflect the appropriate array controls that are compatible with the line regulator and battery control which define the particular cell. The circled numbers within each cell refer to Table 18 which lists the reasons for deleting certain of the possible combinations of regulators and controls in defining these baseline systems. These deletions reflect cases where it appeared illogical to combine certain of the power control or regulation functions in the same system or where one control in a system depends on a specific



<u>ARRAY CONTROL</u>	<u>LINE REGULATION</u>	<u>BATTERY CONTROL</u>
CONFIGURATION 1A:	CONFIGURATION 1A:	(ALL CONFIGURATIONS)
<ul style="list-style-type: none"> • ZENER DIODE SHUNT • ACTIVE SHUNT • PWM SERIES BUCK • MAX. POWER TRACKING SERIES BUCK 	<ul style="list-style-type: none"> • PWM SERIES BUCK • DISS. SERIES BUCK 	<ul style="list-style-type: none"> • SWITCH & RESISTOR • SWITCH, RESISTOR & DISCHARGE BOOSTER
CONFIGURATION 1B AND 1C:	CONFIGURATION 1B:	<ul style="list-style-type: none"> • DISS. CHARGER • DISS. CHARGER & DISCHARGE BOOSTER • PWM (BUCK) CHARGER • PWM (BUCK) CHARGER & DISCHARGE BOOSTER • BOOST CHARGER • BOOST CHARGER & DISCHARGE BOOSTER
<ul style="list-style-type: none"> • NONE • ZENER DIODE SHUNT • ACTIVE SHUNT 	CONFIGURATION 1C:	
	<ul style="list-style-type: none"> • PWM SERIES • BUCK-BOOST 	

Figure 48. Selected Alternative Methods of Implementing Basic Functional Configurations Having Unregulated Main Bus



<u>ARRAY REGULATION</u>	<u>CHARGE REGULATION</u>	<u>DISCHARGE REGULATION</u>
CONFIGURATION 2A:	<ul style="list-style-type: none"> • DISSIPATIVE SERIES REGULATOR • PWM SERIES BUCKING REGULATOR 	PWM BOOST REGULATOR
<ul style="list-style-type: none"> • ACTIVE SHUNT VOLTAGE LIMITER • PWM SERIES BUCKING, VOLTAGE LIMITER • BUCKING MAX. POWER TRACKER-VOLTAGE LIMITER 		
CONFIGURATION 2B:		
<ul style="list-style-type: none"> • BUCK-BOOST REGULATOR 		

Figure 49. Selected Methods of Implementing Basic Functional Configurations Having Regulated Main Bus

Table 17. Summary of Selected Baseline Power System Configurations

Note

- Each configuration (combination of battery control, line regulator and array control) may be used with either AC or DC distribution.
- Applicable array controls indicated by uncircled numbers in each cell.
- Circled numbers in each cell designate reason for deleting certain configurations as listed in Table 18.

**ARRAY
CONTROL
LEGEND**

1. None
2. Zener
3. Active Shunt
4. PWM Buck Series
5. PWM Buck Series + P_{max} Track
6. PWM Series Buck-Boost

BATTERY CONTROLS

		LINE REGULATION				
		1	2	3	4	5
		PWM Buck Line Reg	Diss Line Reg	Boost Line Reg	Bk-Boost Line Reg	No Reg
1	Switch + Resistor	3 (7)(9)	NA (3)	3, 4, 5 (7)(12)	3 (7)(9)	NA (2)
2	Same + Dischg Booster	3 (7)(9)	NA (3)	3, 4 (7)(11)(12)	3 (7)(9)	NA (2)
3	Dissipative Chg'r & Dischg. Sw.	1, 2, 3 (9)	NA (3)	2, 3, 4 (6)(10)(12)	1, 2, 3 (9)	NA (2)
4	Same + Dischg. Booster	1, 2, 3 (9)	NA (3)	2, 3, 4 (6)(11)(12)	1, 2, 3 (9)	NA (2)
5	PWM Buck Chg'r & Dischg. Sw.	1, 2, 3 (9)	NA (3)	2, 3, 4 (6)(10)(12)	1, 2, 3 (9)	NA (2)
6	Same + Dischg. Booster	1, 2, 3 (9)	NA (3)	2, 3, 4 (6)(11)(12)	1, 2, 3 (9)	NA (2)
7	PWM Boost Chg'r & Disch. Sw.	1, 2, 3 (9)	2, 3 (5)(9)	2, 3, 4, 5 (6)(12)	1, 2, 3 (9)	NA (2)
8	Same + Dischg. Booster	1, 2, 3 (9)	NA (4)	2, 3, 4 (6)(11)(12)	1, 2, 3 (9)	NA (2)
9	Diss. Chg. & Boost Dischg. Regulators	NA (1)	NA (1)	NA (1)	NA (1)	3, 4, 5, 6 (8)
10	PWM Buck Chg. & Boost Dischg. Regulators	NA (1)	NA (1)	NA (1)	NA (1)	3, 4, 5, 6 (8)

ARRAY CONTROL LEGEND

1. None
2. Zener
3. Active Shunt
4. PWM Buck Series
5. PWM Buck Series + P_{max} Track
6. PWM Series Buck-Boost

Table 18. Justifications for Deletions of Power System Configurations

1. Not applicable. Array and battery controls provide regulated bus. Additional line regulation not required.
2. Not applicable. Required bus voltage regulation cannot be provided by these battery controls.
3. Not applicable. Power loss in line regulator with maximum voltage at unregulated bus considered excessive.
4. Not applicable. Series dissipative regulator tends to produce constant current load and eliminate possibility of undesirable load sharing.
5. Array Control 1 deleted. Unregulated bus voltage must be limited to minimize voltage drop across dissipative line regulator.
6. Array Control 1 deleted. Must limit unregulated bus voltage to prevent overvoltage at regulated bus.
7. Array Controls 1 and 2 deleted. Active regulator required by battery charge control to provide accurate voltage limit.
8. Array Controls 1 and 2 deleted. Will not provide required $\pm 1/2$ percent bus voltage regulation.
9. Array Controls 4, 5, and 6 deleted. Illogical to use two series bucking regulators in series.
10. Array Control 5 deleted. Illogical to use line regulator if solar array output well regulated. With bucking charge control, array voltage must always exceed battery voltage. Boosting required only during battery discharge and should be included in battery controls.
11. Array Control 5 deleted. Illogical to use discharge booster with maximum power tracking solar array control. Both prevent undesirable load sharing between array and battery.
12. Array Control 6 deleted. Illogical to use two boost regulators in series.

performance characteristic in another. Examples of these are the boost-line regulator systems which require some type of a voltage limiting of the unregulated bus to prevent overvoltage at the line regulator output, or the current-limiting resistor for battery charge control which requires that the applied voltage be controlled by limiting the unregulated bus voltage.

Item 4 of Table 18 refers to the possibility of undesirable battery load sharing at the low end of the unregulated bus voltage range due to the higher current required at this condition by a constant power load characteristic. Since the dissipative regulator functions only as a controlled series resistance to maintain a given output voltage limit, its input current is determined only by the output load for an assumed constant output voltage. As such, the input current is independent of the unregulated bus voltage and undesirable load sharing does not occur.

Item 5 of Table 18 reflects the fact that with a given load the power loss in the series dissipative regulator is a direct function of the input voltage. It was not considered logical, therefore, to use this approach in those systems having a large variation in unregulated bus voltage because of the severe penalty in system efficiency that would result.

Item 7 reflects the need to limit the applied voltage more accurately than can be achieved by the simple zener diode approach to assure full charge of the battery and simultaneously prevent excessive battery voltage. Similarly, as indicated by Item 8, the lack of an array regulator or the use of the simple zener diode approach is not compatible with the assumed $\pm 1/2$ percent bus voltage range of the regulated bus systems.

Item 10 indicates that if a boosting function is required only during those periods of time when the battery is discharging, it is illogical to place this boost regulator in series with the solar array and incur the attendant penalty in system efficiency during sunlight operation, which constitutes the major portion of the total time for any mission.

Item 11 shows that with a maximum power tracking solar array control, the solar array operating voltage is always higher than the voltage of the unregulated bus. This type of array regulator must have the capability of causing the solar array to operate at that voltage corresponding to its maximum power capability.

3.6 SOLAR ARRAY POWER UTILIZATION

As previously discussed under the battery control analysis, those systems which employ an unregulated main bus and a pulsewidth-modulated line regulator and do not include a line booster require that the solar array be designed with the capability of supporting the entire load from near minimum battery voltage to maximum solar array operating voltage. Since the major portion of the load power is usually supplied through a PWM line regulator, it is valid to assume that the characteristic current variation of the load on the unregulated bus as a function of voltage is that of a constant power characteristic. Consequently, the increased load current at the lower voltages requires that the solar array current capability be adequate to support the load at these reduced voltages. This normally produces an excess solar array power capability at higher voltages up to its maximum power point.

A portion of the excess solar array capability at these higher voltages is normally required to charge the battery. For the missions under consideration, the charging power requirements are relatively small compared to this excess array capability and, therefore, the solar array power capability is not efficiently utilized. To minimize the size of the solar array, it is necessary that the maximum power capability of the array be fully utilized at the critical point in the mission. Conversely, those systems which do not make use of the maximum power capability require an increased solar array weight in proportion to the difference between the power available to the loads (that is the power that can be delivered at the worst voltage conditions) and the maximum power capability of the solar array.

A second general type of system includes those that employ the line booster to prevent the need for a solar array current capability equal to the total load requirement at minimum voltage. When a simple resistive battery charge control is used with a momentary line booster and a small margin exists between the array capability (at minimum battery charge voltage) and the load, then, at the beginning of charge, the bus voltage will be reduced to a level only slightly greater than the battery potential. This would also

apply to bucking regulators used for battery charge control if charging is initiated with the regulator in a full "ON" or saturated condition (e.g., spacecraft entering sunlight from an eclipse or reorientation of the solar array following a maneuver). As a result, for these types of systems, the solar array must be designed to operate over a range of voltages from the minimum charging voltage to maximum unregulated bus voltage. However, by modifying the battery charger to turn on in a nonsaturated condition thereby assuring an adequate voltage drop between the main bus and the battery, the solar array may begin charging the battery at a higher array voltage. This approach permits designing the solar array for a specific operating voltage at the critical design point and provides the possibility of optimizing that voltage at the maximum power point of the solar array where maximum battery charging and load capability will exist.

The regulated bus systems are such that the regulated solar array output is at a single voltage which can be optimized for the maximum power point of the solar array. For the interplanetary missions under consideration, however, the solar array voltage capability varies considerably during the course of mission. This imposes another constraint on the selection of battery voltage and regulated bus voltage in that the design of the solar array should match its maximum power point voltage as closely as possible with the regulated bus voltage to minimize the array and system weights.

In order to assess the impact of mismatch between the solar array maximum power point voltage and the operating voltages, a relatively simple computer program was devised. This program determines the degree of matching of these voltages and also determines the critical design points for each of the candidate power systems for each of the missions. The results of these computations were used to determine solar array sizing factors for each case. Investigations of the solar array power capability as a function of mission time, and comparison of these capabilities with the load requirements as a function of mission time clearly indicated that the critical design points would occur at maximum load conditions at encounter, at end-of-life (which could be either minimum or maximum AU depending on particular mission involved) or at the beginning of the mission (cruise phase). Intermediate load conditions and solar array capabilities were always less critical than these three conditions.

The operation of the computer program is as follows. The computer generates the current voltage characteristic of the solar array at the beginning of the mission, encounter and end-of-life from input data which consists of an equation for the current voltage characteristic, the appropriate short-circuit current, the open-circuit voltage, and current and voltage at the maximum power point. Additional input data to the computer program consist of the appropriate ratio of maximum-to-minimum operating voltage for the solar array for the system configuration being analyzed and the power required for the given mission at these minimum and maximum voltage levels for the three discrete points in time within the mission.

The program then assumes that the power required at minimum voltage and minimum AU is just equal to the solar array capability at that condition. Starting at a given minimum voltage level, the computer determines whether the solar array can support the power requirements at minimum and maximum voltages at all times in the mission. The program then gradually increases the minimum voltage in predetermined steps while maintaining the same maximum-to-minimum voltage ratio and maintaining the power requirement at minimum voltage and minimum AU equal to the solar array capability at that voltage. For each step increase in minimum voltage at which all power requirements are satisfied by the solar array, the program calculates the corresponding required value of solar array power at its maximum power point.

These increases in voltage level are continued until such time as a minimum value of solar array power capability at the maximum power point is achieved. In those cases where further increases in operating voltage cause an increase in the maximum power capability of the solar array, the program automatically stops. The computer will not be able to find a solution when the power required at both voltages and all AU conditions cannot be satisfied under the assumption that the minimum AU solar array capability is just adequate to support the load required at minimum voltage.

The program then repeats the operation with the constraint that the power required at maximum voltage at minimum AU is just equal to the solar array capability and again searches for the operating

voltage levels that yield a minimum required capability of the solar array at its maximum power point. The program then performs a similar set of operations assuming the power requirement at minimum voltage to be equal to the solar array capability at conditions corresponding to either encounter or maximum AU as appropriate. Here again, the program shifts the operating voltage range from the given minimum value to increasingly higher values and searches for the solution wherein all power requirements are satisfied and the minimum capability of the solar array at its maximum power point is achieved. Finally, the program performs a fourth set of computations at this second AU condition and in this case assumes the power required at maximum voltage to be just equal to the solar array capability. A fifth and sixth set of computations are performed to cover the third point in the mission when it is not obvious by inspection that the critical design point has been determined by the first four sets of computations.

For these four sets of calculations, the computer then compares the required maximum power point solar array capabilities at 1 AU for each case where solutions were found. That case which yields the lowest value of maximum power capability of the 1 AU solar array is then identified as the critical design point for the mission. By comparing the relative solar array power capabilities at the critical design point and at the maximum power capability of the solar array at 1 AU, a factor is determined which reflects the solar array power capability that must be installed on the spacecraft in order to support a given load at the critical design point. This factor was used in subsequent calculations of the solar array size and weight required for each system configuration for the seven spacecraft models.

It should be pointed out that the loads used in this computer program did not reflect the efficiencies of the elements of the power system other than that of the battery. It was assumed, however, that the ratio of loads at the various voltages and mission times and the ratio of solar array capability at the critical design point to that at the maximum power point at 1 AU would not be materially affected by subsequent calculations which took into account actual component efficiencies of the power system elements. Sample calculations were made which indicated that a reasonable accuracy for these solar array sizing determinations was on the order of

3 percent. The computer program developed for this analysis was necessary because of the large number of systems considered and the fact that it was necessary to investigate all of these systems for each of the seven model spacecraft. The program runs were made on a time-sharing computer system and the results of these analyses are shown in Figures 50 through 54.

For the Mercury Flyby model spacecraft, Figure 50, the alternative power system configurations were divisible into four basic categories. The results of the computer program are illustrated for the critical design point condition for each category. The resulting solar array sizing factor (A) is the ratio of solar array power required at 1 AU at the maximum power point to the power required at maximum load conditions divided by the appropriate power-per-unit weight achievable for the particular solar array configuration at 1 AU. A ratio of 10 w per pound was used for the Mercury and Venus missions. The sizing factor includes a 5-percent contingency to accommodate solar cell or interconnection failures while still maintaining a high probability of successfully providing the required power output throughout the mission.

This factor, therefore, establishes the installed solar array weight-per-unit power at maximum load conditions. It is true that the maximum load conditions may not occur at the critical design point. The analysis, however, determines the relationships of solar array power capability to the load requirements at the several discrete points in the mission simultaneously. Thus, the solar array size required to supply the maximum load condition is based on that solar array capability required to just satisfy the load at the critical design point. If the maximum load point is not at the critical design point, the solar array will have excess capability at this maximum load condition. The computer results in this case define the amount of this excess capability necessary to satisfy the power demand throughout the mission. Expressing the solar array sizing factor in terms of the maximum load condition permits application of this weight factor directly in subsequent system sizing analyses wherein maximum load conditions were used to determine the weight and size of each of the other

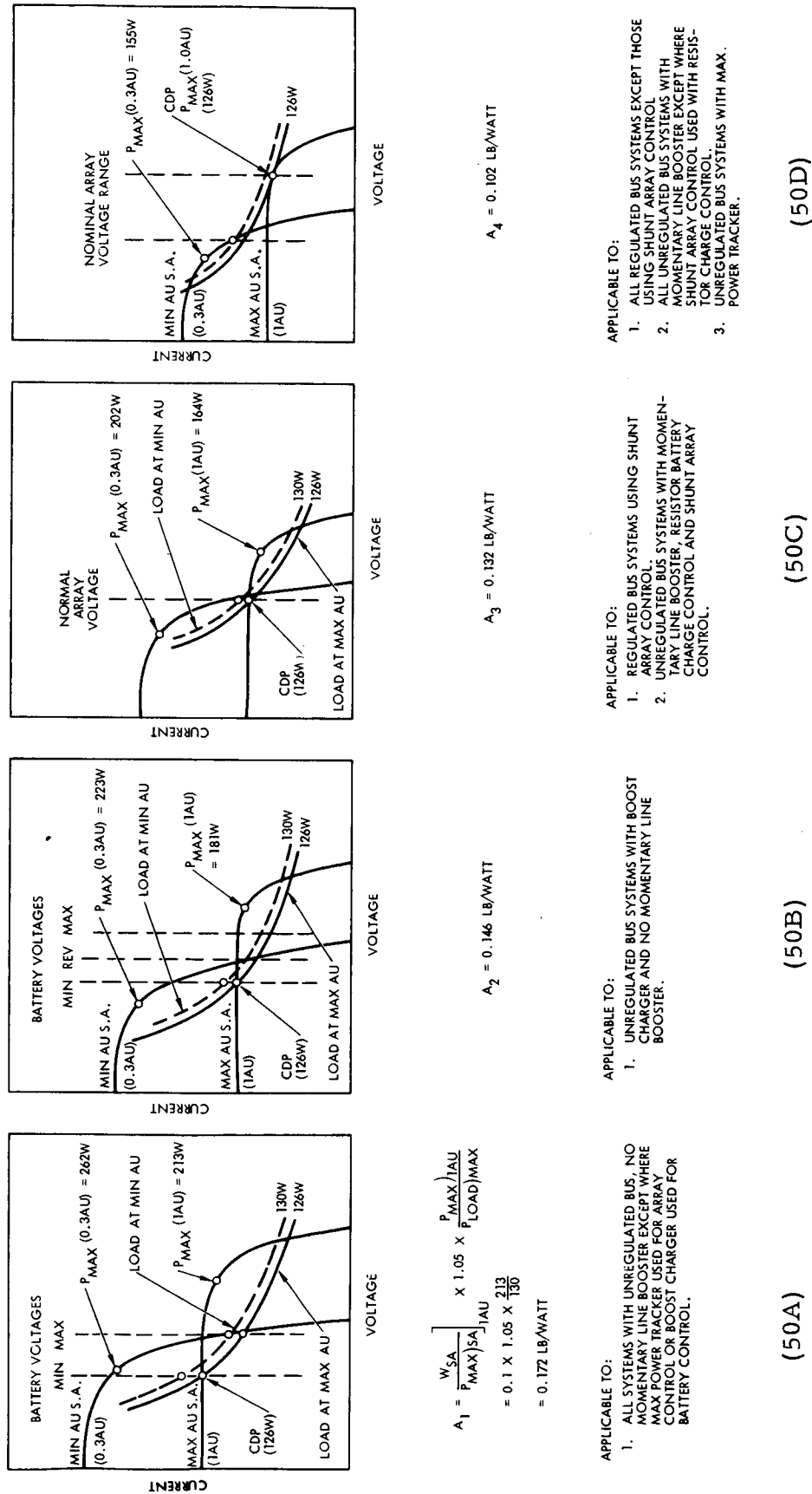


Figure 50. Solar Array Sizing Factors for Mercury Flyby Mission

system components. It was also necessary, in certain cases, to distinguish between maximum power requirements in sunlight and maximum power requirements during battery discharge. These maxima determine the sizing of the subsystem units which operate only in sunlight or during battery discharge.

The dependence of the critical design point condition on the power system configuration is clearly shown for the Mercury Flyby case. The first category of systems, Figure 50A, yields the critical design point at 1 AU with the cruise load of 126 w. Because the applicable systems require the solar array to operate over a relatively wide range of voltages, the critical design point occurs at the minimum operating voltage where a minimum solar array current capability is available. As shown in Figure 50A, battery voltage is constrained at its upper limit by the reduced voltage capability of the minimum AU solar array.

The second category of systems, Figure 50B, illustrates the possible advantage gained by using a boost charger with the battery to overcome this constraint. The operating voltage range is selected such that the low voltage solar array capability at minimum AU is adequate to terminate battery discharge but inadequate to charge the battery by itself. The boost charge regulator permits utilizing the solar array power at a voltage approximating the minimum charging voltage of the battery to fully charge the battery to its maximum voltage level. This increase in the maximum battery voltage relative to the solar array voltage permits reducing the number of series cells required in the solar array for a given battery voltage range in comparison to the first category of systems.

The third category of systems, Figure 50C, includes those systems employing a shunt voltage limiter on the solar array to control bus voltage during the major portion of sunlight operation. The maximum regulated voltage is constrained by the reduced solar array voltage capability at encounter. Thus, in order to achieve a regulated bus, the shunt voltage limiter on the solar array must be active at all times in the mission and the increased voltage capability of the solar array initially at 1 AU is not usable with the shunt control scheme. This constant

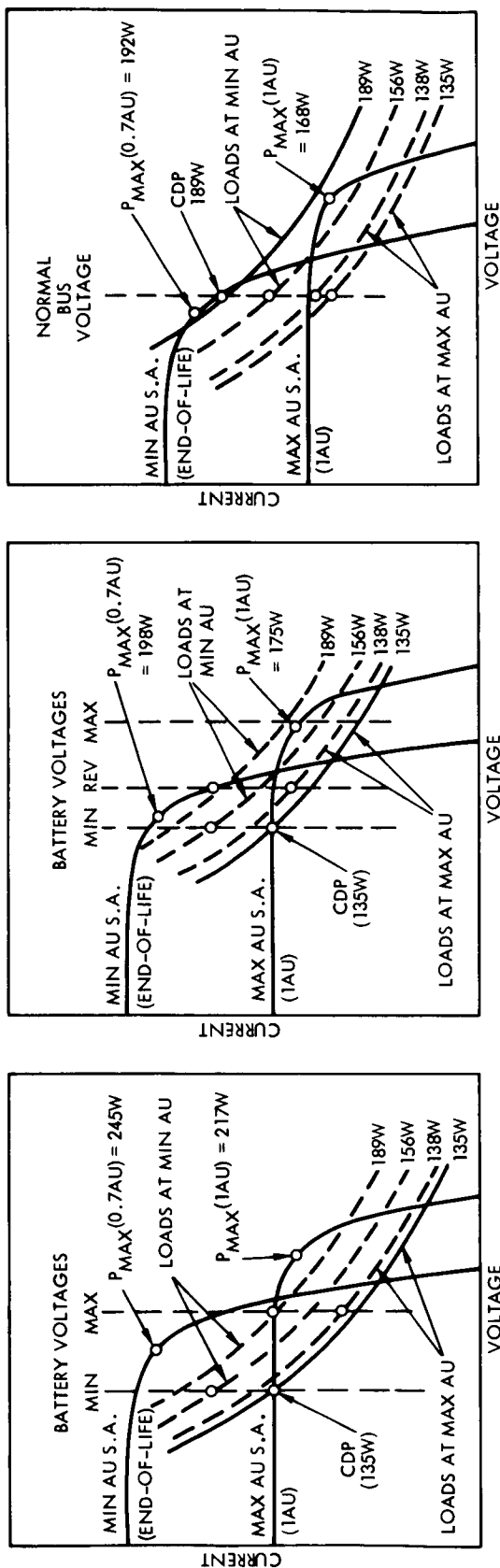
voltage operation of the solar array in this case provides for improved array power utilization in comparison to the first two system categories.

The fourth category of systems, Figure 50D, illustrates the operating points for those systems which employ series pulsewidth modulated regulators for solar array control, and assumes that the design of these regulators is such that they will cause the solar array to operate at a voltage higher than the nominal or regulated bus voltage when required to utilize the increased solar array power capability at higher array voltages. Maximum use may be made of the array capability at the critical design point which produces the smallest array sizing factor. Comparison of these four factors for the Mercury mission shows a total variation of approximately 70-percent in required array size relative to the best system category.

In Figure 51 for the Venus Orbiter No. 1 model, the alternative power system configurations were divisible into three basic categories. The first two of these are similar to the first two of the Mercury Flyby mission. The third category (Figure 51C) illustrates those cases where the normal bus voltage can be selected to match the solar array maximum power capability at the critical design point which occurs at minimum AU. At this voltage the maximum AU solar array power capability was determined to exceed the 189-w load required at this condition. Operation at a single voltage is accomplished by utilizing appropriate series regulators either between the solar array and the main bus or between the main bus and the battery to free the solar array operating voltage from the battery operating voltage variations. Since the critical design point occurs at minimum AU, the shunt regulator approach is not penalized.

Comparing the solar array sizing factors, A , A_2 and A_3 , for this mission shows a variation of approximately 30 percent which is directly reflected in the solar array size and weight for the appropriate system configurations.

For the Venus Orbiter No. 2 model, four categories of systems were produced by the array utilization analyses. The first two of these,



$$A_1 = \frac{W_{SA}}{P_{MAX}(SA)} \times 1.05 \times \frac{P_{MAX}(1AU)}{P_{LOAD}(MAX)} = 0.1 \times 1.05 \times \frac{217}{189} = 0.121 \text{ LB/WATT}$$

APPLICABLE TO:

1. ALL SYSTEM CONFIGURATIONS WITH UNREGULATED MAIN BUS AND NO MOMENTARY LINE BOOSTER EXCEPT WHERE MAX POWER TRACKER USED FOR ARRAY CONTROL OR BOOST CHARGER USED FOR BATTERY CONTROL.

(51A)

$$A_2 = 0.0972 \text{ LB/WATT}$$

APPLICABLE TO:

1. SYSTEM CONFIGURATIONS WITH UNREGULATED BUS, NO MOMENTARY LINE BOOSTER AND BOOST BATTERY CHARGER.

(51B)

$$A_3 = 0.0935 \text{ LB/WATT}$$

APPLICABLE TO:

1. ALL SYSTEMS WITH REGULATED MAIN BUS.
2. ALL SYSTEMS WITH UNREGULATED MAIN BUS AND MOMENTARY LINE BOOSTER IN BATTERY CONTROL.
3. SYSTEMS WITH UNREGULATED MAIN BUS AND MAX POWER TRACKING ARRAY CONTROL

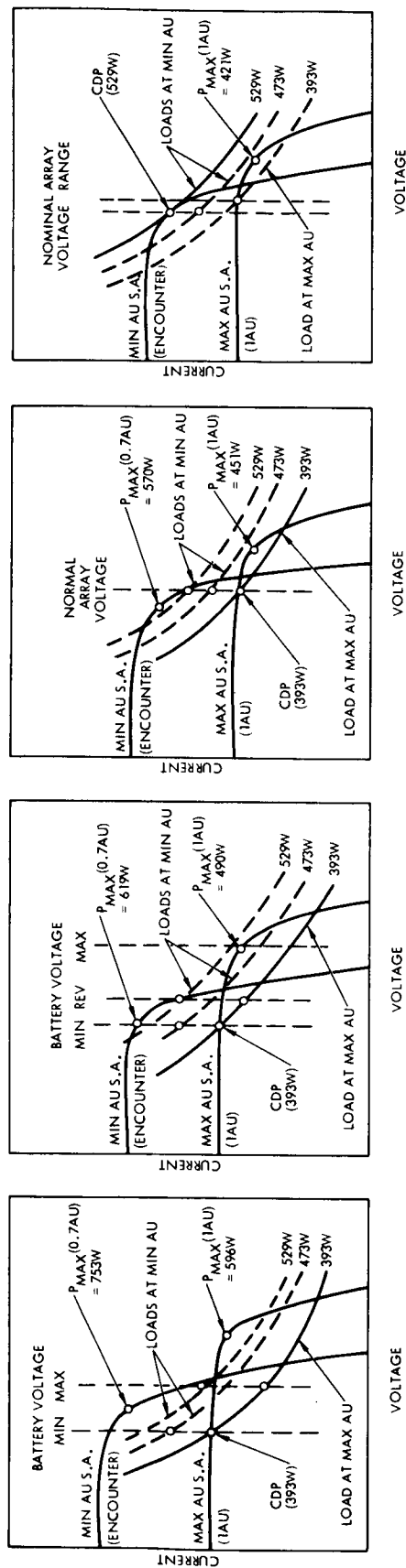
(51C)

Figure 51. Solar Array Utilization Factors for Venus Orbiter No. 1 Mission

as shown in Figures 52A and 52B, are again similar to the first two categories of Mercury Flyby and Venus Orbiter No. 1 models. The relationship of the loads at minimum and maximum AU for the Venus Orbiter No. 2 mission, however, is different from that of Venus Orbiter No. 1 in that the critical design point occurs at maximum AU for those systems which operate at a regulated voltage or a narrow range of voltages. As a result, the third and fourth system categories are produced and are similar to those for the Mercury Flyby mission.

For the Mars Orbiter mission, shown in Figure 53, the solar array sizing calculations were based on the configuration selected by TRW for the Voyager Spacecraft during the JPL funded Voyager studies. This configuration used a fixed, circular solar array on the bottom of the spacecraft and, in order to minimize heat transfer from the solar array into the equipment compartment of the spacecraft, the rear surfaces of the solar array were thermally insulated. As a result, the solar array operating temperatures were significantly higher than could have been achieved with a noninsulated solar array. The advantages gained by eliminating the need for deployment of solar array panels and reducing the temperature excursions of the array were considered to offset the penalty in solar array power capability per unit weight attributable to its higher operating temperature. The specific power factor used for the Mars Orbiter calculations, therefore, is significantly less than the preceding missions at 5.3 w/lb and is reflected in the higher solar array sizing factors. Here again, four categories of systems resulted from the analyses. The total variation in array sizing is shown to be approximately 40 percent.

The results of the array utilization analysis for the three Jupiter missions are illustrated in Figure 54. The variation in the voltage capability of the solar array between minimum and maximum AU conditions is not as pronounced as that of the other missions. For each of the three Jupiter missions, three categories of array sizing factors were determined. For the third category of systems, although the critical design point occurs at maximum AU, the use of a shunt array control



$$A_1 = \frac{W_{SA}}{P_{MAX SA}} \times 1.05 \times \frac{P_{MAX 1AU}}{P_{LOAD MAX}}$$

$$= 0.1 \times 1.05 \times \frac{596}{529}$$

$$= 0.1183 \text{ LB/WATT}$$

APPLICABLE TO:

1. ALL SYSTEM CONFIGURATIONS WITH UNREGULATED MAIN BUS AND NO MOMENTARY LINE BOOSTER EXCEPT WHERE MAX POWER TRACKER USED FOR ARRAY CONTROL OR BOOST CHARGER USED FOR BATTERY CONTROL.

(52A)

$$A_2 = 0.0973 \text{ LB/WATT}$$

APPLICABLE TO:

1. SYSTEM CONFIGURATIONS WITH UNREGULATED BUS, NO MOMENTARY LINE BOOSTER AND BOOST BATTERY CHARGER.

(52B)

$$A_3 = 0.0895 \text{ LB/WATT}$$

APPLICABLE TO:

1. REGULATED BUS SYSTEMS USING SHUNT ARRAY CONTROL.
2. UNREGULATED BUS SYSTEMS WITH MOMENTARY LINE BOOSTER, RESISTOR BATTERY CHARGE CONTROL AND SHUNT ARRAY CONTROL.

(52C)

$$A_4 = 0.0836 \text{ LB/WATT}$$

APPLICABLE TO:

1. ALL SYSTEMS WITH REGULATED MAIN BUS EXCEPT THOSE USING SHUNT ARRAY CONTROL.
2. ALL SYSTEMS WITH UNREGULATED MAIN BUS AND MOMENTARY LINE BOOSTER EXCEPT WHERE SHUNT ARRAY CONTROL USED WITH RESISTOR CHARGE CONTROL.
3. SYSTEMS WITH UNREGULATED MAIN BUS AND MAX POWER TRACKING ARRAY CONTROL.

(52D)

Figure 52. Solar Array Sizing Factors for Venus Orbiter No. 2 Mission

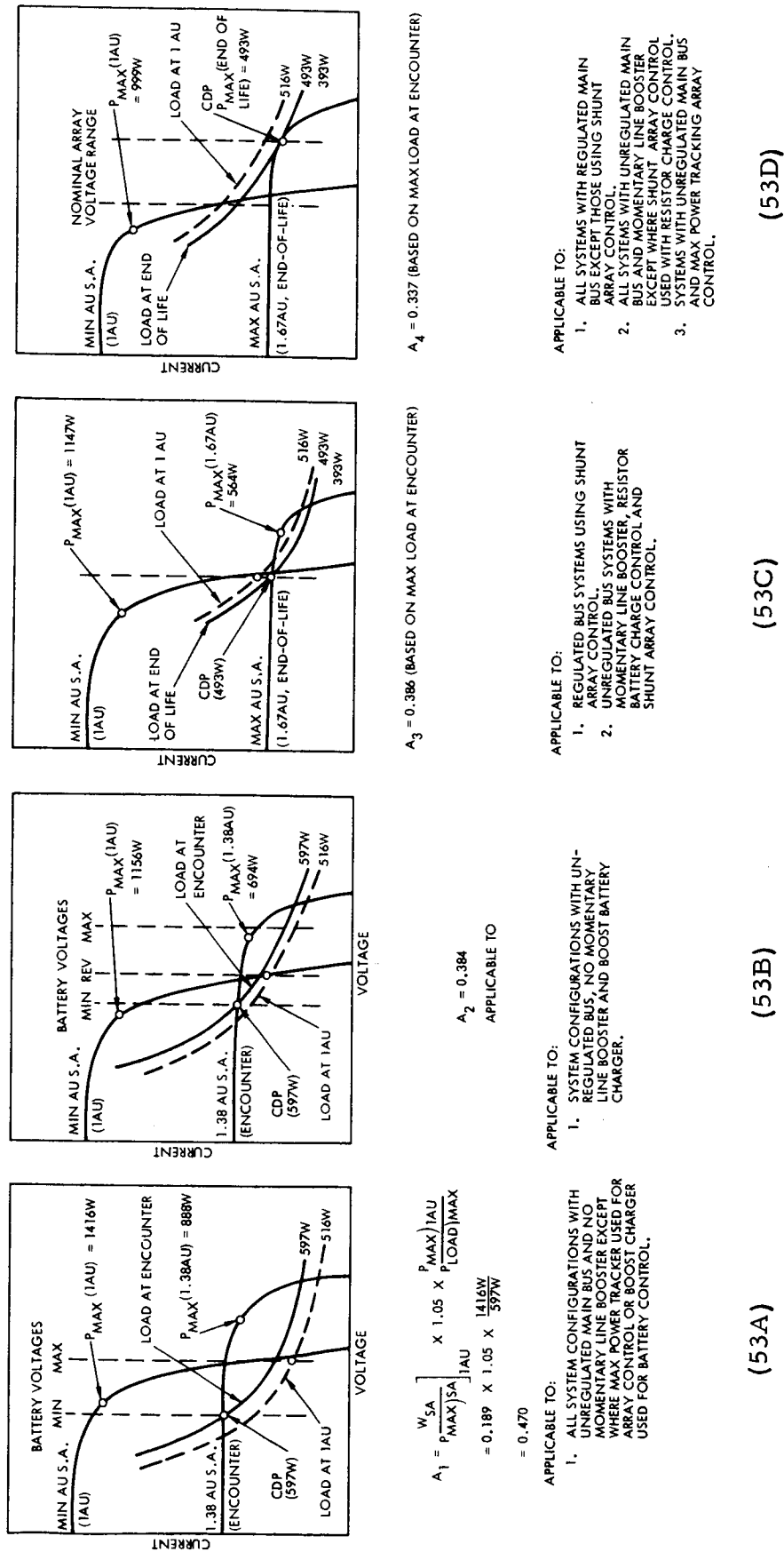
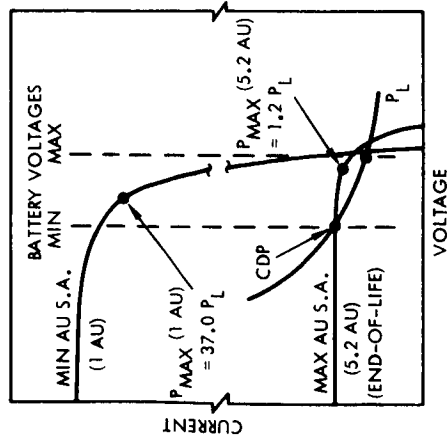


Figure 53. Solar Array Sizing Factors for Mars Orbiter Mission



JUPITER PROBE

$A_1 = 3.46$ (CDP = MIN BATTERY VOLTAGE AT ENCOUNTER)

JUPITER ORBITER NO. 1

$A_1 = 3.88$ (CDP = MIN BATTERY VOLTAGE AT END-OF-LIFE)

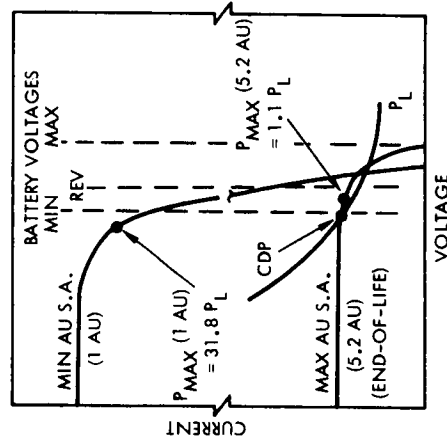
JUPITER ORBITER NO. 2

$A_1 = 1.89$ (CDP = MIN BATTERY VOLTAGE AT ENCOUNTER)

APPLICABLE TO:

1. ALL SYSTEM CONFIGURATIONS WITH UNREGULATED MAIN BUS AND NO MOMENTARY LINE BOOSTER EXCEPT WHERE MAX POWER TRACKER USED FOR ARRAY CONTROL OR BOOST CHARGER USED FOR BATTERY CONTROL.

(54A)



$A_2 = 3.27$ (CDP = MIN BATTERY VOLTAGE AT ENCOUNTER)

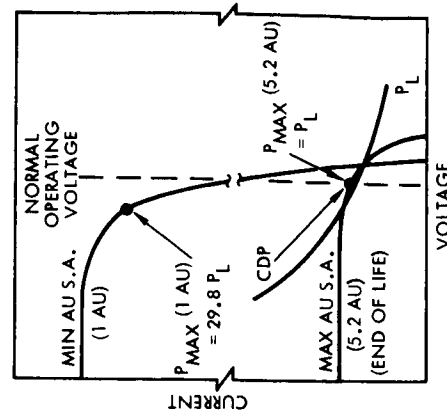
$A_2 = 3.34$ (CDP = MIN BATTERY VOLTAGE AT END-OF-LIFE)

$A_2 = 1.63$ (CDP = MIN BATTERY VOLTAGE AT ENCOUNTER)

APPLICABLE TO:

1. SYSTEM CONFIGURATIONS WITH UNREGULATED BUS, NO MOMENTARY LINE BOOSTER AND BOOST BATTERY CHARGER.

(54B)



$A_3 = 3.12$ (CDP = END-OF-LIFE)

$A_3 = 3.12$ (CDP = END-OF-LIFE)

$A_3 = 1.53$ (CDP = ENCOUNTER)

APPLICABLE TO:

1. ALL SYSTEMS WITH REGULATED MAIN BUS
2. ALL SYSTEMS WITH UNREGULATED MAIN BUS AND MOMENTARY LINE BOOSTER IN BATTERY CONTROL.
3. SYSTEMS WITH UNREGULATED MAIN BUS AND MAX POWER TRACKING ARRAY CONTROL

(54C)

Figure 54. Solar Array Sizing Factors for Jupiter Missions

does not penalize the system because of the lack of a significant voltage difference between the minimum and maximum AU solar arrays. Figure 54 does not indicate a battery-charging capability at this end-of-life critical design point because of the long orbit period and relatively short eclipse duration at Jupiter which requires negligible battery-charging power.

Because of the relatively high power requirements and very large solar array required for the Jupiter Orbiter No. 2 mission, it was considered reasonable to assume that a state-of-the-art advancement to solar array designs having specific power capabilities of 20 w/lb would be appropriate. As a result, the solar array sizing factors are approximately 50 percent of those for the Jupiter probe and Jupiter Orbiter No. 1 models.

The solar array sizing factors are seen to vary by approximately 10 percent for the Jupiter probe case, and by 24 percent for the Jupiter Orbiters. Because of the very large solar array size and weight required to supply the power requirements for these models, the weight penalties resulting from the use of systems which cause the solar array to operate over a relatively large voltage range are very significant.

4. RELIABILITY ANALYSIS

4.1 RELIABILITY WEIGHT OPTIMIZATION METHOD

A primary goal of this study was to develop a method for comparing power system configurations on the basis of reliability and weight in order to select an optimum power system configuration for a given mission. A computer program was developed to calculate the reliability and weight of the large number of candidate power systems which were configured for each of the missions, and to determine the effects of implementing redundancy on the reliability and weight within each system. The problem of redundant effects has been qualitatively approached in the past by the use of characteristic reliability to weight ratios or with figures of merit based on system and/or unit complexity, but these approaches were rejected in favor of a more meaningful quantitative analysis of the problem.

An important consideration in adopting this approach was that the model spacecraft requirements and model system definitions were based, in part, on arbitrary assumptions which would be reflected in the results of the power system optimization analysis. The computer program, however, was developed to provide a useful analytical tool capable of rapidly comparing alternate system configurations for any specific spacecraft application. A major emphasis in the study efforts, therefore, was placed on the development of this program and demonstration of its use in arriving at optimized power system configurations for each of the model spacecraft. Obviously, if the specific recommended optimum system configurations were applied to an actual spacecraft design, the probable variations in detailed spacecraft requirements and constraints from those assumed for this study could lead to a non-optimum power system design. It was anticipated, however, that the results of evaluating a large number of possible system configurations would establish definite trends relative to the general types of power systems which are optimum from the reliability-weight standpoint for the specific types of missions studied. The specific power system designs produced by the optimization process, therefore, provide examples of the use of the computer program

and the analysis of the computer data serves to determine guidelines relative to the types of power system configurations which are optimum for the specified interplanetary missions.

The use of computer programs to select optimum combinations of systems within a spacecraft to produce the most desirable overall spacecraft configuration has been successfully employed by TRW on several projects. This study applied this same basic approach to the power system optimization problem relative to reliability and weight.

The program is organized to accept inputs consisting of the reliability and weight of each unit within a given system configuration, and to combine these units, each of which may be either redundant or nonredundant, in a manner which produces an optimum configuration of that system from the standpoint of reliability and weight. Since specific reliability or weight constraints could not be established for each model, it was necessary to perform these analyses with both weight and reliability as variables. The boundary conditions for these analyses for a given system are clearly established as the minimum weight, minimum reliability, nonredundant configuration and the maximum weight most reliable configuration, where redundancy is employed in all of the units within the system.

The second operation then required by the computer program is to compare alternative system configurations, taking into account their optimized reliability-weight relationships, to determine those systems which provide the lightest weight for a given reliability or the maximum reliability for a given weight. It was considered reasonable to employ a lower limit on reliability of 0.90 for the purposes of this study, although higher reliability values are normally necessary for a practical spacecraft power system design. A sufficiently low limit on reliability was set so that the computer analysis would include consideration of all possible system configurations.

4. 1. 1 Computer Program Description

The power system reliability-weight optimization program determines the best combinations of redundant and nonredundant units within one system configuration as a function of either a reliability or weight allocation. The computer program enumerates all possible combinations

of unit redundancy, and selects those that provide minimum weight for system reliabilities ranging from a minimum of 0.90 to the maximum achievable. These selected combinations then represent the optimum reliability versus weight characteristics for a given system configuration. By comparing these characteristics for all candidate system configurations, the best designs for each mission are determined.

The technique of enumerating all possibilities and then selecting the best combinations would appear to be a cumbersome approach in view of the classical mathematical approaches and dynamic programming techniques which have been used to solve many problems of this type in the past. The discontinuous nature of the unit reliability-weight functions and the interdependence of unit weights, efficiencies, and reliabilities, however, have prevented the adoption of a streamlined solution to the power system optimization problem.

The reliability calculations have been based on the assumption that any single part failure in a nonredundant unit constitutes a power system failure. This simplification has permitted the analysis of a relatively large number of power system configurations leading to the determination of one or more "best" candidates for each mission. The reliability of each unit in the various systems has been established on the basis of its parts count and the part failure rates listed in Table 19. These failure rates have been based primarily on TRW OGO, Vela, and Pioneer spacecraft flight experience. Demonstrated orbital operating times and numbers of parts by type are shown in Tables 20 and 21, respectively. Battery cell failure rates represent estimated values based on the very limited data available for the silver-zinc and silver-cadmium types in space applications.

The matrix shown in Figure 55 represents the basic arrangement of the computer program. Each column represents one essential unit of the system, and each cell represents one of the alternative choices of redundancy in the unit of the appropriate column. Several numbers may be associated with each cell in the matrix, plus additional numbers which are

Table 19. Recommended Failure Rates for Power System Configuration Study

Part Type	Principal Electrical and Other Stress	Spacecraft Equipment Failures/ 10^9 Hr at Case Temperature 30°C
	<u>Rated Power, Percent</u>	
<u>Diode:</u>		
Silicon (< 1 w)	25	5
Silicon power (> 1 w)	25	14
Zener	25	55
<u>Transistor:</u>		
Silicon (< 1 w)	25	28
Silicon power (> 1 w)	25	56
<u>Resistor:</u>		
Carbon composition	25	12
Metal film	25	3
Wirewound, power	25	65
	<u>Rated Voltage, Percent</u>	
<u>Capacitor:</u>		
Ceramic	25	25
Mica, dipped	25	3
Paper, Mylar	25	40
<u>Tantalum:</u>		
Foil	25	21
Solid (series resistance ≥ 3 ohms/v)	25	21
<u>Transformer:</u>		
Low voltage, class H or T insulation	Hot spot $\leq 125^\circ\text{C}$	30 + 30/winding
<u>Inductor:</u>		
Low voltage, class H or T insulation	Hot spot $\leq 125^\circ\text{C}$	30
<u>Relay:</u>		
Base rate, class H or T coil insulation, magnetic latching (2 coils)	Hot spot $\leq 125^\circ\text{C}$	15 (failures/ 10^9 cycles)
<u>Connector:</u>		
Per active pin (soldered)		10
<u>Connector:</u>		
Per active pin (crimped)		5
<u>Connection:</u>		
Soldered		0.5
<u>Connection:</u>		
Welded		0.5
<u>Solar Cell:</u>	Orbital conditions	1
<u>Battery Cell:</u>		
Silver cadmium in 20 cell pack		150
Silver cadmium in 3 cell pack		300
<u>Battery Cell:</u>		
Silver zinc in 15 cell pack		300
Silver zinc in 3 cell pack		600

Table 20. Part Type Demonstrated Orbital Operating Hours
(Vela and OGO)

Part Type	Number of Failures	Operating Hours Vela and OGO
<u>Transistors:</u>		
Silicon	2	106,073,965
<u>Diodes:</u>		
Silicon	1	385,629,667
Zener		7,508,145
<u>Resistors:</u>		
Carbon composition		74,482,179
Metal film		292,450,010
Wirewound		4,374,113
<u>Capacitors:</u>		
Ceramic	1	63,428,620
Dipped mica		2,926,213
Tantalum foil		1,030,847
Tantalum solid		42,916,870
Plastic		233,919
Mylar paper		387,862
<u>Magnetics:</u>		
Transformer		25,782,120
Inductor		1,397,461
Filter		3,281,707
<u>Relays:</u>		
Latching		5,630,944

Table 21. Part Group Total Number
of Orbital Parts (Vela
and OGO)

Part Group	Number of Parts
Transistors	13,989
Diodes	45,855
Capacitors	15,505
Resistors	44,541
Magnetics	3,531
Relays	408

Solar Array	Array Control	Energy Storage	Line Regulator	PCE 1*	PCE 2	PCE 3	PCE 4	PCE 5	PCE 6	PCE 7	PCE 8
R _{SA} A _{SA} (Note 5)	θ _{AC} S _{AC} *UBD	θ _{CR} θ _B θ _{DR} S _{CR} S _{DR} F, *UBE (Note 4)	θ _{LR} S _{LR} *RBD, *RBE	*E1, *D1 ←	*E2, *D2	*E3, *D3	*E4, *D4 — (DC Distribution System) (Note 6)	*E5, *D5	*E6, *D6	*E7, *D7	*E8, *D8 →
	R _{AC1} M _{AC1} N _{AC1}	R _{ES1} , K ₁ M _{CR1} , M _{B1} , M _{DR1} N _{CR1} , N _{CR2}	R _{LR1} M _{LR1} N _{LR1}	R _{1P1} , W _{1P1} η _{1P1E} , η _{1P1D}	R _{2P1} , W _{2P1} η _{2P1E} , η _{2P1D}	R _{3P1} , W _{3P1} η _{3P1E} , η _{3P1D}	R _{4P1} , W _{4P1} η _{4P1E} , η _{4P1D}	R _{5P1} , W _{5P1} η _{5P1E} , η _{5P1D}	R _{6P1} , W _{6P1} η _{6P1E} , η _{6P1D}	R _{7P1} , W _{7P1} η _{7P1E} , η _{7P1D}	R _{8P1} , W _{8P1} η _{8P1E} , η _{8P1D}
	R _{AC2} M _{AC2} N _{AC2}	R _{ES2} , K ₂ M _{CR2} , M _{B2} , M _{DR2} N _{CR2} , N _{DR2}	R _{LR2} M _{LR2} N _{LR2}	R _{1P2} , W _{1P2} η _{1P2E} , η _{1P2D}	R _{2P2} , W _{2P2} η _{2P2E} , η _{2P2D}	R _{3P2} , W _{3P2} η _{3P2E} , η _{3P2D}	R _{4P2} , W _{4P2} η _{4P2E} , η _{4P2D}	R _{5P2} , W _{5P2} η _{5P2E} , η _{5P2D}	R _{6P2} , W _{6P2} η _{6P2E} , η _{6P2D}	R _{7P2} , W _{7P2} η _{7P2E} , η _{7P2D}	R _{8P2} , W _{8P2} η _{8P2E} , η _{8P2D}

NOTES:

- Each vertical column represents single component design.
- Each cell within column represents alternative redundant configuration of particular component.
- Parameters in each column heading are common to all cells in that column.
- Energy storage includes battery, charge control and discharge control.
- Solar array assumed to have single configuration.
- For ac distribution systems, replace PCE columns 1 - 8 with the following:

AC Distribution System							
Gyro Inverter	Main Inverter	TR 1	TR 2	TR 3	TR 4	TR 5	TR 6
η_{GD}, η_{GE}	θ_{MI}, S_{MI}	η_{E1}, η_{D1}	η_{E2}, η_{D2}	η_{E3}, η_{D3}	η_{E4}, η_{D4}	η_{E5}, η_{D5}	η_{E6}, η_{D6}
R_{G1}, W_{G1}	R_{MI1}	R_{1T1}, W_{1T1}	R_{2T1}, W_{2T1}	R_{3T1}, W_{3T1}	R_{4T1}, W_{4T1}	R_{5T1}, W_{5T1}	R_{6T1}, W_{6T1}
η_{G1E}, η_{G1D}	M_{MI1}	η_{1T1E}, η_{1T1D}	η_{2T1E}, η_{2T1D}	η_{3T1E}, η_{3T1D}	η_{4T1E}, η_{4T1D}	η_{5T1E}, η_{5T1D}	η_{6T1E}, η_{6T1D}
R_{G2}, W_{G2}	R_{MI2}	R_{1T2}, W_{1T2}	R_{2T2}, W_{2T2}	R_{3T2}, W_{3T2}	R_{4T2}, W_{4T2}	R_{5T2}, W_{5T2}	R_{6T2}, W_{6T2}
η_{G2E}, η_{G2D}	M_{MI2}	η_{1T2E}, η_{1T2D}	η_{2T2E}, η_{2T2D}	η_{3T2E}, η_{3T2D}	η_{4T2E}, η_{4T2D}	η_{5T2E}, η_{5T2D}	η_{6T2E}, η_{6T2D}
	N_{MI2}						

*Load Power Conditioning Equipment
(Parallel Units)

Figure 55. Reliability - Weight Optimization Matrix

common to all the units of a column. For the cells, the numbers used are as follows:

- R = unit reliability for appropriate level of redundancy
- M = intercept of log weight versus log power plot for particular unit
- N = intercept of efficiency versus log power plot for particular unit
- K = number of batteries
- W = unit weight (when independent of other units)
- η_E = unit efficiency in eclipse (when independent of other units)
- η_D = unit efficiency in daylight (when independent of other units)

For the columns, the numbers used are as follows:

- θ = slope of log weight versus log power plot for each unit
- S = slope of efficiency versus log power plot for each unit.
- π_E = load for particular unit in eclipse* (when independent of other units)
- π_D = load for particular unit in daylight* (when independent of other units)
- F = ratio of battery charge power to discharge power for particular mission.

The computer calculates efficiency and weight for the unit configuration represented by each cell in the matrix according to the following general equations:

$$\text{Efficiency } (\eta) = S \log P + N$$

$$\text{Weight } (W) = MP^\theta$$

From the required output power, P, and the calculated efficiency, the computer determines the input power to each unit. The program proceeds from specified output requirements back through the various series elements of the system to determine required unit power levels and weights, taking into account the required operation of each in sunlight and eclipse.

The matrix is then scanned, and necessary calculations performed to determine total system weight and reliability for each possible combination of system units. Specific calculation methods for the weight of

*Represents only part of total load for array control, energy storage, and line regulator.

the power system are shown in Tables 22 and 23. Terms for these calculations are listed in Table 24.

Initially, it was considered desirable that the analyses be sufficiently flexible such that different types of redundancy could be compared in improving the reliability of an individual unit within the system. As the computer program was developed, however, the number of possible combinations that had to be evaluated within one system became excessive. If one system contains ten units, and each unit within the system has three alternate configurations corresponding to a nonredundant and two alternate redundant configurations, the total number of possible combinations for that one system is 3^{10} . The machine time required to assess the reliability and weight of this large number of configurations and to repeat the operation for approximately 150 different systems for each of the seven missions was clearly excessive. As a result, analyses of each type of unit within the various power system configurations were performed, and preferred methods of implementing redundancy to improve the reliability of each type of unit were selected. These selected methods are discussed in Subsection 4. 2.

This approach, in general, reduced the number of configurations for each unit within a system to two and reduced the number of total combinations necessary to be evaluated for the system from 3^{10} to 2^{10} for a ten-unit configuration. This reduction in the number of operations coupled with the established minimum 0.90 reliability constraint reduced the machine time requirements to a level that was compatible with the scope of the study.

In the actual implementation of this approach in the computer program, it was necessary to deviate from the simple case of one baseline and one redundant version of each unit with the battery and battery controls. The approach adopted consisted of combining the battery and its controls under the heading "Energy Storage" and four alternate configurations for the energy storage were defined as follows:

- A single nonredundant battery with nonredundant controls
- A nonredundant battery with redundant controls
- Redundant batteries each having nonredundant controls
- Redundant batteries each having redundant controls.

Table 22. Weight Calculations for DC Distribution Systems

1.	$P_{LRE} = \frac{\pi_{E1}}{\eta_{1PE}} + \frac{\pi_{E2}}{\eta_{2PE}} + \dots + \frac{\pi_{EN}}{\eta_{NPE}} + \pi_{RBE}$	10.	$P_{CR} = FP_B$
2.	$P_{LRD} = \frac{\pi_{D1}}{\eta_{1PD}} + \frac{\pi_{D2}}{\eta_{2PD}} + \dots + \frac{\pi_{DN}}{\eta_{NPD}} + \pi_{RBD}$	11.	$W_{ES} = KM_{DR} P_{ES}^{\theta_{DR}} + KM_B P_B^{\theta_B} + KM_{BR} P_{CR}^{\theta_{CR}}$
3.	$P_{LRR} = \text{greater of } P_{LRE} \text{ or } P_{LRD}$	12.	$\eta_{CR} = S_{CR} \log \frac{P_{CR}}{K} + N_{CR}$
4.	$W_{LR} = M_{LR} P_{LRR}^{\theta_{LR}}$	13.	$P_{AC} = \frac{P_{LRD}}{\eta_{LRD}} + \frac{P_{CR}}{\eta_{CR}} + \pi_{UBD}$
5.	$\eta_{LRE} = S_{LR} \log P_{LRE} + N_{LR}$	14.	$W_{AC} = M_{AC} P_{AC}^{\theta_{AC}}$
6.	$\eta_{LRD} = S_{LR} \log P_{LRD} + N_{LR}$	15.	$\eta_{AC} = S_{AC} \log P_{AC} + N_{AC}$
7.	$P_{ES} = \frac{P_{LRE}}{\eta_{LRE}} + \pi_{UBE}$	16.	$P_{SA} = \frac{P_{AC}}{\eta_{AC}}$
8.	$\eta_{DR} = S_{DR} \log \frac{P_{ES}}{K} + N_{DR}$	17.	$W_{SA} = A P_{SA}$
9.	$P_B = \frac{P_{ES}}{\eta_{DR}}$	18.	$W_{SYS} = W_{SA} + W_{AC} + W_{ES} + W_{LR} + W_{1P} + W_{2P} + \dots + W_{NP}$

Table 23. Weight Calculations for AC Distribution Systems

1.	$P_{MIE} = \frac{\pi_{E1}}{\eta_{1TE}} + \frac{\pi_{E2}}{\eta_{2TE}} + \dots + \frac{\pi_{EN}}{\eta_{NTE}}$	13.	$P_{ES} = \frac{P_{LRE}}{\eta_{LRE}} + \pi_{UBE}$
2.	$P_{MID} = \frac{\pi_{D1}}{\eta_{1TD}} + \frac{\pi_{D2}}{\eta_{2TD}} + \dots + \frac{\pi_{DN}}{\eta_{NTD}}$	14.	$\eta_{DR} = S_{DR} \log \frac{P_{ES}}{K} + N_{DR}$
3.	$P_{MIR} = \text{greater of } P_{MIE} \text{ or } P_{MID}$	15.	$P_B = \frac{P_{ES}}{\eta_{DR}}$
4.	$W_{MI} = M_{MI} P_{MIR}^{\theta_{MI}}$	16.	$P_{CR} = F P_B$
5.	$\eta_{MIE} = S_{MI} \log P_{MIE} + N_{MI}$	17.	$W_{ES} = K M_{DR} P_{ES}^{\theta_{DR}} + K M_B P_B^{\theta_B} + K M_{CR} P_{CR}^{\theta_{CR}}$
6.	$\eta_{MID} = S_{MI} \log P_{MID} + N_{MI}$	18.	$\eta_{CR} = S_{CR} \log \frac{P_{CR}}{K} + N_{CR}$
7.	$P_{LRE} = \frac{P_{MIE}}{\eta_{MIE}} + \frac{\pi_{GE}}{\eta_{GE}} + \pi_{RBE}$	19.	$P_{AC} = \frac{P_{LRD}}{\eta_{LRD}} + \frac{P_{CR}}{\eta_{CR}} + \pi_{UBD}$
8.	$P_{LRD} = \frac{P_{MID}}{\eta_{MID}} + \frac{\pi_{GD}}{\eta_{GD}} + \pi_{RBD}$	20.	$W_{AC} = M_{AC} P_{AC}^{\theta_{AC}}$
9.	$P_{LRR} = \text{greater of } P_{LRE} \text{ or } P_{LRD}$	21.	$\eta_{AC} = S_{AC} \log P_{AC} + N_{AC}$
10.	$W_{LR} = M_{LR} P_{LRR}^{\theta_{LR}}$	22.	$P_{SA} = \frac{P_{AC}}{\eta_{AC}}$
11.	$\eta_{LRE} = S_{LR} \log P_{LRE} + N_{LR}$	23.	$W_{SA} = A P_{SA}$
12.	$\eta_{LRD} = S_{LR} \log P_{LRD} + N_{LR}$	24.	$W_{SYS} = W_{SA} + W_{AC} + W_{ES} + W_{LR} + W_{1P} + W_{2P} + \dots + W_{NP}$

Table 24. Glossary of Terms

Power Terms

$P_{MIE, MID}$	=	Main inverter output power in eclipse, sunlight
P_{MIR}	=	Main inverter rated output power
$P_{LRE, LRD}$	=	Line regulator output power in eclipse, sunlight
P_{LRR}	=	Line regulator rated output power
P_{ES}	=	Energy storage output power
P_B	=	Battery output power
P_{CR}	=	Battery charger output power
P_{AC}	=	Array control output power
P_{SA}	=	Solar array output power
$\pi_{E1, E2, EN}$	=	Output power in eclipse for power conditioning equipments 1, 2, ---N
$\pi_{D1, D2, DN}$	=	Output power in sunlight for power conditioning equipments 1, 2, ---N
$\pi_{GE, GD}$	=	Output power for gyro inverter in eclipse, sunlight
$\pi_{RBE, RBD}$	=	Direct connected regulated bus load in eclipse, sunlight
$\pi_{UBE, UBD}$	=	Direct connected unregulated bus load in eclipse, sunlight

Efficiency Terms

$\eta_{ITE, 2TE, NTE}$	=	Efficiency in eclipse of transformer rectifiers 1, 2, ---N
$\eta_{ITD, 2TD, NTD}$	=	Efficiency in sunlight of transformer rectifiers 1, 2, ---N
$\eta_{MIE, MID}$	=	Efficiency of main inverter in eclipse, sunlight
$\eta_{GE, GD}$	=	Efficiency of gyro inverter in eclipse, sunlight
$\eta_{IPE, 2PE, NPE}$	=	Efficiency in eclipse of power conditioning equipments 1, 2, ---N

Table 24. Glossary of Terms (Continued)

Efficiency Terms (Continued)

$\eta_{IPD,2PD,NPD}$	=	Efficiency in sunlight of power conditioning equipments 1, 2, ---N
$\eta_{LRE,LRD}$	=	Efficiency of line regulator in eclipse, sunlight
η_{DR}	=	Efficiency of discharge regulator
η_{CR}	=	Efficiency of charge regulator
η_{AC}	=	Efficiency of array control
K	=	Number of batteries
F	=	Ratio of battery charge power to battery discharge power
S_{MI}, N_{MI}	=	Slope and intercept of main inverter efficiency vs power curve
S_{LR}, N_{LR}	=	Slope and intercept of line regulator efficiency vs power curve
S_{DR}, N_{DR}	=	Slope and intercept of discharge regulator efficiency vs power curve
S_{CR}, N_{CR}	=	Slope and intercept of charge control efficiency vs power curve
S_{AC}, N_{AC}	=	Slope and intercept of array control efficiency vs power curve

Weight Terms

$W_{IP,2P,NP}$	=	Weight of power conditioning equipments 1, 2, ---N including main inverter when used
W_{MI}	=	Weight of main inverter
W_{LR}	=	Weight of line regulator
W_{ES}	=	Weight of energy storage
W_{AC}	=	Weight of array control
W_{SA}	=	Weight of solar array
A	=	Weight per unit power output of solar array at maximum load conditions

Weight Terms (Continued)

K	=	Number of batteries
M_{MI}, θ_{MI}	=	Intercept and slope of main inverter weight vs power curve
M_{LR}, θ_{LR}	=	Intercept and slope of line regulator weight vs power curve
M_{DR}, θ_{DR}	=	Intercept and slope of discharge regulator weight vs power curve
M_B, θ_B	=	Intercept and slope of battery weight vs power curve
M_{CR}, θ_{CR}	=	Intercept and slope of charge control weight vs power curve
M_{AC}, θ_{AC}	=	Intercept and slope of array control weight vs power curve

For those cases where the solar array controls and battery controls perform the line regulation function, the appropriate factors are used for the line regulator to permit the computer to calculate its efficiency at 100 percent and its weight at 0. The reliability number for each energy storage configuration contains the reliability of both battery and control. For the solar array, a single configuration defined by its reliability and sizing factor is used for each system. For all remaining units within any system, two configurations, that is, the baseline nonredundant configuration or the preferred redundant configuration, are used. These units are identified as the array control, line regulator, and the several units which combine to perform the load power conditioning function.

A typical example of the computer printout for the optimization of one system for the Venus Orbiter No. 1 mission is illustrated in Table 25. The system configuration is coded in accordance with Table 26 with the exception that solar array type 2 was used to designate array sizing factor A_3 as defined in Subsection 3.6. The 256 combinations represent the number of possible combinations of redundant and nonredundant units within the system. The maximum achievable reliability and the attendant weight for the fully redundant ac and dc distribution systems are shown.

Table 25. Example of Computer Printout for Optimization of One System

VENUS ORBITER NO. 1

SOLAR ARRAY TYPE= 2
ARRAY CONTROL TYPE= 3
ENERGY STORAGE TYPE= 9
LINE REGULATOR TYPE= 5

NO. COMBINATIONS= 256

MAX AC SYSTEM
R= 0.999061 WGT= 201.33

MAX DC SYSTEM
R= 0.998824 WGT= 194.16

AC SYSTEM

MATRIX OF OPTIMA

CONSTRAINT	FEASIBLE	MIN WEIGHT	RELIABILITY	CONFIGURATION....
1	256	111.35	0.919231	1 1 1 1 1 1 1 1
2	256	111.35	0.919231	1 1 1 1 1 1 1 1
3	256	111.35	0.919231	1 1 1 1 1 1 1 1
4	256	111.35	0.919231	1 1 1 1 1 1 1 1
5	255	111.71	0.924020	2 1 1 1 1 1 1 1
6	251	112.20	0.929767	2 1 1 1 1 1 1 2
7	242	113.32	0.932956	2 1 1 1 1 2 1 2
8	232	113.83	0.937484	1 1 1 2 1 1 1 1
9	220	114.19	0.942368	2 1 1 2 1 1 1 1
10	203	114.68	0.948229	2 1 1 2 1 1 1 2
11	185	115.79	0.951482	2 1 1 2 1 2 1 2
12	167	117.64	0.957681	2 2 1 2 1 1 1 1
13	145	118.13	0.963638	2 2 1 2 1 1 1 2
14	118	119.26	0.966944	2 2 1 2 1 2 1 2
15	89	121.26	0.970605	2 2 1 2 1 2 2 2
16	69	125.54	0.977802	2 2 1 2 2 2 2 2
17	52	184.94	0.983678	2 3 1 2 1 1 1 2
18	34	186.42	0.987053	2 3 1 2 1 2 1 2
19	16	189.06	0.990790	2 3 1 2 1 2 2 2
20	4	194.48	0.998137	2 3 1 2 2 2 2 2

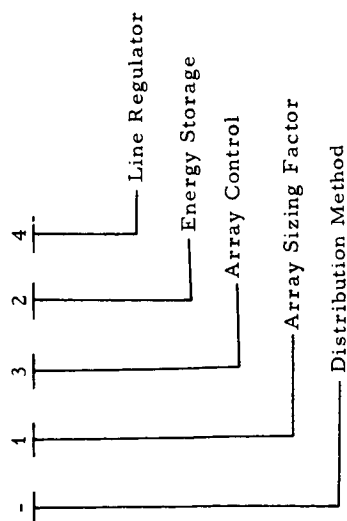
DC SYSTEM

MATRIX OF OPTIMA

CONSTRAINT	FEASIBLE	MIN WEIGHT	RELIABILITY	CONFIGURATION....
1	255	109.18	0.900587	2 1 1 1 1 1 1 1
2	251	109.53	0.912548	1 1 1 1 1 1 1 2
3	248	109.53	0.912548	1 1 1 1 1 1 1 2
4	242	109.88	0.917301	2 1 1 1 1 1 1 2
5	233	109.90	0.920628	1 1 1 1 1 1 2 2
6	223	110.25	0.925423	2 1 1 1 1 1 2 2
7	208	112.01	0.930668	1 1 1 2 1 1 1 2
8	193	112.36	0.935516	2 1 1 2 1 1 1 2
9	170	112.73	0.943799	2 1 1 2 1 1 2 2
10	150	114.23	0.947887	1 1 1 2 1 2 2 2
11	130	114.59	0.952825	2 1 1 2 1 2 2 2
12	107	116.13	0.959137	2 2 1 2 1 1 2 2
13	87	117.47	0.961937	2 1 1 2 2 2 2 2
14	66	118.00	0.968309	2 2 1 2 1 2 2 2
15	49	120.56	0.972503	1 2 1 2 2 2 2 2
16	30	120.92	0.977569	2 2 1 2 2 2 2 2
17	19	183.56	0.983324	1 3 1 2 1 2 2 2
18	10	183.91	0.988446	2 3 1 2 1 2 2 2
19	5	187.13	0.992728	1 3 1 2 2 2 2 2
20	2	187.49	0.997899	2 3 1 2 2 2 2 2

Table 26. Power System Configuration Code

Example Configuration Code:



Code Identification:

<u>Distribution Method</u>		<u>Energy Storage</u>
—	AC Distribution	1 Disconnect switch plus current limiting resistor
(no symbol)	DC Distribution	2 Disconnect switch plus current limiting resistor plus discharge booster
<u>Array Sizing Factor</u>		3 Dissipative bucking charger and discharge switch
1	Sizing Factor A ₁	4 Dissipative charger, discharge switch and discharge booster
2	Sizing Factor A ₂	5 PWM bucking charger and discharge switch
3	Sizing Factor A ₃	6 PWM bucking charger, discharge switch and discharge booster
4	Sizing Factor A ₄	7 PWM boost charger and discharge switch
<u>Array Control</u>		8 PWM boost charger, discharge switch and discharge booster
1	None	9 Dissipative charger and boost discharge regulator (normal voltage battery)
2	Zener Shunt	10 PWM bucking charger and boost discharge regulator (normal voltage battery)
3	Active Shunt	11 PWM bucking charger and boost discharge regulator (low voltage battery)
4	PWM Series Buck	
5	Max. Pwr. Tracker-Buck	
6	PWM Series Buck-Boost	

Line Regulator

- 1 PWM bucking line regulator
- 2 Dissipative bucking line regulator
- 3 Boost line regulator
- 4 Buck-boost line regulator
- 5 No line regulator

The computer optimization results for a series of 20 reliability constraints, starting from 0.90 and increasing of 0.995, are shown in Table 25. For each reliability constraint, the number of feasible combinations of redundant and nonredundant units within the system which meet or surpass the reliability constraint are listed. The weight of each of the feasible combinations is computed and the configuration which yields minimum weight for each of the reliability constraints is selected. Under the configuration column, the digits represent the individual units within the system; 1) indicating baseline or nonredundant configuration of that unit; 2) indicating a redundant configuration. The first column represents the selected configuration for the array control, the second column is for the energy storage, the third column represents the configuration of the line regulator, and the remaining five columns represent the power conditioning equipment. In the case of the energy storage, four numbers are possible:

- 1) Indicates a single battery with nonredundant controls
- 2) Indicates a single battery with redundant controls
- 3) Indicates redundant batteries, each having nonredundant controls
- 4) Indicates redundant batteries, each having redundant controls.

Since no line regulator is required with this system (2395), the line regulator column contains only a 1 designation.

Progressing from the first reliability constraint where all the units within the subsystem are nonredundant, redundant configurations of selected units within the system are added as the reliability constraint is increased. In each case the added redundancy is selected such as to achieve a minimum system weight for the appropriate reliability constraint. For the 20th constraint, four ac system configurations are possible. In this case, the minimum weight system which achieves the 0.995 reliability level is that which employs redundancy in all units except the battery charge controls.

Similarly for the dc system the printout shows selected minimum weight system configurations for each of the reliability constraints. The maximum achievable reliability in the ac distribution system is always higher than that of the dc system because of its fewer parts. However,

the dc system, which employs converters to supply the load power requirements, is better from a weight standpoint because the efficiency of these converters is slightly greater than that of the series combination of inverter and TR units used in the ac system. These differences are quite small and occurred consistently throughout all of the computer runs.

Having evaluated each system configuration for a particular mission to ascertain its lightest weight combination of redundant and nonredundant units for a given reliability constraint, the computer program then performed a second operation which consisted of scanning all of the available optimized system configurations, at each reliability constraint, to rank all of them in order of weight. An example of the computer printout for this operation is shown in Table 27. System identifications in the column headed "CASE" are in accordance with the coding shown in Table 26.

In the Venus Orbiter No. 1 mission, only two of the three solar array sizing factors identified in Subsection 3.6 for this mission were used in the computer runs. As a result, a "1" indicates sizing factor A, and a "2" indicates factor A_3 for the first digit of the code. This omission in the computer program penalized those systems employing boost battery chargers (energy storage type 7) with respect to weight. Subsequent sample calculations were performed for these systems using the correct sizing factor (A_2) with the result that their weights were decreased by approximately 5 percent. Although the relative ranking of these systems was thereby improved, the changes were not sufficiently large to affect the selection of optimum systems.

This ranking by type is accomplished for a given constraint by determining the lightest weight system that meets or surpasses that particular reliability value. This approach introduces some inaccuracies in the analysis because of the granularity of the selected 20 reliability levels. It is possible that within a given range of reliabilities the lightest weight system may just meet the given reliability level but a slightly higher weight system could provide the best system configuration between that level and the next constraint. The error introduced by this granularity is not considered significant. The possibility of failing to identify an optimum system configuration is considered remote because the best systems tended to dominate all others over the entire range of reliability constraints.

Table 27. Example of Ranking by Type for Given Reliability Constraint, Venus Orbiter No. 1 Mission

RANKING BY	TYPE FOR CONSTRAINT	NO.	19 (R = 0.990)		NO.	WEIGHT	REL	CASE
NO.	WEIGHT	REL	CASE		NO.	WEIGHT	REL	CASE
1	187.13	0.992728	2 3 9 5		83	220.36	0.998140	1 4 3 3
2	189.06	0.990790	-2 3 9 5		84	220.39	0.991752	-2 2 6 3
3	189.28	0.992349	2 3 10 5		85	221.05	0.991821	-2 2 4 3
4	191.24	0.990412	-2 3 10 5		86	221.18	0.990945	-1 1 7 4
5	191.68	0.997808	2 4 9 5		87	221.62	0.990255	-2 3 8 1
6	193.14	0.990700	-2 4 9 5		88	222.25	0.990484	-2 3 2 1
7	193.78	0.997428	2 4 10 5		89	222.37	0.991029	-1 4 3 3
8	194.54	0.997636	2 5 9 5		90	222.53	0.991683	-2 2 8 3
9	195.27	0.990322	-2 4 10 5		91	222.88	0.993018	1 3 5 1
10	195.66	0.992258	2 3 6 3		92	224.31	0.992251	2 3 6 4
11	196.05	0.990528	-2 5 9 5		93	224.54	0.993139	1 3 1 1
12	196.11	0.992327	2 3 4 3		94	224.59	0.992847	1 3 7 1
13	196.66	0.997255	2 5 10 5		95	224.83	0.992320	2 3 4 4
14	197.74	0.990321	-2 3 6 3		96	225.06	0.998280	1 1 3 1
15	197.75	0.992189	2 3 8 3		97	225.70	0.991080	-1 3 5 1
16	198.01	0.992419	2 3 2 3		98	225.87	0.992509	-1 2 5 3
17	198.20	0.990150	-2 5 10 5		99	226.52	0.992182	2 3 8 4
18	198.21	0.990390	-2 3 4 3		100	226.92	0.990314	-2 3 6 4
19	199.03	0.997801	2 6 9 5		101	227.08	0.992412	2 3 2 4
20	199.85	0.990252	-2 3 8 3		102	227.15	0.991168	-1 1 3 1
21	199.89	0.997336	2 4 6 3		103	227.45	0.990909	-1 3 7 1
22	200.18	0.990481	-2 3 2 3		104	227.46	0.991201	-1 3 1 1
23	200.31	0.997406	2 4 4 3		105	227.45	0.990383	-2 3 4 4
24	200.61	0.990693	-2 6 9 5		106	227.49	0.992338	-1 2 7 3
25	200.97	0.993015	1 3 5 3		107	229.16	0.990245	-2 3 8 4
26	201.18	0.997421	2 6 10 5		108	229.79	0.990475	-2 3 2 4
27	201.45	0.990230	-2 4 6 3		109	229.96	0.992169	1 2 7 2
28	201.89	0.990300	-2 4 4 3		110	230.31	0.993008	1 3 5 4
29	201.97	0.997267	2 4 8 3		111	231.33	0.992315	1 2 3 3
30	202.18	0.998051	2 5 1 3		112	231.98	0.993129	1 3 1 4
31	202.23	0.997498	2 4 2 3		113	232.03	0.992837	1 3 7 4
32	202.25	0.993136	1 3 1 3		114	232.50	0.998270	1 1 3 4
33	202.46	0.997758	2 5 7 3		115	233.24	0.991070	-1 3 5 4
34	202.52	0.992844	1 3 7 3		116	234.69	0.991158	-1 1 3 4
35	202.79	0.990315	-2 6 10 5		117	235.00	0.990899	-1 3 7 4
36	203.34	0.991077	-1 3 5 3		118	235.01	0.991191	-1 3 1 4
37	203.57	0.990162	-2 4 8 3		119	235.71	0.991518	2 2 6 1
38	203.88	0.990941	-2 5 1 3		120	236.42	0.991588	2 2 4 1
39	203.89	0.990391	-2 4 2 3		121	237.92	0.991450	2 2 8 1
40	204.11	0.990649	-2 5 7 3		122	238.00	0.993061	1 3 3 1
41	204.13	0.997475	2 1 6 1		123	239.35	0.992405	-1 2 7 2
42	204.54	0.997545	2 1 4 1		124	240.55	0.992551	-1 2 3 3
43	204.71	0.991198	-1 3 1 3		125	241.08	0.991122	-1 3 3 1
44	204.93	0.990906	-1 3 7 3		126	241.53	0.992275	1 2 5 1
45	205.77	0.990369	-2 1 6 1		127	243.14	0.991509	2 2 6 4
46	206.20	0.990439	-2 1 4 1		128	243.24	0.992105	1 2 7 1
47	206.33	0.998097	1 4 5 3		129	243.85	0.991578	2 2 4 4
48	206.34	0.997407	2 1 8 1		130	245.05	0.991755	-2 2 6 1
49	207.60	0.998219	1 4 1 3		131	245.35	0.991440	2 2 8 4
50	207.88	0.997925	1 4 7 3		132	245.43	0.993051	1 3 3 4
51	208.01	0.990301	-2 1 8 1		133	245.81	0.991824	-2 2 4 1
52	208.10	0.990986	-1 4 5 3		134	247.32	0.991686	-2 2 8 1
53	209.46	0.991107	-1 4 1 3		135	248.62	0.991112	-1 3 3 4
54	209.68	0.990816	-1 4 7 3		136	248.96	0.992266	1 2 5 4
55	210.06	0.998237	1 1 5 1		137	250.67	0.992095	1 2 7 4
56	210.52	0.992596	1 3 7 2		138	251.23	0.992512	-1 2 5 1
57	211.56	0.997465	2 1 6 4		139	252.69	0.991745	-2 2 6 4
58	211.77	0.998065	1 1 7 1		140	253.02	0.992341	-1 2 7 1
59	211.89	0.991125	-1 1 5 1		141	253.45	0.991814	-2 2 4 4
60	211.97	0.991515	2 2 6 3		142	254.97	0.991676	-2 2 8 4
61	211.98	0.997535	2 1 4 4		143	256.82	0.992318	1 2 3 1
62	212.59	0.991585	2 2 4 3		144	258.88	0.992502	-1 2 5 4
63	213.31	0.990359	-2 1 6 4		145	260.65	0.992331	-1 2 7 4
64	213.64	0.990955	-1 1 7 1		146	264.25	0.992308	1 2 3 4
65	213.74	0.990429	-2 1 4 4		147	267.04	0.992554	-1 2 3 1
66	213.79	0.997397	2 1 8 4		148	274.68	0.992545	-1 2 3 4
67	214.06	0.991447	2 2 8 3					
68	215.03	0.993058	1 3 3 3					
69	215.48	0.990974	-1 3 7 2					
70	215.56	0.990291	-2 1 8 4					
71	216.87	0.992261	2 3 6 1					
72	217.12	0.992272	1 2 5 3					
73	217.40	0.992330	2 3 4 1					
74	217.49	0.998227	1 1 5 4					
75	217.64	0.991119	-1 3 3 3					
76	218.67	0.992102	1 2 7 3					
77	219.09	0.992192	2 3 8 1					
78	219.20	0.998055	1 1 7 4					
79	219.38	0.990324	-2 3 6 1					
80	219.43	0.991116	-1 1 5 4					
81	219.64	0.992422	2 3 2 1					
82	219.92	0.990393	-2 3 4 1					

The method to reduce this data in order to define the optimum system configurations as a function of weight and reliability is as follows. Starting with the ranking by type of Constraint No. 1 (reference Table 27), the minimum weight system was identified and the listing was then scanned to determine the next system of higher reliability that yielded a minimum increase in weight. This eliminated from consideration those systems of lower reliability and higher weight than the first system. The optimum systems were recorded and the procedure was then repeated until a system was found having a reliability equal to or greater than a higher constraint or a weight heavier than the minimum weight system of the next higher reliability constraint. The ranking by type for this higher constraint was then scanned in the same way. This procedure was continued through the highest reliability systems listed in the ranking by type for Constraint No. 20. With this approach, the optimum systems were therefore identified over the entire reliability range. These systems dominated all other system configurations because they represent the minimum achievable weight for a given reliability level. Conversely, all of the systems rejected were either less reliable for an equivalent weight or heavier for an equivalent reliability. The systems identified as optimum then constitute an envelope of minimum weight maximum reliability configurations. For each of these configurations, the reliability versus weight matrix of optima was plotted to arrive at a graphic comparison of the several optimum system types.

4.2 RELIABILITY IMPROVEMENT METHODS

Several conventional techniques are available to the power system designer in maximizing the reliability of a power system. These are:

- a) The selection of systems of inherently high reliability.
- b) The derating of parts with respect to thermal, electrical and mechanical stresses.
- c) The selection and screening of parts.
- d) The implementation of redundancy in the system design.

In considering the effect on power system reliability of alternative power system configurations, the approach taken was to establish a large number of feasible system configurations and evaluate each with the aid of a computer. As described previously under baseline system configurations, the selected baseline systems resulted from logical implementations of several different basic functional configurations. Although it is clear that all possible designs cannot be covered in this manner, the range of systems considered is adequate to permit realistic comparisons of various power system approaches. The assessment of the reliability of each unit within a particular power system configuration is based on the parts count of the selected design for that particular unit and standard failure rates for each part. It is recognized that variations of these selected unit designs will have an impact on the parts count and resultant reliability. However, these variations, in general, constitute second order effects and the selected parts count and resultant reliability values for each particular unit design are representative.

Consideration of the impact of part derating and part selection and screening on the reliability of the various power systems is eliminated from the study by assuming a 25 percent maximum stress level for all of the parts and further assuming the use of high-reliability parts with adequate screening. These assumptions are reflected in the failure rates used for the generic part types in the reliability analyses.

As a result of the selected study approach and the assumptions made relative to parts, the variable remaining in considering methods of improving the reliability of power systems was that of redundancy. Newer unconventional approaches to improving power system reliability, such as the self-regulating and protecting (SRAP) concept being investigated by TRW Systems under contract NAS 5-9178, were not considered in this program. The development of such concepts has not yet progressed to the point where a realistic assessment of their impact on reliability and weight of power systems can be ascertained.

With proper parts application and screening, and with adequate derating with respect to thermal, mechanical, and electrical stresses, the possibility of a failure should be virtually eliminated with the exception of potential wearout failure modes. It was not the purpose of this study to investigate the realism of part failure rates when correct derating and proper parts application policies are followed. Whether attributable to undetected manufacturing defects or incorrectly calculated stress levels, the fact remains that failures in space applications have occurred. This experience has been used as the most realistic basis for determining the failure rates of the generic part types. The selected failure rates represent a major assumption in the analysis of power system reliability. But the benefits to be derived from this study program lie not so much in the absolute reliability numbers that result from the calculations, but rather in the fact that it has permitted the comparative evaluation of a large number of power system configurations on a common basis.

4.2.1 Implementation of Redundancy

Specific methods of implementing redundancy in the units of the various systems have been selected for the system optimization analyses. The investigations leading to these selections have included consideration of the failure modes of each type of unit, the effects of unit failures on system operation and the effects of implementing redundancy on unit weight and performance.

Four basic approaches to implementing redundancy were considered for each type of unit: parallel, standby, quad, and majority voting. The reliability equations and basic configuration for each are described in the following paragraphs.

Since each part of a nonredundant unit has its own failure rate, the general equation for the probability of survival is:

$$P_S = e^{-\lambda t}$$

where

P_S = probability of survival or reliability

λ = the summation of the failure rates for all parts

t = total operating time required.

Figure 56 shows a basic system configuration of "N" elements in series. The equation for the probability of survival of the system is

$$P_S = P_1 \times P_2 \times \text{----} \times P_n$$

where

$P_1 \longrightarrow P_n$ are the reliabilities of each element.

Figure 57 shows a parallel redundant system comprised of two groups of 1 through "N" series elements. Each of the two parallel groups is completely independent and either one can perform the required function.

The probability of survival is:

$$P_S = 1 - \left[(1 - P_A) (1 - P_B) \right]$$

where

P_A and P_B are the survival probabilities of the independent strings.

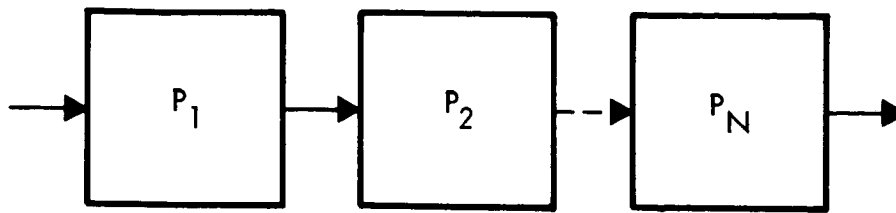


Figure 56. Basic System Reliability Model

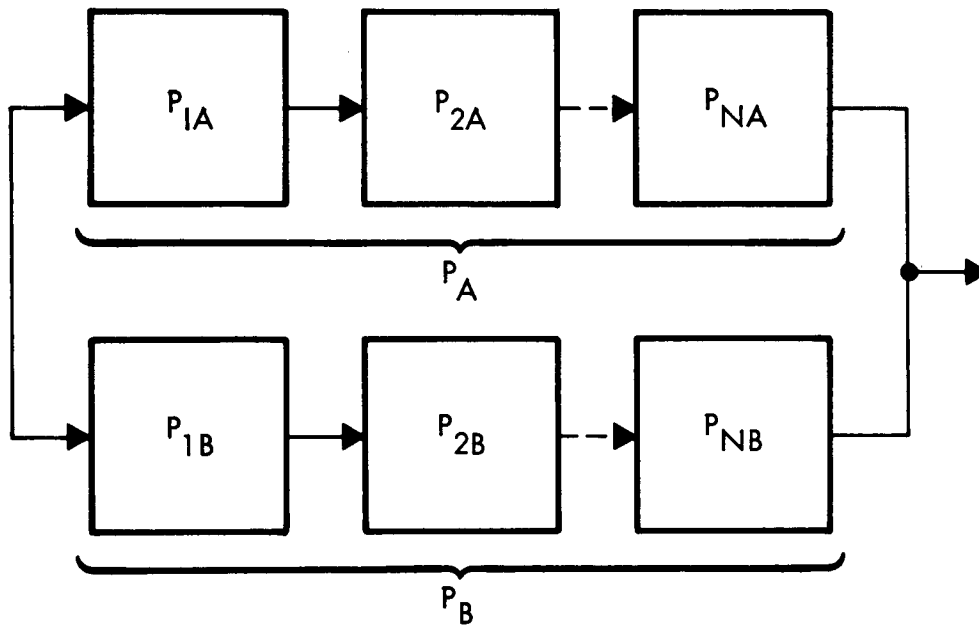


Figure 57. Parallel Redundant System Reliability Model

Parallel operating channels have limited usage because there are some failure mode conditions which they cannot correct. For example, one of the two parallel channels could fail in a manner which causes their common output voltage to go above limits.

In the standby redundant configuration of Figure 58, there are two parallel channels, but only one is operating at any time. This configuration requires additional circuitry to sense a failure in the operating channel and a switching element to transfer to the standby elements in case of a primary element failure.

The equation for probability of survival is:

$$P_S = 1 - \left[(1 - P_1 P_{SW}) (1 - P_2 P_{SW}) \right]$$

where

P_1 and P_2 are the reliabilities of the independent channels, and

P_{SW} = the reliability of the failure sensing and switching elements.

Standby redundancy is generally used for power circuits since it does not cause a significant loss in efficiency.

Quad redundancy is normally implemented at the part level and is illustrated in Figure 59. Either string can perform the required function. The reliability of this configuration is:

$$P_S = 1 - (1 - P_1^2)^2$$

where

P_1 = the reliability of a single part.

The quad configuration is normally not used for series power handling circuits because of its poor efficiency.

Figure 60 shows a block diagram of a majority voting configuration. Two out of the three elements must be operative in order to perform the required function. The probability of survival is:

$$P_S = 1 - \left[(1 - P_1 P_2) (1 - P_2 P_3) (1 - P_1 P_3) \right]$$

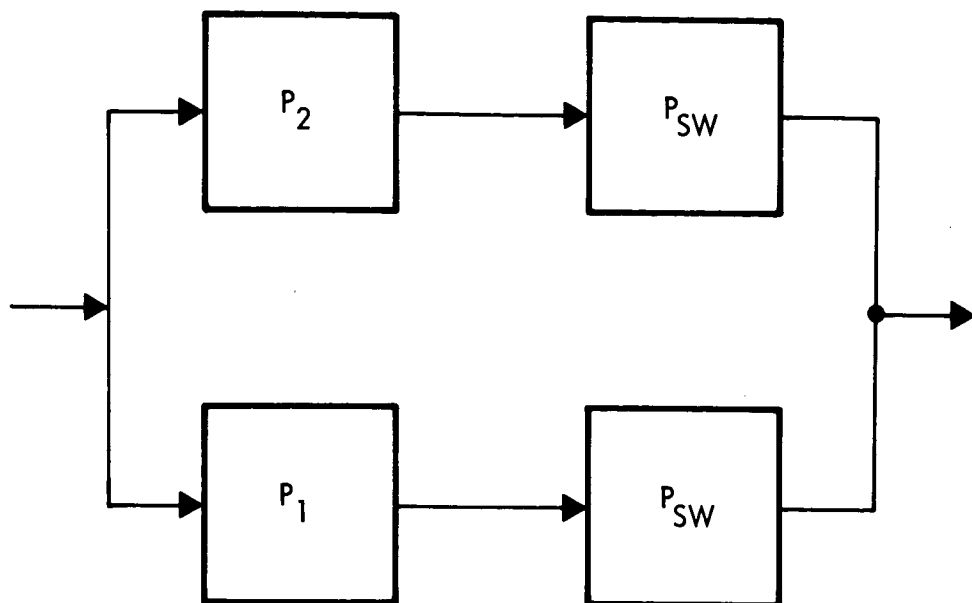


Figure 58. Standby Redundant System Reliability Model

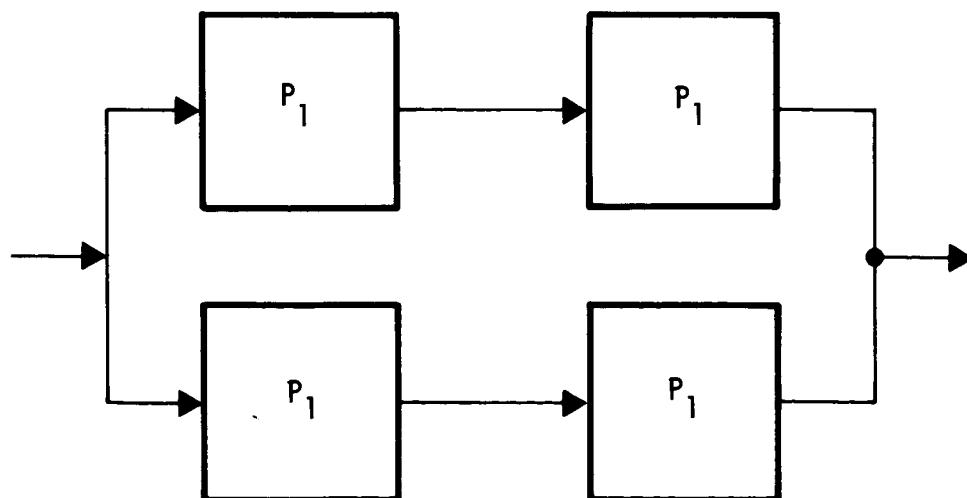


Figure 59. Quad Redundant System Reliability Model

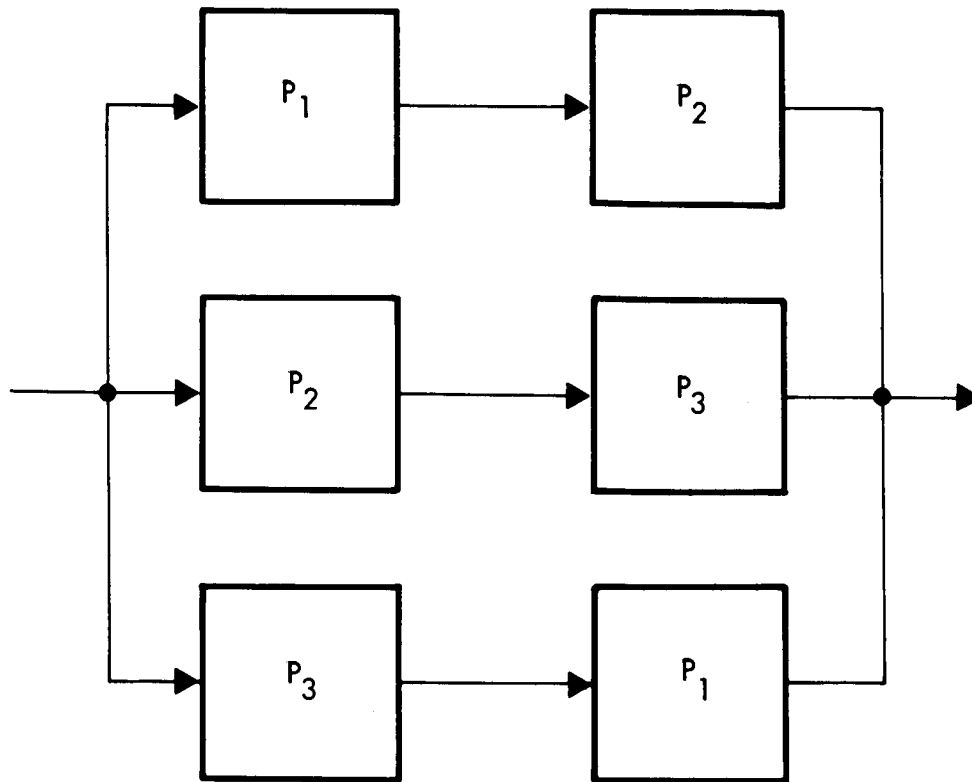


Figure 60. Majority Voting System Reliability Model

where

P_1 , P_2 , and P_3 are the reliabilities of each element.

In most cases $P_1 = P_2 = P_3$, therefore

$$P_S = 1 - (1 - P_1^2)^3$$

Majority voting redundancy is generally applied to low-power sensing circuits.

4.2.2 Selected Redundant Configurations and Parts Counts

The power systems have been divided into the following units, each of which may have many design configurations:

- Solar array
- Array control

- Battery control
- Battery
- Line regulator
- Load power conditioning units
(ac or dc distribution)

4.2.2.1 Solar Array

The solar array configuration is the same for either a baseline system or a redundant system and includes multiple-parallel interconnections of series strings of cells to minimize the effects of cell or connection open-circuit failures on the output power of the array.

4.2.2.2 Array Controls

Five specific array control designs have been considered:

- Zener diode shunt
- Active dissipative shunt
- Pulsewidth modulated series bucking regulator
- Pulsewidth modulated series bucking regulator
with maximum power tracking
- Pulsewidth modulated buck-boost regulator.

The zener diode voltage limiter design is the same for the baseline and redundant configurations and uses multiple-parallel shunt circuits, each controlling a parallel section of the array. If a diode shorts, the solar power will be degraded by $1/N$ where N is the number of parallel zener diodes. Series diodes between the zener diode connection and the common solar array bus prevent current flow through a shorted zener diode from the other parallel array sections. If a zener diode opens, the remaining diodes will limit total array voltage.

The active shunt redundant design uses the majority voting configuration for the voltage sensing and error amplifying stages as illustrated in Figure 61, and uses the quad part configuration for the power transistors and output filter. Figure 61a shows that the nonredundant configuration of the voltage sensing and error amplifier is composed of

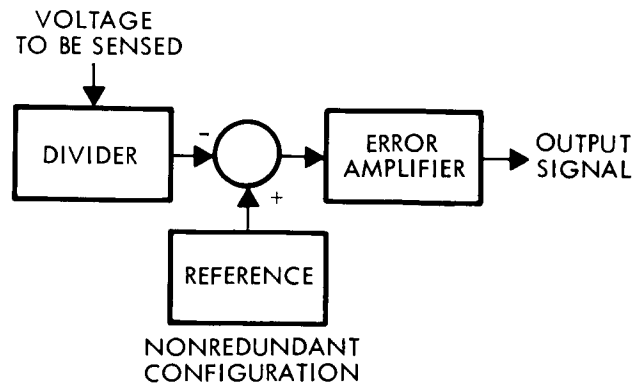


Figure 61a. Nonredundant Voltage Sensing and Error Amplifier Block Diagram

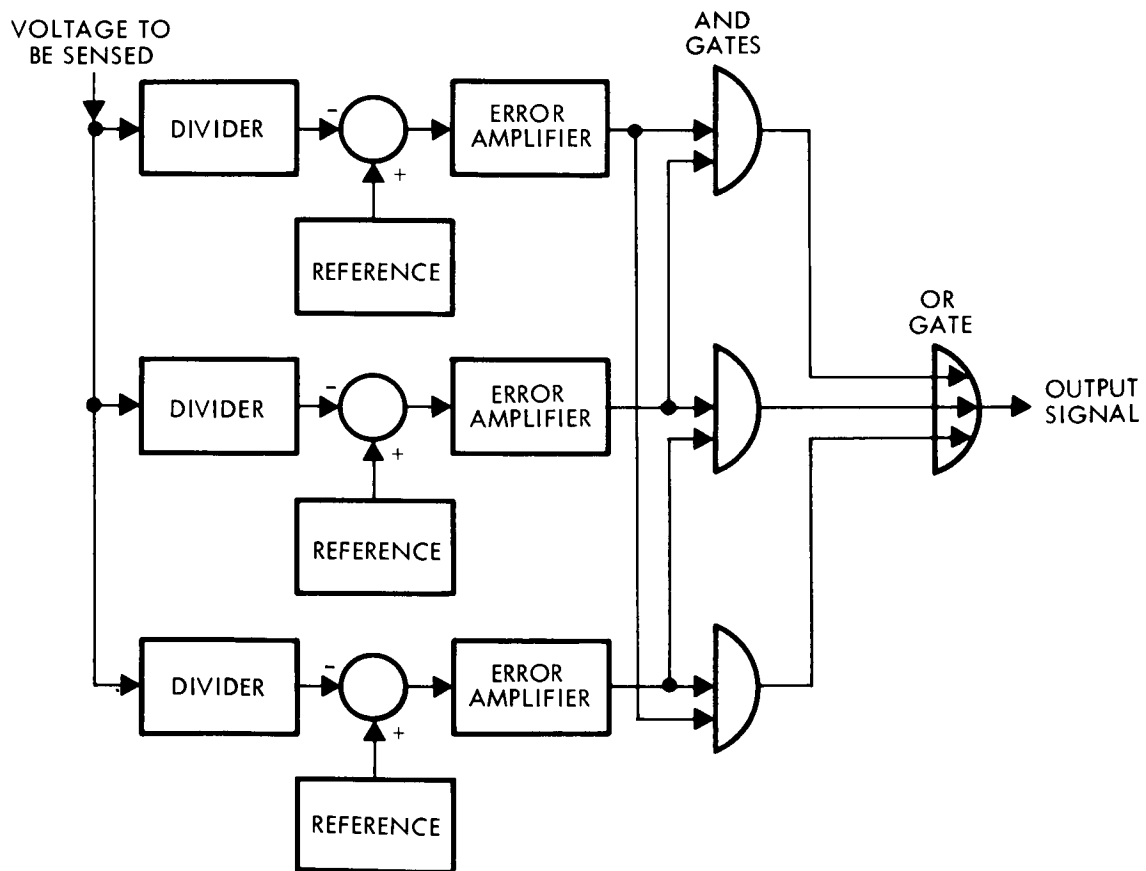


Figure 61b. Majority Voting Redundant Configuration of Voltage Sensing and Error Amplifier

a voltage divider that reduces the magnitude of the sensed voltage to a level comparable to the reference, a precision voltage reference, a summing point, and an error amplifier stage. The redundant majority voting block diagram is illustrated in Figure 61b. It has three non-redundant parallel circuits plus three AND gates and an OR gate. Each AND gate receives two amplified signals and if they are correct the output signal is obtained.

The problem in design with this approach is that the total gain of the circuit varies by a factor of 3 to 1 depending on the failure modes, and it has to be considered to ensure that the regulation or stability is not affected. The quad part configuration is permissible in this case for the shunt power elements because they become active only when there is excessive solar array power in relation to the load demand and do not, therefore, degrade system efficiency.

The pulsewidth-modulated series bucking regulator uses a switching series transistor that controls the power from the solar array to the spacecraft loads. The quad component configuration is not used for this series switch since it would cause a significant decrease in system efficiency. Parallel-operating regulators cannot be used because if a switching transistor shorts, the full solar array voltage will appear on the output and the other parallel regulator could not control for this condition. Therefore, the standby redundant configuration is used and if a failure occurs, the failed regulator is switched out and the standby regulator is energized to control the array output. This approach will produce an output transient during the switching interval; however, all of the systems include a battery and line filters which will tend to minimize the effects of this momentary power interruption. The failure-sensing circuits monitor the output voltage and generate the transfer signal if the output voltage is not within tolerance. A sufficient time delay is designed into the circuitry so that erroneous transfer is not allowed during start-up or load-switching transients. The maximum power tracking regulator and the buck-boost regulator also use the standby redundancy configuration. The parts count for baseline and redundant configurations of each array control are shown in Tables 28 and 29.

Table 28. Array Controls, Baseline Parts Count

Unit	Resistors			Diodes			Capacitors			Transistor		Magnetics			Relays		Other/ Comments
	Carbon Composition	Metal Film	Wire Power	General- Purpose	Rectifiers	Zener	Ceramic	Tantalum Foil	Tantalum Solid	< 1 W	> 1 W	Transformers	Chokes	Mag-Amps	General 4 Sets	Latching 2 Coil	
Zener Diodes						15											
Active Shunt		13	4			1	1	3		4	3						
PWM Buck		21	4	13	1	2	2	3		6	2	3	2	1			
PWM Buck Maximum Power Tracker		40	4	16	1	4	3	3	4	16	2	6	2	1			
PWM Buck-Boost		21	3	13	1	2	1	3		6	2	4	1	1			

Table 29. Array Controls, Redundant Parts Count

Unit	Resistors			Diodes			Capacitors			Transistor		Magnetics			Relays		Other/ Comments
	Carbon Composition	Metal Film	Wire Power	General- Purpose	Rectifiers	Zener	Ceramic	Tantalum Foil	Tantalum Solid	< 1 W	> 1 W	Transformers	Chokes	Mag-Amps	General	Latching 2 Coil	
Zener Diodes						15											
Active Shunt (Power Elements)		4			3			3		3							Quad parts
Active Shunt (Controls)	15					1	2			6							Majority voting
PWM Buck	47	4	4	17	1	4	2	3	2	16	2	3	2	1		1	Standby
PWM Buck Maximum Power Tracker	66	4	4	20	1	6	3	3	6	26	2	6	2	1		1	Standby
PWM Buck-Boost	47	3	3	17	1	4	1	3	2	16	2	4	1	1		1	Standby

NOTE: Quantities shown are for each element of the applicable redundant configuration
(i.e., total quantity per unit = number shown x 4 for quad, x 3 for majority voting
and x 2 for standby redundancy).

4.2.2.3 Battery Controls

Standby redundancy cannot be used for these controls because of the extreme difficulty in sensing a failure or out-of-tolerance condition over the wide range of charge and discharge operating conditions. Instead, the majority voting redundancy is used for the low-level signals and logic and part redundancy is used for the power circuits. The selected methods of implementing part redundancy are shown in Figure 62.

The redundant transformer, Figure 62(a), consists of two series transformers with parallel primary and secondary windings which are interconnected. The parallel windings protect against open-circuit failures and the series transformers are used to protect against turn-to-turn shorts in one winding. The disadvantages of this approach are that each winding must be capable of full load current rating and also full input voltage rating. Each transformer is twice as large as a simple nonredundant transformer and the total VA rating of the magnetics is four times normal. The same technique is used for a choke but the effect of an inductance change to 50 percent of normal, should a winding develop a turn-to-turn short, must be considered in the design.

Figure 62(b) shows a transistor and its redundant equivalent which is composed of two parallel strings of two transistors in series. If one series transistor develops a short, the remaining good transistor maintains normal operations. The diode in the base circuit of the upper transistor protects against a collector to base short which could otherwise produce uncontrolled base current to the other transistors. The base resistors are needed to protect the current-driving signal source if a transistor base-to-emitter short develops and to cause current sharing among the four transistors.

The disadvantages of this configuration are that the normal current gain is reduced to one-half, and all four transistors must have the same power rating as the single nonredundant transistor. The system must be designed to accommodate wide variations in gain both for normal and failure modes.


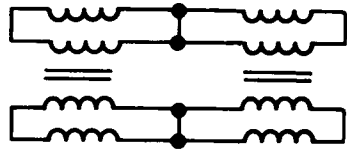
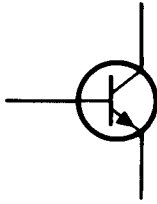
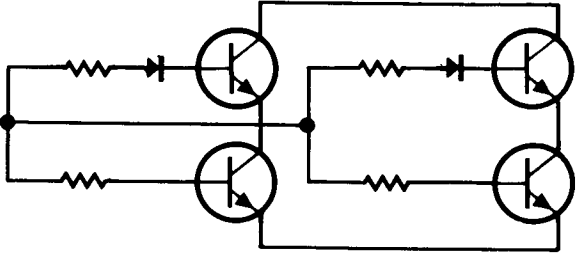

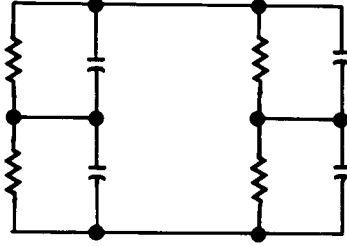




COMPONENT	REDUNDANT COMPONENT
a) MAGNETIC 	 INSULATE BETWEEN PRIMARY AND SECONDARY
b) TRANSISTOR 	
c) CAPACITOR 	
d) RESISTORS 	
e) DIODES 	

Figure 62. Methods of Implementing Part Redundancy

Figure 62(c) shows the nonredundant and the redundant capacitor configurations. The redundant capacitor has two parallel strings of two series capacitors. Resistors are placed in parallel with the capacitors to cause equal divisions of voltage. This is particularly important for tantalum capacitors where a normal unbalance in leakage current can cause unequal division of voltage. This unbalance in voltage may produce voltage reversal on the capacitors during discharge and a resultant failure.

The disadvantages of this configuration are its increased size and weight and the fact capacitance can vary from 0.5 C to 1.5 C. If not considered in the design, this variation can produce excessive ripple or charge regulator instability.

The normal failure mode of the resistor is to drift, open or develop a partial short, and not a complete end-to-end short. The redundant resistor Figure 62(d) is two resistors in parallel. The problem of the redundant resistor is its resistance variation under failure mode conditions.

The redundant diode configuration, Figure 62(e), contains two parallel strings of two diodes in series. The problem of the redundant diode is its increased power loss and change in output voltage when one diode shorts. The zener or reference diode cannot be implemented in this manner and still maintain the voltage accuracy required. Whenever a voltage must be sensed and compared to a reference in a redundant design, the majority voting circuit must be used to maintain a close regulation tolerance (± 1 percent). A precision voltage divider also cannot be obtained by the quad redundant approach.

The relays for discharge control are used in a circuit level majority voting redundant configuration.

In past equipment designs, current levels were normally detected by a magnetic current monitor and its associated ac inverter circuitry. This method does not lend itself to any redundant configuration without undue complexity. As a result, the selected battery controls use a shunt to sense current and a dc amplifier circuit to amplify the low-level signal. This design is much easier to implement in a majority voting redundant configuration.

Tables 30 and 31 list the battery control parts counts for the non-redundant and redundant designs of each type of battery charger and its associated controls.

4.2.2.4 Battery

Silver-zinc batteries were selected for the 0.3 and 5.2 AU probes. Silver-cadmium batteries were chosen for the Mars, Venus and Jupiter orbiters. Two redundant configurations have been selected for analysis. The first of these consists of two parallel batteries, each containing 20 AgCd or 15 AgZn cells, and each capable of satisfying the total energy storage requirement. These numbers of cells are based on providing approximately the same 20- to 32-volt ranges of voltages for all missions. Each battery is used with its own control circuitry which may be either baseline or redundant. This approach was used for all power system configurations.

The second redundant battery configuration consists of three batteries in a two-out-of-three majority voting configuration with each containing only three series cells and each connected to the main power bus through a bucking charge regulator and a boosting discharge regulator.* This approach is only applied as a second alternative redundant battery configuration to those systems which are configured with a regulated main bus. Each of the three batteries has an installed capacity equal to one-half that of the required total battery capacity based on 50 percent maximum depth of discharge. The principal advantage of this second redundant battery configuration is the reduction in number of series-connected cells per battery and the attendant improvement in battery reliability. A second advantage is the reduced total battery weight (150 percent of baseline) in comparison to the first redundant approach (200 percent of baseline). The charge and discharge regulators may be either baseline or redundant.

* This configuration represents one method of applying the TRW Modular Energy Storage and Control concept (MESAC). This concept has been developed and tested under a company-sponsored research program.

Table 30. Battery Controls, Baseline Parts Count

Unit	Resistors			Diodes			Capacitors			Transistor		Magnetics			Relays		Other/Comments
	Carbon Comp.	Metal Film	Wire Power	General Purpose	Rectifiers	Zener	Ceramic	Tantalum Foil	Tantalum Solid	<1W	>1W	Transformers	Chokes	Mag-Amps	General 4 Sets	Latching 2 Coil	
Buck - Resistor		41	2	6	1	3			3	20		3	2			2	Used with systems having unregulated main bus
Buck Resistor & Line Booster		69	2	8	4	4	2	1	6	31	2	3	2	1		2	
Buck Diss. Charger		49	1	4	1	4		1	2	23	2					1	
Buck Diss. Charger & Line Booster		77	1	6	4	5	2	1	5	34	4	3	2	1		1	
PWM Buck Charger		49	2	4	2	2	2	1	3	23	2		2			1	
PWM Buck Charger & Line Booster		77	2	6	5	3	4	2	6	34	4	3	4	1		1	
PWM Buck-Boost Charger		65	2	6	1	4	1	2	6	20	1	1	1	1		1	
PWM Buck-Boost Charger & Line Booster		92	4	8	5	5	1	4	8	32	3	2	3	2			Used with systems having regulated main bus
Diss. Regulator		13	5			1	1	2		4	3						
PWM Buck Regulator		21	4	13	1	2	2	2		6	2	2	2	1			

Table 31. Battery Controls, Redundant Parts Count

Unit	Resistors			Diodes			Capacitors			Tran- sistor		Magnetics				Relays		Other/Comments
	Carbon Comp.	Metal Film	Wire Power	General Purpose	Rectifiers	Zener	Ceramic	Tantalum Foil	Tantalum Solid	<1W	>1W	Transformers	Chokes	Mag-Amps	General 4 Sets	Latching 2 Coil		
Buck Resistor			2	6	1	3			3	22	2	3	2	1		2	Quad Comp. Majority Voting	
Buck Resistor & Line Booster	44	4	2	8	4	4	1	1	6	33	2		2			2	Quad Comp. Majority Voting	
Buck Diss. Charger	65	4	1	4	1	4	1	1	2	25	4	3	2	1		1	Quad Comp. Majority Voting	
Buck Diss. Charger & Line Booster	45	6	1	6	4	5	1	1	5	36	2		2	1		1	Quad Comp. Majority Voting	
PWM Buck Charger	71	4	2	2	2	2	2	1	3	25	4	3	2			1	Quad Comp. Majority Voting	
PWM Buck Charger & Line Booster	45	6	2	2	5	3	1	1	6	36	1	1	1	1		1	Quad Comp. Majority Voting	
PWM Buck-Boost Charger	71	2	2	9	1	4	3	2	6	22	3	2	3	2		1	Quad Comp. Majority Voting	
PWM Buck-Boost Charger & Line Booster	65	2	4	6	5	5	1	4	8	34							Quad Comp. Majority Voting	
PWM Buck-Boost Charger & Line Booster	90	2	4	8	5	5	1	4									Quad Comp. Majority Voting	
Diss. Regulator			5			1	1	2		6	2	2	2	1			Quad Comp. Majority Voting	
PWM Buck Regulator	13	2	4	4	1		1	2		8							Quad Comp. Majority Voting	
	19			9	2	2	1										Quad Comp. Majority Voting	

Note: Quantities listed are for each element of the applicable redundant configuration (i.e., total quantity per unit = number shown x 4 for quad and x 3 for majority voting redundancy).

Note: Quantities listed are for each element of the applicable redundant configuration (i.e., total quantity per unit = number shown x 4 for quad and x 3 for majority voting redundancy).

4.2.2.5 Line Regulators

The following designs were selected for the line regulators:

- Pulsewidth-modulated series bucking regulator
- Series dissipative regulator
- Pulsewidth-modulated boost regulator
- Pulsewidth-modulated buck-boost regulator.

Because of the requirement to minimize weight and losses, standby redundancy configurations are used for the line regulators. However, there will be a momentary loss of power to the load equipment during the transfer to the redundant channel. Certain loads, for example a digital memory, must be protected during the power shutdown. This is normally done by having the failure-sensing circuits give advance warning to these types of loads. Typically, this warning signal initiates required inhibit and sequencing functions within the load equipment before the output voltage of the power supply has deviated significantly from steady-state conditions.

Tables 32 and 33 are the part counts for the baseline and redundant configurations of each line regulator.

4.2.2.6 Load Power Conditioner

The components used for load power conditioning have been analyzed with respect to the specific load requirements of each model spacecraft to define specific equipment groupings and performance requirements. The equipment for those systems using dc power distribution are as follows:

- 3 ϕ 400 Hz gyro inverter
- Central converter (dc to dc)
- Transmitter converter (high or low voltage)
- Computer — sequencer converter (low voltage)
- Television converter (high voltage)
- Experiment converter (low voltage)
- Experiment converter (high voltage)

Table 32. Line Regulators, Baseline Parts Count

Unit	Resistors			Diodes			Capacitors			Transistor		Magnetics			Relays		Other/Comments
	Carbon Comp.	Metal Film	Wire Power	General Purpose	Rectifiers	Zener	Ceramic	Tantalum Foil	Tantalum Solid	<1W	>1W	Transformers	Chokes	Mag-Amps	General 4 Sets	Latching 2 Coil	
PWM Buck		21	4	13	1	2	2	2		6	2	2	2	1			See Note
Diss. Series		13	5			1	1	2		4	3						
Boost		16	2	6	3	2	2	2		6	2	3	2	1			
Buck-Boost		21	3	13	1	2	2	2		6	1	3	1	1			

Note: Boost line regulator also applicable to boost discharge regulator for battery in regulated bus systems

Table 33. Line Regulators, Redundant Parts Count

Unit	Resistors			Diodes			Capacitors			Transistor		Magnetics			Relays		Other/Comments
	Carbon Comp.	Metal Film	Wire Power	General Purpose	Rectifiers	Zener	Ceramic	Tantalum Foil	Tantalum Solid	<1W	>1W	Transformers	Chokes	Mag-Amps	General 4 Sets	Latching 2 Coil	
PWM Buck		47	4	17	1	4	2	2	2	16	2	2	2	1		1	Standby
Diss. Reg.		39	5	4		3	1	2	2	14	3					1	Standby
Boost		42	2	10	3	4	2	2	2	16	2	3	2	1		1	Standby
Buck-Boost		47	3	17	1	4	2	2	2	16	1	3	1	1		1	Standby
<p>Note: Quantities listed must be doubled to determine total unit parts count. Boost line regulator also applicable to boost discharge regulator for battery in regulated bus systems.</p>																	

The equipment selected for systems using ac power distribution are as follows:

- 3 ϕ 400 Hz gyro inverter
- Main inverter (dc to ac)
- Transmitter transformer-rectifier (TR) (high voltage or low voltage)
- Equipment TR
- Television TR (high voltage)
- Experiment TR (low voltage)
- Experiment TR (high voltage)

A distinction is being made between high voltage outputs and low voltage outputs. At high voltage, the transformer designs are heavier due to increased insulation requirements and the output filter capacitors are larger.

Each spacecraft will have its own set of equipment due to the variation in the equipment and the experiments to be performed. Standby redundancy has been selected for all the load power conditioning equipment.

Tables 34 through 61 list the parts counts for Power Conditioning Equipment.

4.2.3 Failure Mode Effects

In the implementation of the preferred standby redundant method in the majority of the series regulators and load power conditioning equipment, it is necessary that consideration be given to the operation of the failure detection and switching circuits in the event of a malfunction. Whereas the use of quad parts or majority voting redundancy will, in event of failure of any individual part within the unit, produce a negligible effect on its performance, standby redundancy presupposes the presence of an out-of-tolerance condition as a result of any part failure within the unit.

Although, in specific instances, it may be desirable to sense both the input and outputs of a given unit, the approach selected herein uses failure-detection circuitry which only monitors the output voltage of standby redundant units. Since a part failure can produce either an overvoltage or undervoltage condition at the output of the unit, the failure-detection circuitry must be capable of monitoring the output voltage over its normal range and detecting any sustained excursion either above or below that specified range.

Since the power system regulation and power conditioning units are in most cases common to other power system units at both their inputs and outputs, it is always necessary to perform analyses of the effects of failures in one unit on the performance of the other units in the power system. When properly implemented, failure detection and standby redundant switching eliminate the possibility of steady state failure mode conditions. As a result, these failure-effects analyses are primarily related to transient conditions which exist in the system subsequent to the fault and prior to the time that the redundant switching functions operate.

Typically, failures in any of the low power control circuitry will tend to produce a deviation of the output of the given unit from its specified range of operating values. It is rare that a failure of this type can produce a deleterious effect on other units within the system unless a prolonged exposure to this out-of-specification condition occurs. Time delays are essential in the implementation of standby redundancy to prevent switching from the operative channel to the redundant channel in the event of a transient condition at the output terminals of the unit. These time delays can be made relatively short and the anticipated out-of-specification conditions resulting from control circuit failures will therefore not exist for a sufficiently long period of time to damage other equipment.

The major area of concern with the implementation of standby redundancy is the ability of this approach to protect against catastrophic failures of major power handling elements within the system which produce a direct short circuit at the input terminals of the unit. A failure of this type obviously can impose a sizable overload on other

power system units which supply power to the particular unit in which the failure has occurred. In those systems having a capability of the battery discharging into such a fault, the overload currents will be very large. It is clear that these large fault currents cannot be relied on to clear the short circuit. The major problem occurring then with such fault conditions is that the series units within the power system may be subjected to damage from excessive overloads produced by failures in another unit prior to the time the standby redundant switching circuitry in the failed unit has operated.

The most suitable technique for protecting against failures of this type and to prevent damage to other units in the power system until the failed unit has been switched out and the standby unit has switched in is to provide a fusing element in series with capacitors, transistors and diodes which, if failed in the short-circuit mode, would produce a direct short circuit of the power bus. These fusing elements can be of many types. In addition to a fuse itself, the use of small wire-size leads on capacitors and low power-rated wire-wound resistors in series with capacitors have been employed with success.

Detailed analysis of specific failure modes and effects must include the characteristics of filters used in the power system units and the ability of these filters to effect a time delay in the appearance of an overcurrent condition in other units as a result of a short circuit within a particular unit. The presence of filter capacitors will normally provide a low impedance source of stored energy to supply fault current within the unit for a limited period of time. Similarly, the associated filter inductor will limit the rise time of input current to the unit. However, the effect of these filters is twofold in that, depending upon the particular location of the malfunction within the unit, the filter may delay the manifestation of a failure at the output terminals of the unit. Thus, the ability of the filters is decreased in giving a degree of protection against overloads in other units of the power system until the standby redundancy in the failed unit operates to remove a fault.

Another time related factor is that the failures of transistors, which are considered the most critical elements in the event of an overload, are often thermal failures, and although the relatively small thermal mass of these devices permits rapid rises in temperature, there may be a lag between the application of the overload condition and the manifestation of this overload as an excessive junction temperature.

Design tradeoffs are necessary between the characteristics of the filters, the magnitudes of fault currents and the time delays used in the fault removal or standby redundant switching circuitry. These time delays in standby redundant circuitry should be minimized whenever possible. The faster the unit reacts to the failure and switches to its standby channel the lower will be the input current to the failed channel, assuming a short circuit within that channel. The question of relay current interruption capability can be resolved more readily without excessively large contact ratings on the switching relays if the time delay is minimized. The delay in switching to a redundant channel, however, must be adequate to permit similar switching operations in units which constitute a load on the particular unit in consideration.

As an example, it is assumed that an inverter is supplying a series of TR units and one of the essential TR units is built in a standby redundant configuration. A short circuit failure within that TR unit will persist for an estimated 20 to 25 msec until its logic and control circuitry has detected the malfunction and the relay has switched from the operating channel to the redundant channel. During this period of time, the inverter will be subject to increasing load current and its output voltage will tend to fall. If this reduction of output voltage is instantly detected by the standby switching circuitry in the inverter, the inverter will switch to its redundant channel unnecessarily.

Although it might appear that the time delay for standby redundant switching circuitry would become progressively larger as one started from the loads and worked back through the power system towards the source, this does not appear to be the case because of the action of the filters that are common to all of the units. It is essential that detailed analyses of these effects be made at the circuit level in the design of all power system units. Time delay circuits were included

Table 34. Load Power Conditioning Equipment, Baseline Parts Count,
Mercury Flyby, AC Distribution System

Unit	Resistors			Diodes			Capacitors				Transistors		Magnetics			Relays		Other / Comments
	Carbon Compound	Metal Film	Wire Power	General Purpose	Rectifiers	Zener	Ceramic	Tantalum Foil	Tantalum Solid	Plastic	< 1W	> 1W	Transformers	Chokes	Mag-Amps	General 4 Sets	Latching 2 Coil	
Gyro Inverter 3 ϕ (400~)		38	9	6	6		14	1	3		9	6	6	1				
Main Inverter		5		4			2	1			2	2	4	1				
Transmitter TR (HV)					8				2	2			1					
Equipment TR (LV)					14			2	5				1					
TV TR (HV)					12				4	2			1					
Experiment TR (LV)																		
Experiment TR (HV)					12				5	1			1					

in all of the selected unit designs that employ standby redundancy for this study and are reflected in the parts counts assigned to each of the various units.

A final consideration in the interactions between units, in the event of a failure, is the design of units with sufficient oversizing to prevent their damage due to a fault in another series unit of the power system. However, this approach tends to significantly penalize unit weight and efficiency. Reliability considerations normally dictate part stress levels on the order of 25 percent of the manufacturers rating. Thus, in the event of a failure, there exists some capability to support overloads or to blow fuses. Failures can always be hypothesized, however, which produce direct short circuits on an element of the power system, and normal derating would not protect the power system element in this case. As a result, current-limiting circuitry is always preferred over unit oversizing to protect against overloads.

Table 35. Load Power Conditioning Equipment, Redundant Parts Count, Mercury Flyby, AC Distribution System

Unit	Resistors			Diodes			Capacitors				Transistors		Magnetics			Relays		Other / Comments
	Carbon Compound	Metal Film	Wire Power	General Purpose	Rectifiers	Zener	Ceramic	Tantalum Foil	Tantalum Solid	Plastic	< 1W	> 1W	Transformers	Chokes	Mag-Amps	General 4 Sets	Latching 2 Coil	
Gyro Inverter 3 ϕ (400~)		54	6	21	6	1	14	1	10		13	6	6	1			5	Standby
Main Inverter		10		10		1	2	1	2		5	2	4	1			2	Standby
Transmitter TR (HV)		15		6	8	1			4	2	3		1				1	
Equipment TR (LV)		19		6	14	1		2	7		3		1				1	
TV TR (HV)		18		6	12	1			6	2	3		1				1	
Experiment TR (LV)							NOT		REQUIRED									Standby
Experiment TR (HV)		18		6	12	1		7	1		3		1					Standby

Note: Parts count listed for one of two identical standby redundant channels in each unit.

Table 36. Load Power Conditioning Equipment, Baseline Parts Count, Mercury Flyby, DC Distribution System

Unit	Resistors			Diodes			Capacitors				Transistors		Magnetics			Relays		Other / Comments
	Carbon Compound	Metal Film	Wire Power	General Purpose	Rectifiers	Zener	Ceramic	Tantalum Foil	Tantalum Solid	Plastic	<1W	>1W	Transformers	Chokes	Mag-Amps	General 4 Sets	Latching 2 Coil	
Transmitter Converter (HV)		6		4	8		2	1	3	2	2	2	4	1				
Gyro Inverter 3 ϕ (400~)		38	6	6	6		14	1	3		9	6	6	1				
Main Converter (LV)		6		4	12		2	1	6		2	2	4	1				
TV Converter (HV)		6		4	12		2	1	4	2	2	2	4	1				
Computer and Sequencer Converter (LV)		6		4	8		2	1	4		2	2	4	1				
Experiment Converter (HV)		6		4	12		2	1	5	1	2	2	4	1				
Experiment Converter (LV)				Not Required														

Table 37. Load Power Conditioning Equipment, Redundant Parts Count, Mercury Flyby, DC Distribution System

[illegible]

Note: Parts count listed for one of two identical standby redundant channels in each unit.

Table 38. Load Power Conditioning Equipment, Baseline Parts Count,
Venus Orbiter No. 1, AC Distribution System

Unit	Resistors			Diodes			Capacitors			Transistor			Magnetics			Relays		Other/ Comments
	Carbon Comp.	Metal Film	Wire Power	General Purpose	Rectifiers	Zener	Ceramic	Tantalum Foil	Tantalum Solid	Plastic	<1W	>1W	Transformers	Chokes	Mag-Amps	General 4 Sets	Latching 2 Coil	
Gyro Inverter		38	6	6	6		14	1	3		9	6	6	1				
Main Inverter		5		4			2	1			2	2	4	1				
Transmitter TR (LV)					12				6				1					
Equipment TR (LV)					14				7				1					
T.V. TR (HV)	NOT REQUIRED																	
Experiment TR (LV)					6				3				1					
Experiment TR (HV)					12				3	3			1					

Table 39. Load Power Conditioning Equipment, Redundant Parts Count,
Venus Orbiter No. 1, AC Distribution System

Unit	Resistors			Diodes			Capacitors			Transistor			Magnetics			Relays		Other/ Comments
	Carbon Comp.	Metal Film	Wire Power	General Purpose	Rectifiers	Zener	Ceramic	Tantalum Foil	Tantalum Solid	Plastic	< 1W	> 1W	Transformers	Chokes	Mag-Amps	General 4 Sets	Latching 2 Coil	
Gyro Inverter		54	6	21	6	1	14	1	10		13	6	6	1			5	Standby
Main Inverter		10		10		1	2	1	2		5	2	4	1			2	
Transmitter TR (LV)		15		6	12	1			8		3		1				1	
Equipment TR (LV)		16		6	14	1			9		3		1				1	
T. V. TR (HV)	NOT REQUIRED																	
Experiment TR (LV)		12		6	6	1			5		3		1				1	
Experiment TR (HV)		20		6	12	1			5	3	3		1				1	Standby

Note: Parts count listed for one of two identical standby
redundant channels in each unit.

Table 40. Load Power Conditioning Equipment, Baseline Parts Count,
Venus Orbiter No. 1, DC Distribution System

Unit	Resistors			Diodes			Capacitors			Transistor			Magnetics			Relays		Other/ Comments
	Carbon Comp.	Metal Film	Wire Power	General Purpose	Rectifiers	Zener	Ceramic	Tantalum Foil	Tantalum Solid	Plastic	<1W	>1W	Transformers	Chokes	Mag-Amps	General 4 Sets	Latching 2 Coil	
Transmitter Converter (LV)		6		4	12		2	1	6		2	2	4	1		General 4 Sets		
Gyro Inverter		38	6	6	6		14	1	3		9	6	6	1				
Main Converter (LV)		6		4	12		2	1	6		2	2	4	1				
TV Converter (HV)	NOT REQUIRED																	
Computer-Sequencer Converter (LV)		6		4	8		2	1	4		2	2	4	1				
Experiment Converter (HV)		6		4	12		2	1	3	3	2	2	4	1				
Experiment Converter (LV)		6		4	6		2	1	3		2	2	4	1				

Table 41. Load Power Conditioning Equipment, Redundant Parts Count,
Venus Orbiter No. 1, DC Distribution System

Unit	Resistors				Diodes			Capacitors			Transistor			Magnetics			Relays		Other/ Comments
	Carbon Comp.	Metal Film	Wire Power	General Purpose	Rectifiers	Zener	Ceramic	Tantalum Foil	Tantalum Solid	Plastic	< 1W	> 1W	Transformers	Chokes	Mag-Amps	General 4 Sets	Latching 2 Coil		
Transmitter Converter (LV)		21		10	12	1	2	1	8		5	2	4	1			1	1	↔ Standby
Gyro Inverter		54	6	21	6	1	14	1	10		13	6	6	1			5		
Main Converter (LV)		21		10	12	1	2	1	8		5	2	4	1			1		
TV Converter (HV)	NOT REQUIRED																		
Computer-Sequencer Converter (LV)		19		10	8	1	2	1	6		5	2	4	1			1		
Experiment Converter (HV)		24		10	12	1	2	1	5	3	5	2	4	1			1		
Experiment Converter (LV)		18		10	6	1	2	1	5		5	2	4	1			1	1	

Note: Parts count listed for one of two identical standby
redundant channels in each unit.

Table 42. Load Power Conditioning Equipment, Baseline Parts Count,
Venus Orbiter No. 2, AC Distribution System

Unit	Resistors			Diodes			Capacitors				Transistors		Magnetics			Relays		Other / Comments
	Carbon Compound	Metal Film	Wire Power	General Purpose	Rectifiers	Zener	Ceramic	Tantalum Foil	Tantalum Solid	Plastic	< 1W	> 1W	Transformers	Chokes	Mag-Amps	General 4 Sets	Latching 2 Coil	
Gyro Inverter 3 ϕ (400~)		38	6	6	6		14	1	3		9	6	6	1				
Main Inverter		5		4			2	1			2	2	4	1				
Transmitter TR (HV)					8				2	2			1					
Equipment TR (LV)					14			2	5				1					
TV TR (HV)					12				4	2			1					
Experiment TR (LV)					8			3	1				1					
Experiment TR (HV)					6				2	1			1					

Table 43. Load Power Conditioning Equipment, Redundant Parts Count,
Venus Orbiter No. 2, AC Distribution System

Unit	Resistors			Diodes			Capacitors				Transistors		Magnetics			Relays		Other / Comments
	Carbon Compound	Metal Film	Wire Power	General Purpose	Rectifiers	Zener	Ceramic	Tantalum Foil	Tantalum Solid	Plastic	<1W	>1W	Transformers	Chokes	Mag-Amps	General 4 Sets	Latching 2 Coil	
Gyro Inverter 3 ϕ (400~)		54	9	21	6	1	14	1	10		13	6	6	1			5	Standby
Main Inverter		10		10			2	1	2		5	2	4	1			2	
Transmitter TR (HV)		15		6	8	1			4	2	3		1				1	
Equipment TR (LV)		19		6	14	1		2	7		3		1				1	
TV TR (HV)		18		6	12	1			6	2	3		1				1	
Experiment TR (LV)		16		6	8	1		3	3		3		1				1	
Experiment TR (HV)		15		6	6	1			4	1	3		1				1	Standby

Note: Parts count listed for one of two identical standby
redundant channels in each unit.

Table 44. Load Power Conditioning Equipment, Baseline Parts Count,
Venus Orbiter No. 2, DC Distribution System

Unit	Resistors			Diodes			Capacitors				Transistors		Magnetics			Relays		Other/ Comments
	Carbon Compound	Metal Film	Wire Power	General Purpose	Rectifiers	Zener	Ceramic	Tantalum Foil	Tantalum Solid	Plastic	<1W	>1W	Transformers	Chokes	Mag-Amps	General 4 Sets	Latching 2 Coil	
Transmitter Converter (HV)		6		4	8		2	1	3	2	2	2	4	1				
Gyro Inverter 3 ϕ (400~)		38	6	6	6		14	1	3		9	6	6	1				
Main Converter (LV)		6		4	12		2	1	6		2	2	4	1				
TV Converter (HV)		6		4	12		2	1	4	2	2	2	4	1				
Computer and Sequencer Converter (LV)		6		4	8		2	1	4		2	2	4	1				
Experiment Converter (HV)		6		4	6		2	1	2	1	2	2	4	1				
Experiment Converter (LV)		6		4	8		2	2	4		2	2	4	1				

Table 45. Load Power Conditioning Equipment, Redundant Parts Count, Venus Orbiter No. 2, DC Distribution System

Unit	Resistors			Diodes			Capacitors				Transistors		Magnetics			Relays		Other / Comments
	Carbon Compound	Metal Film	Wire Power	General Purpose	Rectifiers	Zener	Ceramic	Tantalum Foil	Tantalum Solid	Plastic	<1W	>1W	Transformers	Chokes	Mag-Amps	General 4 Sets	Latching 2 Coil	
Transmitter Converter (HV)		21		10	8	1	2	1	5	2	5	2	4	1			1	Standby
Gyro Inverter 3 ϕ (400~)		54	6	21	6	1	14	1	10		13	6	6	1			5	
Main Converter (LV)		21		10	12	1	2	1	8		5	2	4	1			1	
TV Converter (HV)		21		10	12	1	2	1	6	2	5	2	4	1			1	
Computer and Sequencer Converter (LV)		21		10	8	1	2	1	6		5	2	4	1			1	
Experiment Converter (HV)		21		10	6	1	2	1	4	1	5	2	4	1			1	
Experiment Converter (LV)		21		10	8	1	2	2	6		5	2	4	1			1	Standby

Note: Parts count listed for one of two identical standby redundant channels in each unit.

Table 46. Load Power Conditioning Equipment, Baseline Parts Count,
Mars Orbiter, AC Distribution System

Unit	Resistors			Diodes			Capacitors				Tran- sistors		Magnetics			Relays		Other / Comments
	Carbon Compound	Metal Film	Wire Power	General Purpose	Rectifiers	Zener	Ceramic	Tantalum Foil	Tantalum Solid	Plastic	< 1W	> 1W	Transformers	Chokes	Mag-Amps	General 4 Sets	Latching 2 Coil	
Gyro Inverter 3ϕ (400~)		38	6	6	6		14	1	3		9	6	6	1				
Main Inverter		5		4			2	1			2	2	4	1				
Transmitter TR (HV)					8				2	2			1					
Equipment TR (LV)					14			2	5				1					
TV TR (HV)					12				4	2			1					
Experiment TR (LV)					14			3	4				1					
Experiment TR (HV)					6				2	1			1					
Experiment TR (HV)					6				2	1			1					

Table 47. Load Power Conditioning Equipment, Redundant Parts Count,
Mars Orbiter, AC Distribution System

Unit	Resistors			Diodes			Capacitors				Transistors		Magnetics			Relays		Other / Comments
	Carbon Compound	Metal Film	Wire Power	General Purpose	Rectifiers	Zener	Ceramic	Tantalum Foil	Tantalum Solid	Plastic	<1W	>1W	Transformers	Chokes	Mag-Amps	General 4 Sets	Latching 2 Coil	
Gyro Inverter 3 ϕ (400~)		54	6	21	6	1	14	1	10		13	6	6	1			5	Standby
Main Inverter		10		1.0	8	1	2	1	2		5	2	4	1			2	
Transmitter TR (HV)		15		6	14	1			4	2	3		1				1	
Equipment TR (LV)		19		6	12	1		2	7		3		1				1	
TV TR (HV)		18		6	14	1			6	2	3		1				1	
Experiment TR (LV)		19		6	14	1		3	6		3		1				1	
Experiment TR (HV)		15		6	6	1			4	1	3		1				1	
Experiment TR (HV)		15		6	6	1			4	1	3		1				1	Standby

Note: Parts count listed are for one of two identical standby
redundant channels in each unit.

Table 48. Load Power Conditioning Equipment, Baseline Parts Count,
Mars Orbiter, DC Distribution System

Unit	Resistors			Diodes			Capacitors				Transistors		Magnetics			Relays		Other / Comments
	Carbon Compound	Metal Film	Wire Power	General Purpose	Rectifiers	Zener	Ceramic	Tantalum Foil	Tantalum Solid	Plastic	<1W	>1W	Transformers	Chokes	Mag-Amps	General 4 Sets	Latching 2 Coil	
Transmitter Converter (HV)		6		4	8		2	1	3	2	2	2	4	1				
Gyro Inverter 3 ϕ (400~)	38	6	6	6	6		14	1	3		9	6	6	1				
Main Converter (LV)	6			4	12		2	1	6		2	2	4	1				
TV Converter (HV)	6			4	12		2	1	4	2	2	2	4	1				
Computer and Sequencer Converter (LV)	6	6		4	8		2	1	4		2	2	4	1				
Experiment Converter (HV)	6	6		4	12		2	1	2	1	2	2	4	1				
Experiment Converter (LV)	6	6		4	14		2	2	7		2	2	4	1				
Experiment Converter (HV)	6	6		4	12		2	1	2	1	2	2	4	1				

Table 49. Load Power Conditioning Equipment, Redundant Parts Count,
Mars Orbiter, DC Distribution System

Unit	Resistors			Diodes			Capacitors				Transistors		Magnetics			Relays		Other / Comments
	Carbon Compound	Metal Film	Wire Power	General Purpose	Rectifiers	Zener	Ceramic	Tantalum Foil	Tantalum Solid	Plastic	< 1W	> 1W	Transformers	Chokes	Mag-Amps	General 4 Sets	Latching 2 Coil	
Transmitter Converter (HV)		21		10	8	1	2	1	5	2	5	2	4	1			1	Standby
Gyro Inverter 3 ϕ (400~)		54	6	21	6	1	14	1	10		13	6	6	1			5	
Main Converter (LV)		21		10	12	1	2	1	8		5	2	4	1			1	
TV Converter (HV)		21		10	12	1	2	1	6	2	5	2	4	1			1	
Computer and Sequencer Converter (LV)		21		10	8	1	2	1	6		5	2	4	1			1	
Experiment Converter (HV)		21		10	12	1	2	1	4	1	5	2	4	1			1	
Experiment Converter (LV)		21		10	14	1	2	2	9		5	2	4	1			1	
Experiment Converter (HV)		21		10	12	1	2	1	4	1	5	2	4	1			1	Standby

Note: Parts count listed are for one of two identical standby
redundant channels in each unit.

Table 50. Load Power Conditioning Equipment, Baseline Parts Count,
Jupiter Flyby, AC Distribution System

Unit	Resistors			Diodes			Capacitors				Tran- sistors		Magnetics			Relays		Other / Comments
	Carbon Compound	Metal Film	Wire Power	General Purpose	Rectifiers	Zener	Ceramic	Tantalum Foil	Tantalum Solid	Plastic	< 1W	> 1W	Transformers	Chokes	Mag-Amps	General 4 Sets	Latching 2 Coil	
Gyro Inverter 3 ϕ (400~)		5		4			2	1			2	2	4	1				
Main Inverter					6				2	1			1					
Transmitter TR (HV)					14			2	5				1					
Equipment TR (LV)					12				4	2			1					
TV TR (HV)					14			3	4				1					
Experiment TR (LV)					10				4									
Experiment TR (HV)										1			1					

Table 51. Load Power Conditioning Equipment, Redundant Parts Count,
Jupiter Flyby, AC Distribution System

Unit	Resistors			Diodes			Capacitors				Transistors		Magnetics			Relays		Other / Comments
	Carbon Compound	Metal Film	Wire Power	General Purpose	Rectifiers	Zener	Ceramic	Tantalum Foil	Tantalum Solid	Plastic	<1W	>1W	Transformers	Chokes	Mag-Amps	General 4 Sets	Latching 2 Coil	
Gyro Inverter 3 ϕ (400~)		10		10		1	2	1	2		5	2	4	1			2	Standby
Main Inverter		15		6	6	1			4	1	3		1				1	
Transmitter TR (HV)		19		6	14	1		2	7		3		1				1	
Equipment TR (LV)		18		6	12	1			6	2	3		1				1	
TV TR (HV)		19		6	14	1		3	6		3		1				1	
Experiment TR (LV)		17		6	10	1			6	1	3		1				1	Standby

Note: Parts count listed are for one of two identical standby
redundant channels in each unit.

Table 52. Load Power Conditioning Equipment, Baseline Parts Count,
Jupiter Flyby, DC Distribution System

Unit	Resistors			Diodes			Capacitors				Tran- sistors		Magnetics			Relays		Other / Comments
	Carbon Compound	Metal Film	Wire Power	General Purpose	Rectifiers	Zener	Ceramic	Tantalum Foil	Tantalum Solid	Plastic	< 1W	> 1W	Transformers	Chokes	Mag-Amps	General 4 Sets	Latching 2 Coil	
Transmitter Converter (HV)		6		4	6		2	1	3	1	2	2	4	1				
Gyro Inverter 3ϕ (400~)	NOT REQUIRED																	
Main Converter (LV)		6		4	12		2	1	6		2	2	4	1				
TV Converter (HV)		6		4	12		2	1	4	2	2	2	4	1				
Computer and Sequencer Converter (LV)		6		4	8		2	1	4		2	2	4	1				
Experiment Converter (HV)		6		4	12		2	1	2	1	2	2	4	1				
Experiment Converter (LV)		6		4	14		2	2	7		2	2	4	1				

Table 53. Load Power Conditioning Equipment, Redundant Parts Count, Jupiter Flyby, DC Distribution System

Unit	Resistors			Diodes			Capacitors				Transistors		Magnetics			Relays		Other/ Comments
	Carbon Compound	Metal Film	Wire Power	General Purpose	Rectifiers	Zener	Ceramic	Tantalum Foil	Tantalum Solid	Plastic	<1W	>1W	Transformers	Chokes	Mag-Amps	General 4 Sets	Latching 2 Coil	
Transmitter Converter (HV)	21			10	6	1	2	1	5	1	5	2	4	1			1	Standby
Gyro Inverter 3 ϕ (400~)	NOT REQUIRED																	
Main Converter (LV)	21			10	12	1	2	1	8		5	2	4	1			1	
TV Converter (HV)	21			10	12	1	2	1	6	2	5	2	4	1			1	
Computer and Sequencer Converter (LV)	21			10	8	1	2	1	6		5	2	4	1			1	
Experiment Converter (HV)	21			10	12	1	2	1	4	1	5	2	4	1			1	
Experiment Converter (LV)	21			10	14	1	2	2	9		5	2	4	1			1	Standby

Note: Parts count listed are for one of two identical standby redundant channels in each unit.

Table 54. Load Power Conditioning Equipment, Baseline Parts Count,
Jupiter Orbiter No. 1, AC Distribution System

Unit	Resistors			Diodes			Capacitors				Transistors		Magnetics			Relays		Other / Comments
	Carbon Compound	Metal Film	Wire Power	General Purpose	Rectifiers	Zener	Ceramic	Tantalum Foil	Tantalum Solid	Plastic	<1W	>1W	Transformers	Chokes	Mag-Amps	General 4 Sets	Latching 2 Coil	
Gyro Inverter 3 ϕ (400~)		38	6	6	6		14	1	3		9	6	6	1				
Main Inverter		5		4			2	1			2	2	4	1				
Transmitter TR (HV)					8				2	2			1					
Equipment TR (LV)					14			2	5				1					
TV TR (HV)					12				4	2			1					
Experiment TR (LV)					14			3	4				1					
Experiment TR (HV)					10				4	1			1					

Table 55. Load Power Conditioning Equipment, Redundant Parts Count, Jupiter Orbiter No. 1, AC Distribution System

Unit	Resistors			Diodes			Capacitors				Transistors		Magnetics			Relays		Other/ Comments
	Carbon Compound	Metal Film	Wire Power	General Purpose	Rectifiers	Zener	Ceramic	Tantalum Foil	Tantalum Solid	Plastic	<1W	>1W	Transformers	Chokes	Mag-Amps	General 4 Sets	Latching 2 Coil	
Gyro Inverter 3 ϕ (400~)		54	6	21	6	1	14	1	10		13	6	6	1			5	Standby
Main Inverter		10		10		1	2	1	2		5	2	4	1			2	
Transmitter TR (HV)		15		6	8	1			4	2	3		1					
Equipment TR (LV)		19		6	14	1		2	7		3		1				1	
TV TR (HV)		18		6	12	1			6	2	3		1				1	
Experiment TR (LV)		19		6		1		3	6		3		1				1	
Experiment TR (HV)		17		6		1			6	1	3		1				1	Standby

Note: Parts count listed are for one of two identical standby redundant channels in each unit.

Table 56. Load Power Conditioning Equipment, Baseline Parts Count,
Jupiter Orbiter No. 2, DC Distribution System

Unit	Resistors			Diodes			Capacitors				Transistors		Magnetics			Relays		Other/ Comments
	Carbon Compound	Metal Film	Wire Power	General Purpose	Rectifiers	Zener	Ceramic	Tantalum Foil	Tantalum Solid	Plastic	<1W	>1W	Transformers	Chokes	Mag-Amps	General 4 Sets	Latching 2 Coil	
Transmitter Converter (HV)		6		4	8		2	1	3	2	2	2	4	1				
Gyro Inverter 3 ϕ (400~)	38		6	6	6		14	1	3		9	6	6	1				
Main Converter (LV)	6			4	12		2	1	6		2	2	4	1				
TV Converter (HV)	6			4	12		2	1	4	2	2	2	4	1				
Computer and Sequencer Converter (LV)	6			4	8		2	1	4		2	2	4	1				
Experiment Converter (HV)	6			4	6		2	1	2	1	2	2	4	1				
Experiment Converter (HV)	6			4	12		2	1	4	2	2	2	4	1				

Table 57. Load Power Conditioning Equipment, Redundant Parts Count,
Jupiter Orbiter No. 2, DC Distribution System

Unit	Resistors			Diodes			Capacitors				Transistors		Magnetics			Relays		Other / Comments
	Carbon Compound	Metal Film	Wire Power	General Purpose	Rectifiers	Zener	Ceramic	Tantalum Foil	Tantalum Solid	Plastic	< 1W	> 1W	Transformers	Chokes	Mag-Amps	General 4 Sets	Latching 2 Coil	
Transmitter Converter (HV)		21		10	8	1	2	1	5	2	5	2	4	1			1	Standby
Gyro Inverter 3 ϕ (400~)		54	9	21	6	1	14	1	10		13	6	6	1			5	Standby
Main Converter (LV)		21		10	12	1	2	1	8		5	2	4	1			1	
TV Converter (HV)		21		10	12	1	2	1	6	2	5	2	4	1			1	
Computer and Sequencer Converter (LV)		21		10	8	1	2	1	6		5	2	4	1			1	
Experiment Converter (HV)		21		10	6	1	2	1	4	1	5	2	4	1			1	
Experiment Converter (HV)		21		10	12	1	2	1	6	2	5	2	4	1			1	Standby

Note: Parts count listed are for one of two identical standby
redundant channels in each unit.

Table 58. Load Power Conditioning Equipment, Baseline Parts Count,
Jupiter Orbiter No. 2, AC Distribution System

Unit	Resistors			Diodes			Capacitors				Transistors		Magnetics			Relays		Other / Comments
	Carbon Compound	Metal Film	Wire Power	General Purpose	Rectifiers	Zener	Ceramic	Tantalum Foil	Tantalum Solid	Plastic	< 1W	> 1W	Transformers	Chokes	Mag-Amps	General 4 Sets	Latching 2 Coil	
Gyro Inverter 3 ϕ (400~)		38	6	6	6		14	1	3		9	6	6	1				
Main Inverter		5		4			2	1			2	2	4	1				
Transmitter TR (HV)					8				2	2			1					
Equipment TR (LV)					14			2	5				1					
TV TR (HV)					12				4	2			1					
Experiment TR (HV)					6				2	1			1					
Experiment TR (HV)					12				4	2			1					

Table 59. Load Power Conditioning Equipment, Redundant Parts Count,
Jupiter Orbiter No. 2, AC Distribution System

Unit	Resistors			Diodes			Capacitors				Transistors		Magnetics			Relays		Other/ Comments
	Carbon Compound	Metal Film	Wire Power	General Purpose	Rectifiers	Zener	Ceramic	Tantalum Foil	Tantalum Solid	Plastic	< 1W	> 1W	Transformers	Chokes	Mag-Amps	General 4 Sets	Latching 2 Coil	
Gyro Inverter 3 ϕ (400~)		54	6	21	6	1	14	1	10		13	6	6	1			5	Standby
Main Inverter		10		10		1	2	1	2		5	2	4	1			2	
Transmitter TR (HV)		15		6	8	1			4	2	3		1				1	
Equipment TR (LV)		19		6	14	1		2	7		3		1				1	
TV TR (HV)		18		6	12	1			6	2	3		1				1	
Experiment TR (HV)		15		6	6	1			4	1	3		1				1	
Experiment TR (HV)		18		6	12	1			6	2	3		1				1	Standby

Note: Parts count listed are for one of two identical standby
redundant channels in each unit.

Table 60. Load Power Conditioning Equipment, Baseline Parts Count,
Jupiter Orbiter No. 2, DC Distribution System

Unit	Resistors			Diodes			Capacitors				Transistors		Magnetics			Relays		Other/ Comments
	Carbon Compound	Metal Film	Wire Power	General Purpose	Rectifiers	Zener	Ceramic	Tantalum Foil	Tantalum Solid	Plastic	<1W	>1W	Transformers	Chokes	Mag-Amps	General 4 Sets	Latching 2 Coil	
Transmitter Converter (HV)		6		4	8		2	1	3	2	2	2	4	1				
Gyro Inverter 3 ϕ (400~)	38		6	6	6		14	1	3		9	6	6	1				
Main Converter (LV)		6		4	12		2	1	6		2	2	4	1				
TV Converter (HV)		6		4	12		2	1	4	2	2	2	4	1				
Computer and Sequencer Converter (LV)		6		4	8		2	1	4		2	2	4	1				
Experiment Converter (HV)		6		4	10		2	1	4	1	2	2	4	1				
Experiment Converter (LV)		6		4	8		2	2	4		2	2	4	1				

Table 61. Load Power Conditioning Equipment, Redundant Parts Count, Jupiter Orbiter No. 2, DC Distribution System

Unit	Resistors			Diodes			Capacitors				Transistors		Magnetics			Relays		Other / Comments
	Carbon Compound	Metal Film	Wire Power	General Purpose	Rectifiers	Zener	Ceramic	Tantalum Foil	Tantalum Solid	Plastic	<1W	>1W	Transformers	Chokes	Mag-Amps	General 4 Sets	Latching 2 Coil	
Transmitter Converter (HV)		21		10	8	1	2	1	5	2	5	2	4	1			1	Standby
Gyro Inverter 3 ϕ (400~)		54	6	21	6	1	14	1	10		13	6	6	1			5	
Main Converter (LV)		21		10	12	1	2	1	8		5	2	4	1			1	
TV Converter (HV)		21		10	12	1	2	1	6	2	5	2	4	1			1	
Computer and Sequencer Converter (LV)		21		10	8	1	2	1	6		5	2	4	1			1	
Experiment Converter (HV)		21		10	10	1	2	1	6	1	5	2	4	1			1	
Experiment Converter (LV)		21		10	8	1	2	2	6		5	2	4	1			1	Standby

Note: Parts count listed are for one of two identical standby redundant channels in each unit.

4.3 EFFECT OF RELIABILITY IMPROVEMENTS ON UNIT WEIGHT AND EFFICIENCY

4.3.1 Electronic Equipment

Parametric curves were prepared for each unit design showing its weight and efficiency as functions of output power. Since the power system weight is largely determined by the weights of the battery and solar array, it is imperative that the efficiency of each series element in the system be taken into account in the system optimization calculations. The effects of implementing the preferred redundant configurations in each unit on their weights and efficiencies were calculated. The resultant data is shown in Figures 63 through 80.

Every attempt has been made to make the weight and efficiency data for regulation, control, and conditioning equipment representative of feasible designs. In calculating efficiency, the losses in all the following elements were accounted for:

- Input filter (capacitor and inductor)
- Transformers
- Rectifiers — both forward losses and recovery losses
- Output filter (capacitor and inductor)
- Transistor — both saturated and switching losses
- Error amplifier losses
- Logic losses
- Failure sensing losses.

The same items were accounted for in calculating the weight. An allowance was also made for the packaging of the units, the mechanical assembly, and the electrical connectors.

One of the most significant design parameters affecting unit efficiency and weight is the switching frequency of the inverter and pulse-width modulated regulator circuits. Preliminary designs were made at switching frequencies ranging from 400 Hz to 20 kHz. A figure-of-merit relating both unit efficiency and weight was selected as the product of the

unit losses in percent times the unit weight. Comparisons of the figure-of-merit as a function of frequency for different types of switching units showed a minimum at 6 kHz. Figure 81 is a plot of the loss-weight product versus switching frequency for a 100-w bucking series regulator. At frequencies lower than 6 kHz, the losses decrease but are more than offset by the increased weights of the magnetics and filters. At frequencies greater than 6 kHz, the weight decreases but the increased losses become the predominant characteristic. A 6-kHz switching frequency was selected, therefore, for all ac circuits with the exception of the gyro inverters, which require a 400-Hz output.

4.3.2 Batteries

Parametric weight data for both the silver-cadmium and silver-zinc batteries are shown in Figure 82 as a function of rated capacity and the maximum discharge power level for each mission. Calculations were performed for each mission based on an allowable depth of discharge of 50 percent to permit the subsequent determination of battery weight directly as a function of discharge power in the computer analysis of each system configuration.

Two methods of implementing battery redundancy were selected for analysis. The first of these uses parallel redundancy with each battery sized to support the entire mission requirements. This approach was used for all system configurations. The second method employs two-out-of-three majority voting redundancy with low voltage, three-cell batteries. This approach was applied as a second alternative redundant battery configuration to those system configurations having a regulated main bus. The weight curves for these low voltage batteries are shown in Figure 83. Here again, the weights are plotted for both silver-cadmium and silver-zinc types as functions of rated capacity and discharge power for each mission.

The use of low voltage batteries for the larger power levels considered in the seven model spacecraft produced required cell capacity ratings of up to 430 amp-hr. By way of comparison, the largest capacity rating required with the 20 cell silver-cadmium battery was calculated to

be 110 amp-hr. Although available silver-cadmium cells do not approach these ratings, flight experience with silver-zinc cells of up to 500-amp-hr capacity has been gained in certain booster applications. The development of equally large silver-cadmium cells is considered to be definitely feasible. The lack of extensive experience with large capacity cells, however, is reflected in an assumed 100 percent higher failure rate for the individual cells in the low voltage batteries in comparison to the 20-cell silver-cadmium or 15-cell silver-zinc batteries for each mission.

Battery charging power requirements were calculated for each mission on the basis of an assumed average 80 percent w-hr efficiency and the applicable ratio of discharge time to charge time. For the three Jupiter missions and the Mercury probe, the long charging period available was reflected in a charging power requirement of less than 1 percent of the discharge power level. For the Mars and Venus orbiting missions the results of these calculations were expressed as the ratio of charge power to discharge power for the maximum eclipse orbits. The ratios (F) used for each mission are as follows:

Mercury and Jupiter missions:	$F = 0.010$
Venus Orbiter missions:	$F = 0.180$
Mars Orbiter mission:	$F = 0.236$

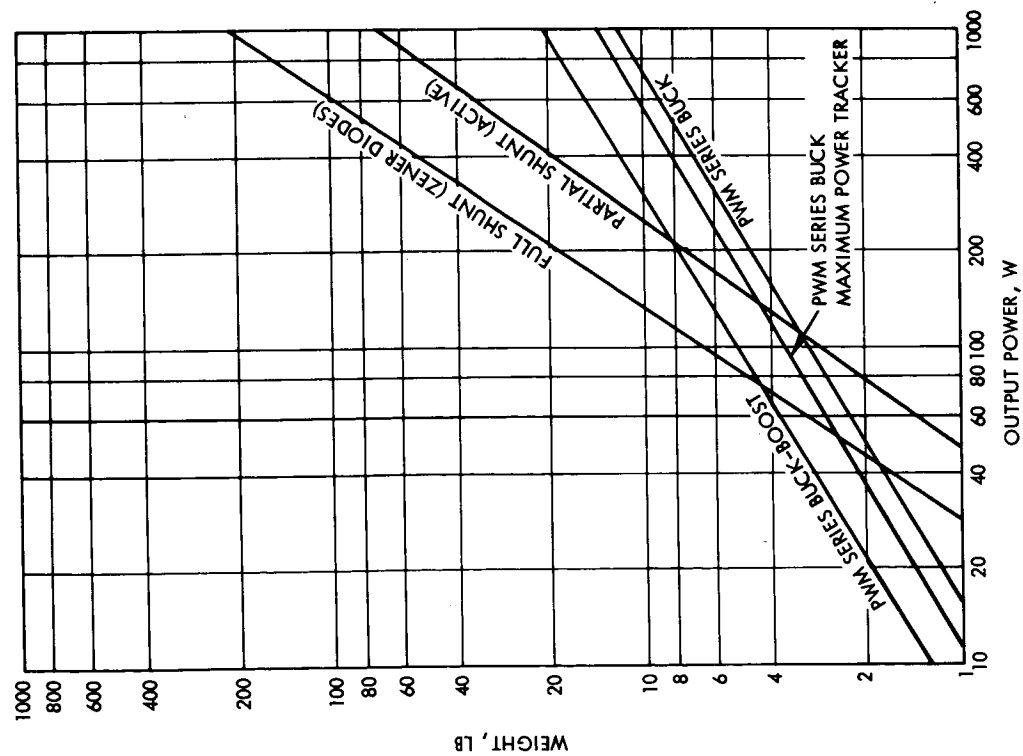


Figure 63. Array Controls, Baseline, Weight versus Power Output

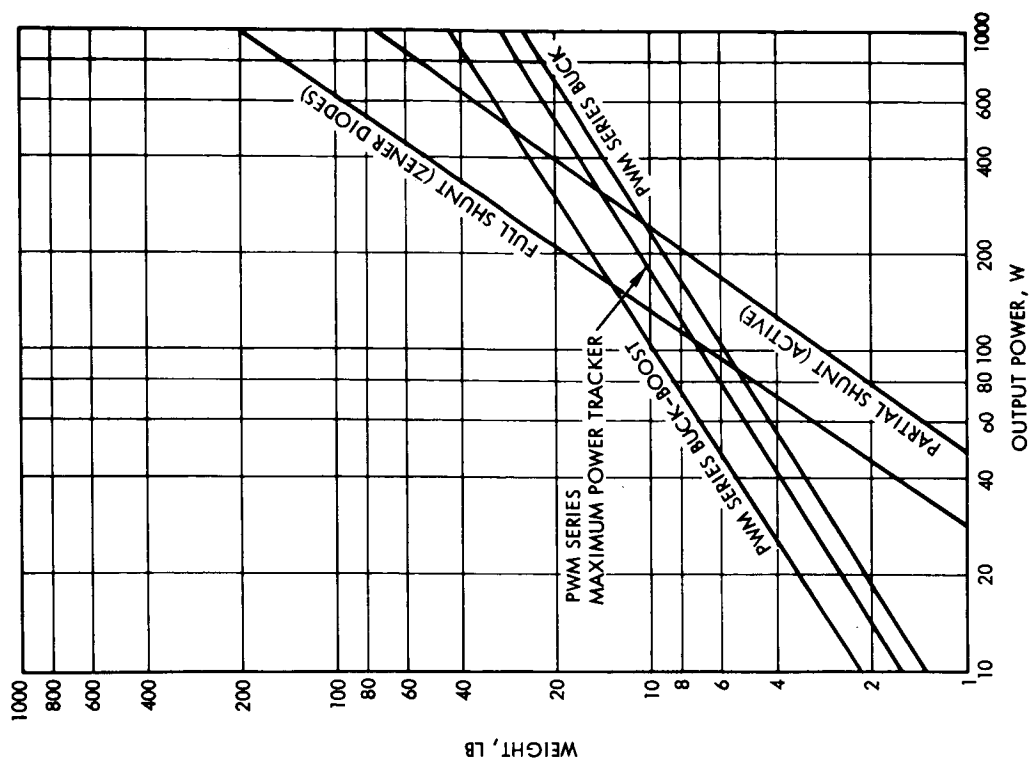


Figure 64. Array Controls, Redundant, Weight versus Power Output

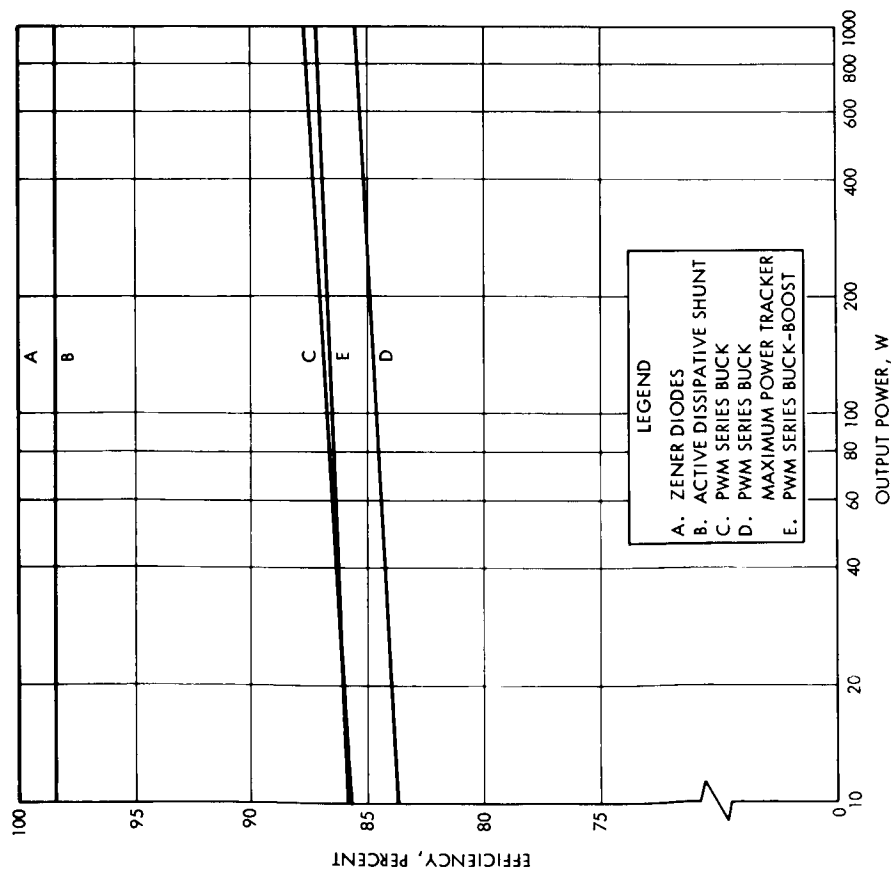


Figure 65. Array Controls, Baseline, Efficiency versus Power Output

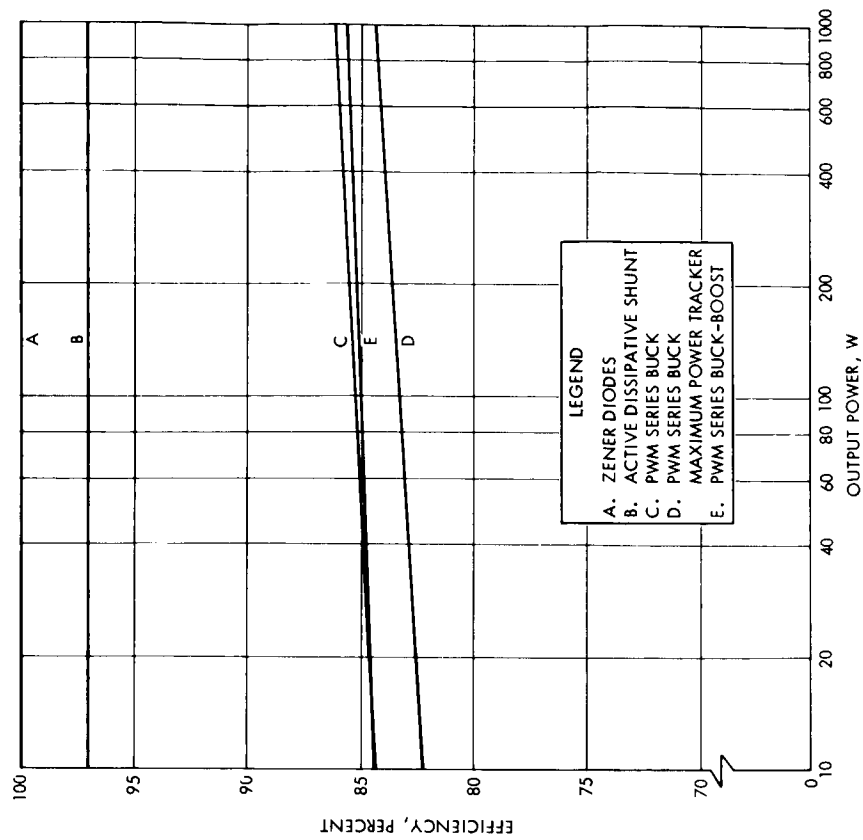


Figure 66. Array Controls, Redundant, Efficiency versus Power Output

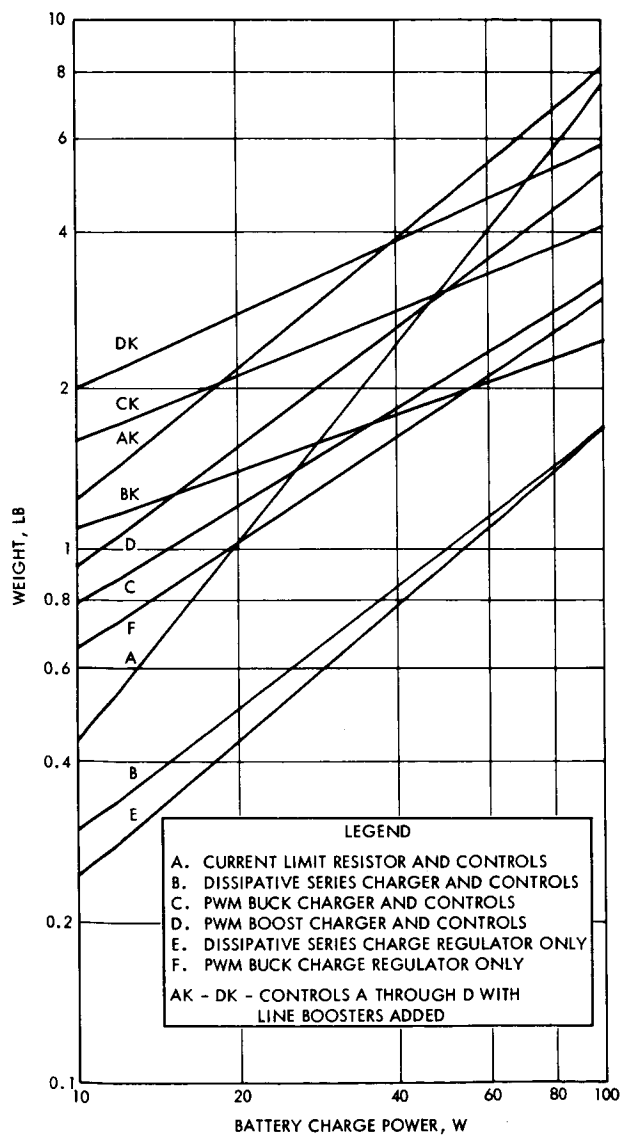


Figure 67. Battery Controls, Baseline, Weight versus Power Output

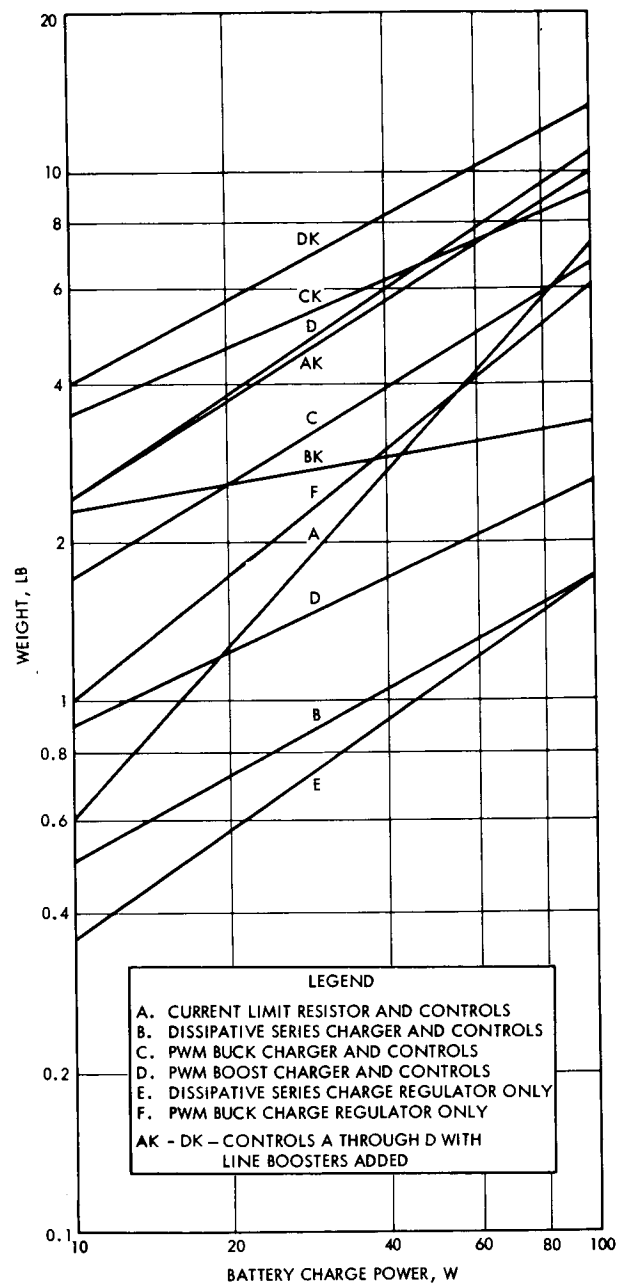


Figure 68. Battery Controls, Redundant, Weight versus Power Output

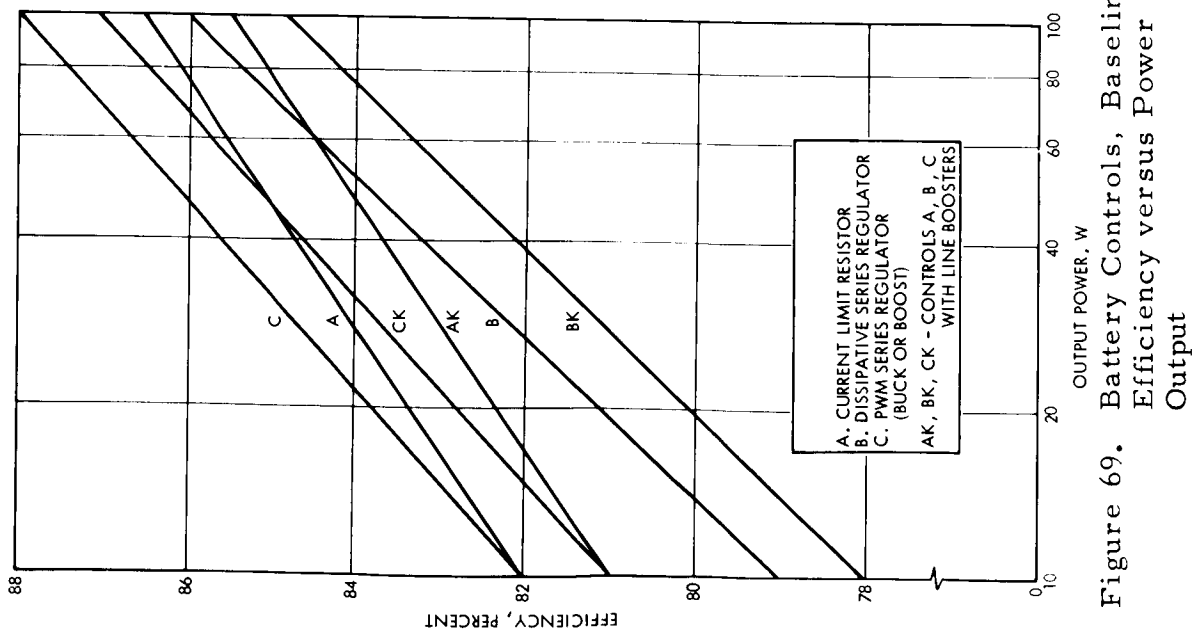


Figure 69. Battery Controls, Baseline, Efficiency versus Power Output

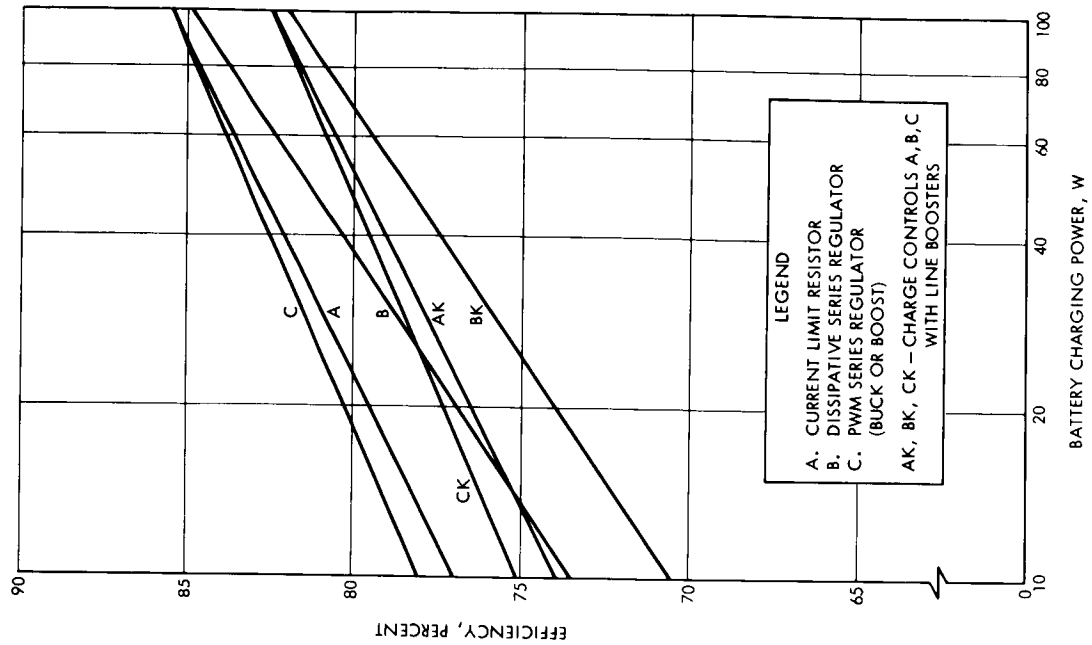


Figure 70. Battery Controls, Redundant, Efficiency versus Power Output

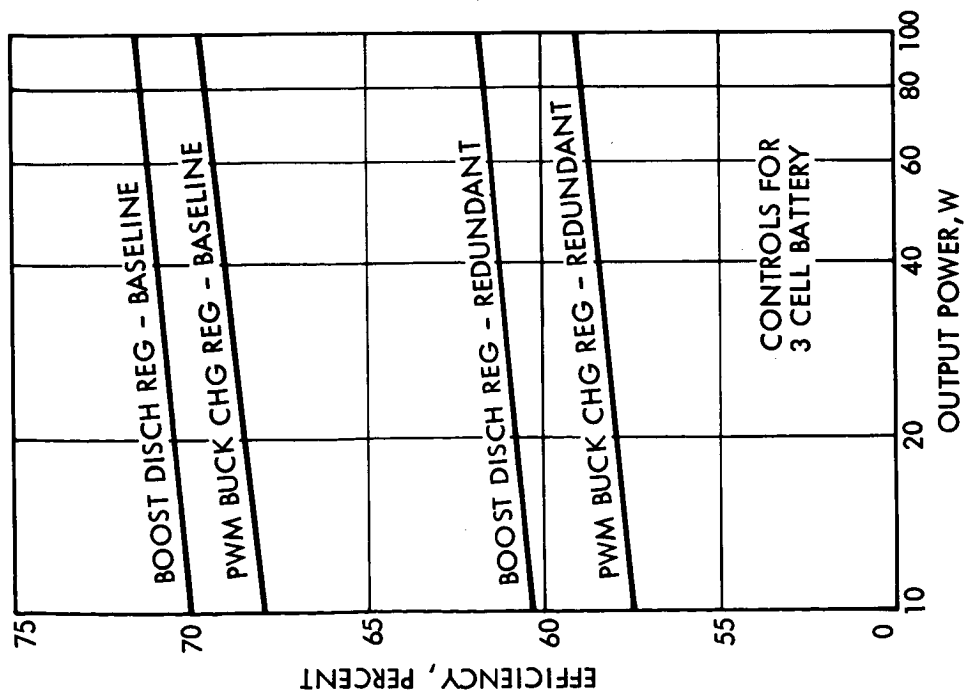


Figure 71. Low Voltage Battery Controls, Efficiency versus Power Output

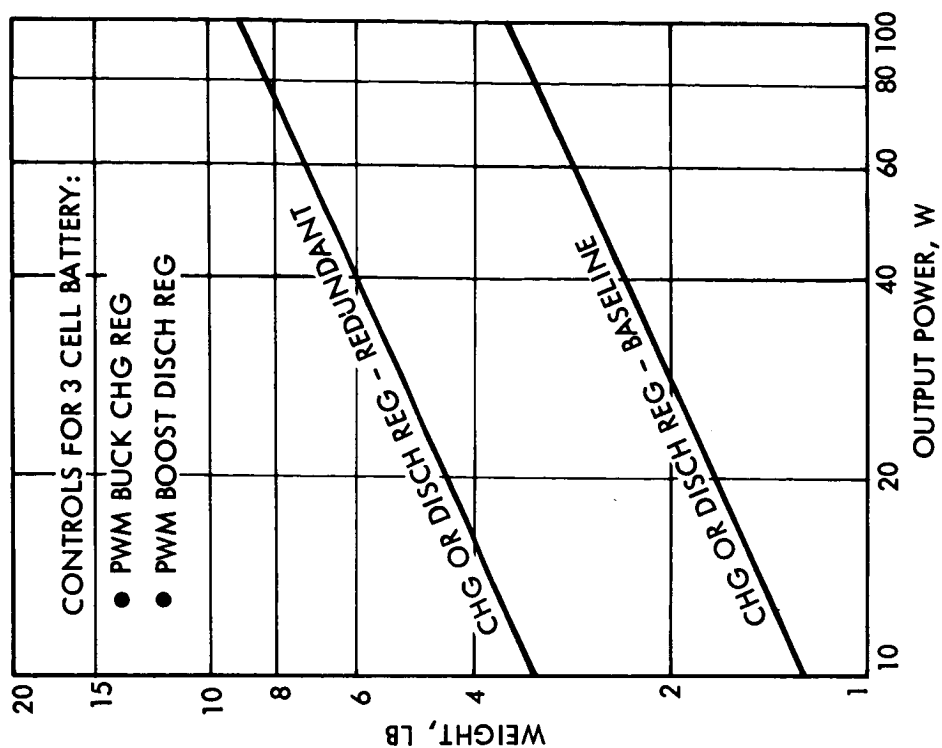


Figure 72. Low Voltage Battery Controls, Weight versus Power Output

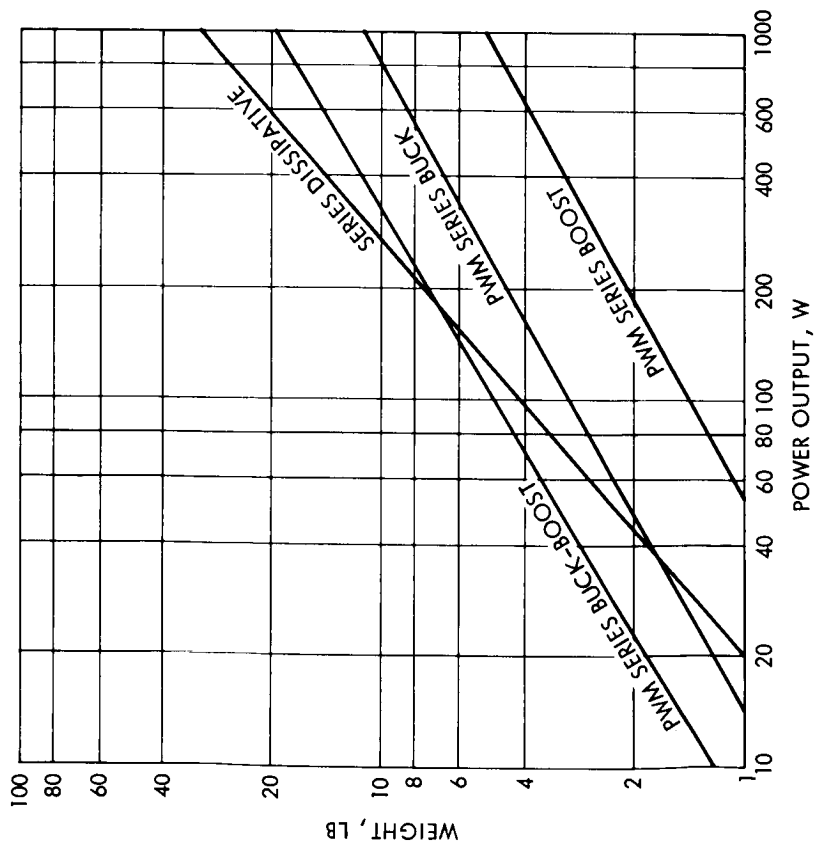


Figure 73. Line Regulator, Baseline, Weight versus Power Output

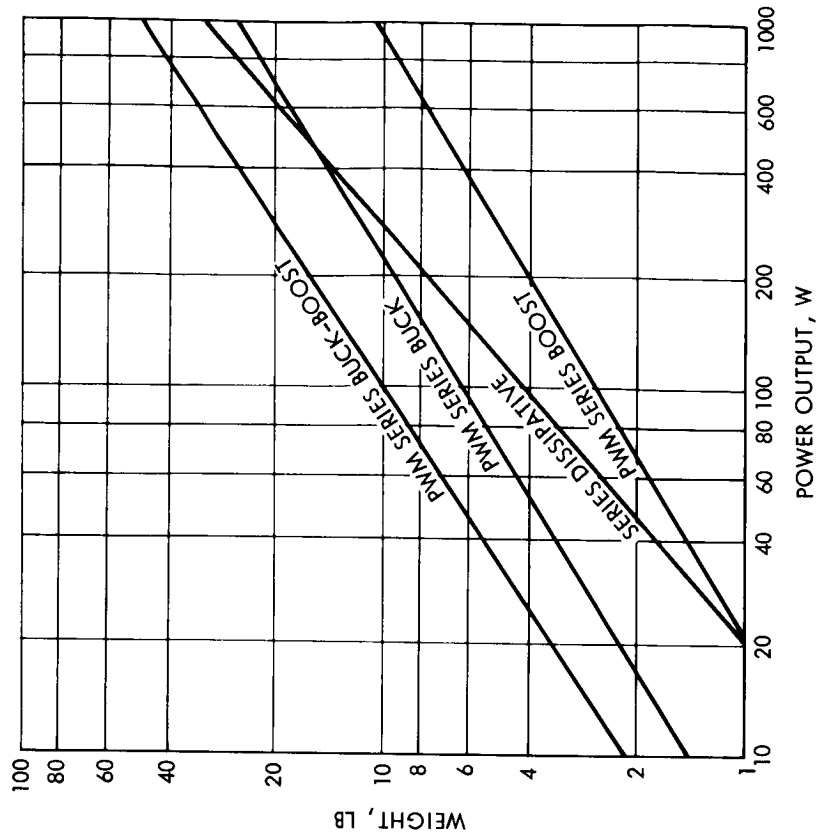


Figure 74. Line Regulator, Redundant, Weight versus Power Output

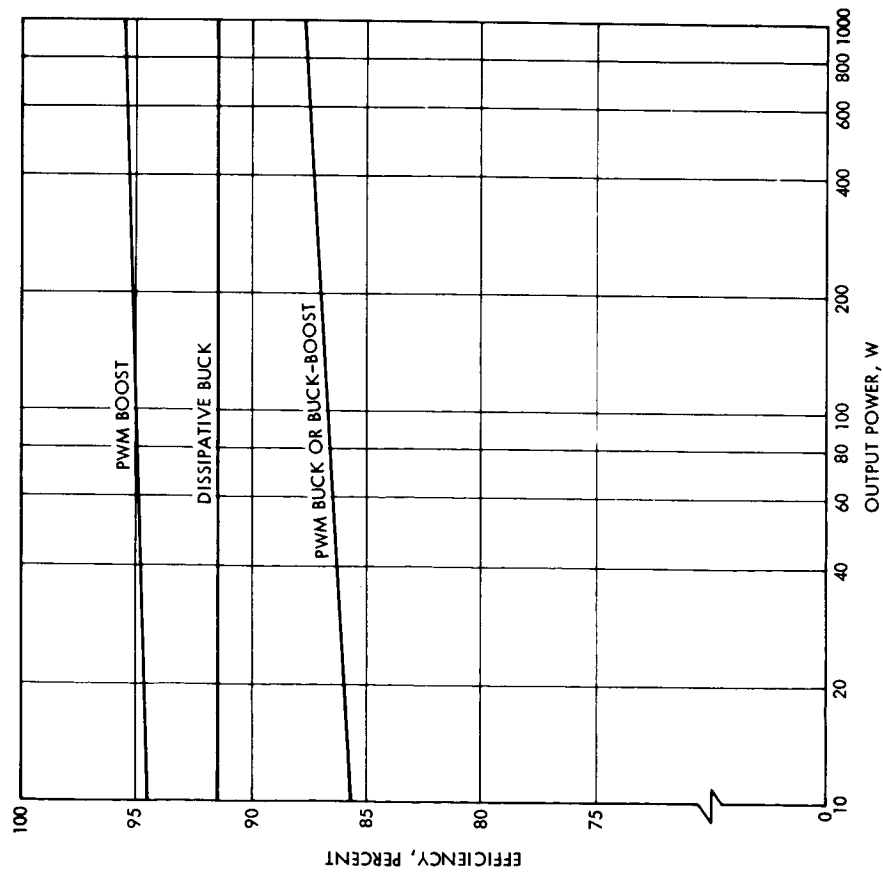


Figure 75. Line Regulator, Baseline, Efficiency versus Power Output

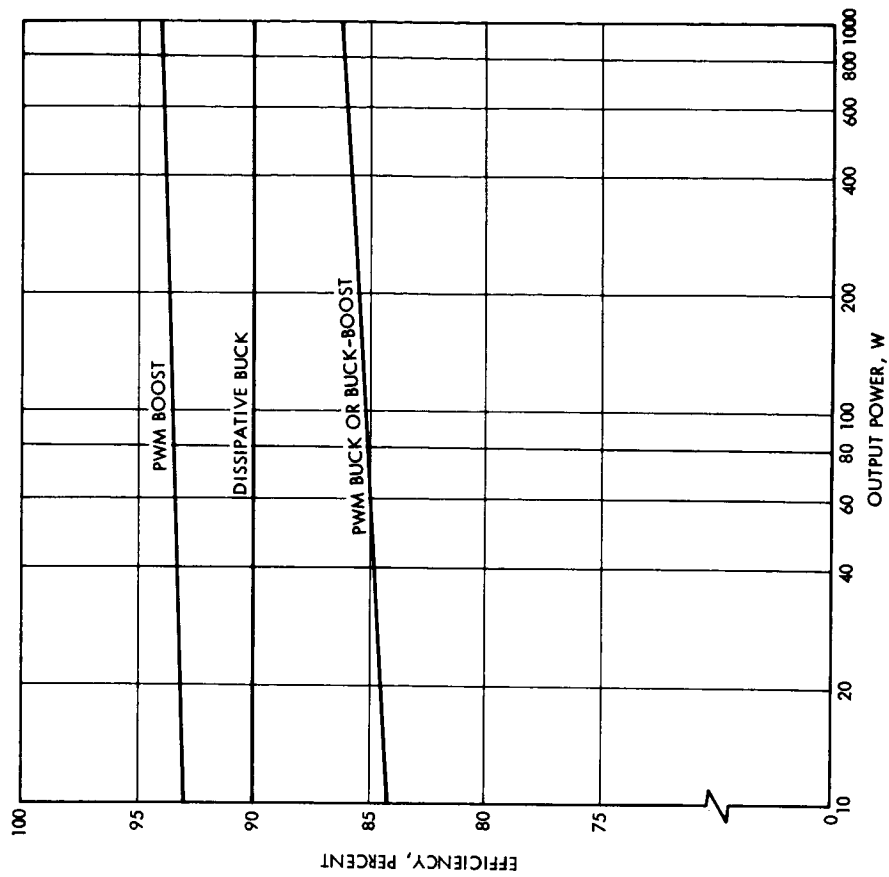


Figure 76. Line Regulator, Redundant, Efficiency versus Power Output

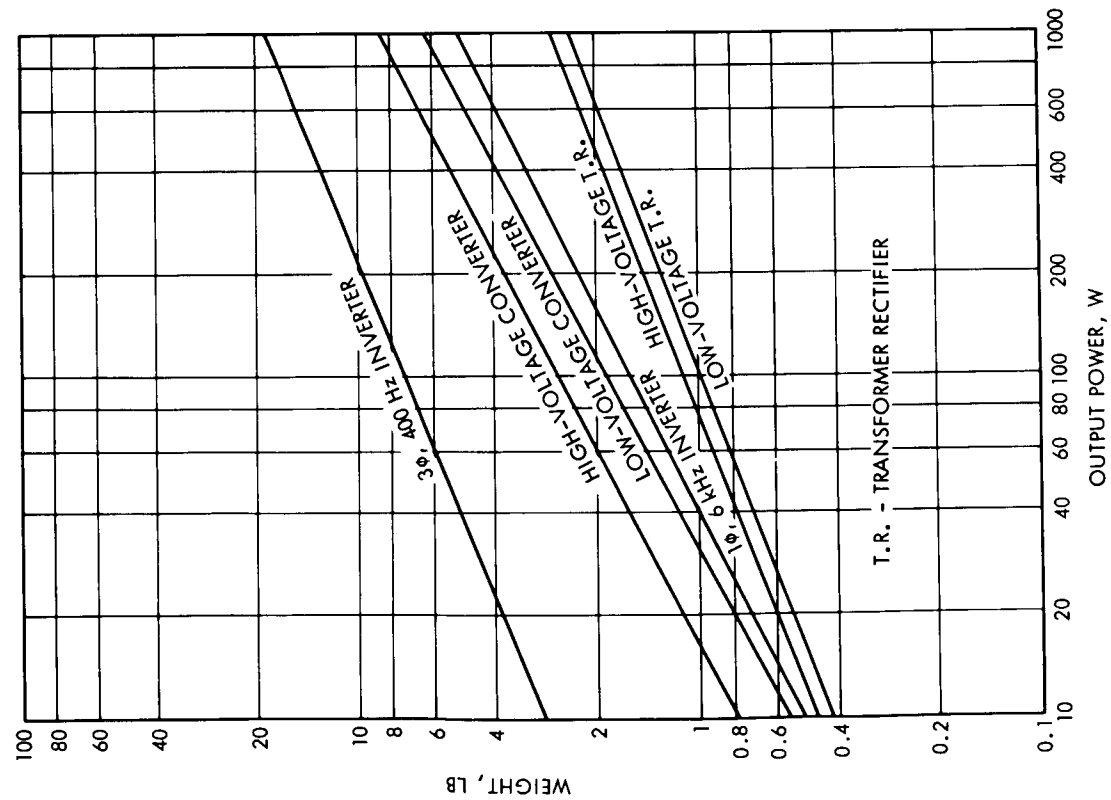


Figure 77. Load Power Conditioning Equipment, Baseline, Weight versus Power Output

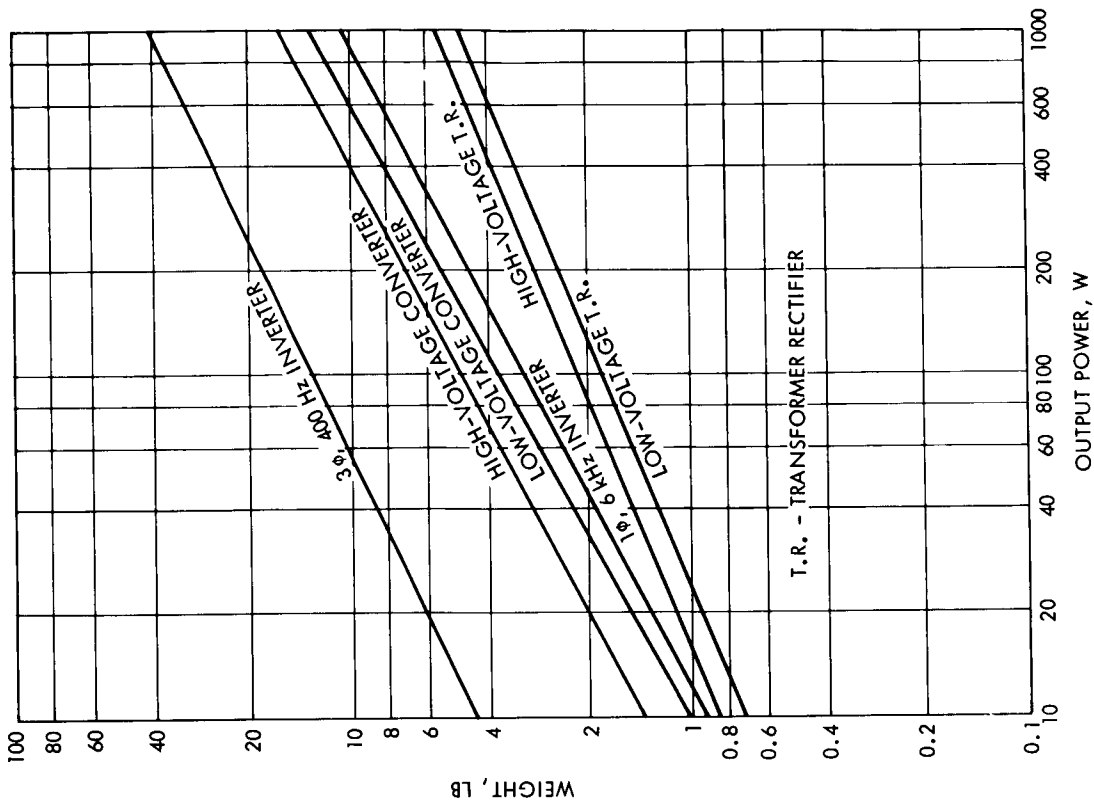


Figure 78. Load Power Conditioning Equipment, Redundant, Weight versus Power Output

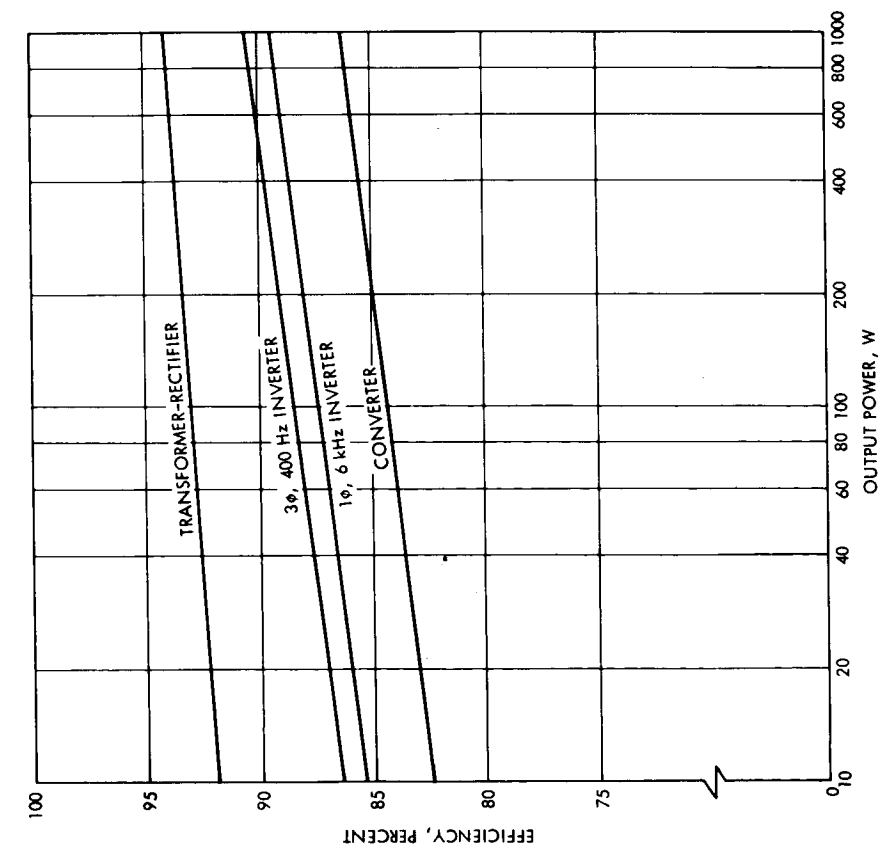


Figure 79. Load Power Conditioning Equipment, Baseline, Efficiency versus Power Output

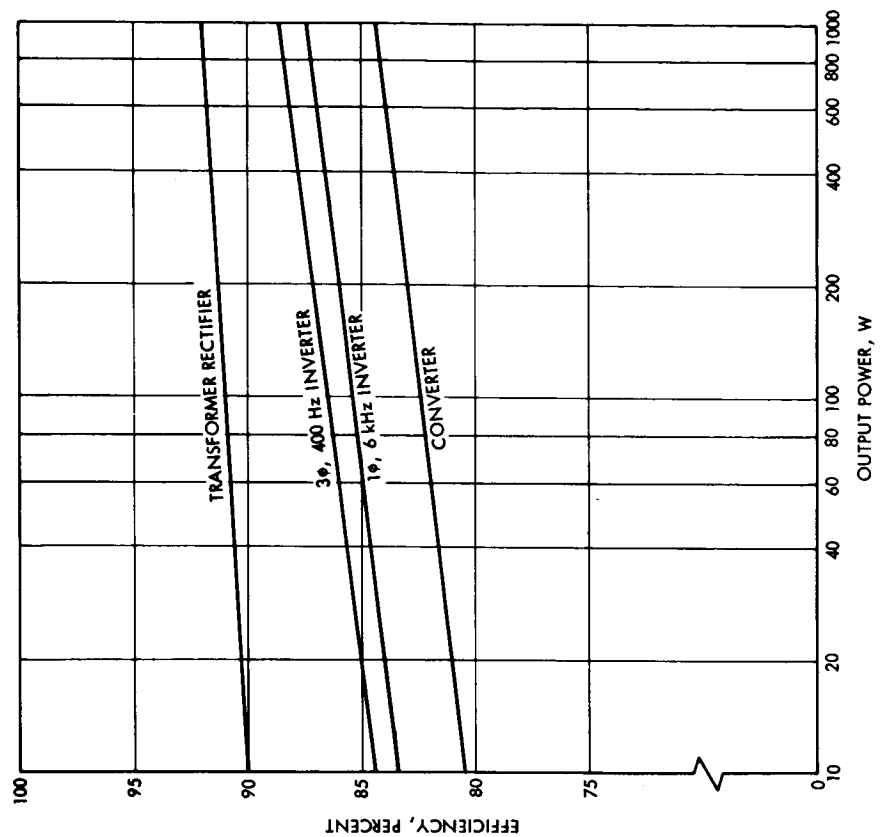


Figure 80. Load Power Conditioning Equipment, Redundant, Efficiency versus Power Output

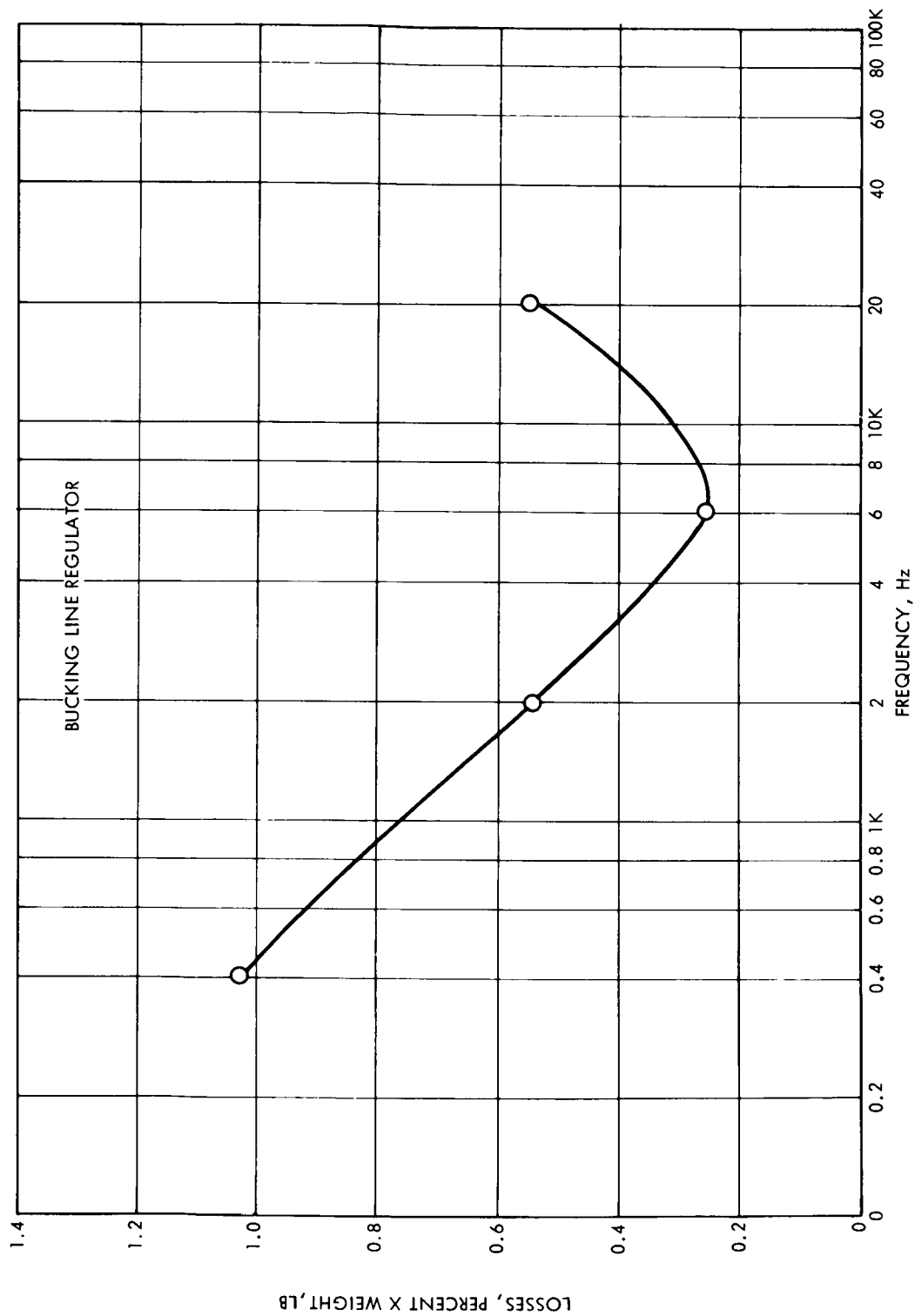


Figure 81. Bucking Line Regulator Power Loss Weight Product versus Switching Frequency

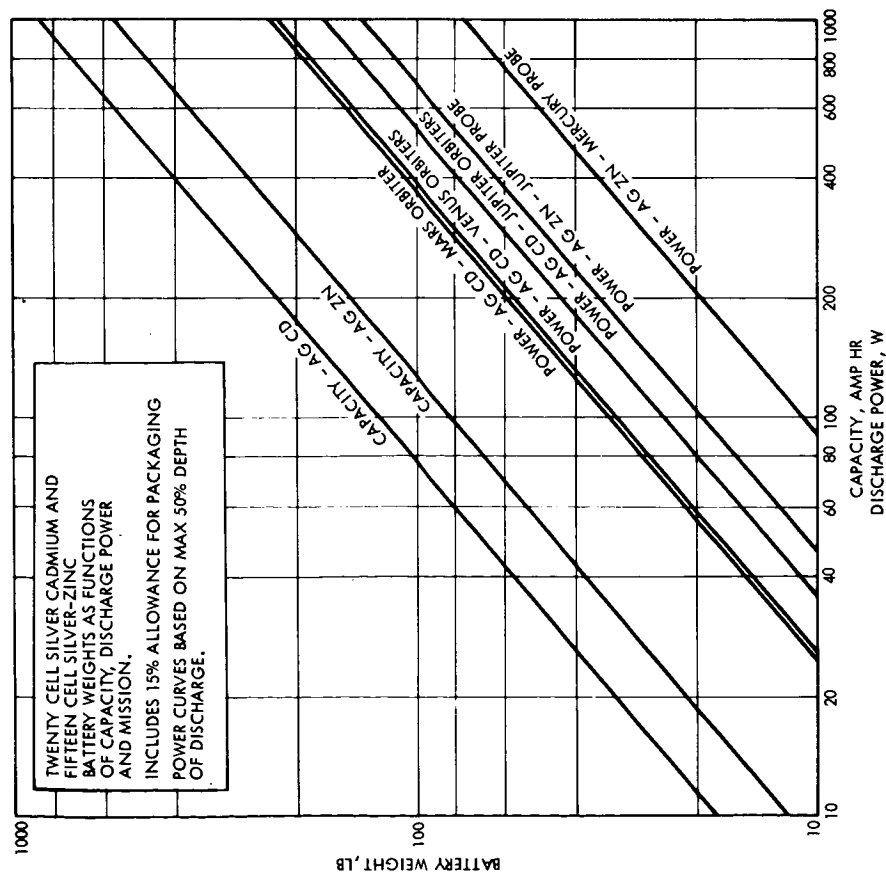


Figure 82. Twenty-cell Silver-cadmium and Fifteen-cell Silver-zinc Battery Weights, Baseline

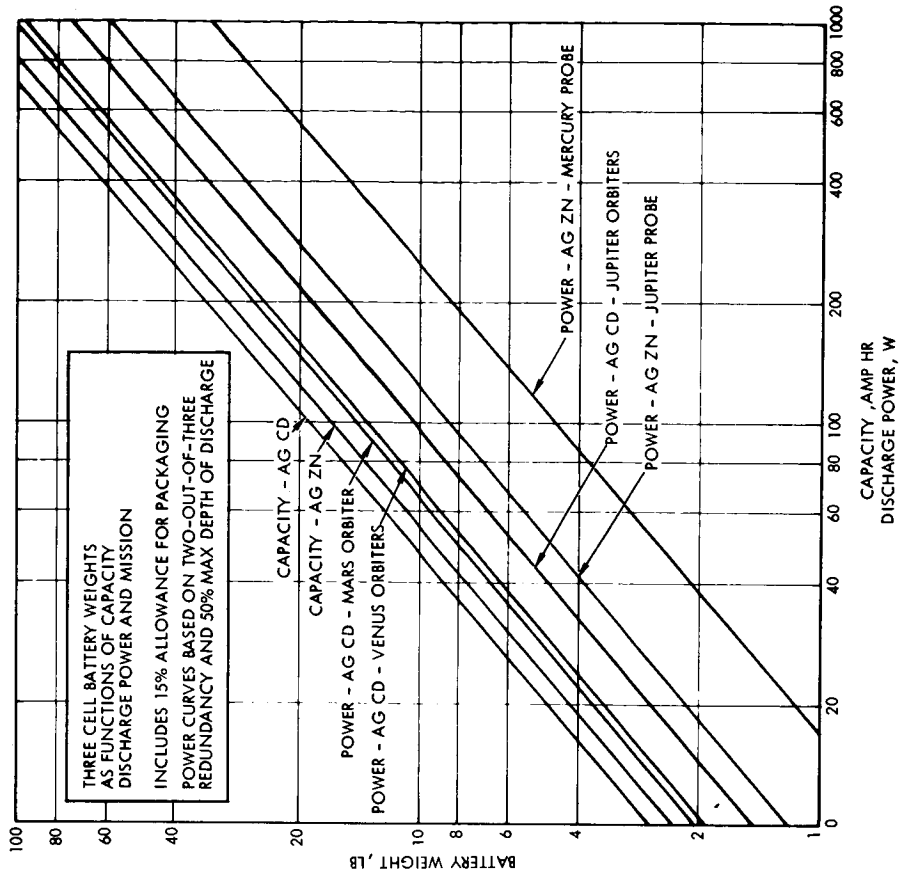


Figure 83. Three-cell Battery Weights, Redundant

4.4 RESULTS OF RELIABILITY-WEIGHT OPTIMIZATION

4.4.1 Venus Orbiter No. 1

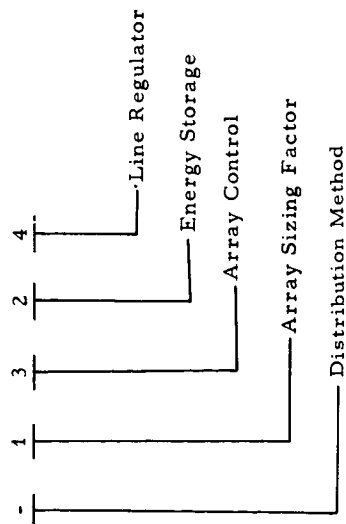
The results of the optimization analysis for the Venus Orbiter No. 1 model are illustrated in Figure 84. The points plotted here represent the optimum system configurations as a function of reliability and weight over the complete range of reliabilities. Five different system configurations were identified as optimum and all of these employ a regulated bus system approach. All other system configurations analyzed fall above the locus of optima plotted on the curve. This locus of points has no meaning between the particular points identified. Although systems exist at these intermediate reliability levels, their weights are always higher than the weight of the next higher reliability system plotted on the curve.

A comparison of these five optimum system configurations for the Venus Orbiter No. 1 mission is shown in Figure 85. This is a plot of the matrix of optima (Reference Table 25) for each of the systems, as determined by the computer analysis of each of the candidate systems. Systems 2395 and 2495 employ 20-cell silver-cadmium batteries with charge and discharge regulators to control the regulated bus (Reference, Configuration Code, Table 62). A large increase in weight is required for these systems to achieve reliabilities greater than 0.98 because of the need to change from nonredundant to fully redundant batteries at this point. Since the battery weight is a relatively large portion of the total system weight for this mission, a characteristic large increase in weight at intermediate reliability levels was found to exist in all systems using 100 percent battery redundancy.

The reliability-weight relationship for these types of systems results from starting with a minimum weight, nonredundant system and selectively adding redundancy to the control, regulation and conditioning equipment. This yields a relatively large increase in reliability for small increase in weight. When reliabilities of approximately 0.977 are achieved, all the electronic equipment is in its redundant configuration. Any further increase in reliability requires that the battery be made redundant. When this is done, it is possible to then minimize the system weight at these increased reliabilities by returning to the baseline configurations of selected units within the system. Further increases in reliability are then

Table 62. Configuration Code

Example Configuration Code:



Code Identification:

<u>Distribution Method</u>		<u>Energy Storage</u>
--	AC Distribution	1 Disconnect switch plus current limiting resistor
(no symbol) DC Distribution		2 Disconnect switch plus current limiting resistor plus discharge booster
<u>Array Sizing Factor</u>		3 Dissipative bucking charger and discharge switch
1	Sizing Factor A ₁	4 Dissipative charger, discharge switch and discharge booster
2	Sizing Factor A ₂	5 PWM bucking charger and discharge switch
3	Sizing Factor A ₃	6 PWM bucking charger, discharge switch and discharge booster
4	Sizing Factor A ₄	7 PWM boost charger and discharge switch
<u>Array Control</u>		8 PWM boost charger, discharge switch and discharge booster
1	None	9 Dissipative charger and boost discharge regulator (normal voltage battery)
2	Zener Shunt	10 PWM bucking charger and boost discharge regulator (normal voltage battery)
3	Active Shunt	11 PWM bucking charger and boost discharge regulator (low voltage battery)
4	PWM Series Buck	
5	Max. Pwr. Tracker-Buck	
6	PWM Series Buck-Boost	

Line Regulator

- 1 PWM bucking line regulator
- 2 Dissipative bucking line regulator
- 3 Boost line regulator
- 4 Buck-boost line regulator
- 5 No line regulator

achieved by again making the electronic equipment redundant until the maximum redundant configuration of the system is reached at a reliability of approximately 0.999.

Systems 23115 and -23115 employ low-voltage batteries in a two-out-of-three majority voting configuration. This alternative approach to implementing battery redundancy in a regulated bus system produces a significant weight advantage at reliability levels between 0.98 and 0.997. Since this approach was used only in a redundant battery configuration, the system weight remains high at lower reliabilities. In order to achieve reliabilities higher than 0.997 with this approach it is necessary to make the battery controls redundant. This produces a significant decrease in system efficiency, a correspondingly large increase in system weight and the highest reliability of all systems considered.

4.4.2 Venus Orbiter No. 2

The locus of optimum systems for Venus Orbiter No. 2 is shown in Figure 86. As indicated in Figure 87, the low voltage battery system, 34115, offers a significant weight advantage at the intermediate reliability levels. The remaining eight optimum systems are closely grouped with respect to weight over the whole reliability range. For this mission the unregulated bus systems 1171, 3161 and 3141 are competitive with the regulated bus systems. As is true with Venus Orbiter No. 1, the maximum reliability is achievable with the low voltage system configuration. The weight penalty associated with this maximum reliability, however, represents a smaller weight penalty on a percentage basis in comparison to the competitive systems than for the lower power Venus Orbiter No. 1 mission. System 1151, although optimum at one reliability level, is not competitive over the remainder of the reliability range.

4.4.3 Mercury Flyby

The Mercury Flyby mission represents the shortest time duration of the seven missions considered in the study. As a result, the minimum reliability for a given system based on a nonredundant configuration of that system was determined to exceed 0.90 by considerable margin. The 20 reliability constraints were therefore revised to reflect a range from 0.93 to 0.9995. The locus of optimum system configurations for this

mission is illustrated in Figure 88. Eight system configurations were determined to be optimum at different reliability values over the entire reliability range. Four of these systems are of the unregulated bus type and four of them utilize the regulated bus technique.

The locus of optima for each of these systems is plotted in Figure 89. The achievable reliability and weights of all the systems are fairly closely grouped. Systems 1171 and -1171, however, were generally higher in weight than the other systems over the range of reliabilities, and, since each of these systems appears as the optimum at only a single reliability value, these systems are considered to be less desirable approaches. The low-voltage battery configurations 34115 and -34115 for this study are shown to be approximately 20 percent higher in weight than the majority of the systems at their maximum reliability values. These lower voltage battery systems are also seen to be characteristically higher in weight at the lower reliability levels because they were analyzed only in redundant battery configuration. At intermediate reliability values ranging from approximately 0.99 to 0.9992 the regulated bus systems (3495 and 34115) offer the lightest weight approach. Unregulated bus systems 3141 and -3141 are optimum at higher and lower reliability values.

4.4.4 Mars Orbiter

The locus of optimum systems for the Mars Orbiter mission is illustrated in Figure 90. Nine different system configurations were determined to be optimum at various values of reliability over the entire range. The optimized reliability versus weight relationship for each of these nine systems is illustrated in Figure 91. Here again, the lines connecting points serve only to facilitate examination of the data and as such have no meaning relative to achievable reliability and weight of the various systems.

At reliabilities between 0.9 and approximately 0.97, the majority of these optimum systems are relatively closely grouped in weight. Two higher weight systems exist within the lower reliability range and these systems, 2323 and 2321, may be observed to be only optimum at a reliability level of slightly greater than 0.99. The weight penalty associated with these two systems at all other reliability levels is considered sufficient justification for eliminating them from further consideration.

The characteristic step increase in weight produced by changing from the nonredundant to redundant battery configurations is seen to occur at reliabilities of approximately 0.98 for five of the systems. It is significant that four of the unregulated bus systems can achieve a reliability of approximately 0.99 prior to the need for adding redundant batteries. At this reliability level, systems 3423 and -3423 offer a significant weight advantage. At the higher reliability levels between 0.997 and 0.999, the regulated bus systems 3495 and unregulated bus systems 3161 and 3141 all are competitive from a weight standpoint.

4.4.5 Jupiter Flyby

The locus of optimum power system configurations for the Jupiter Flyby mission is illustrated in Figure 92. Four different systems were determined to be optimum at various specific reliability levels over the total range. Comparison of the optimized weight and reliability for each of these four systems is shown in Figure 93. The maximum achievable reliability is seen to be relatively low in comparison to the previously discussed mission. This results from the much longer mission time required to reach Jupiter.

The advantage of regulated bus systems employing a shunt solar array regulator is apparent because the solar array is operated at its maximum power point at the critical design point and this power is delivered directly to the load power conditioning equipment without incurring efficiency penalties in series regulators. The inefficiency of charge and discharge regulators produces a minimal effect on the system because of the very low-battery utilization requirement on a nonorbiting mission of this type. The ac distribution system is shown to produce a significant advantage in reliability for this particular mission. The weight penalty associated with this advantage in comparison to the less reliable lighter-weight dc systems shown is approximately 6 percent.

The optimum power system weights vary from approximately 800 to 900 lb which clearly exceeds the allowable weight for this mission. Referring to Table 1, the estimated spacecraft weight is 650 lbs including payload. The assumption that state-of-art solar arrays at 0.1 lb/watt would be used for this mission is therefore not valid. Since the solar array constitutes the major portion of the system weight, a 0.5 lb/watt design,

or better, is essential to the feasibility of this model mission. However, such a change would not appear to affect the selection of optimum systems.

4.4.6 Jupiter Orbiters

The locus of optima for the Jupiter Orbiter No. 1 mission is plotted in Figure 94. Only four system configurations comprise this locus. The plot of the individual optimized weight versus reliability for each of these four systems is shown in Figure 95. The same four systems were determined to be optimum for the Jupiter Orbiter No. 2 mission as shown in Figure 96. The individual plots for this mission are shown in Figure 97. For both of these missions, the regulated bus systems employing the shunt regulator for solar array control were determined to be optimum. Characteristically, the AC versions produced the higher achievable reliabilities and the low voltage battery systems yielded the maximum achievable reliability.

The resultant optimum power system weights for the Jupiter Orbiter No. 1 mission represent 60 to 70 percent of the estimated spacecraft weight of 1620 lbs. Thus, a lighter weight array design is essential to perform this mission with the assumed loads. For the Jupiter Orbiter No. 2 mission, the lighter 0.5 lb/w array design was assumed and the resultant optimum system weights represent less than 20 percent of the 8430-lb spacecraft weight.

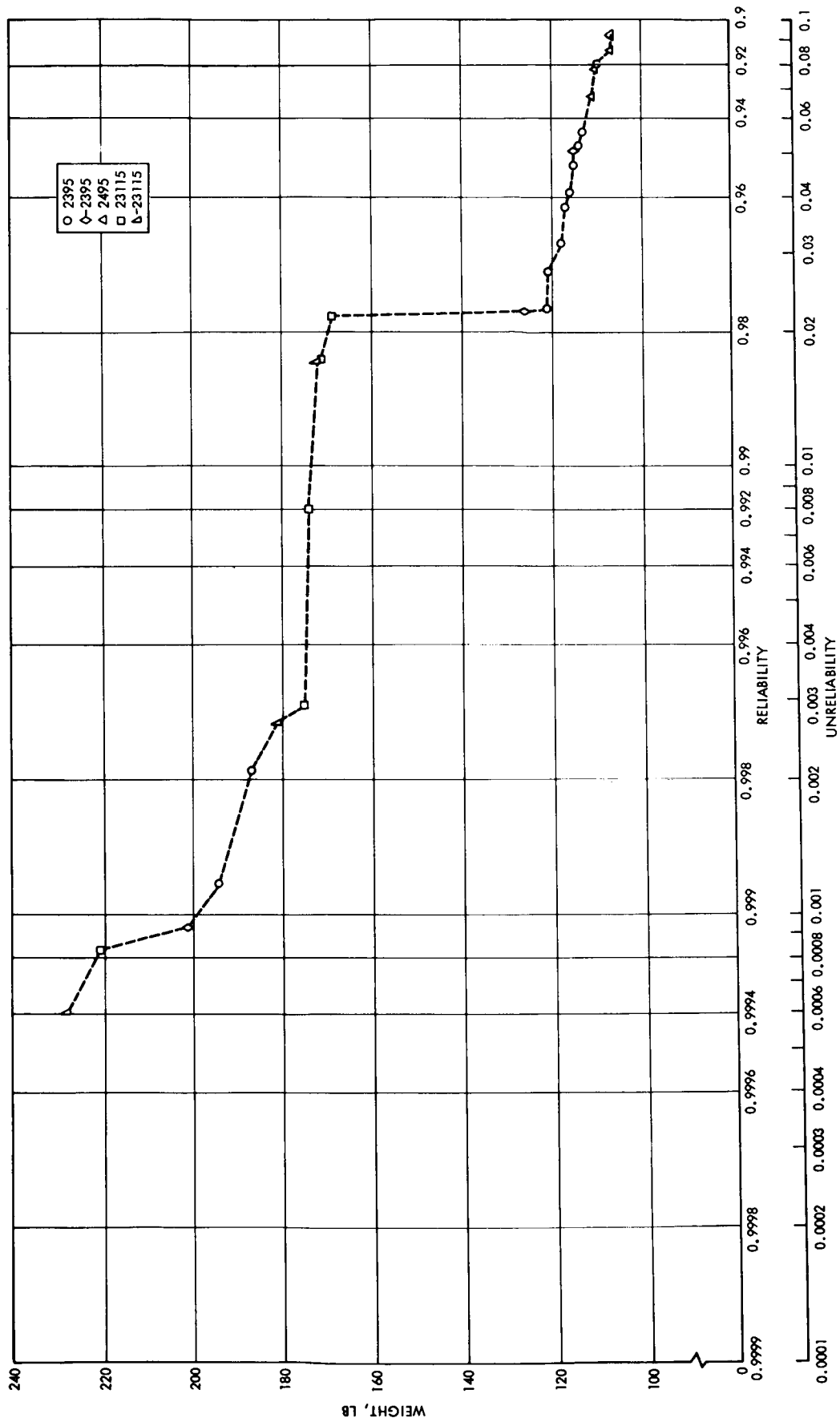


Figure 84. Locus of Optimum System Configurations, Venus Orbiter No. 1

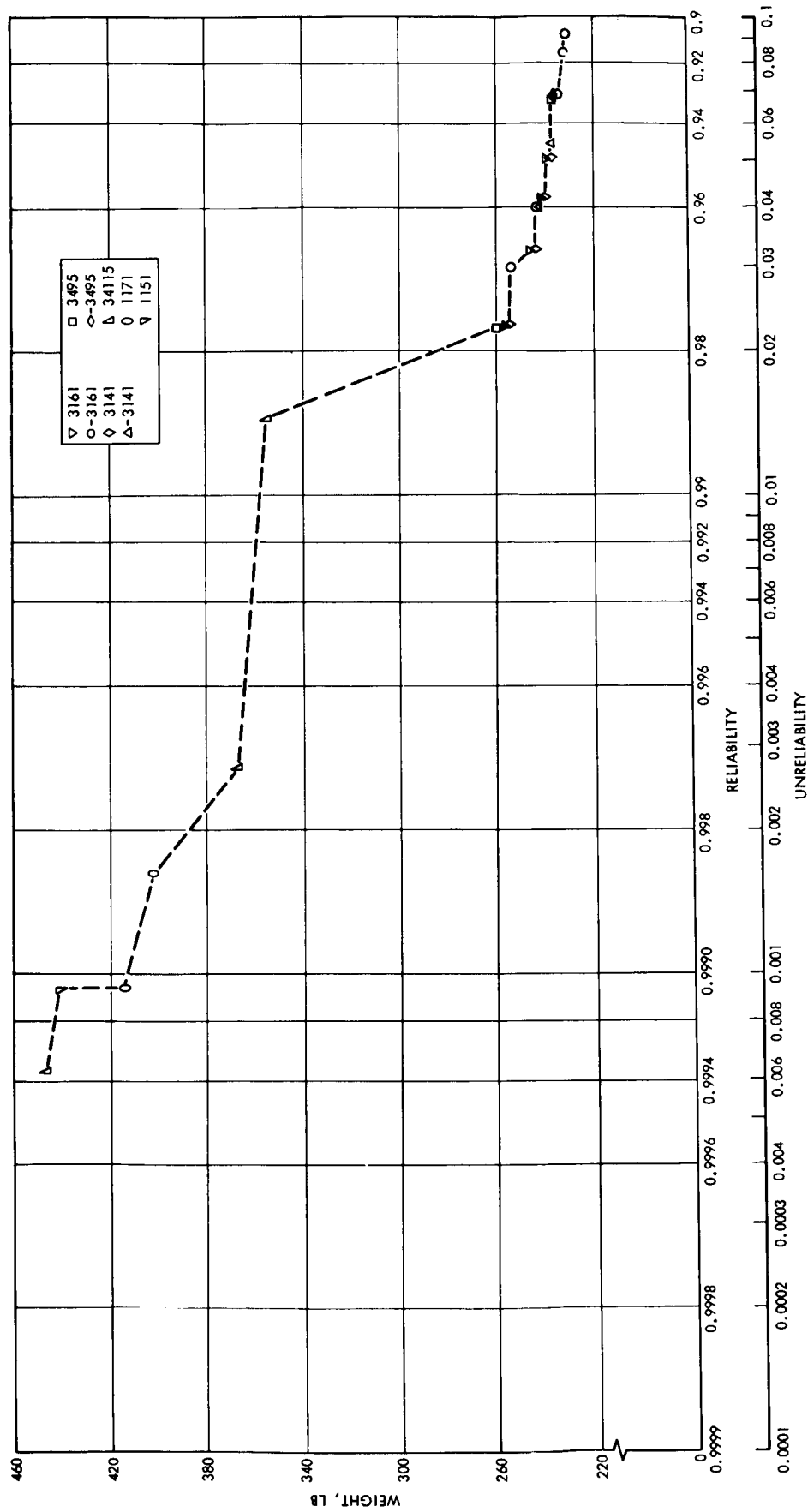


Figure 86. Locus of Optimum System Configurations, Venus Orbiter No. 2

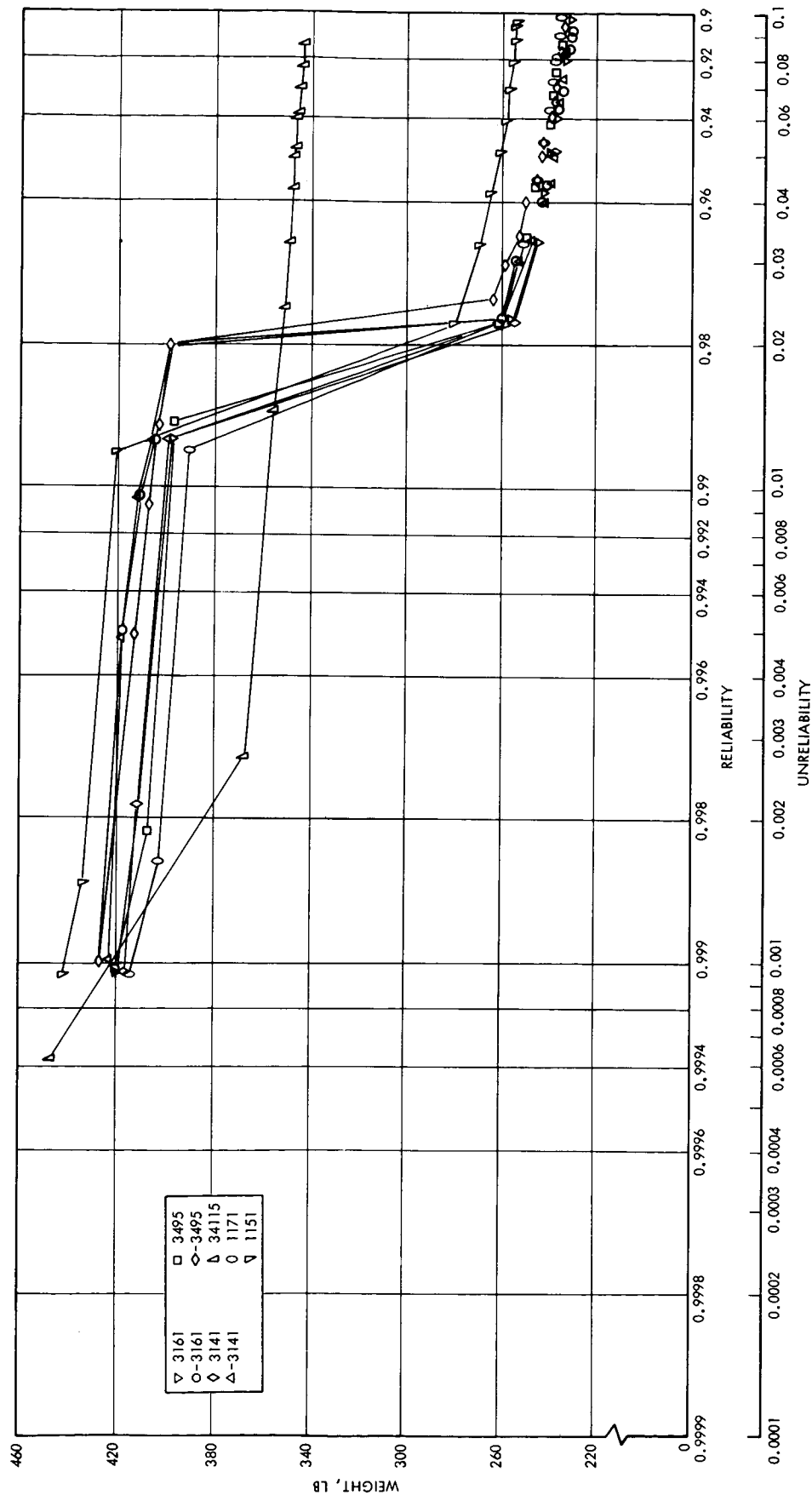


Figure 87. Comparison of Optimum System Configurations, Venus Orbiter No. 2

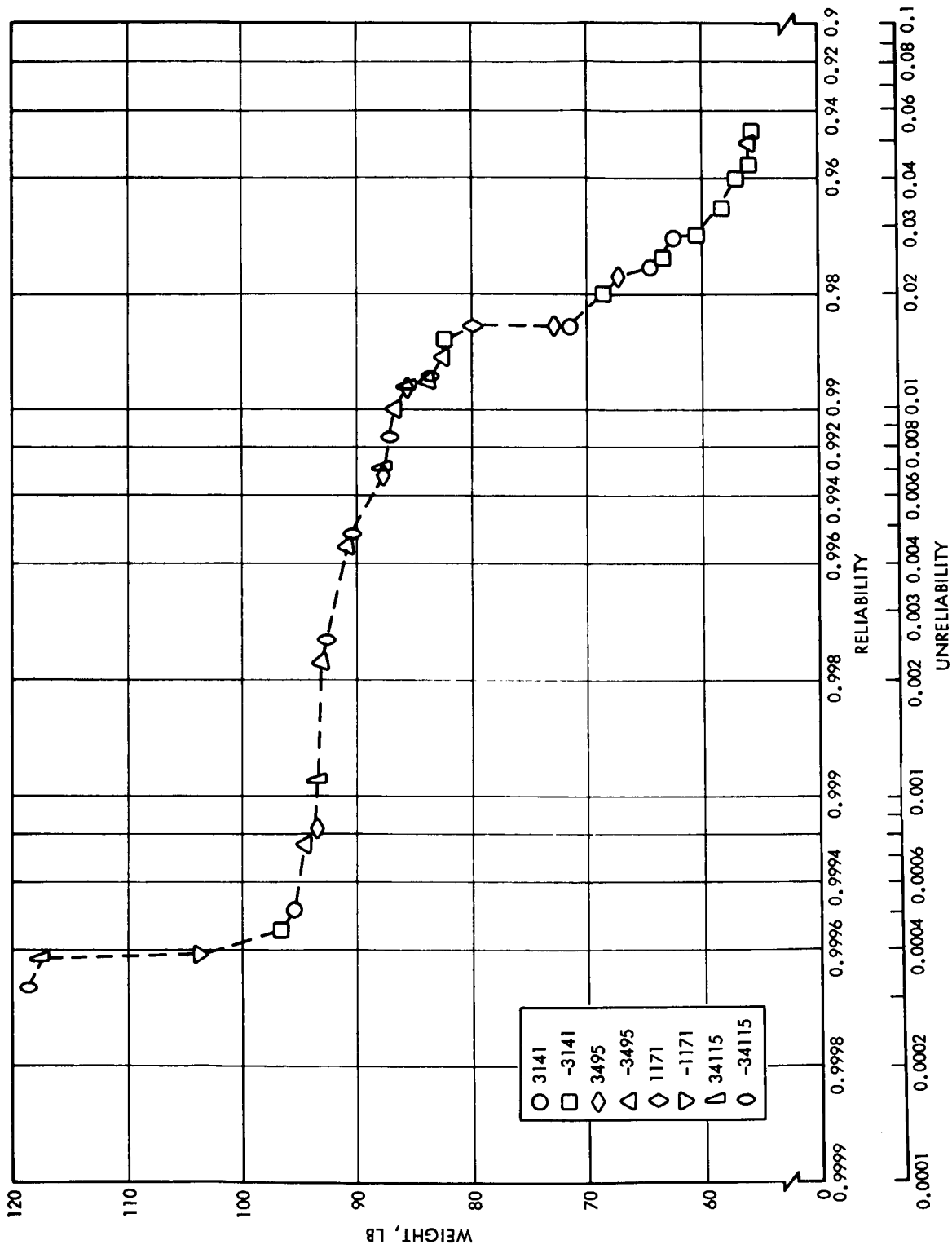


Figure 88. Locus of Optimum System Configurations, Mercury Flyby

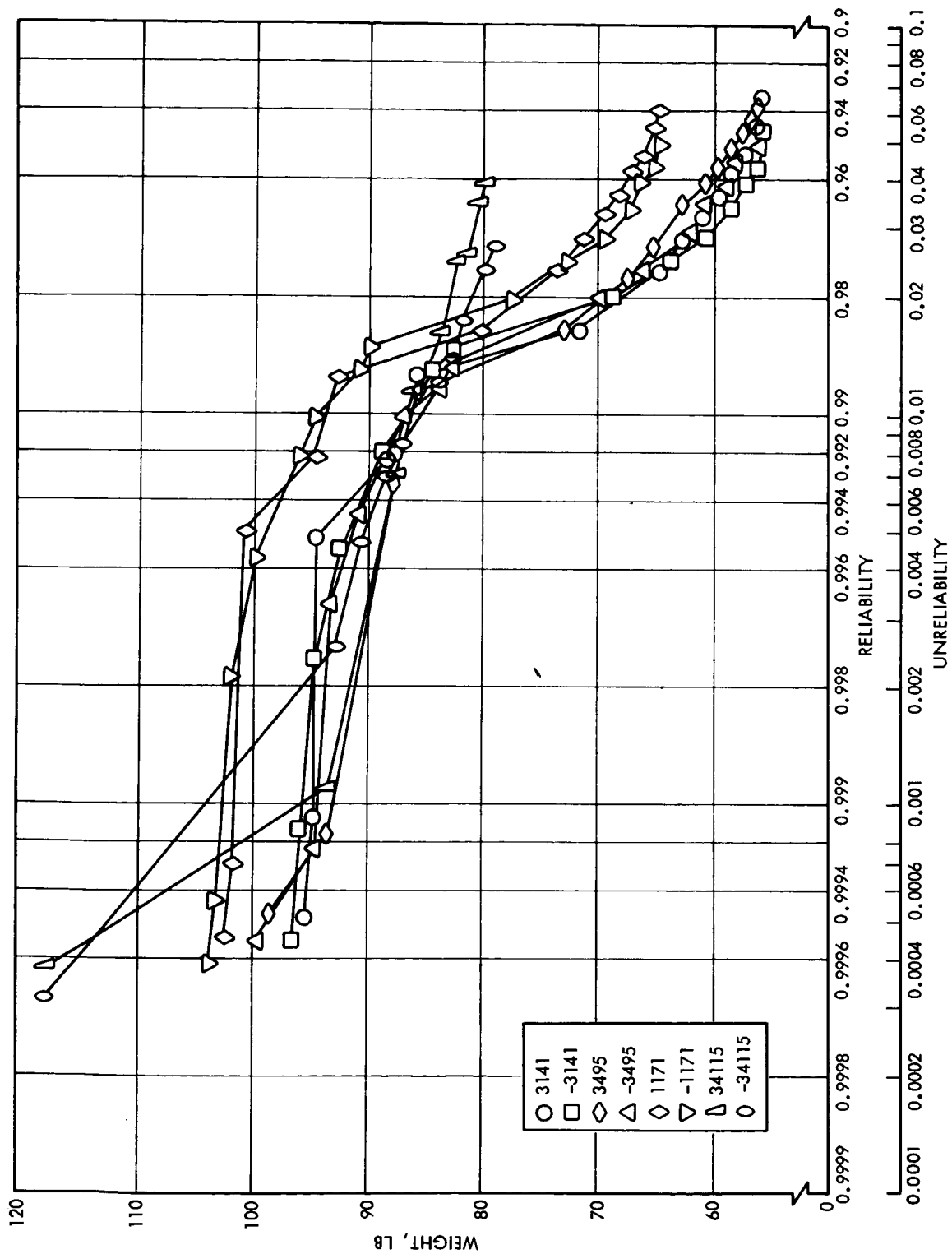


Figure 89. Comparison of Optimum System Configurations, Mercury Flyby

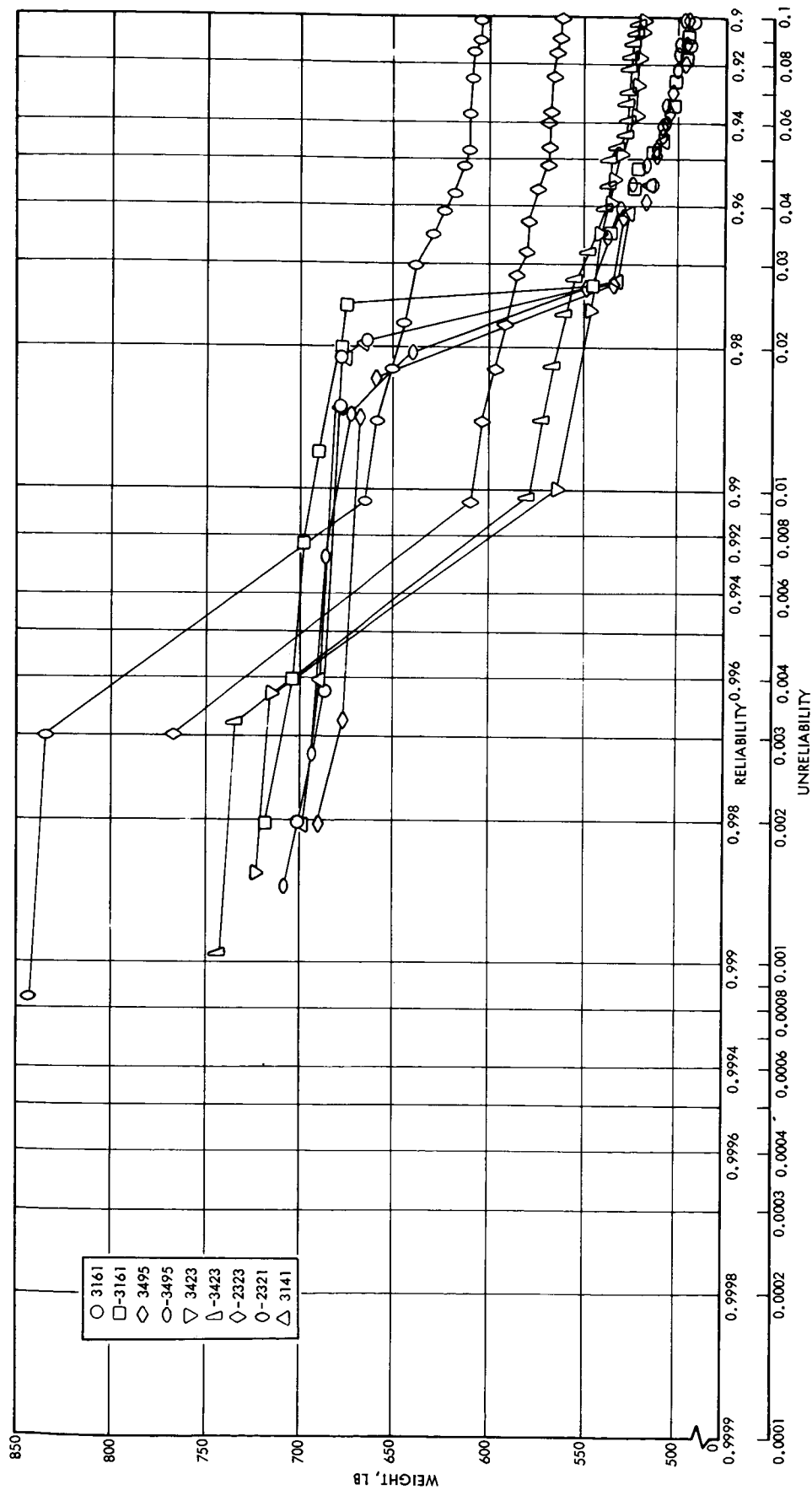


Figure 91. Comparison of Optimum System Configurations, Mars Orbiter

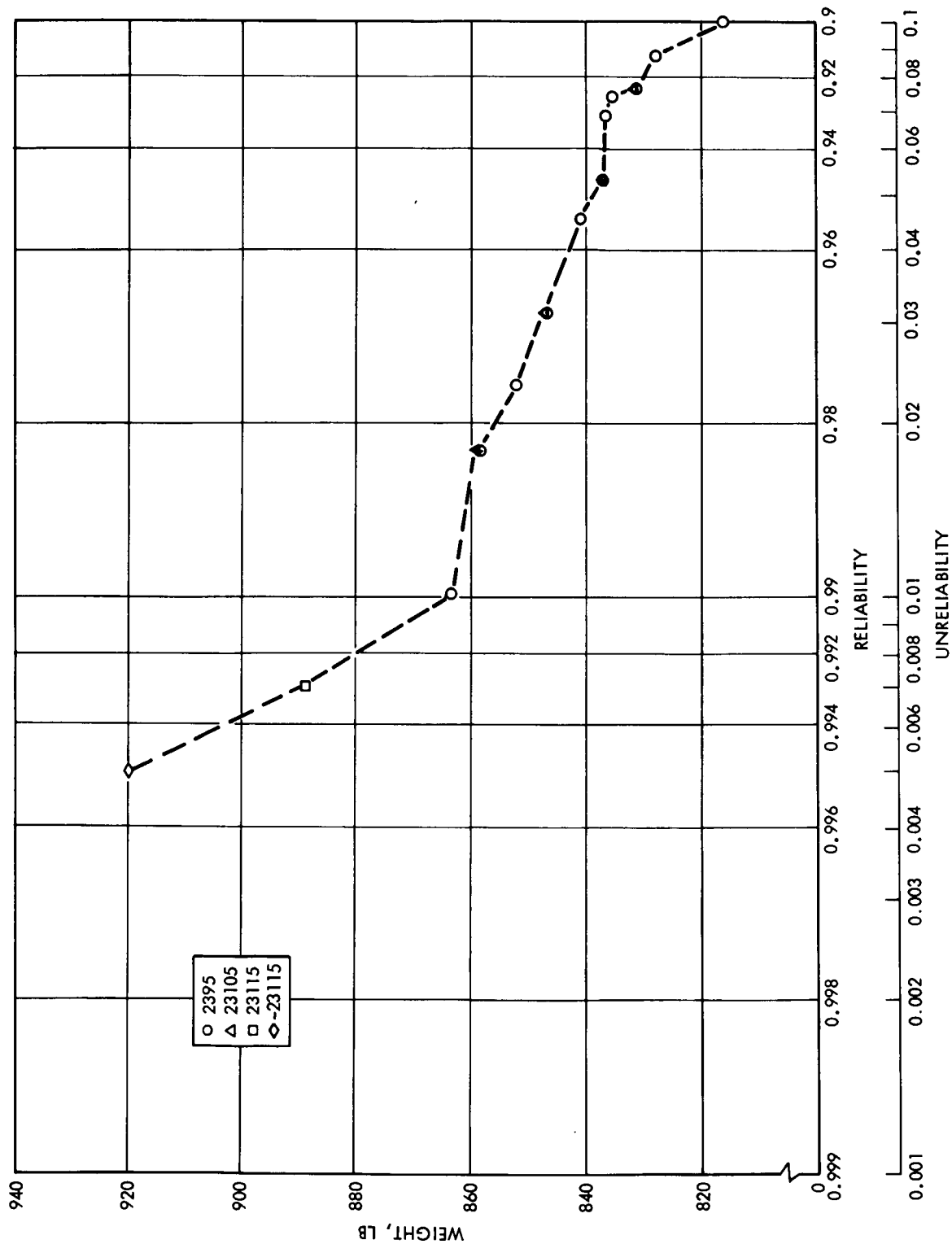


Figure 92. Locus of Optimum System Configurations, Jupiter Flyby

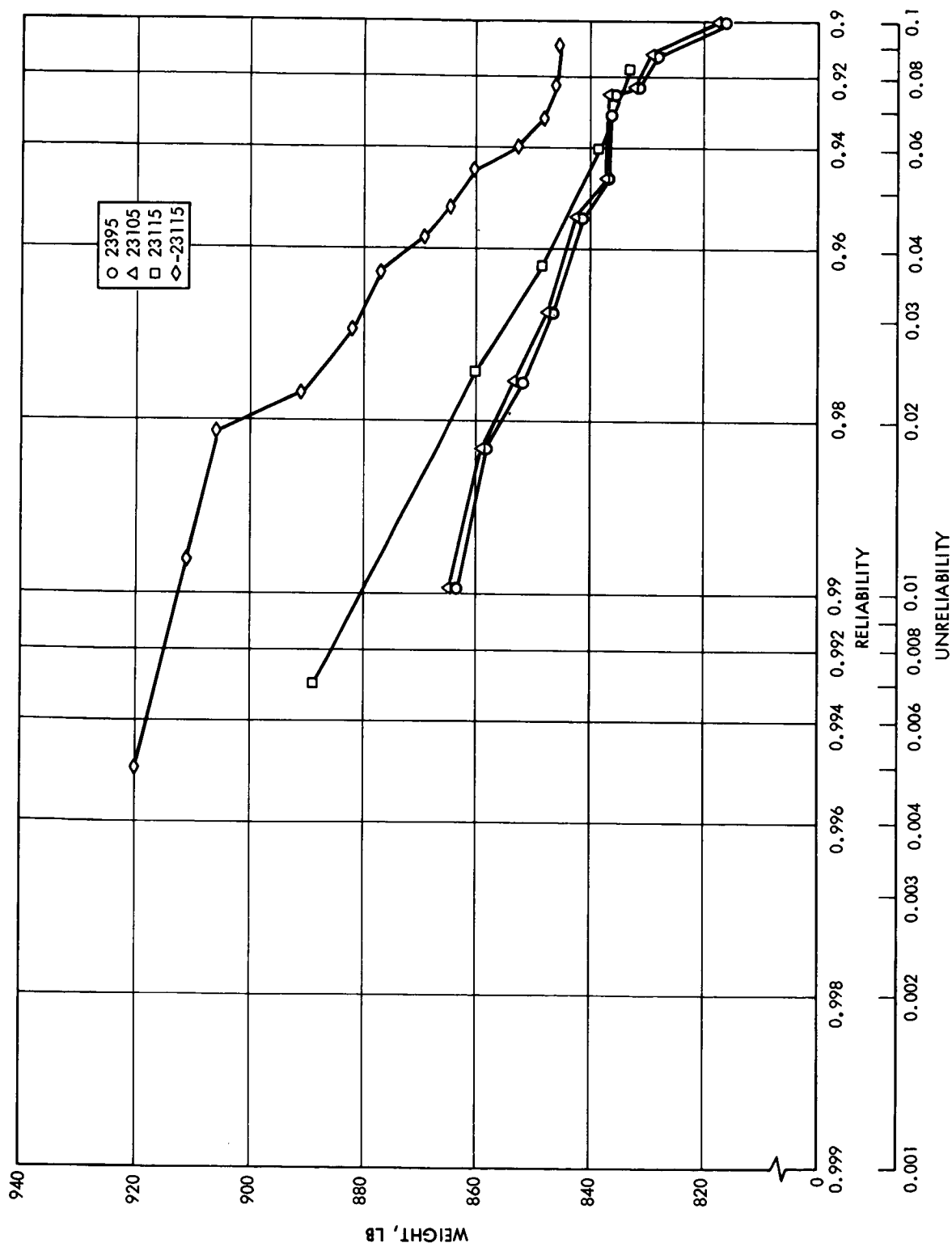


Figure 93. Comparison of Optimum System Configurations, Jupiter Flyby

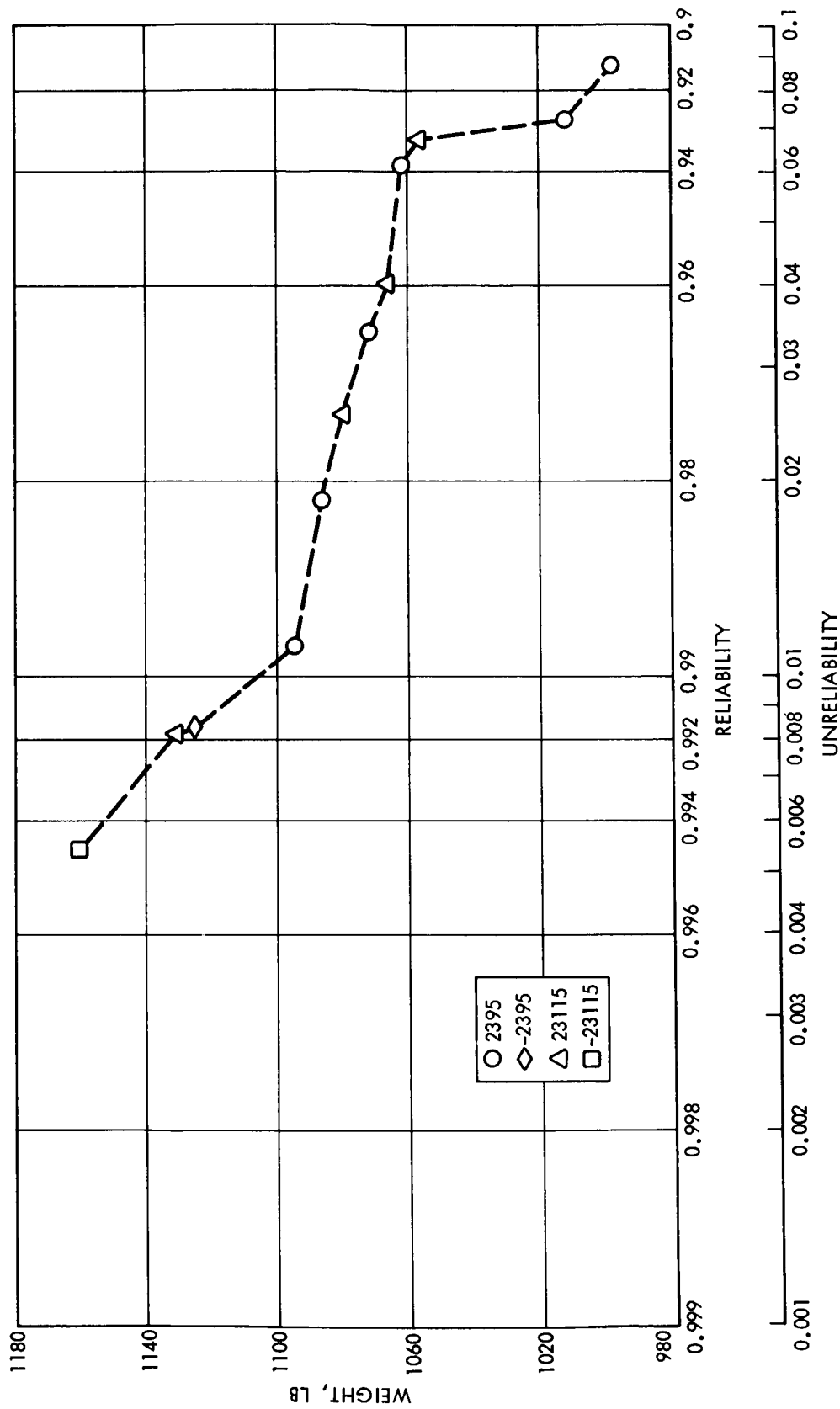


Figure 94. Locus of Optimum System Configurations, Jupiter Orbiter No. 1

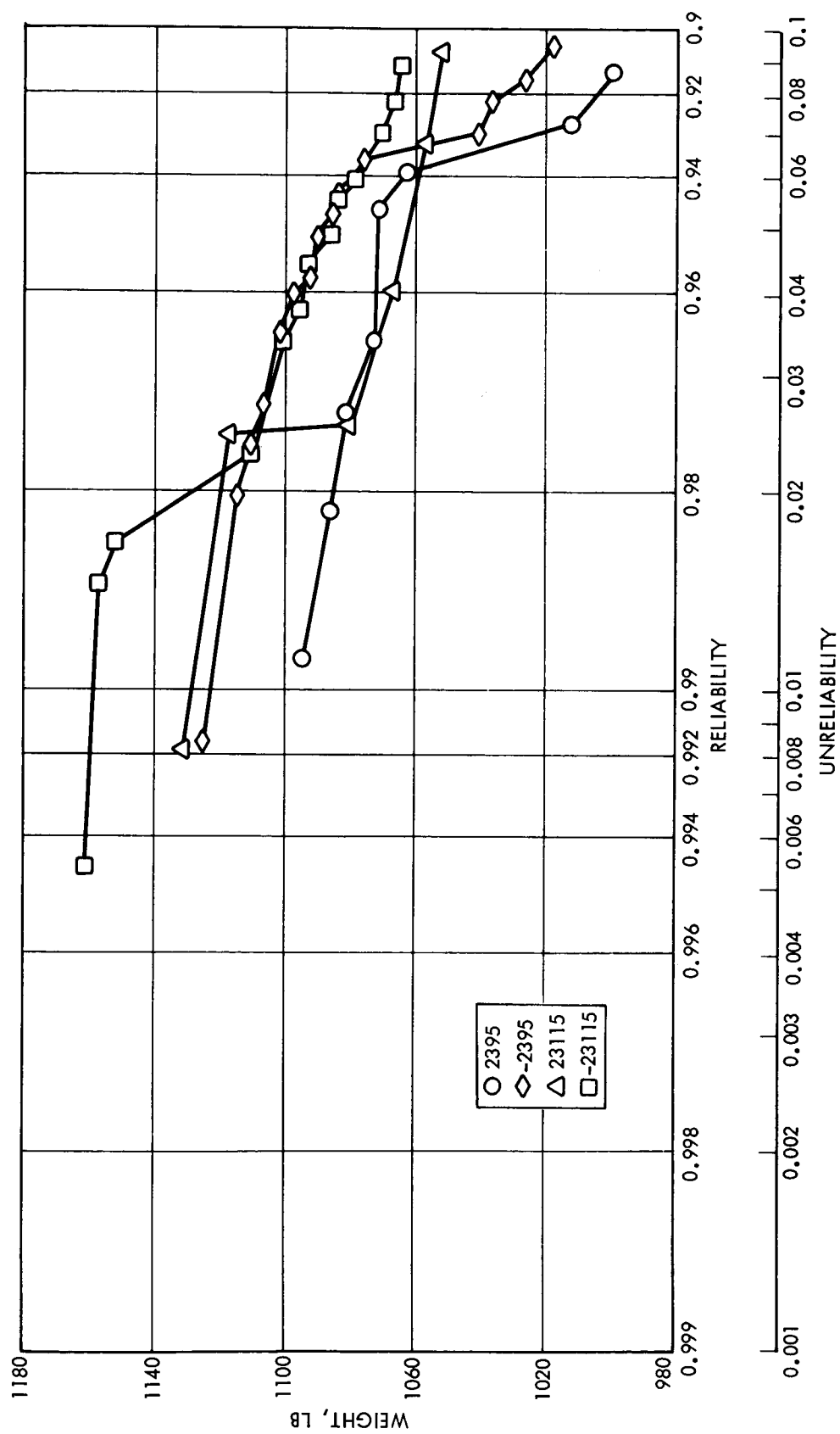


Figure 95. Comparison of Optimum System Configurations, Jupiter Orbiter No. 1

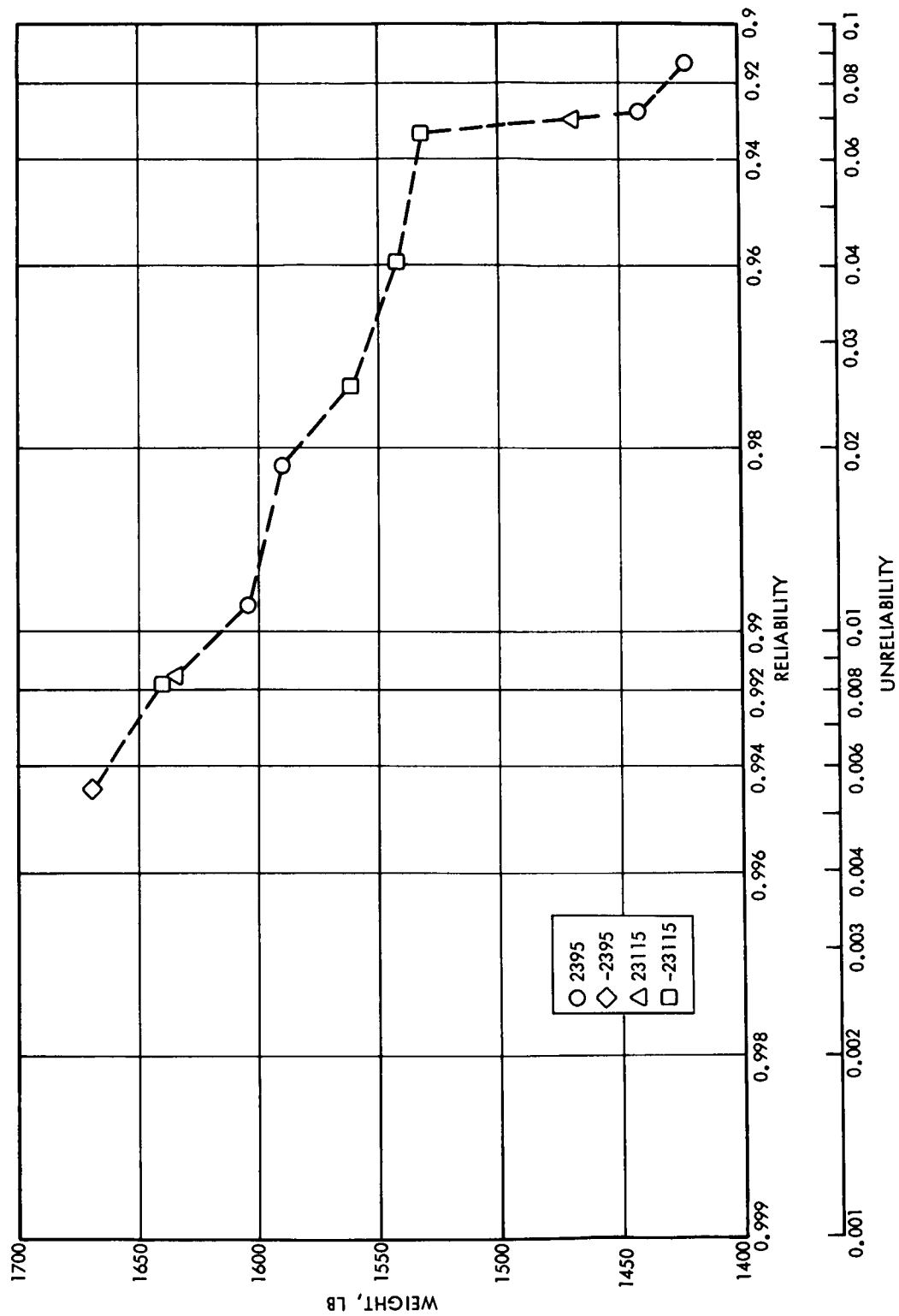


Figure 96. Locus of Optimum System Configurations, Jupiter Orbiter No. 2

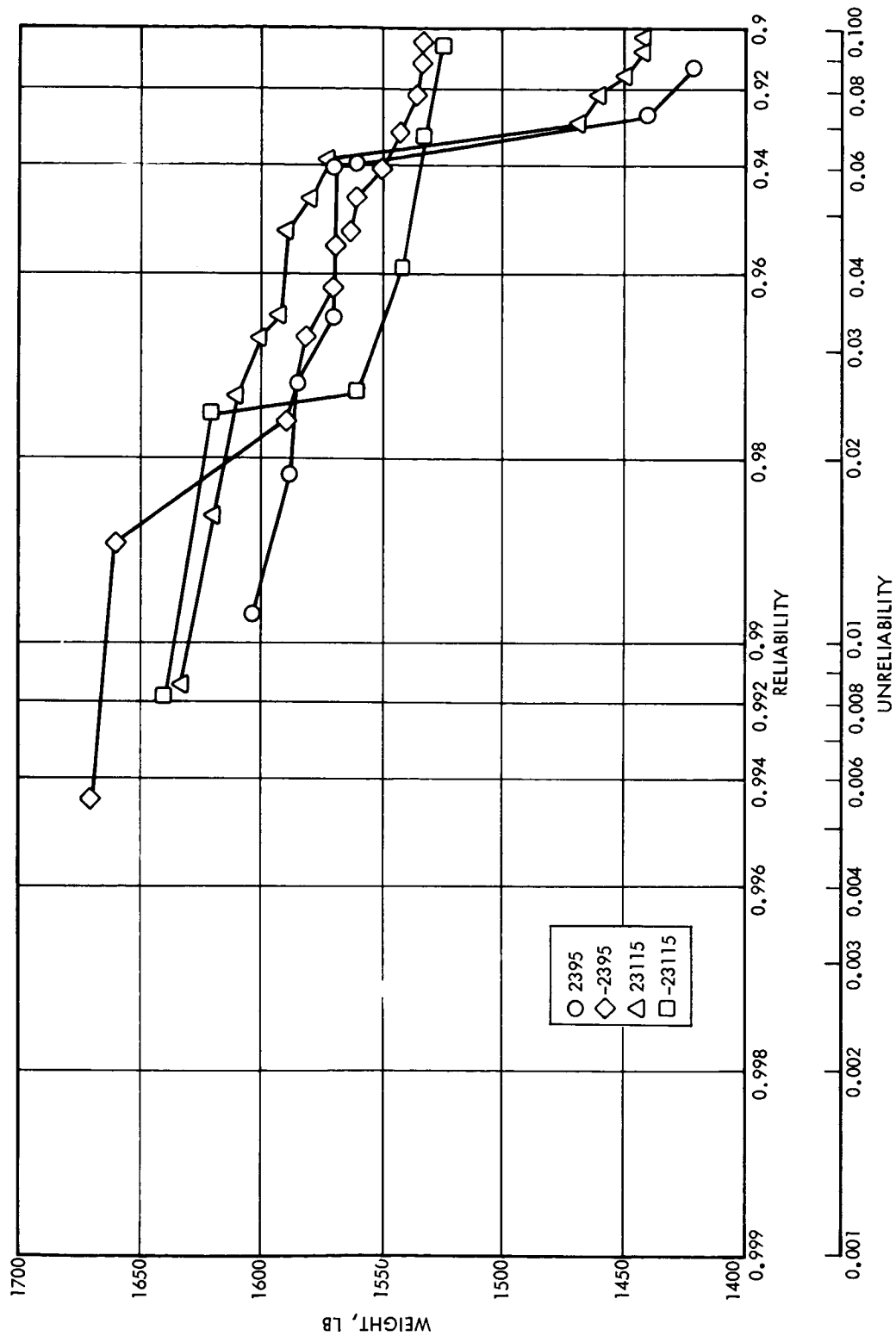


Figure 97. Comparison of Optimum System Configurations, Jupiter Orbiter No. 2

5. QUALITATIVE SYSTEM COMPARISONS

5.1 ELECTROMAGNETIC COMPATIBILITY

One of the most important interface considerations which influence the design of spacecraft power systems is that of electromagnetic compatibility (EMC). Since the power system has some type of conductive interface with each equipment on the spacecraft, interference generated by the power subsystem will exist at these interfaces. In addition, interference, generated by any of the equipments using this power, can use the power subsystem as a medium to couple interference to any other equipment.

As a result of these considerations and the fact that EMC problems are often not fully appreciated by power system designers, emphasis was placed on this aspect of the power system interface studies for this program.

Typical problem areas of incompatibility occur in two distinctive areas:

- a) Effects of electromagnetic interference on phenomena being measured by spacecraft experiments.
- b) Effects of electromagnetic interference on spacecraft electronic systems by various coupling methods.

In the first area, the effect is generally due to the electric and magnetic fields created by the power system equipment and the distribution system. These fields may modulate or change the electromagnetic fields existing in and around the spacecraft or may dominate the space fields so as to make them unmeasurable.

In the second area, interference may couple voltages and/or currents into sensitive electronic circuits and cause irregular behavior of the affected system.

The spectral distribution of the power system interference may be classified into two general categories. The first is discrete line spectra at the regulator switching frequency, converter switching frequency and/or the frequency of ac distribution. Harmonics generally exist above

general random spacecraft noise out to the region of 5 to 10 mc. The second type noise is transient in nature existing at turn on—turn off occurrences. The continuous-spectrum nature of transients may be quite large in amplitude when integrated over the bandwidth of the affected system, and consequently the systems will respond to this energy.

While any system will respond to energy within its passband, some categorization of typical problems is possible for general systems. The magnitude of overall interference problems is generally an inverse function of spacecraft maximum distance for a given power available since data rates are of necessity low for long-distance missions. Consequently, the information bandwidths of experiments and telemetry functions are narrow and the probability of intercepting an intolerable amount of noise is decreased. If the discrete frequencies associated with the power system are above approximately half the maximum data rate, small interference problems should result provided the sensitivities are not excessively high. The nature of the problems, which occur under these conditions, is generally one of sampling. The interference frequencies, which are high compared to the data rate, may be sampled each time a particular data word is transmitted. If the noise frequency and data rates are synchronous, a constant off-set will occur. If they are asynchronous, a modulation of data will occur at some low frequency, dependent upon the difference between the noise frequency and the particular harmonic of the data rate, which results in an inband signal.

Onboard systems, whose outputs are utilized onboard and not transmitted to earth, are not necessarily limited by the data bandwidth. These systems may well have bandwidths which allow them to see the power system interference over a broad range.

Specifically, the primary compatibility problems relating to the spacecraft power system are due to:

- Type of power distribution used (ac or dc)
- Waveform of ac distribution
- Frequency of ac distribution
- Type of voltage regulator circuit used (dissipative or switching type)

- Power circuit grounding
- Power circuit wiring practices
- Power converter "Bandpass Characteristic" to interference at its input.

These compatibility problems can be minimized by the use of judicious circuit design and interference control measures, such as circuit grounding, bonding, shielding, circuit isolation, and filtering.

The impact of EMC considerations on selection of a power system design is divisible into two areas of consideration. The first area concerns the desirability of minimizing the number of power handling units which employ pulsewidth modulation types of switching circuits for regulation and control of the solar array, battery and main power bus. Both series and shunt-type voltage regulators used in spacecraft power systems may employ either switching (pulsewidth-modulated) or dissipative techniques. From the interference generation standpoint, the dissipative type is preferable since it generates negligible interference. In contrast, the pulsewidth-modulated type of regulator is a prolific generator of impulse-type interference.

The second area in which EMC considerations strongly influence power system design is that of selection of the power distribution system. Because of the fewer parts in the ac distribution system it was determined to be the most reliable system. However, in comparing redundant dc systems versus redundant ac systems the differences were only in the third or fourth decimal place of the calculated reliability values. The ac systems were selected with one transformer in the main inverter and a second transformer in each of the transformer-rectifier units. This series transformer configuration produced a penalty in system efficiency which was then reflected in a greater system weight in comparison to the dc systems. Here again, the magnitude of the impact of this poorer efficiency on system weight was not significant. As a result, selection of either ac or dc distribution cannot be based strictly on comparisons of power system reliability and weight.

A squarewave ac versus dc tradeoff performed for a typical state-of-the-art spacecraft indicated, in general, a definite advantage for the dc power distribution system with respect to EMC. The analysis indicated that the dc distribution system could be designed to be acceptably low in interference with proper filtering at its interference producing loads (solenoids, relays, etc.), dc to dc converters and PWM regulators. In contrast, the squarewave ac distribution system inherently produces interference fields due to the transmission of squarewave power throughout the spacecraft. The interference control techniques of slowing pulse rise and fall times, wire twisting and shielding, and proper cable routing reduce the generation and crosscoupling of the switching interference, but not sufficiently in every case.

The necessity of shielding on the ac distribution cabling increases the weight of cabling by approximately 45 percent. For the larger spacecraft, this penalty becomes increasingly significant. The possibility of using higher voltage (>100 v) ac distribution can offset this penalty by reducing load currents and wire sizes. The use of higher voltage dc distribution systems has been limited to about 50 v in the past, based on available transistor voltage ratings. For larger spacecraft, distribution voltages of 100 v or greater (whether ac or dc) would provide significant improvements in the efficiency and weight of the distribution system. Development of parts to provide reliable operation at these higher voltages is considered mandatory to optimize the weight of systems using dc distribution for power levels in the kilowatt range.

5.2 THERMAL CONTROL

The most common interface problem between the power subsystem and spacecraft thermal control system is that of maintaining a relatively close range of operating temperatures for the battery to assure its reliable operation. The typical 50 to 90°F range desired for the battery has, in several spacecraft designs, constituted the single most difficult control problem for the thermal control system. The magnitude of this problem is a function not only of the variations in heat dissipation of the battery which are in turn directly related to its charge rates and charge control methods, but also the influence of other spacecraft equipment, the heat dissipation of which may influence the operating temperature of the battery. Maintaining desirable battery-operating temperatures throughout a mission is a problem common for the most part to all power system configurations, and it does not, therefore, materially effect the selection of power system designs.

A second important thermal interface which could influence the design of the power system is that relating to the thermal control of dissipative regulators. This is particularly true with the shunt dissipative regulator. Techniques have been developed to reduce the magnitude of the heat dissipation in shunt regulators. For the larger spacecraft and for the interplanetary missions studied, however, these techniques may prove inadequate. As a result, the use of series PWM regulators to control the output voltage of the solar array appear clearly advantageous from the thermal control standpoint. The principal advantage of the series regulator is to proportionately reduce the power drawn from the solar array if the load power demand is significantly less than the solar array power capability. This is accomplished by causing the solar array to operate at a voltage and current at which the efficiency with which it converts solar energy into electric power is relatively low.

Concerning the missions investigated in this study, the large variation in solar array capability during the Jupiter mission would produce the largest thermal control problem relative to the use of the shunt regulator. The shunt regulator, however, is most advantageous for the Jupiter missions because of its ability to optimize the operating point of

the solar array at the critical design point of the mission. This advantage is particularly significant because of the very large solar array required for the Jupiter missions; thus it is desirable to add additional complexity to switch-out sections of the solar array during the early phases of the mission when a large excess capability exists. This will reduce the amount of heat dissipation in the shunt regulator such that the thermal control system can accommodate this approach.

5.3 POWER SYSTEM FLEXIBILITY

The term flexibility, as used in this study, pertains to the ability of the power system to tolerate variations in load power requirements during the various mission phases or changes in the specific power characteristics required by the loads without necessitating extensive redesign of the power system or producing detrimental effects on the power system reliability and weight. The first area of concern is the effect of changes in power levels or power characteristics required by the loads when supplied from the dc distribution system. When dc-to-dc converters are used to generate the voltages required by the loads, any variation in load requirements could necessitate the redesign of one or more of these converters. The advantage gained by using an ac distribution system as configured in this study is small in this respect, in that centralized TR units were used wherever possible to minimize the number of parts in the system and to maximize system efficiency. These would also require redesign in the event of load requirement changes.

It is clear that, from the standpoint of flexibility, power system configurations which supply a common ac or dc bus to the loads and permit the load equipment to condition that power as necessary offer large advantages in terms of flexibility. The disadvantage is the duplication of power conditioning functions in the various load equipment with its attendant reduction in system reliability and increase in system weight. This reliability penalty results from the increased number of parts required to provide power conditioning for the essential loads but must also take into account the advantage of having separate power conditioners for the nonessential loads. Obviously, redundancy can be employed in these power conditioning functions to minimize the loss in reliability. As a result, the poorer efficiency of many small power conditioning elements in comparison to centralized power conditioning is the major reason for considering this to be an undesirable approach.

It is extremely difficult to quantitatively trade off the gains in system flexibility against losses in system efficiency. The design of an optimum power system, however, must assume adequate definition of load power requirements and must permit the power system designer to optimize the necessary power conditioning equipment. The approach of supplying an ac bus to all of the load equipment from a central inverter is a compromise,

in this respect, which permits consolidating all power inversion functions into one power system unit and requires transformer rectifier units in the load equipment. If the power requirements of each of these items of load equipment are small, relative to the total power demand, it is reasonable to assume that an advantage will be gained with this approach over that of supplying a dc bus to all of the load equipment and including dc-to-dc converters within each of the loads. The reason for this is that at low power levels the decrease in efficiency of a dc-to-dc converter is larger than that associated with transformer-rectifiers. If a relatively small number of dc-to-dc converters may be used, as occurred for the assumed load power conditioning equipment configurations in this study, then the efficiency of the dc distribution system is improved and the efficiency penalty of having transformers in the main inverter and additional transformers in the TR units tends to offset the apparent efficiency advantage of the ac distribution system.

A second area of consideration relative to load growth is in the power sources and their control and regulation functions. Any increased continuous load power demand will normally require redesign of these power system elements. With respect to transient or peak load demands, however, if the additional load can be supplied from an unregulated bus, then those system configurations which permit the battery to discharge directly to the main bus would appear to have an advantage over the regulated bus system unless these transient load demands can be supplied directly from the battery.

The use of a low-voltage battery with a regulated bus system has a significant disadvantage in this respect. For this type of system, all continuous or transient load demands which exceed the solar array capability must be supplied from the battery through its boost discharge regulator. An increase in steady state or peak loads would necessitate adequate power-handling capability in this regulator. In addition to the probable redesign required, the regulator efficiency at normal load conditions would, as a result, be decreased with an attendant increase in battery and system weight.

A method under investigation by TRW to overcome this disadvantage with a low-voltage battery system is incorporated in the modular energy storage and control (MESAC) system which is based on a modular approach in performing the energy storage function. Each module within such a system contains the low-voltage battery and its charge and discharge regulators. This system has an inherent large degree of flexibility in that load growth can be accommodated by adding modules without necessitating new design or the redesign of any of the other existing modules.

With respect to transient or peak loads, the use of a transient load bus isolated from the main bus and supplied through separate boosters from the batteries, or the use of separate energy sources, such as capacitors or a primary battery, appear to be feasible alternatives to the addition of energy storage modules.

In this study, the low-voltage battery concept was configured with three batteries, two of which are required to support the requirements. In the actual application of the modular energy storage concept, the number of batteries is a variable which can be optimized for the specific use. The analyses leading to the selection of the optimum system must take into account the availability of battery cells of given capacities as well as the reliability-weight tradeoff of using a larger number of batteries in parallel. Thus, it is possible to consider a system as an example having twelve batteries in parallel, ten of which are required to support the mission. The potential advantage is that due to the relatively small number of cells required, an adequate reliability may be achieved with only 20 percent redundancy.

From these general considerations, it appears that the ac distribution approach and the modular energy storage concept offer advantages relative to flexibility in terms of load growth. The reliability weight analyses that have been performed indicate that changes in the battery duty cycle may have a more significant impact on the selection of a power system. Here again the distinction between the regulated bus concept and the unregulated bus concept is made. The former is clearly advantageous for those missions in which battery discharge requirements are relatively small. The Mars Orbiter mission represented the greatest ratio of

eclipse time to sunlight time during its orbiting phase. The study results for this mission showed that certain of the unregulated bus systems offered weight advantages in comparison to the regulated bus systems.

Analyses have shown that if this ratio is further increased, the unregulated bus approach, because of its more efficient energy-storage capability, becomes even more favorable than the regulated bus approach. As a result, consideration of flexibility in terms of variations in the orbit parameters may lead either type of system to become less optimum and possible variations in these parameters must be taken into account in the initial power system design.

5.4 SYSTEM DESIGN CONSIDERATIONS

There are several specific power system design considerations that are common to all power system configurations. These are:

- Command provisions
- Telemetry provisions
- Protection against load faults
- Electromagnetic interference control

5.4.1 Command Provisions

In those spacecraft applications where continuous surveillance from the ground is possible, many operations of the power system can be controlled by ground command. In some cases, this results in a significant simplification of the onboard automatic control circuitry. The approach favored for the interplanetary missions considered in this study is that of providing onboard automatic controls and relying on ground command only as a backup to the onboard control. The reliability of these automatic controls is maximized by the addition of redundancy within the control circuits. Care must be exercised in implementing the backup command circuits to assure that their failure modes are such that they will not cause improper operation of the power system.

The need for automatic controls is particularly important in considering missions with large earth-spacecraft distances such as that of the Jupiter missions. In these missions, the time lapse between the transmittal of telemetry data from the spacecraft and the receipt of that data at the earth can be as great as 50 minutes. This corresponds to a distance of 6 AU. Maximum distances and approximate corresponding one-way transmission times for each of the missions are as follows:

Jupiter:	6 AU	(at encounter)	50 minutes
Mars:	2.6 AU	(end-of-life)	22 minutes
Venus:	1.2 AU	(end-of-life)	15 minutes
Mercury:	1.4 AU	(end-of-life)	12 minutes

For the Jupiter mission, if the reaction time at the ground station is as rapid as five minutes to determine necessary action on receipt of abnormal telemetry data, the corrective action for a possible dangerous situation on the spacecraft would take about two hours. In reviewing typical power system failure modes and effects, it is considered impractical to allow any of these failure modes to exist for that period of time without corrective action.

The second reason for recommending the use of reliable automatic controls is that the penalty in weight resulting from incorporating automatic power system control functions in the spacecraft and in implementing these circuits in a redundant fashion to assure their reliable operation is relatively small. Nevertheless, unforeseen eventualities do exist and, whether they occur within the power system or external to the power system, the desirability of having the flexibility of changing operating modes by command in response to abnormal conditions is clearly advantageous.

Command capability is considered most desirable in those areas relating to battery-charge control and load switching. The safe operation of the battery is dependent upon the ability of the spacecraft thermal control system to maintain desirable operating temperatures. If these operating temperatures are exceeded for reasons of abnormal orientation conditions, abnormal heat dissipation in any spacecraft equipment or abnormal operating conditions of the battery itself, the probability of completing the mission is reduced. Ground command capabilities are considered necessary to terminate battery charging, regardless of the status of the on-board control circuitry, and to restore normal automatic operation when desired. Secondary command requirements relative to battery control are the ability to initiate battery charging at any time as a backup to the automatic on-board charge control function and the provision to adjust battery charge rates or voltage limits to accommodate abnormal operating conditions.

The second command requirement of providing the capability for switching loads may serve as a backup to on-board load sequencing provisions, permit gross adjustments of heat dissipation within the vehicle, control the amount of available battery charging power, or limit battery discharge energy requirements. An automatic control feature in most power systems consists of a battery under voltage sensor which effects an automatic load reduction in the event that battery capacity is inadequate.

The preferred implementation of this feature is to provide a non-essential load bus which can be deenergized in the event of an undervoltage of the battery. All loads not required for survival of the spacecraft should be energized from such a bus since, in the event of a battery undervoltage, the remaining battery capacity is usually relatively small. If battery undervoltage occurs early during an eclipse period, the remaining battery capacity must support all essential or critical loads throughout the remainder of the eclipse period. The voltage setting for this undervoltage disconnect of nonessential loads is critical in that it must be sufficiently high to assure adequate remaining battery capacity for spacecraft survival and, on the other hand, sufficiently low to prevent premature load disconnect.

Here again, the operation of such a load disconnect function could be implemented by relying on a ground command for cases where the surveillance of the spacecraft is continuous and the transmission times are relatively small. Neither of these conditions is applicable to the interplanetary missions considered in this study. As a result, the need for a nonessential load bus and automatic deenergization of that bus in the event of low-battery voltage during discharge is considered imperative. The simplest example of this is the Jupiter Orbiter mission. If such an event were to occur at the beginning of the 1.6-hr. eclipse period, a probable complete loss of power would occur before corrective action could be taken by ground command. Ground command load-switching capabilities are necessary in this case to restore the nonessential loads when desired, and to effect a load reduction prior to entry into each subsequent eclipse if the battery capacity is not recovered.

Another ground command capability often provided in earth-orbiting spacecraft is that for reconditioning batteries. This operation consists of removing a battery from the main system, discharging it completely through an auxiliary load and then returning it to the system for complete recharge. This reconditioning cycle is employed routinely in the storage of battery cells and has been determined to be an effective way of overcoming a major portion of the loss of battery capacity attributable to repeated charge-discharge cycling or long term storage.

Although the numbers of cycles required in the interplanetary missions considered in this study do not appear sufficiently large to necessitate the addition of battery-reconditioning capability, it is considered desirable to include this provision as it is not a significant penalty in weight or reliability and it affords the possibility of extending the mission considerably beyond its design life in the orbiting phase. It also permits diagnosis of suspected battery malfunctions by removing a battery from the system and discharging it through a separate auxiliary load. The battery-reconditioning provision may also serve to restore battery capacity lost through self discharge during an extended cruise phase prior to a spacecraft maneuver or other battery discharge requirement.

Another type of command often employed in power system design is that used to reset automatic switching of a standby redundant unit. This provision is necessitated primarily by practical consideration of pre-launch checkout requirements to ensure that both channels of redundant units are operative. The recommended implementation of standby redundancy and that used in the reliability weight tradeoffs in this study provide for switching from either channel to the second channel in the event of a failure. As such, the possibility of a subsequent failure or apparent failure in the second channel could cause switching back to the failed channel.

The probability of having failures in both channels of redundant units is extremely low; however, the possibility of a failure in an item of load equipment or other power system unit which appears as a failure in the operating channel is much higher. The result of such an apparent failure would be

to switch back to the failed channel and this would, in turn, cause a cycling condition between the two channels until such time as the malfunction which produced this apparent failure was corrected or isolated. It appears clear that with properly designed redundancy in the other power system units and with proper load fault isolation provisions, this cycling condition will be terminated automatically.

Command provisions are recommended, therefore, to provide the following capabilities:

- a) Terminate/initiate battery charging
- b) Change battery charge current/voltage limits
- c) Energize/deenergize nonessential load bus
- d) Energize/deenergize individual nonessential loads
- e) Initiate/terminate battery reconditioning discharge
- f) Select operative channel of standby redundant units

5.4.2 Telemetry Provisions

The judicious implementation of telemetry provisions constitutes an important task in the design of an electrical power system. It may be said that in the event of proper operation of all elements of the power system during a given mission, the telemetry data for the power system will be excessive. On the other hand, in the event of a malfunction within the power system or a malfunction attributed to the power system, the telemetry provisions will be typically inadequate. Whereas in the case of operational satellite systems (such as those used for global communications, navigational, or weather observation networks) power system telemetry provisions may be minimized, the exploratory nature of the interplanetary missions considered in this study amplifies the desirability of maximizing these provisions.

Power system telemetry, however, normally competes with scientific communications and other prime spacecraft functions for the available telemetry channels so that it is a rare case when all desirable engineering measurements can be transmitted. Priorities for selection of telemetry points must therefore be developed for the spacecraft as a whole. To this end, five general categories of telemetry provisions were developed and they are listed in order of descending priority as follows:

- 1) Measurements required for the performance of normal flight operations by ground command.
- 2) Measurements required for the performance of alternate or abnormal modes of operation by ground command.
- 3) Measurements required to verify the performance of specific systems either in flight or during prelaunch checkout activities.
- 4) Measurements required to evaluate detailed performance of critical or newly developed units.
- 5) Measurements required to diagnose malfunctions which may result in a mission failure.

Recommended analog telemetry measurements and the assigned priority for each as applied to electric power systems are illustrated in Table 63. For each parameter listed, the typical range of nominal values, the required variations of each about that nominal value and the desired measurement accuracy are shown. These values reflect the range of typical operating characteristics of the interplanetary mission considered in this study.

The assignment of priorities reflects the possibility of changing battery operating modes or adjusting spacecraft loads by command. As a result, all of the battery parameters and key current measurements are listed as priority 2. Since load adjustments can be made to change shunt regulator heat dissipation, the shunt element temperature measurement is also assigned this higher priority. The remaining parameters are required to verify power system performance (priority 3) or diagnose serious malfunctions (priority 5).

To conserve telemetry channels it is desirable to combine several output voltage measurements of load power conditioners in one word. In this case, only a qualitative indication is provided in the event that one or more voltages deviate from their normal value. When all voltages are correct, a single value telemetry indication will be received.

Table 63. Analog Telemetry Measurements and Priorities

Unit Assembly	Parameter	Nominal Values of Parameter	Required Measurement Range (%)	Desired Measurement Accuracy (%)	Priority	Notes
Solar array	Output voltage	20 to 50 V	50 to 250	3	3	{ Partial shunt regulator only. **Measurement range 98 to 102% for regulated bus systems. *Main bus voltage and current same as solar array voltage and current for shunt array control.
	Output current	5 to 50 A	10 to 150	3	3	
Array regulator	Panel temperature	-200° to +150°C	----	5	3	Reconditioning discharge
	Shunt element voltage	10 to 30 V	0 to 100	5	3	
	Shunt element current	5 to 150 A	0 to 100	5	3	
	Shunt element temperature	-40° to 100°C	----	3	2	
	Series regulator temperature	-40° to 100°C	----	3	5	
	Main bus voltage*	20 to 50 V	70 to 102**	1/2	3	
Battery	Main bus current*	5 to 50 A	10 to 150	3	2	Reconditioning discharge
	Charge current	0.1 to 50 A	0 to 200	0.5	2	
	Discharge current	5 to 100 A	0 to 150	3	2	
	Terminal voltage	3 to 28 V	80 to 120	0.5	2	
	Baseplate temperature	0° to +50°C	----	3	2	
Line regulator	Baseplate temperature	-40° to +100°C	----	3	5	Reconditioning discharge
	Output voltage	20 to 50 V	90 to 110	0.5	3	
	Output current	5 to 50 A	10 to 150	3	2	
Inverter	Output voltage	20 to 50 V ac	90 to 110	0.5	3	Reconditioning discharge
	Output current	5 to 50 A ac	10 to 150	3	2	
	Baseplate temperature	-40° to +100°C	----	3	5	
Converter or transformer-rectifier	Input current	2 to 20 A	20 to 120	3	5	Reconditioning discharge
	Output voltage	3 to 500 V	90 to 110	0.5	3	
	Baseplate temperature	-40° to +100°C	----	3	5	

In addition to the analog measurements listed in the table, discrete status indications are required for all on-off switching functions in the power system. The priorities assigned to these are either 2 or 5 depending on whether command operation of these switching functions is provided. As the transmission time between the spacecraft and the ground station is increased, the importance of these status indications also increases. The reason for this is that the effect of sending a given command cannot be rapidly ascertained and thus the exact status of the on-board controls must be known to minimize the possibility of transmitting a wrong command for the particular situation.

Several of the diagnostic measurements become meaningless if they are not made with high accuracy. Some errors can be eliminated by repeated automatic calibration, but analog systems are usually limited to ± 3 percent accuracy. Several power system measurements need, therefore, pulse modulation telemetry of considerable word length. Sampling rates, however, can be slow in all cases, about one sample every 1 to 10 minutes. During certain mission phases, a speed-up of this rate may be desirable, but telemetry of transient conditions is rarely attempted.

Any telemetry is costly, either in complexity, power consumption, reliability, etc. The simplest parameter to telemeter is voltage, since it needs no further conversion. Biased measurements (suppressed zero) require well-stabilized zener diode networks. Current measurements require conversion into analog voltages with an attendant increased complexity. Temperature measurements suffer from the low accuracy achievable with wide-range thermistors or similar temperature/voltage converters.

Since none of the power system telemetry has a priority 1, the guiding criterion in the implementation of these monitors is to achieve fail-safe designs. Where separate power sources are required to supply dc-bias voltages or ac excitation to the telemetry monitors, it is essential that these power supplies be fused or otherwise protected to assure that their failure will not jeopardize the mission. The most common case where this consideration applies is the inverter necessary to supply ac excitation to magnetic-amplifier-type current monitors. Although more

costly in terms of power consumption, it is recommended that separate inverters be provided for each current monitor and that each inverter be fused to isolate it from the system in event of a short-circuit failure.

5.4.3 Load Fault Protection

In all of the study investigations, the failures considered in calculating the probability of success of the power system were based solely on the reliabilities of the units within the power system. It is recognized that failures in other subsystems of a spacecraft may precipitate failures in the power system itself. The possibility that a given and perhaps non-essential load could fail the power system and the mission cannot be overlooked in actual applications.

In analyzing failure modes of typical load equipment, the predominant failure which can damage the power system is a gross overload produced by shorting of a part connected in a shunt configuration. The distinction made here is between series parts in a load circuit which may short and produce an increase in current and shunt parts which short circuit the power supply output in event of a failure. A detailed failure mode analysis of the load equipment is essential to the optimization of overload protection provisions within any power system.

The providing of overload protection against short circuits in the distribution system wiring itself is not recommended. The probability of short circuit failures in the interconnecting wiring of the spacecraft is normally made extremely low through proper design, manufacturing and installation of the harness assemblies to maintain adequate insulation between circuits and between each circuit and the spacecraft structure.

Several approaches exist for protecting the power system against gross overloads caused by load equipment failures. These are:

- a) Fuse protection for each item of load equipment.
- b) Circuit breaker protection for each (not remotely resettable).
- c) Latching relay with excess current trip.
- d) Individual unit current limiting.

- 1) Solid state series element
 - 2) Series regulator control
- e) Bus undervoltage detection and associated bus disconnect.

5.4.3.1 Fuse Protection for Each Major Component

The use of fusing in the power input to each major load unit constitutes a simple and effective approach to overload protection. Weight penalties and power losses associated with this approach are quite small. One problem with this approach, however, is the relatively high probability of undesired loss of power to the load because of the variability of "blow" values for fuses. This may be further complicated by a wide range of component power requirements or component turn-on current surges. This latter problem may be partly or completely alleviated by use of delayed-blow type fuses.

The use of fuses does introduce another series element in the system reliability model, and the possibility of failure due to environmental factors such as vibration, humidity or shock must be taken into account. Fuses alone can provide adequate isolation of failed nonessential loads. The use of fuses also lends itself to use with redundant essential loads of either parallel or standby types. Operation of the fuse in a standby redundant unit configuration offers an easily detectable signal to effect transfer to the standby unit and helps to protect other series power system units against damage or unnecessary switching in the event of a short circuit prior to its detection and isolation by standby redundant switching provisions in the failed unit.

5.4.3.2 Circuit Breaker Protection for Each Major Component

Circuit breakers offer a second simple approach to load fault isolation. The variability of their trip point is narrower than that of fuses. A prime drawback is the size and weight penalty that will be incurred with their use. If used with a load subject to a wide range of input requirements, circuit breakers are not effective. As in the case of fuses, circuit breakers are a one-shot protection means when used in unmanned applications. The power loss in the protective device is very minimal and a voltage drop of 20 to 100 mv is typical.

5.4.3.3 Latching Relay with Excess Current Trip

This approach is very similar to the use of circuit breakers, including their advantages and disadvantages. The principal difference is the advantage offered by incorporating automatic or ground command controlled reset provisions with the relay approach.

The protective device power loss can be kept to a level comparable to that for circuit breakers.

5.4.3.4 Unit Current Limiting

The use of a separate self-sufficient current limiting device would appear to hold considerable promise if implemented in a solid-state approach. The principal advantages of this approach appear to be a narrow range of operating values and high resistance to environmental effects. Significant disadvantages however are that the series voltage drop and power loss will be appreciable.

Current limiting can also be provided by appropriate current feedback circuits to provide override control of series voltage regulating functions in line regulation or load power conditioning equipment.

If integrated with the load equipment, it is quite possible that an automatically variable current limit point could be achieved to make the limiting value a function of the mode of operation of the unit, and weight and size penalties would be minimized. A large advantage of this approach is that it can be automatically reset. The major disadvantage is that complete isolation of a faulted unit from the power source is not normally achievable.

5.4.3.5 Bus Undervoltage Detection

The use of bus undervoltage detection and consequent automatic removal of all nonessential loads is a relatively effective approach in most circumstances. Provisions to reconnect these loads by command of each individual load is considered desirable. This approach is most effective in detecting large magnitude faults, particularly if the power source has relatively high impedance such as a solar array.

The weight penalty attributable to this form of protection will be quite negligible if provision for on/off control of the loads is provided for other reasons. The reliability of this approach can be maximized through the use of redundancy and the power loss and series voltage drop will be negligible. Insensitivity to small magnitude faults, particularly with a low impedance power source, is the principal area of weakness of this approach.

5.4.4 Electromagnetic Interference Control

The overriding aim in designing for electromagnetic compatibility (EMC) is to prevent any system from having adverse effects on the operation of any other system of the spacecraft. From the packaging and equipment interfacing considerations, there are two fundamental approaches to spacecraft EMC success. The first approach is to utilize individual source suppression on a building block or unit basis. The second approach involves not employing source suppression, but rather shielding the unit containing the interference source and filtering its inputs and outputs.

The first approach, where possible to implement, simplifies the interconnection and interfacing problem, whereas the second approach requires filtering all inputs and outputs and places additional burdens on the designers concerned with spacecraft EMC. Where an internal compatibility problem is essentially nonexistent or the susceptible circuits are easily separated from the high internal interference levels, the second approach is satisfactory. The first proposed approach includes three identifiable EMC actions:

- a) Prevention of the generation of interference at the source. In many cases, it will be found easier to prevent the generation of interference than to prevent its transmittal to susceptible circuits, or to reduce the effect of interference which reaches other circuits.
- b) Prevention of any residual interference, remaining after the above step, from either being conducted or radiated from the generating circuit to any of the susceptible circuits.
- c) Prevention of any remaining interference which reaches the susceptible circuit from adversely affecting performance.

The three above activities are suppression, shielding, and desensitizing. They should be carried out in the entire equipment design, starting with the design of the smallest circuit board all the way through the complete power system with nearby spacecraft equipment taken into consideration.

Shielding and other suppression measures may prove quite ineffective unless supplemented by adequate and consistent grounding. Grounding deficiencies may be the source of problems of internal system interaction, as well as excessive interference propagation and susceptibility to external fields.

Because of the wide range of frequencies involved, careful consideration must be given to the grounding practices employed throughout a spacecraft. The grounding techniques employed must be effective over the entire range of frequencies generated and in the electromagnetic environment in which the spacecraft must operate. The extensive use of solid-state devices greatly increases the susceptibility of circuits to RF energy well beyond their design passband. This must be taken into account in the grounding and shielding practices employed.

A prerequisite to the effective reduction of interference interaction is the establishment of an effective ground plane. When the first functional electronic circuit or module is assembled into a metallic housing or chassis, that housing or chassis becomes its ground plane and, ultimately, the spacecraft structure becomes the ground plane for each unit and all systems. The effectiveness of the ground plane in dissipating undesired electromagnetic energy is dependent upon its proper utilization with respect to the circuitry with which it is associated.

The equipment mountings and structural members of the spacecraft should be electrically bonded together to form a low-impedance reference plane. The mating surface areas between structural members should have an electrically-conductive finish equivalent to bare metal. All units or assemblies of the power system should be electrically bonded to the spacecraft structure via the mounting panels or pads. Bonding should be accomplished by metal-to-metal contact over the entire surface areas, which are held in mechanical contact. Where metal-to-metal contact

cannot be employed, at least two metallic bonding straps of minimum practical length and maximum width compatible with the mechanical considerations should be used.

5.4.4.1 Unit Packaging and Installation

Preventing the generation of unwanted signals begins with the earliest power system concept analyses. First, the types of circuits, waveforms, devices, etc. are chosen and then the specific units, circuits, and parts with favorable EMC characteristics are selected. At this point, the packaging engineer can assist by applying the following measures or by examining the design to ensure that the following have been done:

- a) Proper bonding to the ground plane of all metal, not a direct part of the circuit, will prevent those materials from possibly becoming antennas, resonant circuits, etc. Bonding will also prevent changes in resistance between portions of the structure which would generate rather large interference signals.
- b) Proper suppression of switching transients from electromechanical relays or fast squarewave rise and fall times.
- c) Reduction of generated and coupled interference by proper orientation of components and proper wire routing, twisting, and shielding.
- d) Proper design of the equipment enclosure to prevent the escape of radiated interference energy.

The discrete line spectrum produced by the fast rise and fall times of switching circuits, such as those used in pulsewidth modulated regulators, converters, and inverters, can be greatly reduced by slowing the switching times. The amount of slowing required is a function of the current being switched and the level of interference generation which can be tolerated.

Separation of generating circuits from susceptible circuits is best accomplished by placing them at opposite ends of the equipment or circuit board, or by enclosing one or the other inside a shielded compartment. As an example, a dc-dc converter located at a spacecraft

experiment package should be enclosed in a shielded compartment within the experiment package, with its input/output leads properly bypassed with feedthrough filters.

Of prime importance is the handling of the wiring within the densely packaged equipments which make up the typical spacecraft power system. For purposes of example, it is assumed that one unit is the power distribution unit (PDU), whose function is the distribution of electrical power throughout the spacecraft. A typical PDU measures 6 x 6 x 8 in. and contains circuitry for primary and secondary dc power, squarewave ac power, input and output discrete command circuitry, and relay power switching. Since this unit interfaces with every other equipment on the spacecraft, it can become a coupling medium for interference generated within the PDU, or to any one of the interfaced loads, if improperly designed with respect to EMC. To minimize this coupling and suppress the power switching transients, the following interference control measures must be implemented:

- a) Locate power switching relays in a shielded compartment and decouple the contact circuits with bulkhead mounted, feedthrough filters.
- b) Twist and shield all circuits which generate interference or are susceptible to interference.
- c) Ground the wire shields at each end to maximize their shielding efficiency. Bundle interference-sensitive wiring separately from noisy wiring, including wiring going to interference-sensitive spacecraft equipments.
- d) Locate the squarewave ac power bus in a shielded compartment with its input and output leads shielded to minimize its radiation.
- e) Route ac power, primary dc power, secondary dc power, and commands on separate output connectors to avoid coupling. In passing through these connectors, carry each two-wire circuit on adjacent pins to minimize the circuit area and, in turn, the interference pickup or generation.

These measures are similarly applicable to other units of the power system; particularly dc/dc converters and pulsewidth-modulated regulators.

The packaging activity must, in general, conform to the shielding design and be assisted by the EMC engineer. The enclosure requires attention in the "RF-tight" sealing seams and cover plates and the removal of nonconductive materials from electrical bonding surfaces. It is important that the shielding be electrically continuous with high conductivity across each seam, joint, or other discontinuity. In general, shield thickness is governed by the required mechanical properties for strength rather than by shielding effectiveness requirements.

5.4.4.2 Grounding

For all units energized from the primary dc bus, the power returns should be grounded at a single electrical reference point only. All load returns should be carried to this point on individual conductors. Steady-state loads of less than 1 amp may be returned to structure within or adjacent to the load unit.

If separate power sources are used for individual systems, separate electrical reference points should be established for each system. These points will normally be located at, or adjacent to, the power sources. Exceptions to this criterion may be warranted by the physical separation of the load units.

Secondary power (dc outputs of transformer-rectifiers or converters) returns should be dc isolated from the primary power and connected directly to chassis in each load power conditioner, and at each unit supplied. Power return wires should not carry signal returns except in short runs within a circuit where power and signal returns are necessarily common. In all cases, circuit returns should be individually connected to chassis at the closest accessible point.

In transformer-rectifiers or converters, each secondary power return should be connected to chassis as close as possible to the transformer, in addition to grounding at the output connector. Filter capacitor ground leads should be connected to chassis and maintained as short as possible. Filter capacitors utilizing the case as ground are preferable where practical. In the case of converters or transformer-rectifiers

supplying secondary power to several units in addition to avoiding common dc power returns, care must be taken to provide adequate filtering or decoupling in each load unit to avoid interaction between units. Grounding dc power returns to chassis in each load unit precludes coupling via return lines.

6. CONCLUSIONS AND RECOMMENDATIONS

6.1 CONCLUSIONS

In this study a large number of alternative power system configurations for several typical interplanetary missions were quantitatively compared. The primary study results are the computer program, which was developed to evaluate and optimize the reliability and weight of all candidate system configurations, and the preliminary determination of preferred system configurations for the interplanetary missions specified.

The study included the definition of model missions, model spacecraft configurations, the power requirements for each of these configurations, and the selection of specific designs for the large number of alternative power system functions required in the different system configurations.

6.1.1 Reliability -Weight Optimization Computer Program

The computer program resulting from this study provides a basic tool which can be used to quantitatively compare any set of power system configurations on the basis of reliability and weight. The absence of such a tool in the past has usually restricted the number of alternative system configurations to a relative few that are evaluated for any given mission. Considerable emphasis has then been placed on improving the reliability and minimizing the weight of the particular configuration that appeared best suited to the mission. This approach can obviously lead to the use of a system which is not optimum.

The fact that system considerations other than reliability and weight may strongly influence the selection of a particular power system design cannot be overlooked. Probably, the most significant considerations, other than reliability and weight, are cost and schedule. These considerations often lead to the adaptation of existing flight-proven equipment, which, although cost effective, frequently results in the use of a system that is neither the most reliable nor the least heavy for the new missions. Another consideration tending to deter power system optimization is a requirement that the power system be flexible in supporting a variety of payloads and/or missions; potential schedule improvements and cost savings again provide the reason for such a provision.

The reliability-weight optimization analyses performed in this study excluded spacecraft optimization requirements such as these, and, as a result, specific recommendations of preferred optimized power system designs for each of the interplanetary missions are not obtainable. However, the results of the computer program can provide the power system data needed to optimize the overall reliability and weight of the spacecraft for any specified mission.

Although considerations, such as cost, development time, and multiple missions, exist, the optimum design of any spacecraft requires proper apportioning of the total weight allowance defined by the booster capability among the various systems to achieve maximum complete spacecraft reliability.

The results of the computer runs for the power system define a largely narrowed-down range of system designs and the corresponding reliability and weight for each. These data, together with similar data for the communication system, payload, guidance and control, etc., can be combined in an overall system optimization program to select the optimum spacecraft configuration. Computer programs, capable of performing this type of spacecraft optimization already in use, facilitated the development of the power system optimization computer program for this study. The program approaches are similar in that various alternative configurations of elements within a system are defined, and, on the basis of reliability and weight, comparisons are made of possible combinations of these alternative elements. In this study, these comparisons were made for alternative power system configurations after each power system configuration was first optimized by comparing all combinations of redundant and nonredundant units within that power system configuration. The existence of this computer program permits the rapid development of reliability and weight data for optimized power system designs that can be used as an input to the overall spacecraft optimization process of future programs.

6.1.2 Preferred Power System Configurations

All power system configurations studied in this project were grouped into two categories:

- a) Those that combine the solar array and battery electrically at an unregulated bus.
- b) Those which use regulators on the solar array as well as for charging and discharging of the battery to permit their combination at a regulated bus.

The selection of the optimized configuration as well as the general type of power system was found to be a function of the load power profile of the mission, the solar array characteristics during the mission, and the allocated power system reliability or weight for the particular mission.

The principal advantage of directly generating a regulated bus results from the fact that a single, highly efficient solar array regulator may be used during sunlight operation when the solar array is supporting the load. When the battery is required to support the load for long periods, the losses incurred by battery charge and discharge regulation tend to offset the advantage of efficient solar array utilization obtained through the regulated bus approach. Conversely, unregulated bus systems provide a more efficient method of charging and discharging the battery but require supplementary regulation functions to accommodate the voltage variations of the main bus. These additional regulation functions reduce the efficiency of solar array power utilization in sunlight.

For all of the Jupiter missions, the weight of the very large solar array required to support the assumed loads at sun-spacecraft distances of 5.2 AU, combined with the attendant low utilization of battery energy, resulted in the selection of regulated bus systems for each mission. For the model spacecraft configured for these Jupiter missions, it was determined that solar array designs yielding at least 20w/lb at 1 AU are virtually essential to achieve mission feasibility.

For the Venus Orbiter No. 1 mission, the regulated bus systems were again selected as the optimum configurations over the entire reliability range. For the Venus Orbiter No. 2 mission, the Mercury mission and the Mars Orbiter mission, the regulated and unregulated bus systems were intermixed over the reliability range.

There is a common characteristic among all of the reliability-weight plots for systems that consider the use of a single nonredundant battery, or a fully redundant two-battery approach for the orbiting missions. Starting from a nonredundant system of minimum weight and minimum reliability, a significant reliability gain with only a moderate weight increase can be achieved by first making all of the electronic equipment redundant. To further improve reliability, it was necessary to make the battery redundant; this increased system weight significantly for most of the missions. The reliability gained with the redundant battery permitted the elimination of some of the redundancy in the electronic equipment to minimize weight for intermediate reliability values. Further increases in system reliability are achieved by again making the electronic units redundant with only moderate weight increases.

The relative magnitude of the step increase in weight, incurred by making the battery redundant, is less for the flyby missions than for the orbiting missions. This is due to the fact that battery utilization is relatively small and the battery weight is less dominant in comparison to that of the solar array and conditioning equipment. Where low-voltage batteries are used, the nonredundant configuration was not considered. As a result, the characteristic step increase in weight occurring at intermediate reliability levels is not observed.

It was also noted in the analysis that the variation in particular implementation of a function within the several basic system configurations has a very small effect on the overall system reliability and weight; this was particularly true for the alternative battery charge control designs. The choice between dissipative bucking chargers and pulsewidth-modulated chargers, which of course have a higher efficiency, normally favored the dissipative approach. This results from the fact that the simplicity of the dissipative approach gives a reliability and weight advantage over the switching approach, and the efficiency advantage of the switching approach is not significant in terms of the low battery-charging power required for these model missions.

The selection of optimum systems as a function of reliability and weight was shown to include both ac and dc power distribution approaches. Analysis of the data has shown that the difference in reliability and weight

between an ac and dc distribution scheme is relatively small. As a result, the selection of either an ac or dc distribution system must be made on the basis of additional considerations such as flexibility, fault isolation and electromagnetic compatibility for a particular application.

The results of the power system reliability-weight optimization analyses have shown that for interplanetary probes or orbiting missions having relatively long orbit times and, as a result, relatively short eclipses, the use of power systems that electrically combine the solar array and battery at a regulated bus are usually advantageous.

An extension of this basic system approach which appears to offer significant improvements in system reliability and weight is the Modular Energy Storage and Control (MESAC) concept, which utilizes low-voltage batteries with a regulated bus approach. Although this system, as configured in the study, did not always appear to be optimum, an assumed use of three batteries, when only two are required to perform a mission, does not show the flexibility of this approach. The number of batteries used and the number of batteries required must be analyzed for any particular application to determine the optimum configuration of this low-voltage battery energy-storage concept.

The corollary to this conclusion is that those applications which require a significant amount of battery utilization because of a relatively low sunlight-to-total-orbit-period ratio are best served by power systems that incorporate the simplest battery control functions and an unregulated main bus. If these systems are configured with but one centralized line regulator, the overall weight and reliability of this approach is superior to that of any other approach.

6.1.3 Preferred Power Systems

Preferred power system configurations were determined, in the absence of reliability or weight allocations, by analyzing the results of the weight-reliability optimization for each of the seven model spacecraft. The locus of optimum systems (Section 4) for each model was scanned to determine those configurations which either were predominantly lightest over the entire reliability range or were significantly lighter than the

system having the next higher reliability. A single preferred system could not be selected for each mission because a weight limit or reliability allocation based on an overall spacecraft optimization was not available. The preferred system designations for each model and definitions of the major functional elements for each are as follows:

<u>MODEL</u>	<u>PREFERRED SYSTEMS</u>
Mercury Flyby	141, 495
Venus Orbiter No. 1	395, 3115
Venus Orbiter No. 2	141, 171, 4115
Mars Orbiter	161, 495, 423
Jupiter Flyby	395, 3115
Jupiter Orbiter No. 1	395, 3115
Jupiter Orbiter No. 2	395, 3115
System 141: No solar array voltage control, dissipative battery charger, momentary line booster or PWM bucking line regulator	
System 161: Same as 141 except PWM bucking battery charger	
System 171: Same as 141 except PWM buck-boost battery charger and no momentary line booster	
System 395: Dissipative shunt solar array regulator, dissipative battery-charge regulator, PWM boosting battery-discharge regulator and no line regulator (nominal 28-v battery)	
System 3115: Same as 395 except low voltage battery	
System 423: PWM series bucking solar array voltage limiter, resistive battery charge control, momentary line booster and PWM boosting line regulator	
System 425: Same as 395 except PWM series bucking solar array regulator	
System 4115: Same as 3115 except PWM series bucking solar array regulator	

6.2 RECOMMENDED FUTURE STUDY AREAS

Further development of the power system reliability-weight optimization computer program should be undertaken to improve its adaptability to a specific power system design requirement. This recommended development is divisible into two specific areas of investigation. The first area is the reexamination of several simplifying assumptions made in performing this study and the determination of necessary modifications to the computer program to improve its flexibility. The second area of investigation is the employment of mathematical techniques to solve or simplify the reliability-weight optimization problem without necessitating the enumeration of all possible system combinations.

6.2.1 Optimization Program Refinements

In order to free the computer program from limitations imposed by the study assumptions, it is recommended that the program be applied to an actual spacecraft design and necessary modifications incorporated. One of the more significant of these assumptions relates to the fact that some of the elements in the power system are normally required to perform various system control and protection functions which were not included in the power system models and computer analyses. These additional control and protection functions may include load switching, command, telemetry, overload protection or undervoltage protection provisions which will influence the overall system reliability and weight. However, the general trends and the ranking of systems indicated by the computer runs made thus far should not be significantly affected by such function additions, as the needed additional circuitry can be made highly reliable through redundancy without a significant weight penalty.

It is true, however, that in selecting optimum systems as a function of reliability for a particular mission, several systems were rejected that were very close to the optimum in terms of achievable reliabilities and weights. The possibility exists, therefore, that the addition of protection and control functions can be achieved in a more efficient manner or in a manner which produces a smaller weight increase in one system than in another. Should this prove to be the case, the previous selections of optimum systems need reexamination.

A second assumption made in the study was that the maximum bus power requirements occurred simultaneously with the maximum load demand on the various power conditioning equipment in the system. In an actual application, it is typical that the equipment power requirements vary as a function of time, and, although a maximum average load condition on the main bus may exist, certain of the loads may be deenergized or operated at reduced power during this period. At other times in the mission, particular loads may be significantly increased although the total power at the main bus could be reduced.

Another example of this difference occurs in the proper sizing of the battery, wherein the maximum average load during the battery-discharge period must be defined. Here again the load demand on particular items of power conditioning equipment, such as TR units and converters or inverters, may vary significantly during the discharge period. The sizing of the battery must reflect the average load and the average efficiency of the load power conditioning equipment. The sizing of the load power conditioning equipment must reflect the maximum load under any condition on that item of equipment.

Therefore, modifications of the program are recommended to distinguish between maximum individual load requirements for each item of power conditioning equipment and the maximum bus load requirements.

In many applications, certain of the spacecraft loads can be classified as nonessential to success of the mission, and the failure of load power conditioning equipment that supplies these loads could therefore be tolerated. Such failures would require protection against damaging the essential elements of the power system; however, it is very likely that these protective features would require a smaller weight penalty than the implementation of the redundancy as used in the study to achieve a suitable overall system reliability. Further improvement in the system reliability-weight optimization program would result from incorporating realistic definitions of failure to include the possibility that several nonessential loads could be lost without causing mission failure. Consequently, it is recommended that the computer program be analyzed with respect to the simplifying assumption made for this study that all elements of the power system were in-line in the reliability model.

The recommendation that the optimization program be applied to an actual spacecraft application is further supported by the fact that this would also afford an opportunity to perform realistic tradeoffs of dc versus ac power distribution, and to perform detailed analyses of power system failure modes, effects and corrective measures. These investigations require definition of specific characteristics of the spacecraft and its equipment in addition to the power system requirements, constraints and interfaces in order to yield meaningful results. The best source of such data is an actual spacecraft design.

6.2.2 Mathematical Analysis of Reliability-Weight Characteristics

It is considered entirely feasible that the implementation of partial redundancy at the unit or circuit level would add a large number of intermediate reliability and weight values to the plotted locus of optima for each power system. This could allow approaching very closely a smooth curve of reliability versus weight from the nonredundant system configuration up to the point at which the large increase in weight, due to the implementation of battery redundancy, is required. The possibility of developing a mathematical expression for this curve would then exist.

It is recommended that further analysis be undertaken to determine the possibility of employing classical mathematical techniques in searching for the best combination of redundant and nonredundant units within this range of reliabilities for a given system configuration and a specific weight constraint. This approach would permit a significant simplification in the overall power system optimization process by eliminating the need to calculate the reliability and weight of all possible combinations of redundant and nonredundant units in the search for an optimized configuration.